

TABLE OF CONTENTS

	Page
INTRODUCTION	1
CHAPTER 1 LITERATURE REVIEW	7
1.1 Introduction.....	7
1.2 Design for manufacturing and assembly (DFMA) overview	7
1.2.1 Composites materials.....	8
1.2.2 Matrices.....	8
1.2.3 Reinforcements	9
1.2.4 Composite material forms.....	11
1.3 Composite fabrication processes.....	11
1.3.1 Autoclave cure process	12
1.3.2 Compression moulding process	12
1.4 Cost modeling concepts	13
1.4.1 Analogous estimation model.....	13
1.4.2 Parametric estimation model.....	13
1.4.3 Analytic estimation model	14
1.4.4 Accounting methods	14
1.4.5 Activity based costing.....	14
1.4.6 Process-based cost models.....	15
1.5 Manufacturing cost modeling for composites materials.....	15
1.5.1 ACCEM Power law model	16
1.5.2 1 st order model	17
1.5.3 Hyperbolic model.....	18
1.5.4 Cost optimization models for composites materials	19
1.5.5 Cost modeling of thermoplastic composite compression moulding.....	20
1.5.6 Summary and limitations of existing models.....	21
CHAPTER 2 TOOLING AND ENERGY COSTS ESTIMATION OF COMPRESSION PROCESS MOULDED RANDOMLY ORIENTED STRANDS THERMOPLASTIC EXPERIMENTAL PARTS	23
2.1 Introduction.....	23
2.2 Cycle time simulation and energy cost estimation for ROS parts	23
2.3 Material.....	27
2.4 Flat plate.....	28
2.4.1 Compression moulding process of flat plate.....	28
2.4.1.1 Heating step	28
2.4.1.2 Cooling step	29
2.4.2 Heat transfer processes	29
2.4.3 Numerical simulations	30
2.4.3.1 Heating time simulation.....	30
2.4.3.2 Cooling step simulation	32

2.4.4	Experimental and numerical results.....	34
2.4.5	Heating power simulation results.....	35
2.4.6	Heating energy costs calculations.....	36
2.5	T-shape part	36
2.5.1	Compression moulding process of T-shape part.....	36
2.5.1.1	Heating step	37
2.5.1.2	Cooling step.....	38
2.5.2	Heat transfer processes	38
2.5.3	Numerical simulations	39
2.5.3.1	Heating step simulation.....	39
2.5.3.2	Cooling time simulation.....	42
2.5.4	Experimental and numerical results.....	43
2.5.5	Heating power simulation results.....	44
2.5.6	Heating energy costs calculations.....	45
2.6	L-bracket part.....	46
2.6.1	Compression moulding process of L-bracket	46
2.6.1.1	Heating step	46
2.6.1.2	Cooling step	47
2.6.2	Heat transfer processes	48
2.6.3	Numerical simulations	48
2.6.3.1	Heating step simulation.....	48
2.6.3.2	Cooling step simulation	51
2.6.4	Experimental and numerical results.....	52
2.6.5	Heating power simulation results.....	54
2.6.6	Heating energy costs calculations.....	55
2.7	Tooling costs estimation for manufacturing ROS parts.....	55
2.7.1	Methodology.....	55
2.7.2	Flat mould cost estimation.....	57
2.7.2.1	Flat mould manufacture process	57
2.7.2.2	Flat mould assembly process	57
2.7.2.3	Flat mould cost estimation results.....	58
2.7.2.4	Flat mould costs breakdown	59
2.7.2.5	Estimated and commercial cost comparison for the flat mould.....	60
2.8	T-shape mould cost estimation	61
2.8.1	T-shape mould manufacture process	61
2.8.2	T-shape mould assembly process.....	62
2.8.3	T-shape mould cost estimation results.....	63
2.8.4	T-shape mould cost breakdown	65
2.8.5	Estimated and workshop costs comparison for the T-shape mould.....	66
2.9	L-bracket mould cost estimation.....	67
2.9.1	L-bracket mould manufacture process.....	67
2.9.2	L-bracket mould assembly process.....	68
2.9.3	L-shape mould cost estimation results.....	69
2.9.4	L-bracket mould cost breakdown.....	71
2.9.5	Estimated cost and commercial price comparison for L-shape mould.....	72

2.10	Discussion of results and conclusion	72
CHAPTER 3	TOOLING AND ENERGY COSTS SIZING AND COMPLEXITY SCALING LAWS OF COMPRESSION PROCESS MOULDED RANDOMLY ORIENTED STRANDS THERMOPLASTIC EXPERIMENTAL PARTS	77
3.1	Introduction.....	77
3.2	Energy costs sizing scaling laws for ROS parts.....	77
3.2.1	Flat plate.....	77
3.2.1.1	Heating power simulation results scaling with volume of ROS flat plate	78
3.2.1.2	Heating energy cost calculation results scaling with volume of ROS flat plate	79
3.2.2	T-shape part	79
3.2.2.1	Heating power simulation results scaling with volume of ROS T-shape part	80
3.2.2.2	Heating energy cost calculation results scaling with volume of ROS T-shape part	80
3.2.3	L-bracket part.....	81
3.2.3.1	Heating power simulation results scaling with volume of ROS L-bracket part.....	81
3.2.3.2	Heating energy cost calculation results scaling with volume of ROS L-bracket.....	82
3.2.3.3	ROS part heating energy sizing scaling laws.....	83
3.2.3.4	ROS part heating energy costs sizing scaling laws.....	85
3.2.3.5	ROS parts heating energy complexity scaling laws.....	86
3.3	Tooling costs sizing scaling laws for ROS parts	86
3.4	Tooling costs complexity scaling laws	89
3.5	Discussion of results and conclusion	90
CHAPTER 4	TOOLING AND ENERGY COSTS ESTIMATION FOR COMPRESSION PROCESS MOULDED UNIDIRECTIONAL FIBRE CARBON PREPREG THERMOPLASTIC EXPERIMENTAL PARTS	91
4.1	Introduction.....	91
4.2	Cycle time simulations and energy costs estimation for UD parts	91
4.2.1	Material	92
4.2.2	Compression moulding process of concave part	92
4.2.2.1	Heating step	94
4.2.2.2	Cooling step.....	96
4.2.3	Mathematical model and heat transfer processes.....	96
4.2.4	Numerical simulations	99
4.2.4.1	Heating step simulation.....	99
4.2.4.2	Cooling step simulation	102
4.2.5	Experimental and numerical results.....	104
4.2.6	Heating power simulations	105

4.2.7 Heating energy costs estimation 106

4.3 Tooling costs estimations for manufacturing UD parts107

4.3.1 Concave mould manufacture process 107

4.3.2 Side lock manufacturing process 108

4.3.3 Concave mould assembly process 109

4.3.4 Concave mould cost estimation results 110

4.3.5 Concave mould cost breakdown 111

4.4 Discussion of results and conclusion113

CHAPTER 5 TOOLING AND ENERGY COSTS SIZING AND COMPLEXITY
 SCALING LAWS FOR COMPRESSION PROCESS MOULDED
 UNIDIRECTIONAL CONTINUOUS FIBRE REINFORCED
 THERMOPLASTIC PARTS115

5.1 Introduction115

5.2 Energy costs sizing scaling laws for UD parts.....115

5.2.1 Concave part 116

5.2.1.1 Heating power simulations results for the laminate..... 116

5.2.1.2 Heating power simulation results for the concave mould..... 117

5.2.1.3 Heating energy cost calculation results for concave part..... 117

5.2.2 U-shape part 118

5.2.2.1 Heating energy calculation results for the laminate..... 118

5.2.2.2 Heating power simulation results for hollow square mould 119

5.2.2.3 Heating energy cost calculation results for U-shape part 120

5.2.3 Hollow square part..... 120

5.2.3.1 Heating energy cost calculation results for the laminate 121

5.2.3.2 Heating power simulation results for hollow square mould 121

5.2.3.3 Heating energy cost calculation results for hollow square part 122

5.2.4 Z-shape part 122

5.2.4.1 Heating power calculations results for the laminate 123

5.2.4.2 Heating power simulation results for Z-shape mould..... 123

5.2.4.3 Heating energy cost calculation results for Z-shape part..... 124

5.2.5 Flat plate..... 124

5.2.5.1 Heating power calculation results for the laminate..... 125

5.2.5.2 Heating power simulation results for flat mould 125

5.2.5.3 Heating energy cost calculation results for flat plate..... 126

5.2.6 UD part heating energy sizing scaling laws..... 126

5.2.7 UD part heating energy costs sizing scaling laws..... 128

5.3 Mould costs sizing scaling laws for UD parts129

5.4 Mould costs complexity scaling laws for UD parts132

5.5 Discussion of results and conclusion133

CHAPTER 6 COSTS ESTIMATION FOR THERMOSET COMPOSITE PARTS
 MANUFACTURED BY AUTOCLAVE PROCESS135

6.1 Introduction135

6.2 Flat plate.....137

6.2.1	Process manufacturing time estimation	137
6.2.1.1	Layup time estimation.....	138
6.2.2	Flat mould cost estimation	142
6.3	T-shape part	146
6.3.1	Process manufacturing time estimation	146
6.3.1.1	Lay-up time estimation	147
6.3.2	Tooling costs estimation	151
6.4	L-bracket.....	156
6.4.1	Process manufacturing time estimation	157
6.4.1.1	Layup time estimation.....	157
6.4.2	Tooling costs estimation	163
6.5	Cost analysis	169
6.5.1	Flat mould	171
6.5.2	T-shape part	172
6.5.3	L-bracket part.....	174
6.6	Discussion of results and conclusion	176
CHAPTER 7	MANUFACTURING COST ANALYSIS FOR THERMOPLASTIC COMPOSITE COMPRESSION MOULDED AEROSPACE COMPONENTS	179
7.1	Introduction.....	179
7.2	Manufacturing costs.....	179
7.2.1	Manufacturing cost elements	180
7.2.1.1	Variable costs.....	182
7.2.1.2	Fixed costs	184
7.2.1.3	Overheads costs	186
7.2.1.4	Unit costs	186
7.3	Costs analysis.....	186
7.3.1	ROS parts.....	189
7.3.1.1	Flat plate.....	189
7.3.1.2	T-shape part	191
7.3.1.3	L-bracket part.....	193
7.3.2	UD parts.....	195
7.3.2.1	Concave part	196
7.3.2.2	Hollow square part.....	197
7.3.2.3	U-shape part.....	199
7.3.2.4	Z-shape part	200
7.3.2.5	Flat plate.....	202
7.4	Autoclave process and compression moulding parts manufacturing costs comparisons	203
7.5	Discussion of results and conclusion	204
GENERAL CONCLUSION.....		207
RECOMENDATIONS		211

APPENDIX I	LIST PUBLICATION LIST	213
ANNEX I	FEATURES MANUFACTURING DATA FOR FLAT MOULD.....	215
ANNEX II	FEATURES MANUFACTURING DATA FOR T-SHAPE MOULD ...	219
ANNEX III	FEATURES MANUFACTURING DATA FOR L-SHAPE MOULD ...	223
ANNEX IV	FEATURES MANUFACTURING DATA FOR CONCAVE MOULD	230
ANNEX V	COST CALCULATION EXCEL SPREADSHEET FOR THERMOSET FLAT PLATE MANUFACTURED BY AUTOCLAVE PROCESS.....	235
ANNEX VI	COST CALCULATION EXCEL SPREADSHEET FOR THERMOSET T-SHAPE PART MANUFACTURED BY AUTOCLAVE PROCESS.....	241
ANNEX VII	COST CALCULATION EXCEL SPREADSHEET FOR THERMOSET L-SHAPE PART MANUFACTURED BY AUTOCLAVE PROCESS.....	247
ANNEX VIII	COST CALCULATION EXCEL SPREADSHEET FOR ROS FLAT PLATE MANUFACTURED BY COMPRESSION MOULDING PROCESS	253
ANNEX IX	COST CALCULATION EXCEL SPREADSHEET FOR ROS THERMOPLASTIC T-SHAPE PART MANUFACTURED BY COMPRESSION MOULDING PROCESS	259
ANNEX X	COST CALCULATION EXCEL SPREADSHEET FOR ROS THERMOPLASTIC L-SHAPE PART MANUFACTURED BY COMPRESSION MOULDING PROCESS	265
ANNEX XI	COST CALCULATION EXCEL SPREADSHEET FOR UD THERMOPLASTIC CONCAVE PART MANUFACTURED BY COMPRESSION MOULDING PROCESS	271
ANNEX XII	COST CALCULATION EXCEL SPREADSHEET FOR UD THERMOPLASTIC HOLLOW SQUARE PART MANUFACTURED BY COMPRESSION MOULDING PROCESS....	277
ANNEX XIII	COST CALCULATION EXCEL SPREADSHEET FOR UD THERMOPLASTIC U-SHAPE PART MANUFACTURED BY COMPRESSION MOULDING PROCESS	283

ANNEX XIV	COST CALCULATION EXCEL SPREADSHEET FOR UD THERMOPLASTIC Z-SHAPE PART MANUFACTURED BY COMPRESSION MOULDING PROCESS	289
ANNEX XV	COST CALCULATION EXCEL SPREADSHEET FOR UD THERMOPLASTIC FLAT PLATE MANUFACTURED BY COMPRESSION MOULDING PROCESS	295
	LIST OF BIBLIOGRAPHICAL REFERENCES.....	301

LIST OF TABLES

	Page
Table 1.1	Matrices typical properties.....9
Table 1.2	Typical fibres properties Adapted from Haffner (2002,p.35).....10
Table 2.1	Physical and thermal properties of carbon/PEEK.....27
Table 2.2	Model geometry characteristics for simulation of heating step32
Table 2.3	Model geometry characteristics for simulation of the cooling step33
Table 2.4	Heating step simulation results for flat plate36
Table 2.5	Heating energy and heating energy costs results for.....36
Table 2.6	Geometry characteristics of the heating model.....41
Table 2.7	Geometry characteristics of the cooling model42
Table 2.8	Heating step simulation results for T-shape part45
Table 2.9	Heating energy and heating energy costs results for the T-shape part45
Table 2.10	Geometry characteristics of the heating model at various times for three locations on the middle plan of the ROS flat plate50
Table 2.11	Geometry characteristics of the cooling model52
Table 2.12	Heating step simulation results for L-bracket part.....55
Table 2.13	Heating energy and heating energy costs results55
Table 2.14	Features assembly data for flat mould58
Table 2.15	Flat mould manufacturing costs.....58
Table 2.16	DFMA Flat mould estimated costs59
Table 2.17	Commercial and estimated costs comparison for the flat mould61
Table 2.18	Features assembly data for T-shape mould.....63
Table 2.19	T-shape mould manufacturing costs64

Table 2.20	DFMA T-shape mould estimated costs.....	64
Table 2.21	Workshop and estimated costs comparison for T-shape mould	67
Table 2.22	Features assembly data for L-bracket mould	68
Table 2.23	L-shape mould manufacturing costs	69
Table 2.24	DFMA L-shape mould estimated costs.....	70
Table 2.25	Estimated cost and commercial price comparison for L-shape mould	72
Table 3.1	Heating data and heating power density simulations results scaling with volume of ROS flat plate	78
Table 3.2	Calculated heating energy and heating energy costs scaling with volume of ROS flat plate	79
Table 3.3	Heating data and heating power density simulations results scaling with volume of ROS T-shape part	80
Table 3.4	Calculated heating energy and heating energy costs scaling with volume of ROS T-shape part	80
Table 3.5	Heating data and heating power density simulations results scaling with volume of ROS L-bracket.....	81
Table 3.6	Heating power calculations results scaling with.....	82
Table 3.7	Calculated heating energy and heating energy costs scaling with the volume of ROS L-bracket.....	83
Table 3.8	Heating energy sizing scaling laws for three ROS part forms:Flat plate, T-shape and L-bracket	84
Table 3.9	Heating energy costs sizing scaling laws for three ROS part forms.....	85
Table 3.10	Estimated tooling costs for L-bracket mould, T-shape mould and flat mould scaling with mould projected area	87
Table 3.11	Tooling costs sizing scaling laws for L-bracket mould, T-shape mould and flat mould	88
Table 4.1	Physical and thermal properties of ZiO_2	92
Table 4.2	Surface emissivities	98
Table 4.3	Geometry characteristics of the pre-heating model	101

Table 4.4	Geometry characteristics of the cooling model	103
Table 4.5	Heating power simulation results for the laminate	106
Table 4.6	Heating power simulation results for the concave mould.....	106
Table 4.7	Heating energy and heating energy cost results for concave part.....	106
Table 4.8	Concave mould components assembly data	109
Table 4.9	Concave mould manufacturing cost estimation results	110
Table 4.10	DFMA concave mould cost estimation results	111
Table 4.11	DFMA estimated costs and commercial price comparison for the concave mould.....	113
Table 5.1	Heating data and heating power simulation results for the laminate scaling with the part volume.....	116
Table 5.2	Heating power simulation results for the concave mould scaling with the volume of the mould.....	117
Table 5.3	Calculated heating energy and heating energy costs for the concave part scaling with the part volume.....	118
Table 5.4	Heating energy scaling with the part volume	119
Table 5.5	Heating power simulation results for the hollow square mould scaling with the volume of the mould	119
Table 5.6	Calculated heating energy and heating energy costs for U-shape part scaling with the part volume	120
Table 5.7	Heating energy scaling with part volume	121
Table 5.8	Heating power simulation results for the hollow square mould scaling with the volume of the mould.....	121
Table 5.9	Calculated heating energy and heating energy costs for hollow square parts scaling with part volume.....	122
Table 5.10	Heating energy scaling with part volume	123
Table 5.11	Heating power simulation results for the Z-shape mould scaling with the volume of the mould.....	123

Table 5.12	Calculated heating energy and heating energy costs for Z-shape part scaling with part volume	124
Table 5.13	Heating energy scaling with the volume of flat plate	125
Table 5.14	Heating power simulation results for the flat mould scaling with volume of the mould.....	125
Table 5.15	Calculated heating energy and heating energy costs for flat plate scaling with part volume.....	126
Table 5.16	Heating energy sizing scaling laws for five UD part forms: concave part, hollow square part, U-shape part, Z-shape part, Flat plate.....	127
Table 5.17	Heating energy costs sizing scaling laws for five UD part forms: concave part, hollow square part, U-shape part, Z-shape part, Flat plate.....	129
Table 5.18	Estimated moulds costs for concave mould, hollow square mould, flat mould and Z-shape scaling with mould projected area	130
Table 5.19	Mould costs sizing scaling laws for concave mould, hollow square mould, flat mould and Z-shape mould	131
Table 6.1	The rate categories for the cost calculation.....	135
Table 6.2	Other material costs for making flat plate.....	137
Table 6.3	The flat plate manufacturing time estimation results.....	138
Table 6.4	The flat mould manufacture process data	143
Table 6.5	The costs details for flat mould.....	144
Table 6.6	Other material costs for making a T-shape part by lay-up and autoclave cure	146
Table 6.7	The T-shape part manufacturing time estimation results.....	147
Table 6.8	T-shape mould manufacture process data.....	153
Table 6.9	The cost details for T-shape mould.....	154
Table 6.10	Other material costs for making an L-bracket part by lay-up and autoclave cure	157
Table 6.11	The L-bracket manufacturing time estimation results	158

Table 6.12	The L-shape mould manufacture process data.....	165
Table 6.13	The cost details for L-shape mould.....	167
Table 6.14	Estimated cost for thermoset flat plate.....	171
Table 6.15	Estimated costs for thermoset T-shape part.....	173
Table 6.16	Estimated costs for thermoset L-bracket part	175
Table 7.1	Typical manufacturing costs.....	179
Table 7.2	Industrial data on cost modeling.....	187
Table 7.3	Estimated costs for ROS flat plate.....	190
Table 7.4	Estimated costs for (ROS) T-shape part	192
Table 7.5	Estimated costs for (ROS) L-bracket part.....	194
Table 7.6	Estimated costs for (UD) concave part.....	196
Table 7.7	Estimated costs for (UD) hollow square part.....	198
Table 7.8	Estimated costs for (UD) U-shape part.....	199
Table 7.9	Estimated costs for (UD) Z-shape part	201
Table 7.10	Estimated costs for (UD) flat plate	202
Table 7.11	Comparisons between compression moulding process and autoclave process parts manufacturing costs	204

LIST OF FIGURES

		Page
Figure 0.1	Cost modeling concept.....	4
Figure 2.1	Typical tetrahedral element.....	26
Figure 2.2	Preparation of material.....	27
Figure 2.3	Manufacturing cell for flat plate: (1) placing material in the cutter, 2) cutting of material into strands (manual cutter), (3) distributing randomly of strands in the mould, (4) closing and transferring of the mould to the press, (5) heating of platens, compression moulding of flat plate and then cooling (6) demoulding.....	28
Figure 2.4	Contact heat transfer mechanisms	30
Figure 2.5	Geometry of the model for heating step simulation.....	31
Figure 2.6	Mesh of the model for heating step simulation.....	31
Figure 2.7	Model geometry of the cooling system.....	33
Figure 2.8	Distribution of temperature in the model at heating times: a) 10 s, b) 1000 s.....	34
Figure 2.9	Distribution of temperature in the model at cooling times: a) 10 s , b) 3600 s.....	34
Figure 2.10	Comparison between numerical and experimental temperatures at various times for three locations on the middle plan of the ROS flat plate.....	35
Figure 2.11	a) Cavity mould filled with ROS. b) Experimental set up c) ROS T-shape part.	37
Figure 2.12	Contact heat transfer mechanisms	38
Figure 2.13	Geometry of the model for simulation of heating step	40
Figure 2.14	Mesh of the model geometry for heating step simulation.....	40
Figure 2.15	Model geometry of the cooling system.....	42
Figure 2.16	Distribution of temperature in the model at heating times: a) 30 s, b) 1600 s.....	43

Figure 2.17	Distribution of temperature in the model at cooling times: a) 20 s, b) 1800 s.....	43
Figure 2.18	Comparison between numerical and experimental temperature distributions during the compression moulding process inside the ROS T-shape part	44
Figure 2.19	a) Cavity Mould filled with ROS. b) Experimental set up c) ROS T-shape part.	46
Figure 2.20	CAD of the mould showing the position of the heating cartridges and the rib insert	47
Figure 2.21	Contact heat transfer mechanisms	48
Figure 2.22	Geometry of the model for heating process.....	49
Figure 2.23	Mesh of the model geometry for heating simulation	50
Figure 2.24	Model geometry of the cooling step	51
Figure 2.25	Distribution of temperature in the model at heating times: a) 10 s, b) 2500 s.....	52
Figure 2.26	Distribution of temperature in the model at cooling times: a) 25 s, b) 7300 s.....	53
Figure 2.27	Temperature variation versus time inside the mould and L-bracket part ..	54
Figure 2.28	CAD of flat mould	57
Figure 2.29	Cost breakdown of flat mould.....	60
Figure 2.30	CADs of T-shape mould assembly: a) cavity assembly, b) punch assembly.....	62
Figure 2.31	Cost breakdown of T-shape mould	66
Figure 2.32	CAD of L-bracket mould fixture	68
Figure 2.33	Cost breakdown of L-bracket mould	71
Figure 3.1	Design of ROS flat plate in 3D.....	78
Figure 3.2	Design of the ROS T-shape	79
Figure 3.3	Design of the ROS L-bracket.....	81

Figure 3.4	Heating energy of three ROS parts in function of the part volume: Flat plate, T-shape and L-bracket.....	84
Figure 3.5	Heating energy costs of three ROS parts in function of the part volume: Flat plate, T-shape and L-bracket	85
Figure 3.6	Heating energy consumption scaling with complexity of the part	86
Figure 3.7	Tooling costs vs. projected area for L-bracket mould, T-shape mould and flat mould T-shape mould and flat mould.....	88
Figure 3.8	Moulds costs for L-bracket mould, T-shape mould and flat mould scaling with complexity level of the mould.....	89
Figure 4.1	Manufacturing cell of concave part. (1) preparation of the laminate, (2) placing the laminate in the IR oven, (3) heating the laminate in the IR oven, (4) transfer of heated laminate to press, (5) compression moulding of part, (6) demoulding of the cooled concave part.....	93
Figure 4.2	Experimental setup.....	94
Figure 4.3	Design of Elstein ceramic infrared radiator (HTS series).....	95
Figure 4.4	Position of thermocouples through the thickness of the laminate	95
Figure 4.5	a) Cavity block, (b) Punch block, (c) Top and bottom views of concave part	96
Figure 4.6	Heat transfer mechanisms in the IR oven	98
Figure 4.7	Geometry of the model for simulation of infrared pre-heating step	100
Figure 4.8	Mesh of the model geometry for pre-heating step simulation	102
Figure 4.9	Geometry of the model for cooling step simulation	103
Figure 4.10	Comparison between numerical and experimental temperatures over time for three different locations inside the laminate in z- direction	104
Figure 4.11	Numerical temperature vs. time inside the concave mould	105
Figure 4.12	CAD of two halves of concave mould: cavity and punch	108
Figure 4.13	CAD of side lock	108
Figure 4.14	Concave mould assembly	109
Figure 4.15	Cost breakdown of concave mould.....	112

Figure 5.1	Design of concave part.....	116
Figure 5.2	CAD of U-shape part	118
Figure 5.3	CAD of hollow square part.....	120
Figure 5.4	CAD of Z-shape part.....	122
Figure 5.5	CAD of flat plate.....	124
Figure 5.6	Heating energy of five UD parts in function of part volume: concave part, hollow square part, U-shape part, Z-shape part, Flat plate.....	127
Figure 5.7	Heating energy costs of five UD parts in function of part volume: concave part, hollow square part, U-shape part, Z-shape part, Flat plate.....	128
Figure 5.8	Estimated moulds costs vs. projected area of concave mould, hollow square mould, flat mould and Z-shape mould	131
Figure 5.9	Moulds costs for concave mould, hollow square mould, flat mould and Z-shape mould scaling with complexity level of the mould	132
Figure 6.1	Autoclave equipment	136
Figure 6.2	Design of flat mould for autoclave process with support structure	142
Figure 6.3	Flat mould component	151
Figure 6.4	L-shape mould component.....	152
Figure 6.5	T-shape mould assembly with support structure	152
Figure 6.6	Design of the triangular flat plate	158
Figure 6.7	Design of L-shape mould components: A) L-shape cavity B) L-shape rib cavity	164
Figure 6.8	Design of L-shape mould assembly with support structure.....	164
Figure 6.9	Cost breakdown of the thermoset flat plate	172
Figure 6.10	Cost breakdown of the thermoset T-shape part	174
Figure 6.11	Cost breakdown of the thermoset L-bracket part.....	176
Figure 7.1	Cost breakdown of ROS flat plate	191

Figure 7.2	Cost breakdown of (ROS) T-shape part.....	193
Figure 7.3	Cost breakdown of (ROS) L-bracket part.....	195
Figure 7.4	Cost breakdown of (UD) concave part	197
Figure 7.5	Cost breakdown of (UD) hollow square part.....	198
Figure 7.6	Cost breakdown of (UD) U-shape part	200
Figure 7.7	Cost breakdown of (UD) Z-shape part.....	201
Figure 7.8	Cost breakdown of (UD) flat plate.....	203

LIST OF ABBREVIATIONS

ACCEM	Advanced Composite Cost Estimating Manual
AMTC	Aerospace Manufacturing Technology Center
ATCAS	Advanced Technology Composite Aircraft Structure
BHTC	Bell Helicopter Textron Canada
CAD	Computer Aided Design
CD	Clamping Devices
CDF	Cold Diaphragm Forming
CERs	Cost Estimation Relationships
CNC	Computerized Numerical Control
CRC-ACS	Cooperative Research Centre for Advanced Composite Structures
DFA	Design for assembly
DFM	Design for manufacturing
DFMA	Design for manufacturing and assembly
ETS	École de Technologies Supérieure
FEM	Finite Element Method
MIT	Massachusetts Institute of Technology
MPCM	Manufacturing Process Cost Models
NASA	National Aeronautics and Space Administration
PID	Proportional Integral Derivative
QFs	Quality Functions
RC	Repeat Count
ROS	Randomly Oriented Strands
RPA	Radiators Panels Area
RPN	Radiators Panels Number
RTM	Resin Transfer Molding Process
S	Screws
SHCS	Socket Head Cap Screw
SMC	Sheet Moulding Compound
UD	Unidirectional

XXXII

UQTR Université du Québec à Trois Rivières

US United States

VARTM Vacuum Assisted Resin Transfer Molding Process

LIST OF SYMBOLS AND UNITS OF MEASUREMENTS

Symbol	Unit	Description
A	mm	Area of pocket
C.A	m ²	Cartridges areas
D	mm	Diameter of drilled holes
D ₁	mm	Depth of material removed
D ₂	mm	Depth of material removed from the pocket
H.P.D	w/m ²	Heating power density to reach 380°C
H.P ₁	w	Heating power to reach 361°C
H.P ₂	w	Heating power to reach 375°C
H.P ₃	w	Heating power to reach 381°C
H.P ₄	w	Heating power to reach 394°C
H.P'.D	w/m ²	Heating power density to maintain 380 °C
H.P' ₁	w	Heating power to reach 420°C
H.P' ₂	w	Heating power to maintain 420°C
H.P' ₁ .D	w/m ²	Heating power density to reach 420°C
H.P' ₂ .D	w/m ²	Heating power density to maintain 420 °C
H.T	min	Heating time to reach 380°C
H.T ₁	min	Heating time to reach 361°C
H.T ₂	min	Heating time to reach 375°C
H.T ₃	min	Heating time to reach 381°C
H.T'	min	Heating time to reach 394°C
H.T' ₁	s	Heating time to reach 420°C
H.T' ₂	s	Heating time to maintain 420°C
hr	-	Hour
L ₁	mm	Length of the surface to be milled
L ₂	mm	Length of drilled holes
min	-	Minute
N.H.C	-	Number of heating cartridges
N.R.P	mm	Number of Radiator Panels

P'_1	w	Punch heating power to reach 360 °C
P'_2	w	Punch heating power to maintain 360 °C
P'_3	w	Cavity heating power to reach 360 °C
P'_4	w	Cavity heating power to maintain 360°C
R.P.A	mm	Radiator Panel Area
s	-	Second
t'_1	s	Punch heating time to reach 360°C
t'_2	s	Punch heating time to maintain 360°C
t'_3	s	Cavity heating time to reach 360°C
t'_4	s	Cavity heating time to maintain 360°C
V_L	10^4 mm^3	Volume of the laminate`
V_m	-	Volume of the mould
V_p	10^4 mm^3	Volume of the part`
W	mm	Width of the surface to be milled

INTRODUCTION

During the last decades, the historical data have shown that the advanced composite materials knew drastically increasing uses in the aerospace industry, which has been becoming a promising candidate material to replace conventional metallic materials for several future applications (Eaglesham, 1998) due to many advantages, among them, their high performance such as specific mechanical properties in terms of rigidity and their significant material savings in terms of weight. However, the implementation of more composite structures requires high costs, especially for geometrical complex structures such as frames or ribs, complex layups with thickness and orientation variations by an autoclave process having a long cure cycle, thus, constitutes an economical barrier against their continued increasing uses. The design for manufacture and assembly (DFMA) approach recommends that cost estimation be integrated into the design process, right at the start of product development, in order to ensure competitiveness and economic viability. In other words, it is necessary to develop models for estimating costs, which will guide designers and engineering teams to make the right decisions early in the design of a new part (Curran et al., 2005; Kim et al., 2001). In fact, it has been demonstrated that approximately 70% of a product cost is fixed at the design stage (Boothroyd et al., 1994).

In the case of a newly developed process, cost analysis models based on the characteristics of the manufacturing process are preferred over models considering actual production activities due to a lack of data for parts which have not yet been made. In fact, there are several models were proposed to estimate the manufacturing costs of composites materials but they were limited to some specific process and required experimental studies which need to be improved for accurate cost estimation (Ye, Zhang et Qi, 2009). Currently, several process based costing commercial softwares are available for metals, but there is almost nothing for composite materials and more particularly for compression molding processes of thermoplastic composites. The technique using size and complexity scaling laws in estimating process time suggested by Gutowski et al. (1994) and Haffner et Gutowski (1999), which

depends on the process parameters and the geometry of the part, are quite realistic for resin thermoset composite parts (Barlow et al., 2002; Kaufmann, Zenkert et Mattei, 2008; Ye, Zhang et Qi, 2009). However, while their calculation of production time was complex, the heating energy estimation, on the contrary, was based on basic heat transfer theory, where only the mass of the part was considered. Although there are works covering the estimation and comparison of the manufacturing costs of certain automotive thermoset and thermoplastic injection moulded parts, which show an increase in the costs of thermoplastic parts due to an increase in tool cycle time (Verrey et al., 2006), there is almost nothing providing cost analysis data for thermoplastic composite parts manufactured by compression moulding.

In order to meet the aerospace markets needs with high production volume of complex structures parts in the near future years, it is needed to develop new fast and low-cost manufacturing technology for manufacturing different category of complex and lightweight 3D parts. The compression moulding process is considered as one commercial method having short cycle time and encompasses several different moulding technologies differentiated by the tooling, the pressure application and the material form used. A multidisciplinary research team comprised of many universities was formed to carry out a project aimed at developing compression moulded processes for advanced thermoplastic composites used to produce structural aerospace parts. Moreover, the industrial partners need to know the cost of the composites parts compared to metallic ones,

Scope and research objectives

In order to assure the cost effectiveness of the newly developed thermoplastic composite parts, it is necessary to be able to assess the cost of the manufacturing process. This study is part of the research project presented earlier, aims at developing a cost modeling methodology for estimating the costs of new parts that have not been yet based on limited experiments done by other academic research partners using sizing scaling laws. Moreover to investigate the effect of the process on the costs, on one hand two types of prepreg material were involved in this study: ROS and UD which were processed by two different

compression moulding processes. On the other hand, the cost comparison between identical parts made by thermoset autoclave process and thermoplastic compression moulding process was also studied.

Methodology of the research

For calculating the manufacturing costs of the parts the proposed cost model used Microsoft Excel software was developed in house. The manufacturing costs of the parts include different cost elements and are explicitly given by equation (0.1) (Haffner, 2002).

$$C_{Total} = C_{Material} + C_{Labour} + C_{Energy} + C_{Machinery} + C_{Tooling} + C_{Building} + C_{Workingcapital} + Overheads \quad (0.1)$$

In the Excel spreadsheet, different cost equations were integrated and academic and industrial data were imputed, which represent the cost drivers in the cost model. There are data related to the manufacturing process such the material characteristics, the part geometry and the cycle time. The labour time includes the cycle time of the compression moulding process and the time of the other activities such as preparation and cut of material, demoulding, storage, etc. The reference part could be an experimental part or a virtual part. For an experimental part, the mould costs and the energy consumption were estimated respectively by DFMA and COMSOL multiphysics softwares. These data were imputed in the Excel program for calculating the cost of the part. For a virtual part, by changing the dimension of the part and by keeping the same cycle time, the mould costs and the energy consumption were estimated for iteration n times scaling with the projected mould area and the volume of the part respectively thereby establishing the mould costs sizing scaling laws and energy costs sizing scaling laws. For a new part having a given dimension, the mould costs and the energy costs were calculated by applying the mould costs sizing scaling laws and energy sizing scaling laws already integrated in the Excel program. After imputing the cost data, the Excel program calculates the new costs of different elements and makes the summation to calculate finally the new cost of the part. Figure 0.1 shows the cost modeling concept.

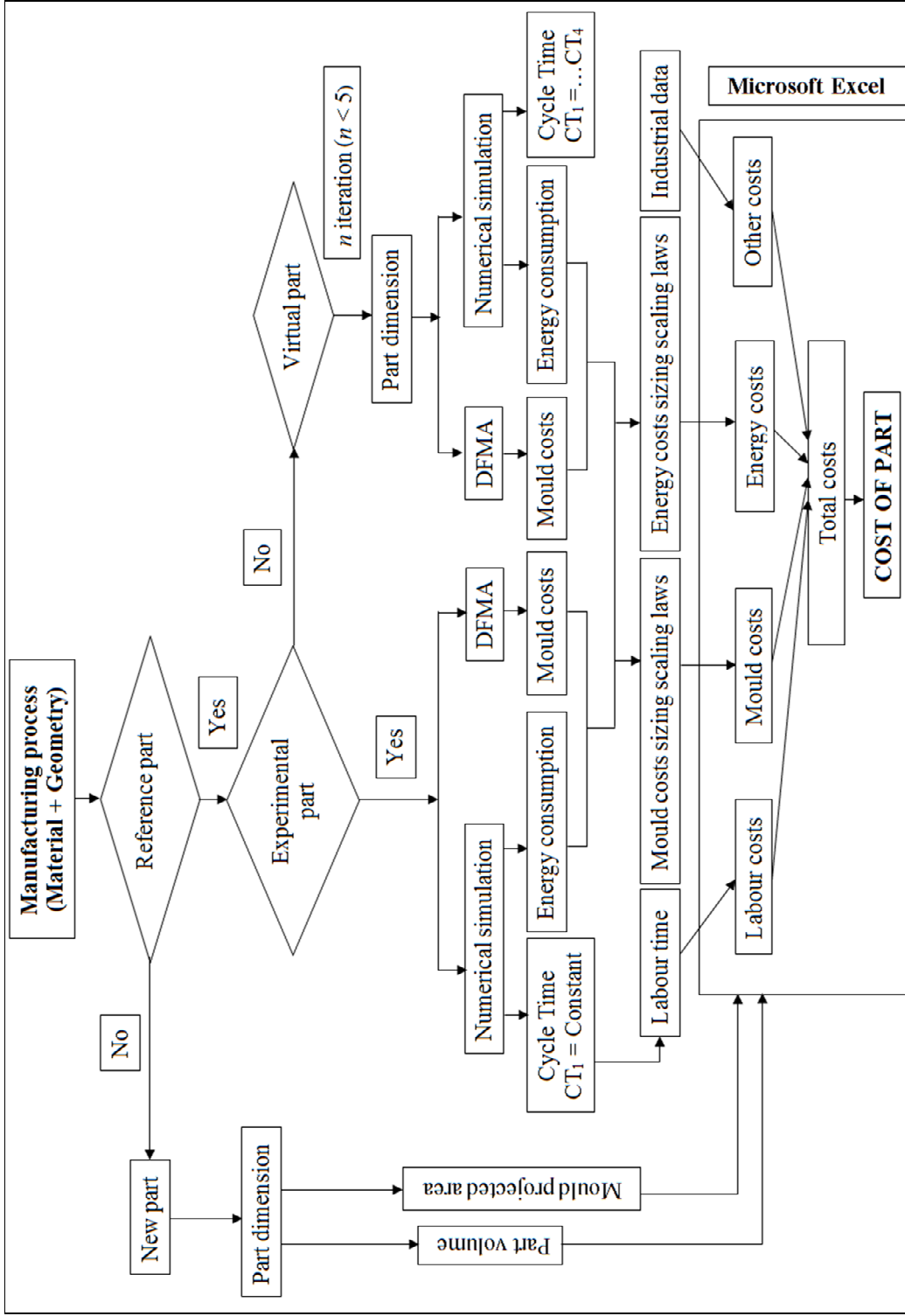


Figure 0.1 Cost modeling concept

Structure of the thesis

This Ph.D thesis consists of seven chapters. The introduction outlines the problem to be addressed, the context, the objectives and the proposed methodology of the research study.

Chapter 1 presents a literature review on composite materials, composite manufacturing processes, cost modeling concepts, general manufacturing cost modeling for composites materials and limitations of existing models.

In chapter 2, the estimations of tooling and energy costs for compression process moulded randomly oriented strands prepreg thermoplastics experimental parts are presented.

Chapter 3 presents the tooling and energy costs complexity sizing and complexity scaling laws for compression process moulded randomly oriented strands prepreg thermoplastics parts.

In chapter 4, the estimations of tooling and energy costs for compression process moulded unidirectional continuous fiber prepreg thermoplastics experimental parts are presented.

Chapter 5 presents the tooling and energy costs complexity sizing and complexity scaling laws for compression process moulded unidirectional continuous prepreg thermoplastics parts.

Chapter 6 presents the costs estimation of thermoset composites parts manufactured by autoclave process and focuses particularly on the estimation of manufacturing times and on the estimation of tooling costs for making the parts.

The chapter 7 presents the general cost model including equations necessary to calculate different cost elements and the total cost per part (Haffner, 2002), the cost analysis for compression process moulded thermoplastic composite parts (ROS parts and UD parts). Cost

comparisons between thermosets composite parts made by autoclave process and thermoplastic composite parts made by compression moulding process were also presented.

Finally, a general conclusion outlines the important results obtained during this study and some recommendations will be suggested for future works.

CHAPTER 1

LITERATURE REVIEW

1.1 Introduction

This chapter is devoted to the literature review on the DFMA concept, composite materials, composite fabrication processes, cost modeling concepts, previous works on manufacturing cost modeling for composites materials including the cost modeling of thermoplastic composite compression moulding and finally on limitations of existing cost models.

1.2 Design for manufacturing and assembly (DFMA) overview

Design for manufacturing and assembly (DFMA) is a methodical approach which consists to analyse the design of a new or existent product in order to reduce its cost and improve its quality. It includes two methodologies applied together in a given process, DFM and DFA. DFM stands for design for manufacturing and DFA stands for design for assembly. DFMA aims to facilitate the manufacturing and assembly of different parts, forming a final product in order to estimate its cost at early design stage through reducing part count and assembly time or changing the geometry and the material of the part.

The DFA approach was developed by Geoffrey Boothroyd, supported by National Science Foundation (NSF) grant at the University of Massachusetts in the mid-1970s. This method can help designers to design parts that would be handled and assembled automatically (Boothroyd, 1974). In early 1980s, Geoffrey Boothroyd et al. developed a DFMA software version which was used by various industrial sectors all over the world particularly U.S industry and presented important manufacturing cost and time savings (Dewhurst et Boothroyd, 1988).

1.2.1 Composites materials

A composite material is defined as a combination of at least two constituents which occupy different phases to produce a material having different characteristics from those of the individual components. Generally, one component is a reinforcement which provides strength and rigidity for example a fibre, a particle or a whisker (Ma, 2011), whereas the other component is a matrix which acts as a bonding agent (Haffner, 2002) for example a polymer, a metal or a ceramic. The composite materials studied in this present research are fibre reinforced polymers by considering a resin based on a polymer as the matrix component.

1.2.2 Matrices

The important functions of the matrix are not only to bind the reinforcement fibres together but it distributes loads uniformly into the whole composite material and protects the fibres against the external damages such as corrosion and abrasion. Among the matrices of the advanced composites commonly used, there are polymer based matrices which can be divided into two main categories, thermoset and thermoplastic resins. Table 1.1 presents the common matrices properties. The thermoset resins are broadly the most used in the aerospace industry due to their high strength-to-weight ratios (Marina, 2011), easy processing and better fibre wetting, but they are often brittle. They cure irreversibly through chemical reaction and heated generally above 200°C which means that they cannot be recycled since they cannot be melted and reshaped after curing. Most popular thermoset composite materials are epoxy, polyester, vinylester.

On the contrary, the thermoplastic resins have the potential to be reshaped thermally by heating and also they can be solidified upon cooling and recycled at the end of the lifespan. It is easy to repair and join parts due to their good welding character. Their processing is difficult due to high melting temperatures and high viscosities, and application of high temperature and pressure is required to achieve acceptable levels of consolidation and crystallization with short cycle times thereby reduce significantly the manufacturing costs

comparatively to thermosets which are expensive. Thermoplastic materials have higher toughness, impact strength and service temperatures than thermoset materials (Marina, 2011). Most popular thermoplastic composite materials are polyamide (PA), Polyetheretherketone (PEEK), and Polyethylene (PE). The thermoplastic composite materials can be processed by different forming methods such as compression moulding, injection moulding and automated tow placement.

Table 1.1 Matrices typical properties
Adapted from Haffner (2002, p.40)

Resin	Density	Strength	Modulus	Strain	Price
Unit	[Kg/m³]	[MPa]	[MPa]	[%]	[\$/kg]
Thermosets					
Epoxy	1190.23	6.896	3.448	7	3.74 - 4.41
Polyester	1107.19	6.207	2.758	4.5	3.52 - 4.63
Vinylester	1107.19	5.517	2.069	3	3.74-4.85
Thermoplastics					
PA	1494.71	102.069	13.793	2.1	66.14-88.18
PEEK	1300.95	102.758	5.517	1.6	88.18-110.23
PE	941.11	24.827	13.793	2.1	1.32-1.76

1.2.3 Reinforcements

As mentioned before the reinforcements used in this research study are the fibres since they are the most regularly employed forms of reinforcing material (Ma, 2011). Commonly the fibres are categorized on various forms depending on the fibres placement in different spatial directions according to the particular application such as linear, superficial and multidimensional geometries. There are three main types of fibres: continuous fibres, discontinuous fibres and hybrids fibres. The continuous fibres include unidirectional fibres (UD) in tape form impregnated with the polymer, fibres fabrics such as woven, braided and knitted. The continuous fibres have naturally preferred orientations. Although (UD)

continuous fibres performs are almost characterised by their high mechanical properties, their forming is limited to simple geometrically parts. The discontinuous fibres were extensively used to made high volume of structural components due to their low manufacturing costs and they present poor mechanical properties .They include aligned fibres, aligned chopped strips, randomly oriented fibres and randomly oriented strands. The hybrids fibres are made by the mixture of discontinuous fibres and continuous fibres in order to manufacture complex parts for example MultiMate (Syncoglas, Belgium) which is composed of a layer of glass weft knit fabric sandwiched between two layers of random glass mat(Marina, 2011). Table 1.2 illustrates the typical fibres properties.

Table 1.2 Typical fibres properties
Adapted from Haffner (2002,p.35)

Fibers	Density	Strength	Modulus	Strain	Price
Unit	[Kg/m³]	[MPa]	[MPa]	[%]	[\$/kg]
Glass					
E- glass	2601.91	2999.21	68.94	5	1.76-2.2
C- glass	2491.19	3302.58	68.94	5	1.76-2.2
S2- glass	2491.19	998.96	82.74	5.3	13.22-17.63
Carbon					
Carbon HS	1799.19	3599.06	220.63	1.6	44.09-66.14
Carbon IM	1799.19	5302.06	303.37	1.8	66.14-88.18
Carbon HM	1799.19	3502.53	379.21	0.4	99.21-198.41
Carbon UHM	1992.95	1999.48	441.26	0.8	242.51-352.74
Aramid					
Aramid LM	1494.71	3599.06	62.05	3.6	44.09
Aramid HM	1494.71	3102.64	117.21	2.4	55.11
Aramid UHM	1494.71	3399.11	179.26	1.3	66.14

Several studies were realised to produce high performance fibres with lower costs for example carbon fibre whose price tends to decrease over time to a value of 5\$/lb. This is due to strong concurrence of important carbon fibres producing countries (Gutowski, 1997).

1.2.4 Composite material forms

As mentioned before, there are several fibre-reinforced composite material forms that are distinguished by the fibres geometry for making high performance components such as:

- Woven composites (woven fabrics, 3Dimension woven, rovings);
- Prepreg tape composites;
- Laminates;
- Sandwich composites.

The decisive selection of material is important in the estimation of final cost of a product especially at the beginning of the design work. This selection depends on the following criteria (Haffner, 2002):

- The mechanical properties of the matrix and the fibre;
- Materials and manufacturing process costs;
- Environmental and health effects.

The glass, carbon and aramid fibres can be used in every manufacturing process but the thermoset and thermoplastic matrix depend on the process selection criteria.

1.3 Composite fabrication processes

The final composite part do not depend only on selecting the matrix, the reinforcement materials but also on selecting the appropriate process and its operating conditions such as equipment and tooling investment costs, production volume, in order to assure the

compatibility between the process and the material by considering the design and the geometry of the part such as shape, surface finish and specified tolerance.

Composite materials can be processed by different manufacturing methods such as forming process (compression moulding, injection moulding, diaphragm forming,...), lay up(hand lay-up, automated tow placement, filament winding,...), impregnation/wetting (pultrusion, resin transfer moulding), curing processes (vacuum bagging, autoclave,..) machining and assembly, without including inspection and quality control steps in these processes. Comparative studies of different long fibre reinforced thermosets composites manufacturing processes showed that the manual processes which were adapted to little production volume according to increasing quality and cost levels are hand lay up or contact moulding, infusion moulding and prepreg moulding whereas some automated processes are costly due to important machinery investment costs and long curing cycle time for example autoclave cure and pultrusion processes.

1.3.1 Autoclave cure process

Commonly, the Autoclave process is a method used for curing prepreg thermoset composites. After stacking prepreg layers on the mould and sealing them with the vacuum bag, the autoclave cure occurs inside the autoclave equipment mechanically and chemically by involving two main factors: Heat and pressure. Mechanically, under the pressure the vacuum is created by removing the trapped air for consolidating the laminate. Chemically, the applied heat creates crosslinks between chains of the polymer and consequently the resin solidifies (Berenberg, 2003; Cauberghs, 2011).

1.3.2 Compression moulding process

The compression moulding process is regularly used for forming thermoplastic composites parts with different geometric forms, since equipment is industrially available in a wide variety of sizes, economical and easy to install. Moreover, the cycle time is relatively short

and assures a better tolerance of the part thickness. Generally, the compression moulding process can be divided into two main steps: heating and pressurizing steps for a definite period of time. In fact, the material placed between two halves mould flows due to application of pressure and heat and acquires the shape of the mould cavity with high dimensional accuracy depending on the mould design, the part is solidified under cooling and is removed after opening of the mould. The matched die was designed in order to get more homogenous pressure distribution and adjust the dimensional tolerance of the part.

1.4 Cost modeling concepts

There are several costs estimation concepts used in industry depending on the context and purpose of estimating costs. The first three models related to the lifecycle of product while the last three models are based on accounting methods, activity based costing, process-based cost models.

1.4.1 Analogous estimation model

The analogous estimation model is based on the comparison between a new project having limited data and any similar project previously completed by an organisation whose estimated cost is available and accurate in such a way to have a reasonable correlation and resemblance level between them using the expert judgment to determine the cost of current project. The analogous method is relatively fast and inexpensive but it is not as accurate as other estimating methods.

1.4.2 Parametric estimation model

A parametric estimating model is a mathematical representation of cost relationships that provide a logical and predictable correlation between the physical characteristics or parameters of a project defined as independent variables and the estimated cost defined as dependent variable. The independent variables are known as cost drivers, and typically may

be physical or operational characteristics associated with the project to be estimated. This model can produce higher levels of accuracy depending on the sophistication and the underlying data built into the model. The parametric cost models are mostly developed at many companies having access to large amount of data (Dysert, 2008).

1.4.3 Analytic estimation model

The analytical estimation model uses accounting information system data of the company. It is the most classical and the most widespread among the all cost estimation methods. As highlighted by El Asli (2008), this model is mainly used during the mass production phase because it needs more detailed information on the product and the manufacturing process and these information are not always available in the design stage.

1.4.4 Accounting methods

The Accounting method is a process which begins with collecting, analyzing, calculating financial income and costs by using cost equations and ends with the preparation of periodical reports for reviewing and controlling cost in order to help managers make decisions. As this method is based on the net present value and on necessary permanent funds for exploitation, calculation of complex assets is difficult and may result in overestimation or underestimation.

1.4.5 Activity based costing

The activity based costing is cost estimation method that based on the activities which cause the indirect cost of the product by identifying the cost drivers and assigning costs for each activity, then making summation of all these activities costs. The weakness of the activity costing method is that it often uses previous and historical data which require substantial resources to integrate them. Moreover, it is expensive and time-consuming.

1.4.6 Process-based cost models

The process-based cost model helps designers make the decision about relevant technologies before beginning the project. This model involves the process and the material to form the part and relates the part design to the processing parameters such as cycle time, machinery capacity, tooling size. It consists to define the purpose of the cost model, to determine the appropriate cost elements which give the final cost of the part, to describe the different steps of the process during which the cost elements are identified with the inputs and outputs, then to generate relationships between the cost parameters and the total manufacturing costs by evaluating eventual risks due to any variation of some inputs integrated in new projects, thus may result in uncertain estimated costs.

The process-based cost models are rather used and adopted than the other cost estimation models for applications related to development of high performance structures because they use mathematical equations describing the process mapping and manufacturing conditions and measure its performance by determining the parameters influencing.

The major drawback of process-based cost models is high investments in time and cost to develop them. Furthermore, these models require a good knowledge in process engineering and in evaluating manufactured parts.

1.5 Manufacturing cost modeling for composites materials

During the periods of developing the composite manufacturing technologies, many research works were realized for elaborating different cost models for composites materials. Among the common Manufacturing Process Cost Models (MPCM) mentioned in the literature are:

- The manufacturing Cost Model for Composites (Ramkumar, Vastava et Saha, 1991), the joint MIT and Boeing developed Composite Optimization Software for Transport Aircraft Design Evaluation (Mabson et al., 1994);
- ACCEM model which was developed in Advanced Composite Cost Estimating Manual by Northrop Corporation for the US air force (LeBlanc et al., 1976). This model consists to develop a computerized methodology for estimating recurring costs. The computerized estimating program describes the manufacturing process flow in different steps in such way to calculate the production time for each operation by deriving equations of the production time in function of processing parameters such as complexity of the part using the power law, thereby the cost of each step can be calculated by multiplying the production time by the cost rate. The ACCEM model is accepted generally by industry. Depending on the data used for the regression, these models are quite accurate in general but not able to account for any variations on the part design such as size and complexity or process improvements.

1.5.1 ACCEM Power law model

The ACCEM power law model developed by the US Air Force and Northrop Corporation is accepted generally by industry. In the case of existing historical production data, the power law model can be used to calculate the processing time t using the following equations:

$$t = A.x^r \Leftrightarrow x = \left(\frac{t}{A}\right)^{\frac{1}{r}} \quad (1.1)$$

$$\log(t) = \log(A.x^r) \Leftrightarrow \log(t) = \log(A) + r \log(x) \quad (1.2)$$

Where x is the part size, A and r are defined using log function.

1.5.2 1st order model

First order model developed by Gutowski et al. (1994) is a theoretical cost model based on the physics of the production process for estimating the manufacturing process time of advanced composites parts.

Gutowski and his disciples: (Haffner, 2002; Neoh, 1995) proposed a method to estimate the process time of each processing step using hyperbolic model depending on two process parameters, the velocity constant v_0 and a time constant τ_0 , where x is the extensive variable in the process (length, area or volume). Finally the total process time is given by summing of all the process step times. Neglecting the effects of the 2nd order oscillation on the process time the step response of a 1st order dynamic system can be written as:

$$v = -a \cdot \tau_0 \Rightarrow v = -\frac{dv}{dt} \cdot \tau_0 \Leftrightarrow \frac{dv}{v} = -\frac{dt}{\tau_0} \Rightarrow \frac{v}{v_0} = e^{-t/\tau_0} \quad (1.3)$$

Where v is the velocity, a is the acceleration.

Considering the boundary conditions, the velocity becomes:

$$\Rightarrow v = v_0 \cdot \left(1 - e^{-t/\tau_0}\right) \quad (1.4)$$

This model requires less expertise and historical data than the previous statistical methods and is adapted easily to the process changing conditions and they must meet five boundaries conditions while using process scaling laws. As the process time scales with size and complexity of the design part using regression analysis, the first order model shows certain correlations with ACCEM model (Haffner et Gutowski, 1999). Although the theoretical cost model was developed and applied widely, it is limited to estimate the costs of some common thermoset processes such as Hand Layup, Resin transfer Molding, Automated Tow placement, Pultrusion, Double Diaphragm Forming and Assembly.

1.5.3 Hyperbolic model

The hyperbolic model was developed by G. Mabson from Boeing Commercial Airplane Group as an approximation result of 1st order model (Haffner, 2002) in order to find the solution of the equation (1.4). By applying the integration operations and using the size scaling form, the process time t can be obtained under the form:

$$\Rightarrow t = \tau_0 \cdot \sqrt{\left(\frac{L}{v_0 \cdot \tau_0} + 1\right)^2 - 1} \quad (1.5)$$

Where L is the size of part for a given process.

All these models used the same methodology of analyzing cost drivers in the manufacturing process level in such a way to capture all the costs associated with a given process, including materials, labor, overhead costs, recurring and nonrecurring costs of production. These models provide more accurate cost estimates for manufacturing composites, but require detailed knowledge of processing time.

The first order model was applied by other researchers to develop others cost estimation models such as:

- Web based cost estimation models used in Massachusetts Institute of Technology (MIT) which is applicable to estimate the time and the cost of different processes, help designers make process decision and select the tactics of cost reductions;
- Process Cost Analysis Database (PCAD) was used in NASA/Boeing ATCAS initiative for modelling the manufacturing processes time and assembly costs (Neoh, Gutowski et Dillon, 1995);

- Cost estimation model adopted by (Ye, Zhang et Qi, 2009) who proposed an optimization method to estimate the processing time of manufacturing composites waved beam using autoclave cure by modifying the model parameters;
- Cost estimation model used by (Barlow et al., 2002) for modelling the labour cost of aircraft composite parts made by VARTM and RTM manufacturing process.

There are intelligent cost estimation models for composite manufacturing such as:

- Design decision support system developed by (Eaglesham, 1998) which provides designers with the activity cost data by searching and arranging existing information for making better decision about their design;
- knowledge-based system developed by (Shehab et Abdalla, 2002) for cost modelling of product manufactured by machining and injection moulding process which uses an intelligent technique able to select material and process based on the CAD softwares and on the manufacturing parameters and to estimate the production and assembly cost using the life cycle of the product.

1.5.4 Cost optimization models for composites materials

(Pantelakis et al., 2009) optimized the manufacturing processes of composite material components regarding to product's quality and cost . Their concept was applied for the case of thermoplastic composite helicopter canopies manufactured by 'Cold' Diaphragm Forming (CDF) process. The adopted methodology was based on the consideration of the process thermal cycle in order to decide the component's quality and cost. Material dependent Quality Functions (QFs) and process dependent Cost Estimation Relationships (CERs) were determined according to quality and cost sensitivity analysis. QFs and CERs were exploited to derive the optimal thermal cycle. The process thermal cycle is numerically simulated to allow for its virtual application on the material. A new software tool is developed to execute the optimization procedure. CDF heating system configuration along with the optimal thermal cycle for producing helicopter canopies were obtained.

(Verrey et al., 2006) proposed a parametric technical cost model for manufacturing cost comparison of carbon fibre reinforced thermoplastic and thermoset plant automotive floor pans made by two resin transfer moulding processes (RTM) at production volumes of 12.5k and 60k parts per year by considering representative geometry features. The cost comparisons showed that a cost increase of 35% for thermoplastic resin against thermoset system due to 22% increase in thermoplastic RTM thermal cycle. This increase is due to two necessary thermoplastic RTM moulds/press units versus one thermoset RTM mould/press unit. Moreover, the cost optimization analysis adopting pertinent plant strategies showed important cost savings due to the reduction of non-crimp fabric carbon rejects.

1.5.5 Cost modeling of thermoplastic composite compression moulding

(Åkermo et Åström, 2000) developed a cost model for estimating the costs of moulding of three different thermoplastic composite components and they compared them to those of compression moulding of a thermoset sheet moulding compound (SMC) and stamping of sheet metal. A Microsoft Excel program has been developed to calculate the part cost using the developed model, in which the manufacturing costs included of equipment cost, tooling cost, labor cost, and material cost. The results showed that steel components are the most cost-competitive for long annual production series (more than 100,000 components), the profitability threshold depends on the size and geometrical complexity of components and that sheet metal stamping component cost was dominated by equipment costs. On the contrary, thermoplastic components have an economic advantage in intermediate production series and the raw materials cost dominates (excess of 100,000 components per year) as part size increased.

For optimization and reduction of composites compression moulding process cycle time and then the reduction of their costs(Abrams et Castro, 2003) developed a relevant process model for Sheet Moulding Compound (SMC) composite automotive parts manufactured by compression moulding. This model was based on the measurement of the SMC material parameters required to predict molding forces of truck body panels in order to reduce the

process cycle time (using Newtonian mechanical laws). The moulding force comparison between the experimental values and the predicted results showed the validity of the model.

1.5.6 Summary and limitations of existing models

From the literature review presented in this section, there are many research studies were conducted by several authors on manufacturing cost modelling and analysis of the composites in different industrial domains for accurate cost estimation or for cost optimization. In fact, the majority of these studies focused on some specific processes of thermoset composite production and a little research work was done to develop cost estimation models for thermoplastic composite compression moulding process in particular in aerospace industry. As compression molding process of thermoplastic composites is relatively new and the cost data are almost nonexistent thereby the cost models presented are based on rudimentary assumptions.

For example, according to (Åkermo et Åström, 2000) the obtained results on cost analysis of carbon/thermoplastic composite parts manufactured by compression molding process, it is difficult to really get relevant data imputed into the cost estimate model (several important factors may be neglected in the modeling cost program such as machining and trimming, inspection, size and complexity, study of the microstructure of parts to be manufactured and the parameters of the process for optimal cost reduction, overheads, cutting tool, etc..).

For the tooling, they assumed that the mould costs depends on several parameters such as size and complexity of the manufactured part, heating and cooling, moulding pressure and production volume. The modelling of mould costs was based on approximations and assumptions using an interpolation or an extrapolation of some provided data for simple geometry components and on complexity levels for complex geometry components by scaling with mould size. Consequently, for simple geometries, the mould costs estimation is not precise since it did not use a validating method of assumed values. For complex geometries, the mould costs were approximated arbitrary in function of the mould size, thus

contradicting to the design complexity definition since the complex part is a part which has more bends exceeding 30 degrees and the part complexity depends on its shape and it is given by the type of curvatures according to the experimental study of CRC-ACS' industrial partners(Kumar et Kendall, 1999).

For equipment, the cost of the press was based on 8 years lifecycle assumptions whereas an industrial hydraulic press is still in use for more than 30 years; this leads to an equipment maintenance significant difference between assumption-based costs and the actual costs. The power cost for equipment category was estimated annually based on the amperage of the fuse such as the power cost is the quotient of fuse divided by 1200 Ampere multiplied by annual rate of 52k Euro/year. This power estimation is not accurate since it did not give the necessary power to be used for each equipment category.

The cost model developed by (Barlow et al., 2002)which was based on finite element method for estimating the manufacturing costs of an aerospace carbon fibre composite components using the advanced technologies is not able to calculate all the cost elements involved except the recurring labor and material costs.

The proposed cost model will be developed in this thesis in order to calculate different costs elements. The chapter 2 presents the study on the estimations of tooling and energy costs for compression process moulded randomly oriented strands prepreg thermoplastics

Experimental parts.

CHAPTER 2

TOOLING AND ENERGY COSTS ESTIMATION OF COMPRESSION PROCESS MOULDED RANDOMLY ORIENTED STRANDS THERMOPLASTIC EXPERIMENTAL PARTS

2.1 Introduction

The conducted study in this chapter is divided into two sections. The first section presents the methodology and the results of estimating energy costs for randomly oriented strands prepreg thermoplastic experimental parts manufactured by compression moulding process. The process energy includes heating energy and mechanical energy. It was demonstrated that the mechanical energy cost per part was very low and can be neglected (Cardonne, 2015). Thus, they can be integrated in investment costs calculation of the press. The second section presents the methodology and the results of estimating the tooling costs used for manufacturing these categories of parts.

2.2 Cycle time simulation and energy cost estimation for ROS parts

This section consists to simulate the cycle time and calculate the energy costs for three ROS parts forms such as flat plate, T-shape and L-bracket. The process cycle time includes the heating time and the cooling time. For heating step, the heating time included two periods: heating and dwelling. The heating time was simulated using the transient thermal analysis module of the commercial COMSOL Multiphysics® software by solving numerically heat transfer equation (2.1) based on the 3D finite elements method. It is about to determine the transient temperature distribution versus the heating time in the whole compression moulding system including the platens, the moulds and the ROS parts.

$$\rho_i C_{p_i} \frac{\partial T}{\partial t} = \nabla \cdot (k_i \nabla T) + Q_s \quad (2.1)$$

Where ρ_i , C_{p_i} and k_i are respectively the density, the specific heat capacity and the thermal conductivity of the considered materials ($i=1,2$: CF/PEEK , steel) and Q_s is the volume heat source.

During the processing cycle time two heat transfer modes were occurred: conductive and convective. In order to calculate the conduction heat transfer between the composite part, the platens and the mould. These components were considered as solids blocks in contact with no internal heat generation. It was assumed that the contact resistance effects were neglected at the interface between the solids (perfect contact). The time-dependent study was selected in order to assess the evolution of temperature in the ROS parts by steps of time. The boundary thermal conditions during the heating stage were as follows:

- The external convective heat transfer between the platens, the mould, and the air was occurred according to formula (2.2);

$$k_i \Delta T = h(T_{air} - T) \quad (2.2)$$

Where h is the heat transfer coefficient for natural convection, T_{air} is the air temperature assumed to be constant at 22°C.

- The initial value of temperature in the whole model depends on each case study;
- The necessary power density applied at the heating cartridges areas was adjusted using formula (2.3).

$$Power\ density * (T < 380 [degC]) + power\ density * (T > 380 [degC]) \quad (2.3)$$

In order to assure the uniformity of the temperature throughout the composite part, the desired temperature has to be maintained at 380°C for a given time. During the dwelling period the power density applied to the heating cartridges has to be reduced to an adequate value.

For cooling step, the boundary thermal conditions were : the initial value of temperature in The whole model was fixed to 380°C; the heat source was stopped. The speed and the temperature of the cooler were considered to be constant.

During the whole cycle the upper surface of higher platen and the lower surface of the bottom platen were insulated and the processing geometry model was meshed with 3D free tetrahedral elements, which can be adapted to different simulations. Each element has four nodes and can be generated automatically by default algorithm for solid modeling. The element size parameters should be controlled and adjusted in order to create the meshing of the geometry and run the model study. However, these changes can produce different mesh qualities. It was stated that minimum element quality greater than the value 0.1 is required to get good simulation results by refining the meshing. The heat transfer module of COMSOL Multiphysics software uses isoparametric nodal finite elements for linear approximation where parametric and local interpolations are the same. Each node has one degree of freedom which, is the temperature according the three axis (x, y, z). A typical tetrahedral element having four local nodes is schematized in Figure (2.1).

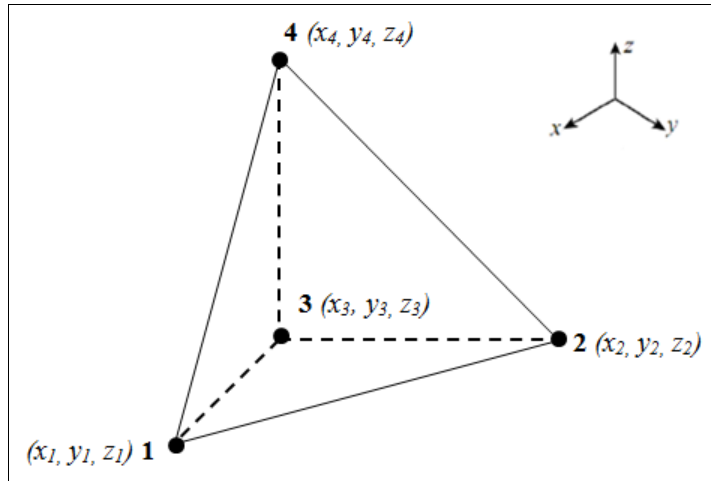


Figure 2.1 Typical tetrahedral element

The thermal power P can be given by equation (2.4).

$$P = \sum_{i=1}^2 \rho_i \cdot V_i \cdot C_{p_i} \cdot \Delta T / \Delta t \quad (2.4)$$

Where $\Delta T / \Delta t$ is the heating rate, V_i is the material volume. The other parameters have already been mentioned. The heating power was calculated by multiplying the power density to the number and the area of heating cartridges. From the simulated cycle time and using the formula (2.4) the heating power was deducted for each step of heating time and the temperature scale corresponding to different heating rates. The heating energy consumptions were calculated using the heating step simulation results by applying equation (2.5). The heating energy costs were calculated by applying equation (2.6) using the energy rate of 0.0457 (\$/kWh) according to 2015 Hydro-Quebec data.

$$\text{Total heating energy Consumption} = \sum_i^n P_i (\text{heating power}) \times t_i (\text{heating time}) \quad (2.5)$$

$$\text{Heating energy costs / part} = \text{Total energy Consumption} \times \text{Energy rate} \quad (2.6)$$

2.3 Material

The material used in this study is CF/PEEK with short carbon fibre unidirectional prepreg tape. The prepreg tape can be slit and chopped by manual or automatic cutter into strands with different sizes. The preparation of material is shown in Figure 2.2.

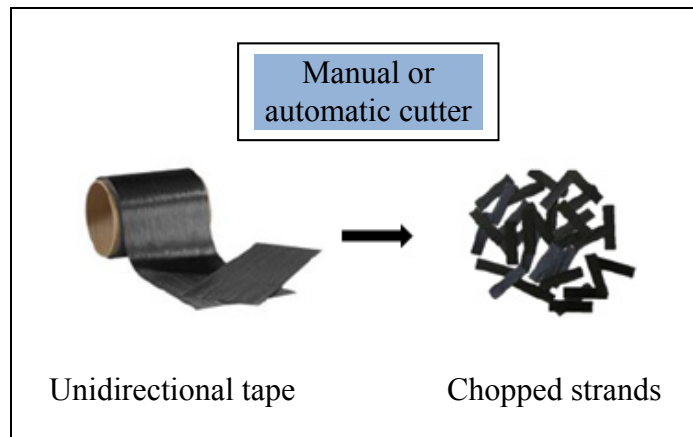


Figure 2.2 Preparation of material
Reproduced and adapted with the permission
of Leblanc et al. (2014b, p.2)

The studied parts were made of chopped strands which were distributed in such way to assure their random orientation in steel moulds (ROS). The thermal and physical proprieties of the steel material were obtained directly from the database of the COMSOL software. Table 2.1 presents the thermal and physical proprieties of carbon/PEEK.

Table 2.1 Physical and thermal properties of carbon/PEEK
Taken from Levy (2014)

Proprieties	Unit	Carbon/PEEK
Density	(kg/m ³)	1540
Specific heat	J.kg ⁻¹ .K ⁻¹	1320
Thermal conductivity	W.m ⁻¹ .K ⁻¹	0.75

2.4 Flat plate

2.4.1 Compression moulding process of flat plate

The studied part was a flat plate of 355.6 mm x 304.8 mm x 6 mm, made of long discontinuous fibre strands of 25.4 mm x 12.7 mm x 6 mm, that were slit manually or automatically from unidirectional prepreg tape of 304.8 mm wide and 61% volume fraction. The six step of the manufacturing cell of the flat plate included preparation and moulding phases are shown in Figure 2.3.

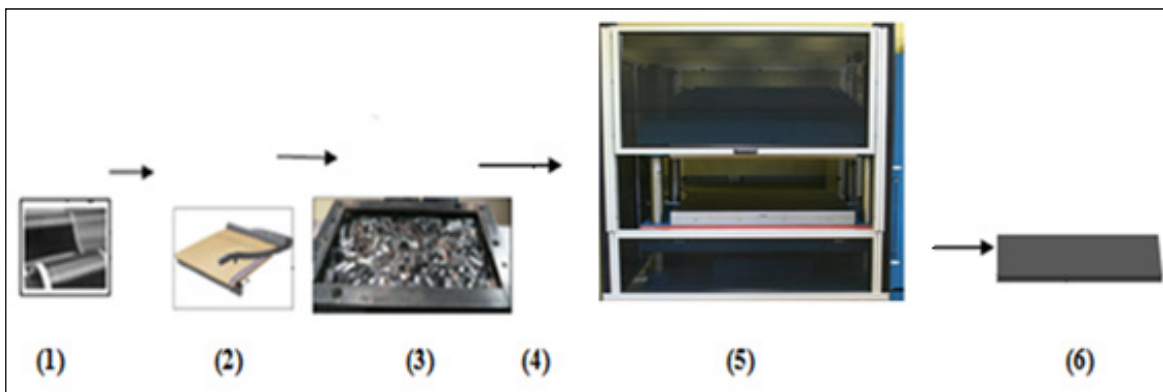


Figure 2.3 Manufacturing cell for flat plate: (1) placing material in the cutter, (2) cutting of material into strands (manual cutter), (3) distributing randomly of strands in the mould, (4) closing and transferring of the mould to the press, (5) heating of platens, compression moulding of flat plate and then cooling (6) demoulding

Reproduced and adapted with the permission
of Picher-Martel et Selezneva (2011) and Roy (2014)

The compression moulding cycle comprised heating and cooling steps while a constant pressure of 34 bars was applied to the mould during the whole cycle (Selezneva et al., 2012).

2.4.1.1 Heating step

After the placement of the material, the mould was closed and transferred to a Wabash 100 Tons hot press which had two steel square platens of 914.4 mm each side and of 85.73 mm

thickness. The 16 parallel heating cartridges integrated into each platen yielded a thermal power of 28 kW. The temperature of the platens was controlled par PID controller. Three thermocouples used to measure the temperature of the material during the cycle were inserted at three positions on the middle plan of the ROS flat plate through three slots inside the mould. They were connected to a wireless transmitter sending signals to a computer for data acquisition. The temperature of the composite flat plate was increased from ambient temperature up to 380°C (heating period), and then maintained for about 20 minutes (dwelling period) (Roy, 2014).

2.4.1.2 Cooling step

The heating system was stopped at the end of the heating step and the plate started to cool down from 380°C to around 50°C by cooling channels integrated inside the platens. Afterwards, the cooled plate was removed from the press(Roy, 2014; Selezneva et al., 2012).

2.4.2 Heat transfer processes

The conduction and convection heat transfer mechanisms which occurred between flat plate, the flat mould and the platens are presented in Figure 2.4.

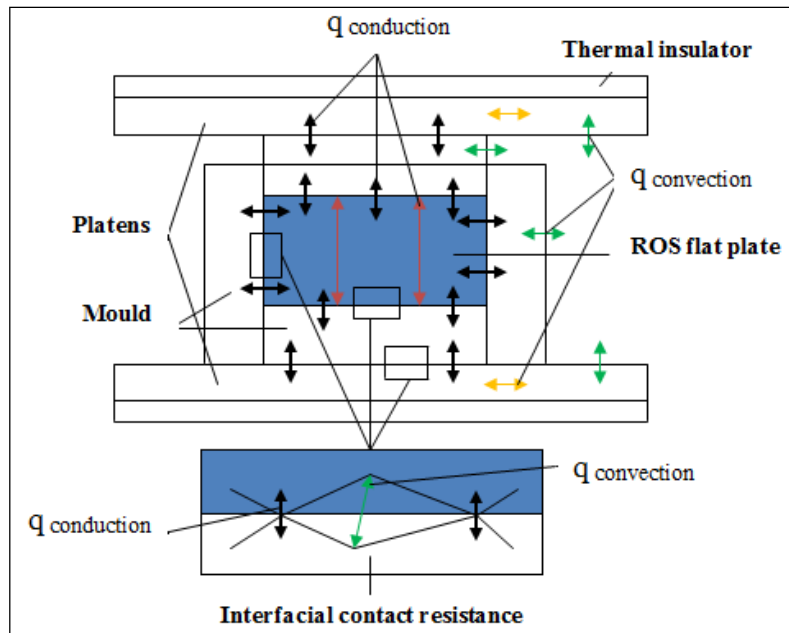


Figure 2.4 Contact heat transfer mechanisms

2.4.3 Numerical simulations

2.4.3.1 Heating time simulation

The heating time included two periods: heating and dwelling. The heating time was simulated using the transient thermal analysis module of the commercial COMSOL Multiphysics software by numerically solving the heat transfer equation (2.1) based on the 3D finite elements method. The model was composed of two press platens, a frame, two plate moulds and the ROS flat plate. These components were considered as solid blocks in contact. The model also included 16 cylindrical heating cartridges with a radius of 5 mm and 914.4 mm long inserted into each platen. The heating cartridges were symmetric with respect to the ROS flat plate. Figure 2.5 shows the geometry of the model for the simulation of the heating process.

The time-dependent study was selected in order to assess the evolution of the temperature in the ROS flat plate by time steps. The time to heat to 380 °C was defined, ranging from 0 to

7260 s, with 5 s steps. The following boundary thermal conditions were present at the heating stage: the initial air temperature value was set to 20 °C; the initial temperature value in the whole model was set to 22 °C, and the required power density needing to be applied at the heating cartridge areas was adjusted using formula (2.3).

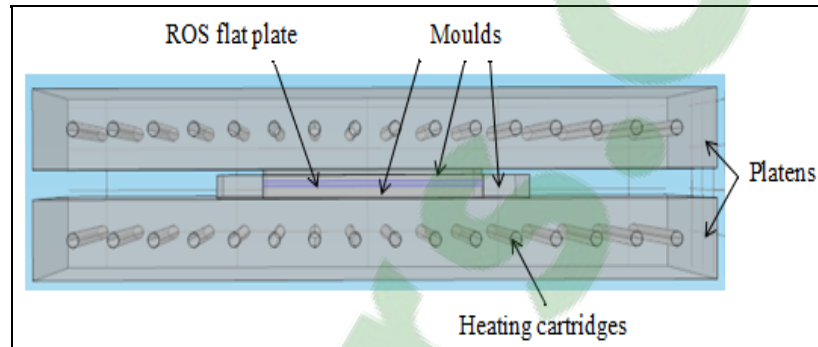


Figure 2.5 Geometry of the model for heating step simulation

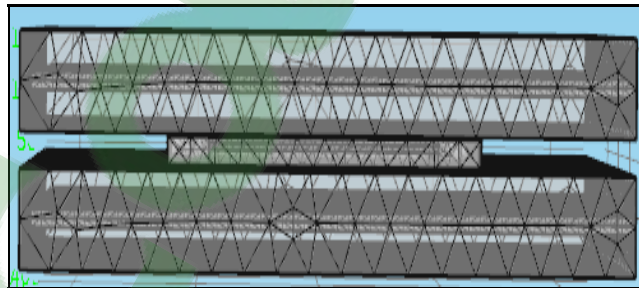


Figure 2.6 Mesh of the model for heating step simulation

As results, It was found that the required power density needing to be applied at the heating cartridge areas in order to reach the processing temperature (380 °C) was 33500 kw/m², and that needed to achieve temperature uniformity throughout the part was 4000 kw/m² (the dwelling period). The upper surface of the higher platen and the lower surface of the bottom platen were insulated. Figure 2.6 shows the mesh of the model geometry for heating simulation. The heating cartridges were symmetric with respect to the ROS flat plate. The model geometry characteristics for simulation of heating step are presented in Table 2.2.

Table 2.2 Model geometry characteristics for simulation of heating step

Domains		Nature	Dimensions (x,y,z) (mm)	Position (x,y,z) (mm)
Platens	Bottom	Steel block	914.4 x 914.4 x 85.725	(0,0,0)
	Top			(0,0,117.125)
Mould frame		Steel block	482.6 x 431.8 x 25.4	(0,0,55.5625)
Mould plate	Bottom	Steel block	335.6 x 304.8 x 12.7	(0,0,49.2125)
	Top			(0,0,67.9125)
ROS flat plate		Solid block (CF/PEEK)	335.6 x 304.8 x 6	(0,0,58.5625)
Heating cartridges (16)	Bottom	Steel solid cylinder	r = 5 , L = 914.4	(- 443,403.41,15) (- 443,349.62,15) (- 443,295.83,15) (- 443,242.04,15) (- 443,188.25,15) (- 443,134.46,15) (- 443,80.67,15) (- 443,26.97,15) (- 443,-26.82,15) (- 443,-80.61,15) (- 443,-134.4,15) (- 443,-188.19,15) (- 443,-241.98,15) (- 443,-295.77,15) (- 443,-349.56,15)
	Top			Symmetrical positions

2.4.3.2 Cooling step simulation

For cooling stage, the cooling channels were added to the geometry of the model. Each tube has the radius of 5 mm. The cooling time was defined in the range from 0 to 3700 s with a step of 5 s to cool down from 380°C to around 50°C. The following boundary thermal conditions were present at the cooling stage: the initial temperature value in the whole model was set to 380 °C The velocity of the flowing air was 35 m/s. The model geometry of the

cooling system is shown in Figure 2.7. The model geometry characteristics for cooling step simulation are presented in Table 2.3.

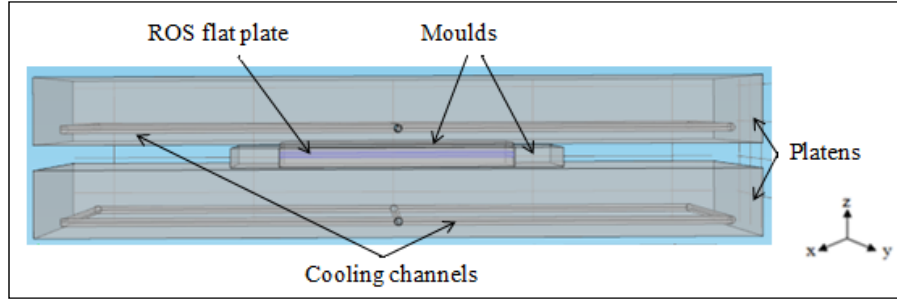


Figure 2.7 Model geometry of the cooling system

Table 2.3 Model geometry characteristics for simulation of the cooling step

Domains	Nature	Dimensions (mm)		Position (x,y,z) (mm)	
		Radius	Length		
Cooling channels	Solid steel cylinder	5	845	x- axis	(- 420,- 420,-23)
					(- 420,420,-23)
				y-axis	(420,- 420,-23)
					(- 420,-420,-23)
				x- axis	(- 420,- 420, 94.12)
					(- 420,420,94.12)
		40	40	x- axis	(- 420,0,- 23)
					(420,- 420,94.12)
				y-axis	(- 420,- 420,94.12)
					(- 460,0,94.12)
				x- axis	(420,0,- 23)
					(- 460,0,- 23)
	(420,0,94.12)				
	(- 420,0,94.12)				

2.4.4 Experimental and numerical results

The distribution of the calculated temperature throughout the model at heating times of 10 and 1000 s are presented in Figure 2.8. The distribution of the calculated temperature throughout the model at cooling times of 10 and 3600 s are presented in Figure 2.9.

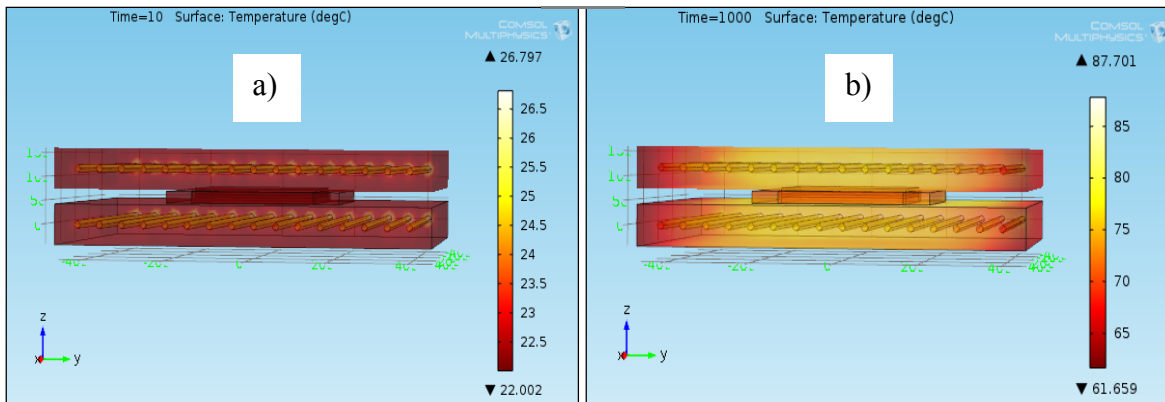


Figure 2.8 Distribution of temperature in the model at heating times: a) 10 s, b) 1000 s

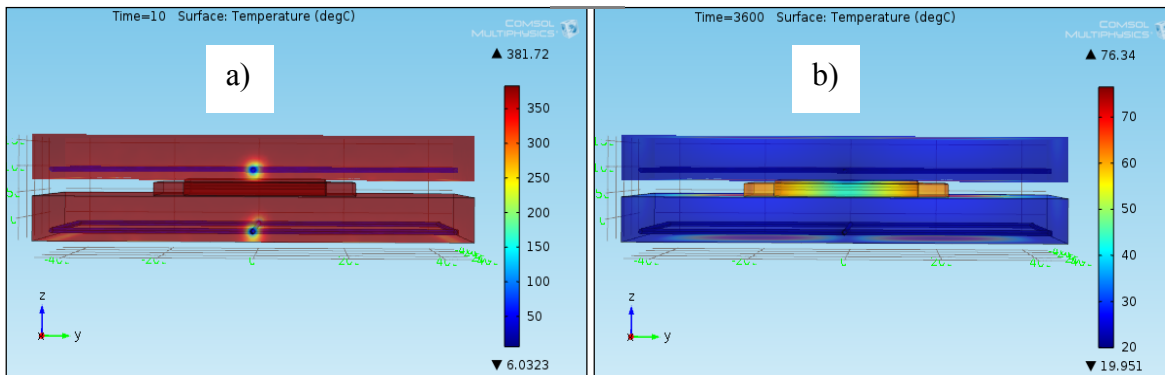


Figure 2.9 Distribution of temperature in the model at cooling times: a) 10 s , b) 3600 s

The obtained numerical results of the transient temperature for the present model were compared to experimental data (Selezneva, 2013). Figure 2.10 shows the comparison between the experimental temperatures and the numerical results at various times for three locations on the middle plan of the ROS flat plate which are : center $(0,0,0)$; corner 1 $(-160,125,0)$ and corner 2 $(140,-120,0)$.

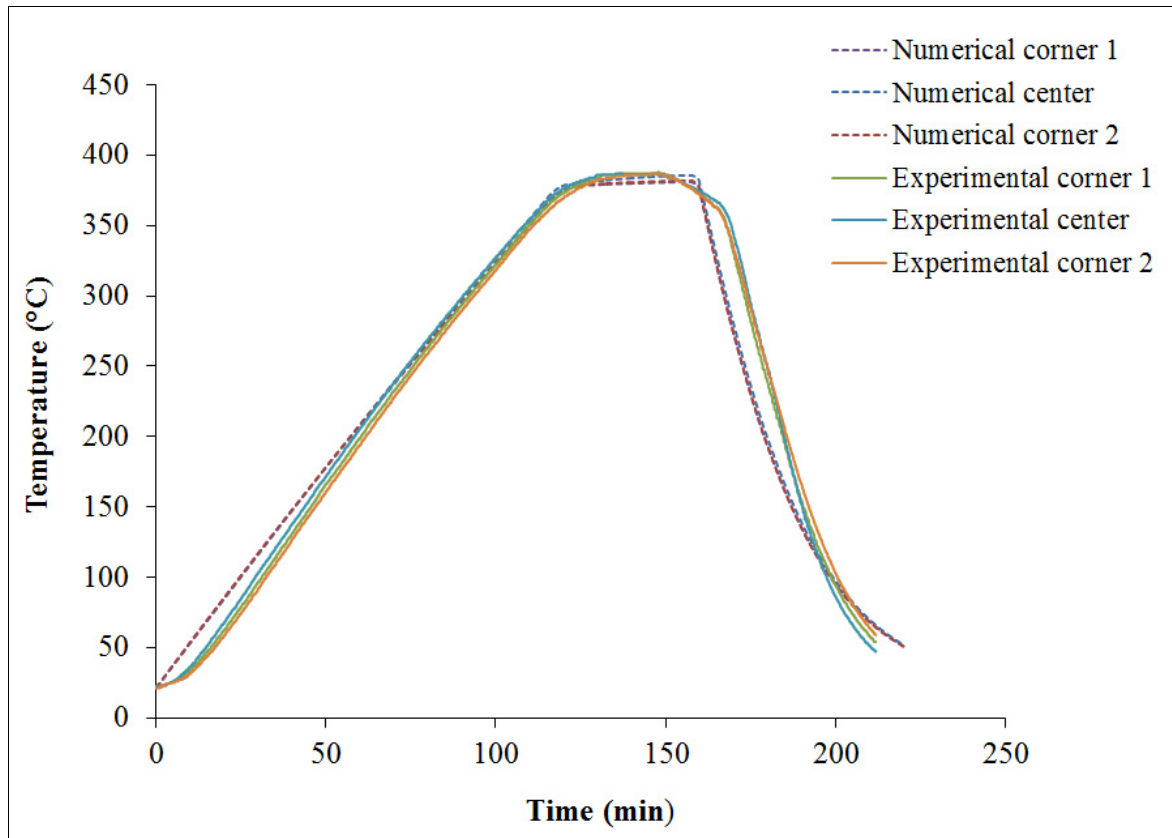


Figure 2.10 Comparison between numerical and experimental temperatures at various times for three locations on the middle plan of the ROS flat plate

2.4.5 Heating power simulation results

As mentioned in previous section, the heating time was simulated using the transient thermal analysis module of the commercial COMSOL Multiphysics software basing on 3D FEM. In order to reach the processing temperature and to get the temperature uniformity throughout the flat plate the necessary heat source rate applied at the surfaces of heating cartridges was adjusted using formula (2.3).

From Figure 2.10 and using equation (2.3) the heating power was deducted for each step of heating time and the temperature scale corresponding to different heating rates. Table 2.4 presents the heating step simulation results for flat plate.

Table 2.4 Heating step simulation results for flat plate

V_p (10^4 mm^3)	H.P.D (w/m^2)	H.T (min)	H.P'.D (w/m^2)	H.T' (min)	N.H.C	C.A (m^2)
65.0321	33500	134	4000	23	32	0.02871

2.4.6 Heating energy costs calculations

From Table 2.4 and applying equations (2.5) and (2.6), the heating energy and the heating energy costs were calculated. Table 2.5 presents the heating energy and the heating energy costs results for the flat plate.

Table 2.5 Heating energy and heating energy costs results for the ROS flat plate

V_p (10^4 mm^3)	Total heating energy (kwh)	Energy rate (\$/kwh)	Energy costs (\$)
65.0321	70.144	0.0457	3.205

2.5 T-shape part

2.5.1 Compression moulding process of T-shape part

The T-shape part was composed of a rib and a flange. The rib measured 82.44 mm x 25 mm x 3.17 mm and of the flange, 82.44 mm x 82.44 mm x 3.17 mm (Figure 2.11c). The part was made of discontinuous fibre strands which were slit manually or automatically from unidirectional prepreg tape. These strands were placed in the mould cavity and distributed such as to assure their random orientation (Figure 2.11a). The experimental setup of manufacturing T-shape part is shown in Figure 2.11b.

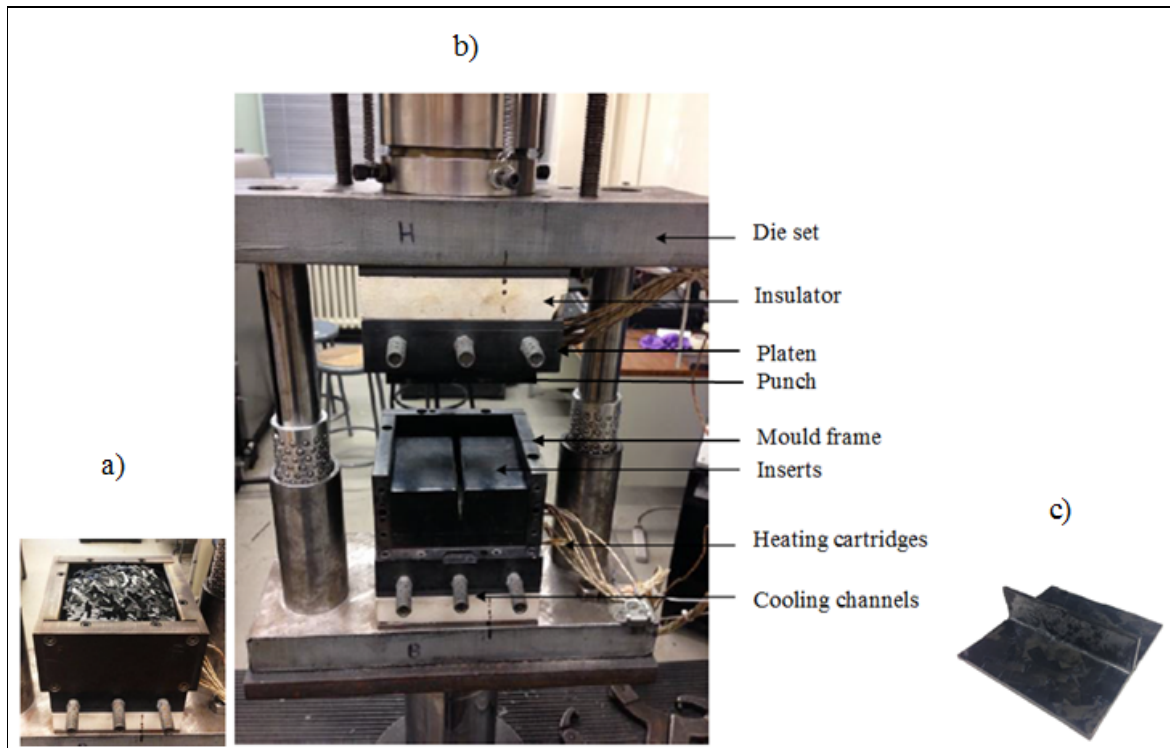


Figure 2.11 a) Cavity mould filled with ROS. b) Experimental set up.
 c) ROS T-shape part
 Reproduced and adapted with the permission of LeBlanc et al. (2014a)

2.5.1.1 Heating step

The cavity and the punch of the mould were fixed to two H-13 steel platens measuring 101.6 mm x 101.6 mm, and the whole fixture was mounted to a 250 kN MTS press. After the material was placed in the cavity mould which was assembled with two inserts and frames, the mould was closed. The platens were heated using four heating cartridges and were controlled by two auto-tuning PID controllers. An initial pressure of 10 bars was applied during heating. When the processing temperature was reached, a pressure of 30 bars was applied for a dwell of 15 minutes and during cooling step. Two thermocouples used to measure the temperature of the material during the cycle were inserted through the mould (LeBlanc et al., 2014a).

2.5.1.2 Cooling step

At the end of the heating step, the mould and the part started to cool down from 380 °C to ambient temperature at a rate of 10°C/min, using compressed air flowing through cooling channels in the mould platens. The cooled part was subsequently removed (LeBlanc et al., 2014a).

2.5.2 Heat transfer processes

The conduction and convection heat transfer mechanisms which occurred between T-shape part, the T-shape mould and the platens are presented in Figure 2.12.

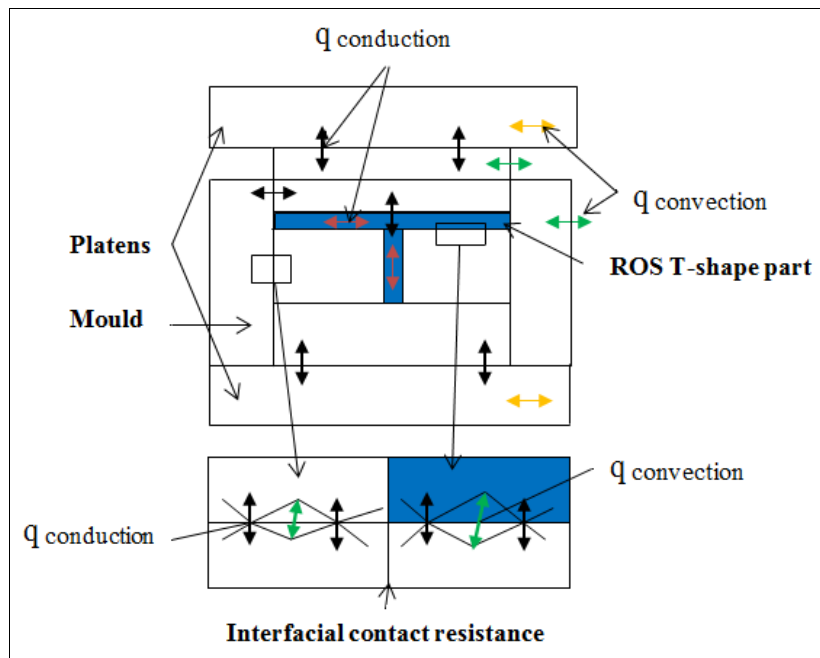


Figure 2.12 Contact heat transfer mechanisms

2.5.3 Numerical simulations

2.5.3.1 Heating step simulation

The heating time included two periods: heating and dwelling. It was simulated using the transient thermal analysis module of the commercial COMSOL Multiphysics software by solving the heat transfer equation (2.1) numerically, based on the 3D finite elements method. The model comprised two platens, the frame, the two inserts, two plate moulds, the ROS T-shape part, and two insulators. These components were considered as solid blocks in contact. The model also included 4 cylindrical heating cartridges with a radius of 3.834 mm and a length of 101.6 mm inserted in each platen. Figure 2.13 shows the geometry of the model used to simulate the heating process. The time-dependent study format was selected in order to enable a time step assessment of the evolution of the temperature in the ROS T-shape part. The heating time to reach a temperature of 380 °C was defined in the range of 0 to 2730 s, with 5 s steps. The following boundary thermal conditions were present at the heating stage: for the convective heat transfer, the initial air temperature value was set to 20°C; the initial value for the temperature in the whole model was set to 25 °C, and the required power density needing to be applied at the surfaces of the heating cartridges was adjusted using the formula (2.3).

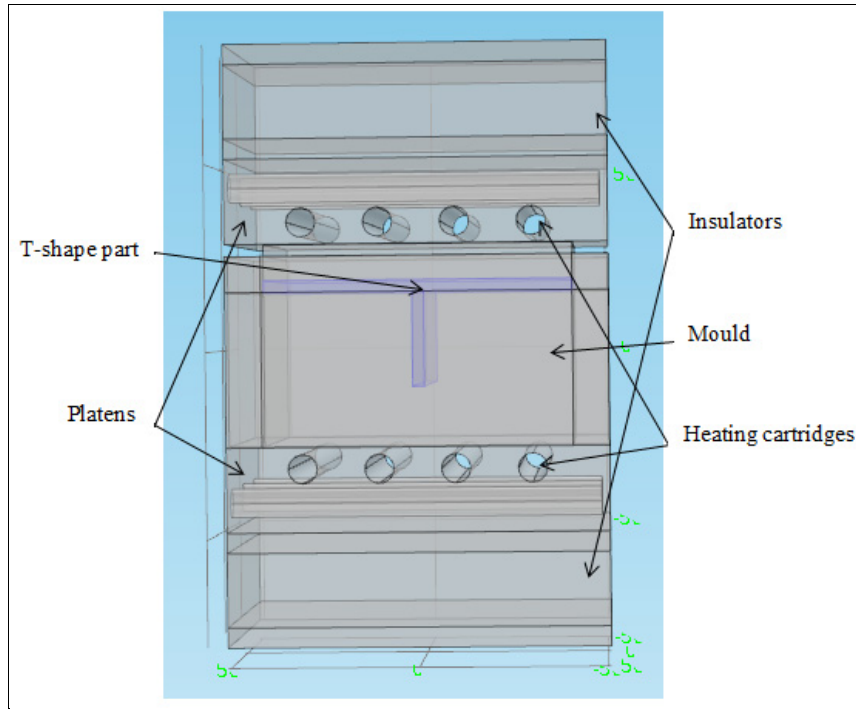


Figure 2.13 Geometry of the model for simulation of heating step

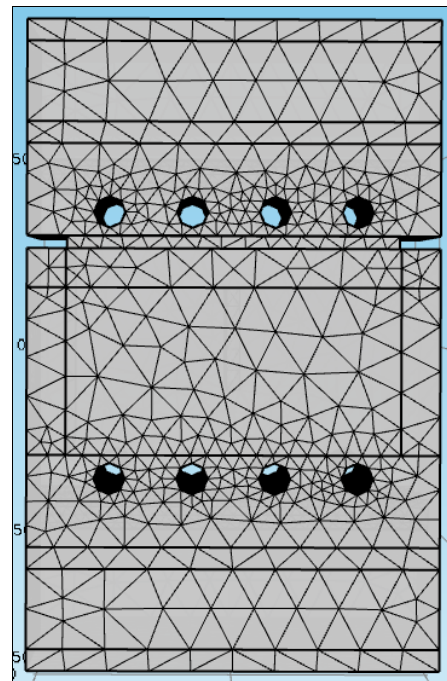


Figure 2.14 Mesh of the model geometry for heating step simulation

As results, it was found that the required power density needing to be applied to the heating cartridges in order to reach the processing temperature (380 °C) was 54000 kw/m², and that needed to achieve temperature uniformity throughout the part was 16000 kw/m² (the dwelling period). The upper surface of the higher platen and the lower surface of the bottom platen were insulated. Figure 2.14 shows the mesh of the model geometry for heating step simulation. The geometry characteristics of the heating model are presented in Table 2.6.

Table 2.6 Geometry characteristics of the heating model

Domains		Nature	Dimensions (x,y,z) (mm)	Position (x,y,z) (mm)
Platens	Bottom	Steel block	101.6 x 101.6 x 22.62	(0,0,39.88)
	Top			(0,0,-36.71)
Cavity mould		Steel block	101.6 x 101.6 x 50.8 Thickness : 9.58	(0,0,0)
Punch		Steel block	82.44 x 82.44 x 9.58	(0,0,23.42)
Mould plate	Bottom	Steel block	101.6 x 101.6 x 5.36	(0,0, -50.7)
	Top			(0,0,53.87)
ROS T-shape part		Solid block (CF/PEEK) (2)	Flange: 82.44 x 82.44 x 3.17 Rib: 82.44 x 25.4 x 3.17	(0,0,17.4) (0,0,3.12)
Insulators (2)		Top	101.6 x 101.6 x 19.74	(0,0,66.42)
		Bottom	101.6 x 101.6 x 19.74	(0,0,-63.25)
Heating cartridges (8)	Bottom	Steel solid cylinder	r = 3.834 ; L = 101.6	(-10.16,-50.8,-31.15) (-30.48,-50.8,-31.15) (10.16,-50.8,-31.15) (30.48,-50.8,-31.15)
	Top			(-10.16,-50.8,34.32) (-30.48,-50.8,34.32) (10.16,-50.8,34.32) (30.48,-50.8,34.32)

2.5.3.2 Cooling time simulation

For the cooling stage, the cooling channels were added to the geometry of the model, and were connected to cylindrical holes drilled. The cooling time was defined in the 0 to 2000 s range, with a 5 s step to cool down from 380°C to ambient temperature. The following boundary thermal conditions were present at the cooling stage: the initial temperature value in the whole model was set at 380 °C. The upper surface of the higher platen and the lower surface of the bottom platen were insulated. The velocity of the flowing air was 50 m/s. The model geometry of the cooling system is shown in Figure 2.15. The geometry model characteristics for simulation of cooling step are presented in Table 2.7.

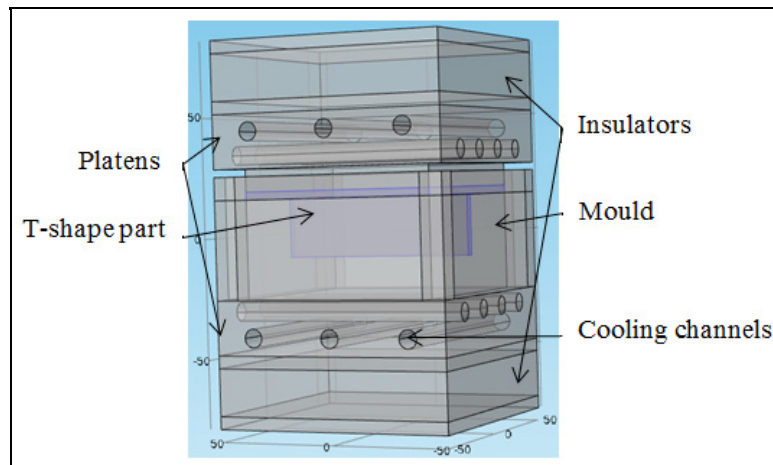


Figure 2.15 Model geometry of the cooling system

Table 2.7 Geometry characteristics of the cooling model

Domains	Nature	Dimensions (mm)		Position (x,y,z) (mm)	
		Radius	Length		
Cooling channels	Machined cylindrical holes	3.834	101.6	Bottom	(-50.8,0,-40.73)
					(-50.8,34.5,-40.73)
					(-50.8,-34.5,-40.73)
				Top	(-50.8,0,43.9)
					(-50.8,34.5,43.9)
					(-50.8,-34.5,43.9)

2.5.4 Experimental and numerical results

The distribution of the calculated temperature throughout the model at heating times of 30 and 1600 s are presented in Figure 2.16. The distribution of the calculated temperature throughout the model at cooling times of 20 and 1800 s are presented in Figure 2.17.

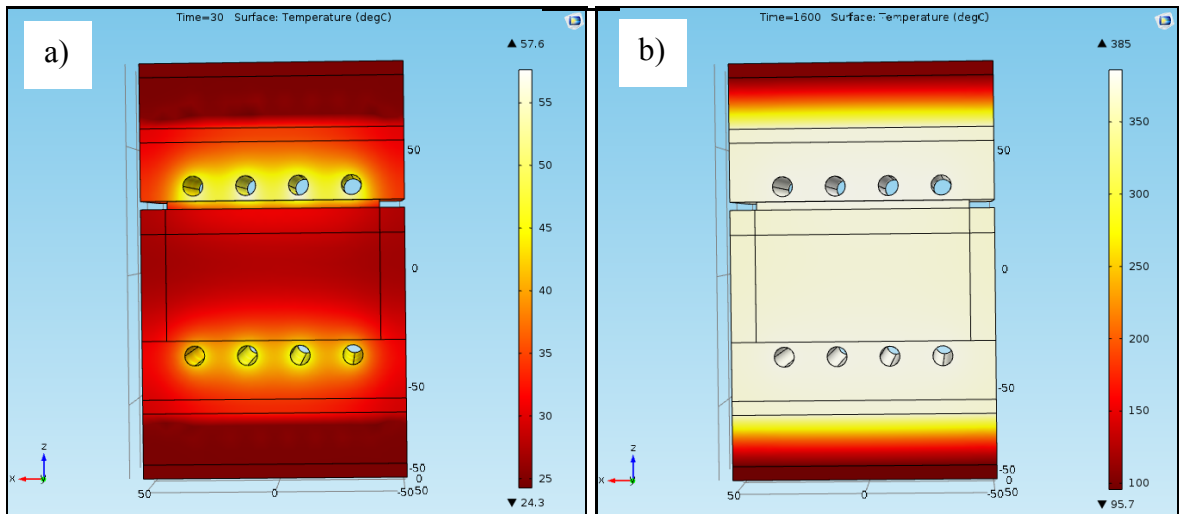


Figure 2.16 Distribution of temperature in the model at heating times: a) 30 s, b) 1600 s

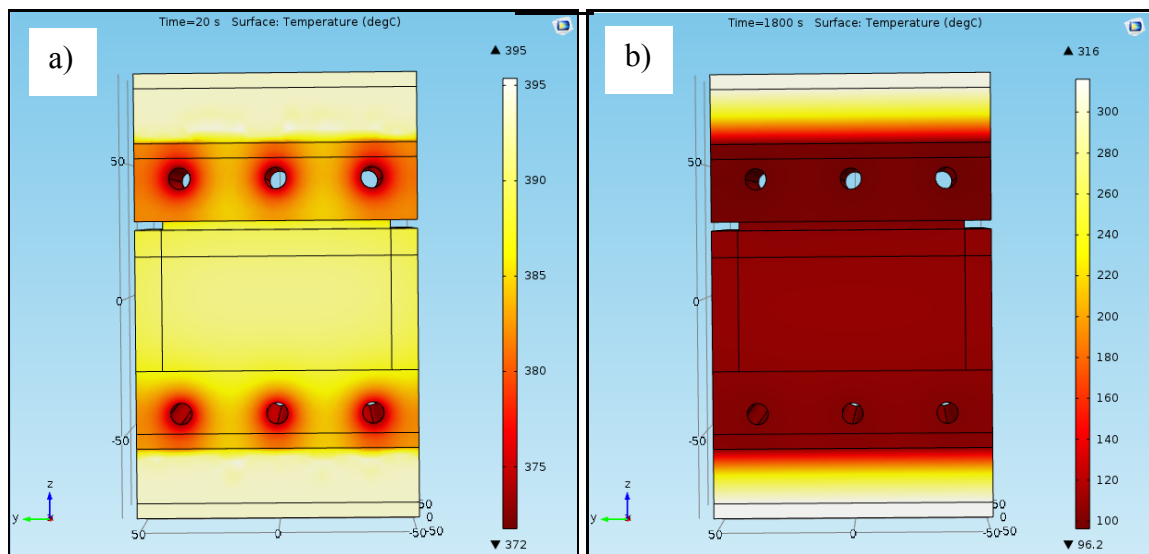


Figure 2.17 Distribution of temperature in the model at cooling times: a) 20 s, b) 1800 s

The transient temperature numerical results obtained for the present model were compared to experimental data (LeBlanc, 2014a). Figure 2.18 shows a comparison between experimental and numerical temperature distributions during the compression moulding process inside the ROS T-shape part.

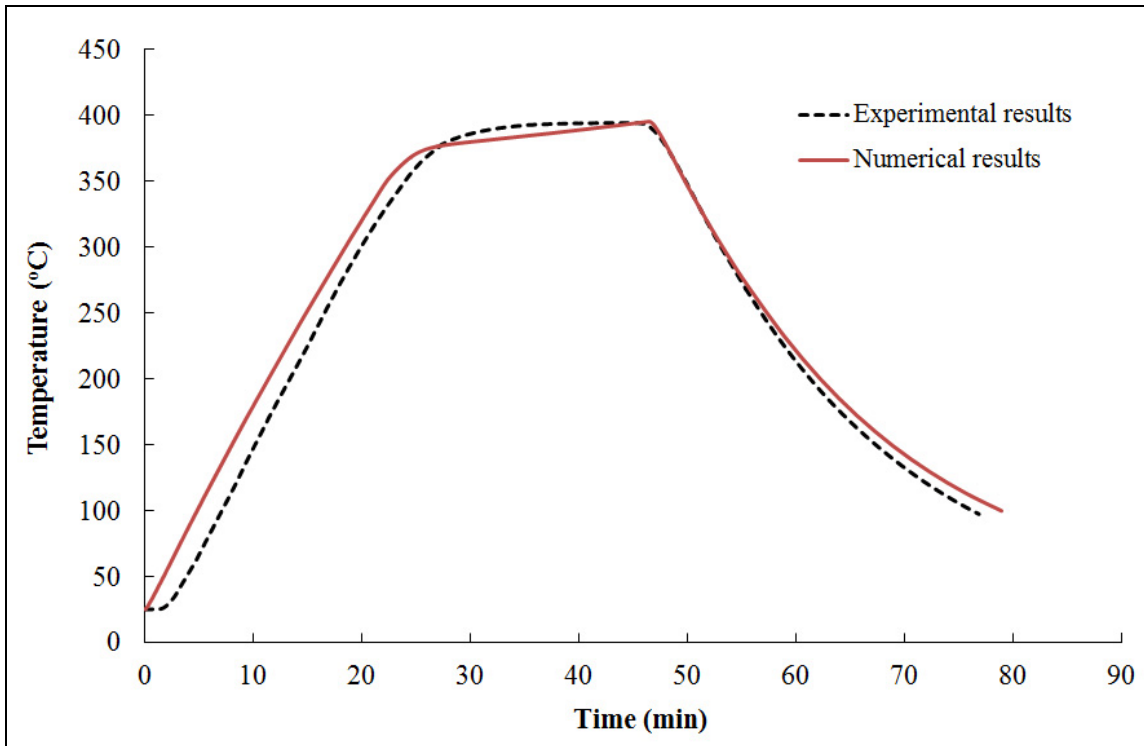


Figure 2.18 Comparison between numerical and experimental temperature distributions during the compression moulding process inside the ROS T-shape part

2.5.5 Heating power simulation results

As mentioned in the previous section, the heating time was simulated using the transient thermal analysis module of the commercial COMSOL Multiphysics software (based on 3D FEM). In order to reach the processing temperature and obtain temperature uniformity throughout the part, the required heat source rate needing to be applied at the surfaces of heating cartridges was adjusted using formula (2.3).

From Figure 2.18 and using formula (2.3) and applying equation (2.4), the heating curve can be divided into four approximated straight lines such that the heating power can be deduced for each heating time step and temperature scale corresponding to different heating rates. Table 2.8 presents the heating step simulation results for T-shape part.

Table 2.8 Heating step simulation results for T-shape part

<i>N.H.C</i>		8	H.P ₁	H.T ₁	H.P ₂	H.T ₂	H.P ₃	H.T ₃	H.P ₄	H.T ₄
			(w)	(min)	(w)	(min)	(w)	(min)	(w)	(min)
C.A	(m ²)	0.00244	1056	23	388	3	119	4	312	15
H.P.D	(w/m ²)	54.000								
H.P'.D	(w/m ²)	16.000								

2.5.6 Heating energy costs calculations

From Table 2.8 and applying equations (2.5) and (2.6) the heating energy and the heating energy costs were calculated .Table 2.9 presents the heating energy and the heating energy costs results for T-shape part.

Table 2.9 Heating energy and heating energy costs results for the T-shape part

Part volume (10 ⁴ mm ³)	Total heating energy (kwh)	Energy rate (\$/kwh)	Energy costs (\$)
2.817	0.6098	0.0457	0.0278

2.6 L-bracket part

2.6.1 Compression moulding process of L-bracket

The L-bracket part, having a width of 75 mm, a leg length of 115 mm, a thickness of 6.4 mm, and a rib height of 40 mm (Figure 2.19c), was made of short fibre strands that were slit manually or automatically from unidirectional prepreg tape of a thermoplastic composite bulk moulding compound. These strands were placed in the mould cavity and distributed such as to assure their random orientation (Figure 2.19a). The experimental setup of manufacturing L-bracket is shown in Figure 2.19b.

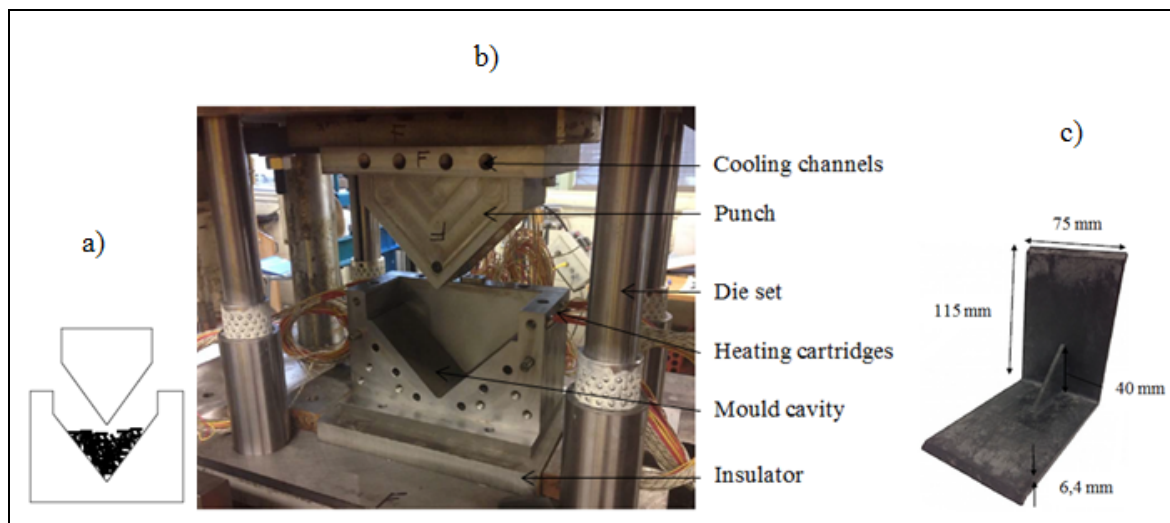


Figure 2.19 a) Cavity Mould filled with ROS. b) Experimental set up.
c) ROS L-bracket

Reproduced and adapted with the permission of Leblanc et al. (2014b, p.7)

2.6.1.1 Heating step

After assembling the P20 steel machined mould, which was composed primarily of the cavity and the punch, and was fixed on the die set, the whole tool was then installed in a General Motors 40 Ton press. The mould was coated with two Frekote 700-NC release agents, and the material was placed and distributed randomly in the cavity mould. A rib insert was integrated

in the punch in order to add a rib feature. After the mould was closed, its heating was started. The punch was heated with four 600 Watt heating cartridges aligned vertically, while the cavity was heated with four 1000 Watt heating cartridges positioned at 45° with the horizontal axis. The temperature of the mould was controlled by means of two auto-tuning PID controllers from the Watlow Company. Two thermocouples used to measure the temperature of the material during the cycle were inserted through the mould. When the processing temperature was reached, it was maintained for 10 minutes, and a pressure of 40 bars was applied on the material (LeBlanc et al., 2014b). The CAD of the mould on exploded view is shown in Figure 2.20.

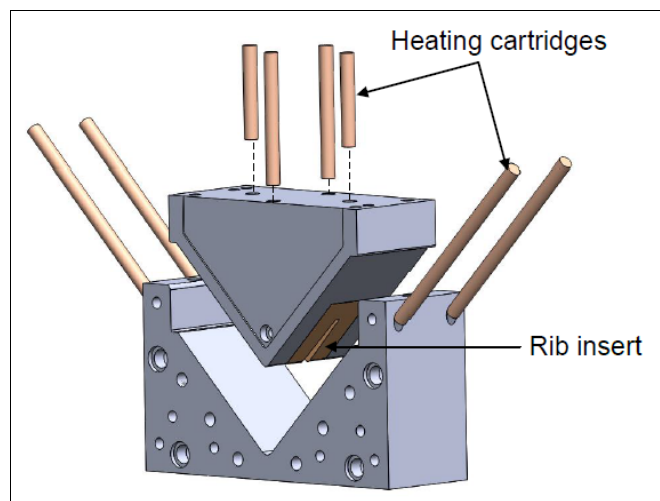


Figure 2.20 CAD of the mould showing the position of the heating cartridges and the rib insert
Taken from Leblanc et al. (2014b, p.7)

2.6.1.2 Cooling step

At the end of the heating step, the mould started to cool down from the processing temperature to ambient temperature at a rate of 5°C/min using compressed air flowing through cooling channels. Afterwards, the mould was disassembled, and the part was removed (LeBlanc et al., 2014b).

2.6.2 Heat transfer processes

The conduction and convection heat transfer mechanisms which occurred between L-bracket, the L-shape mould and the platens are presented in Figure 2.21.

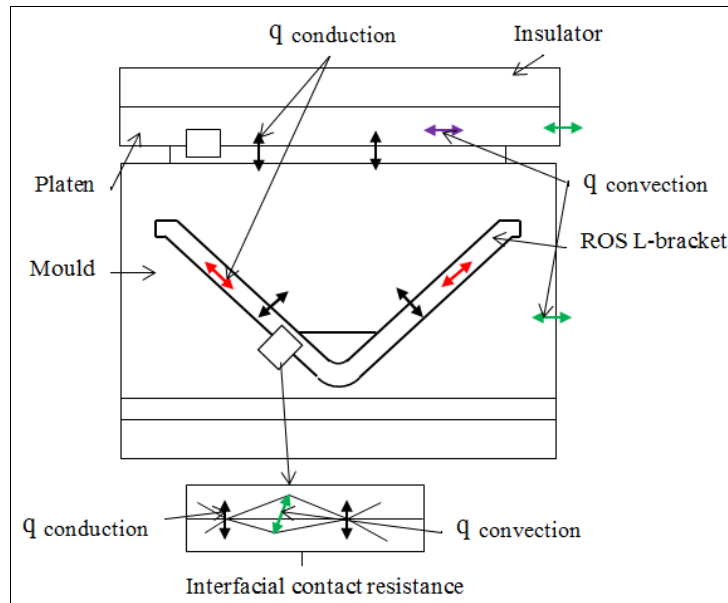


Figure 2.21 Contact heat transfer mechanisms

2.6.3 Numerical simulations

2.6.3.1 Heating step simulation

The heating time included two periods: heating and dwelling. The heating time was simulated using the transient thermal analysis module of the commercial COMSOL Multiphysics software by solving the heat transfer equation (2.1) numerically, based on the 3D finite elements method. The model was composed of a steel block simulating the platen and the mould (the punch and the cavity), the L-shape block simulating ROS L-bracket part and two blocks simulating two insulators. These components were considered as solid blocks in contact. The model included also 8 cylindrical heating cartridges having a radius of 4.687 mm, four of them have 132.45 mm length inserted in the cavity at 45° with vertical axis and

the others with 85.35 mm and 62.75 mm lengths were inserted vertically in the punch. Figure 2.22 shows the geometry of the model used to simulate the heating process. The time-dependent study format was selected in order to enable a time step assessment of the evolution of the temperature in the ROS L-bracket. The heating time to reach 380 °C was defined in the 0 to 2800 s range, with 5 s steps. The following boundary thermal conditions were present at the heating stage: for the convective heat transfer, the initial value of air temperature was set to 20 °C; the initial temperature value in the whole model was set to 85 °C. The required power densities needing to be applied to the heating cartridges, having lengths of 132.45 mm, 85.35 mm and 62.75 mm, in order to reach the processing temperature (375°C) were 125103 kw/m², 76386 kw/m² and 103885 kw/m² respectively, using formula (2.7).

$$\text{Power density} * (T < 375[\text{degC}]) + \text{power density} * (T > 375[\text{degC}]) \quad (2.7)$$

In order to attain the processing temperature (380°C) and obtain temperature uniformity throughout the part, the required power density needing to be applied to the heating cartridges having a length of 132.45 mm was 24000 kw/m², while for those having lengths of 85.35 mm and 62.75 mm, it was 18000 kw/m² (the dwelling period); the upper surface of the higher platen and the lower surface of the mould cavity were insulated.

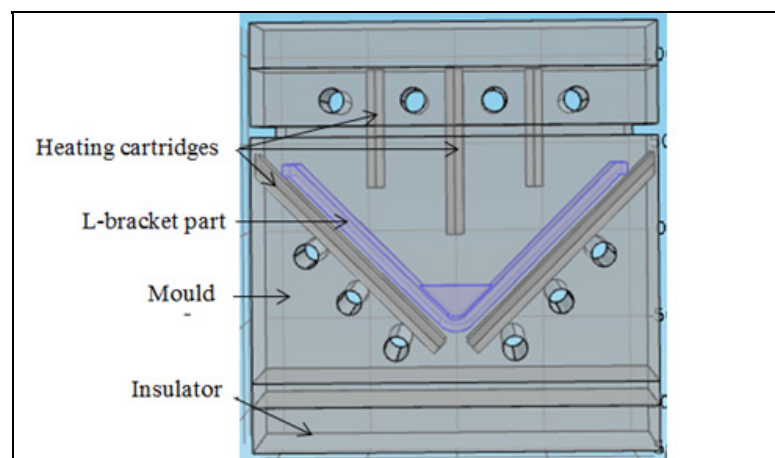


Figure 2.22 Geometry of the model for heating process

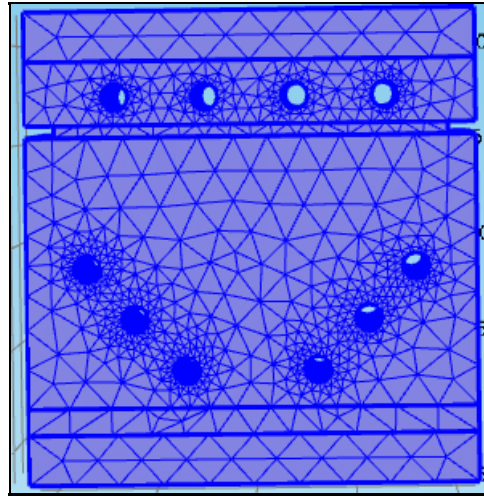


Figure 2.23 Mesh of the model geometry for heating simulation

Figure 2.23 shows the mesh of the model geometry for heating simulation. The geometry characteristics of the heating model are presented in Table 2.10.

Table 2.10 Geometry characteristics of the heating model

Domains		Nature	Dimensions (x,y,z) (mm)		Position (x,y,z) (mm)
Cavity- punch-platen		Steel block	219.375 x 125.625 x 182.642		(0,0,0)
ROS L-bracket		Solid (CF/PEEK)	2 Legs : 115 x 75 x 6.4 Rib : Height = 40 Thickness = 6.4		(0,0,-37)
Insulators (2)		Top	219.375 x 125.625 x 24.375		(0,0,103.508)
		Bottom	219.375 x 125.625 x 24.375		(0,0,-103.508)
Heating cartridges (8)	Bottom	(4) Steel solid cylinder	r = 4.687 mm, L = 13.45		(9,18.75,-62)
					(-9,18.75,-62)
	Top	(4) Steel solid cylinder	(2)	r = 4.687 mm, L = 85.35	(44.062,0,25.969) (-44.062,0,25.969)
(2)			r = 4.687 mm, L = 62.75	(0,33.06,0.656) (0,-33.06,0.656)	

2.6.3.2 Cooling step simulation

For the cooling stage, the cooling channels were added to the geometry of the model, and were connected to drilled cylindrical holes. The cooling time was defined in the 0 to 7400 s range, with a 5 s step, to cool down from 380°C to ambient temperature. The following boundary thermal conditions were present at the cooling stage: the initial value of temperature in the whole model was fixed to 380 °C. The upper surface of the higher platen and the lower surface of the mould cavity were insulated. The velocity of the flowing air was 10 m/s. The model geometry of the cooling system is shown in Figure 2.24. The geometry model characteristics for simulation of the cooling step are presented in Table 2.11.

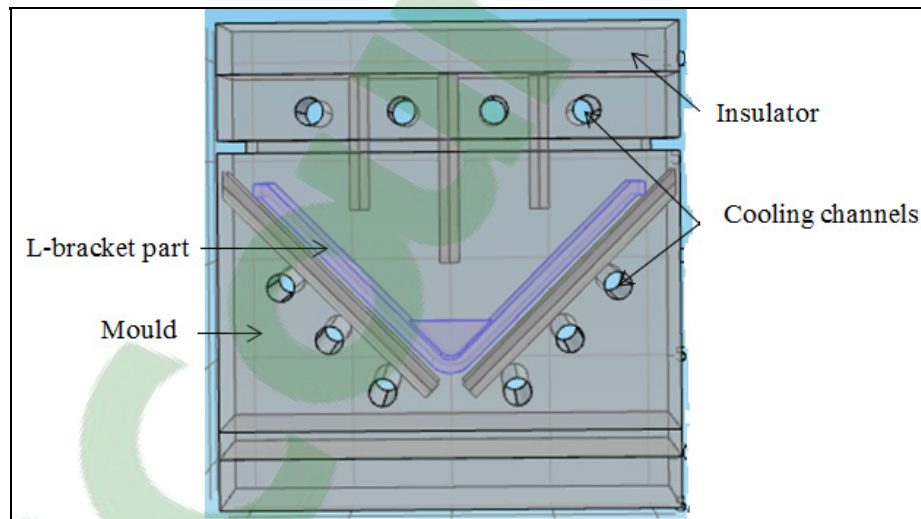


Figure 2.24 Model geometry of the cooling step

Table 2.11 Geometry characteristics of the cooling model

Domains	Nature	Dimensions (mm)		Position (x,y,z) (mm)	
		Radius	Length		
Cooling channels	Machined cylindrical holes	6.562	125.62	Bottom	(32,-62.81,-60)
					(-32,-62.81,-60)
					(57,-62.81,-35)
					(-57,-62.81,-35)
					(80,-62.81,-10)
				(-80,-62.81,-10)	
				Top	(65.812,-62.81,73.625)
					(21.937,-62.81,73.625)
					(-21.937,-62.81,73.625)
					(- 65.812,-62.81,73.625)

2.6.4 Experimental and numerical results

The distribution of the calculated temperature throughout the model at heating times of 10 and 2500 s are presented in Figure 2.25. The distribution of the calculated temperature throughout the model at cooling times of 25 and 7300 s are presented in Figure 2.26.

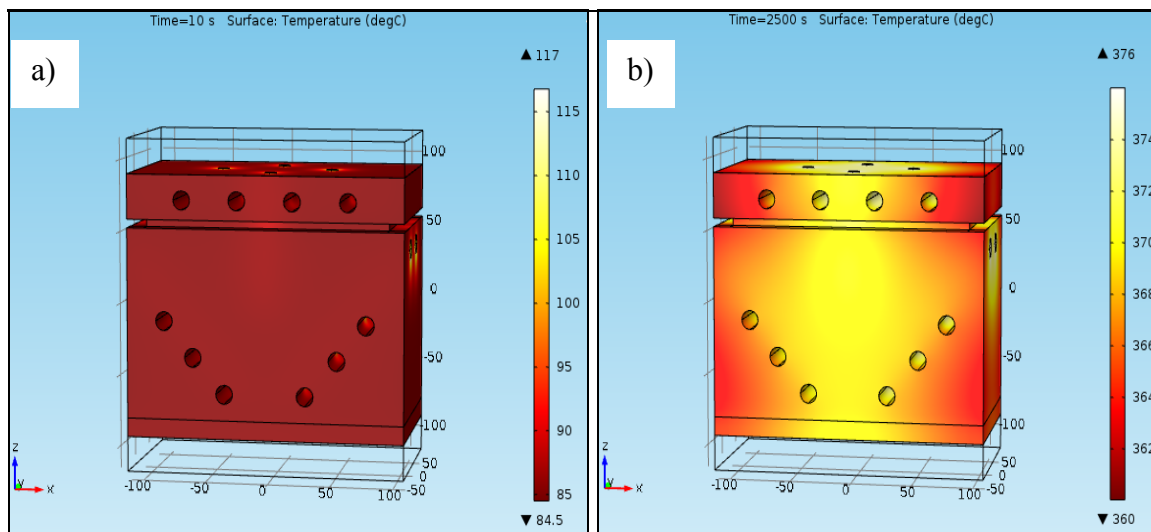


Figure 2.25 Distribution of temperature in the model at heating times: a) 10 s, b) 2500 s

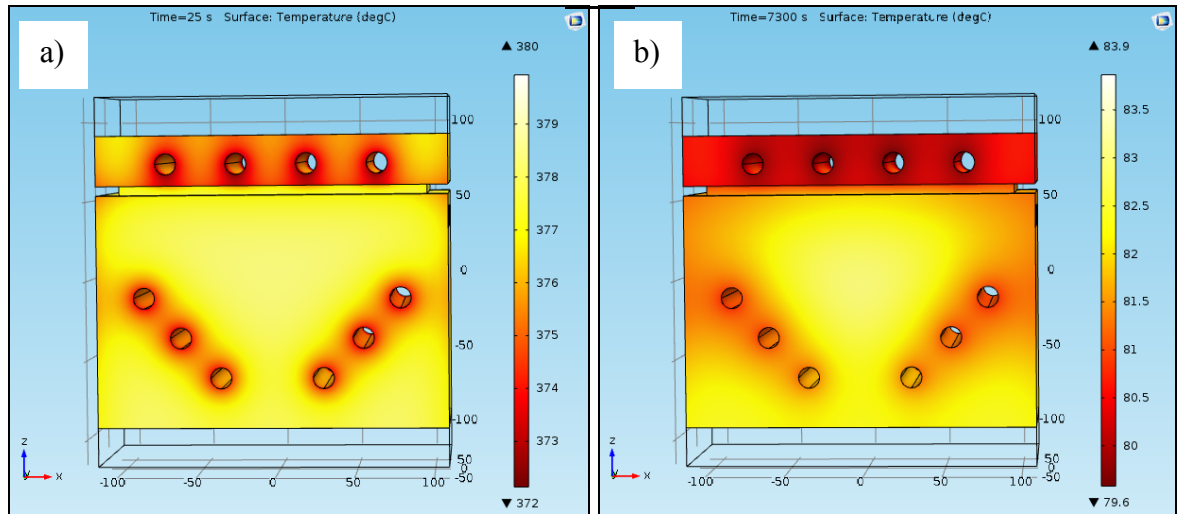


Figure 2.26 Distribution of temperature in the model at cooling times: a) 25 s, b) 7300 s

The numerical results of the transient temperature obtained for the present model were compared to experimental data (LeBlanc, 2014b). Figure 2.27 shows the temperature variation in function of time inside the ROS L-bracket part and the mould.

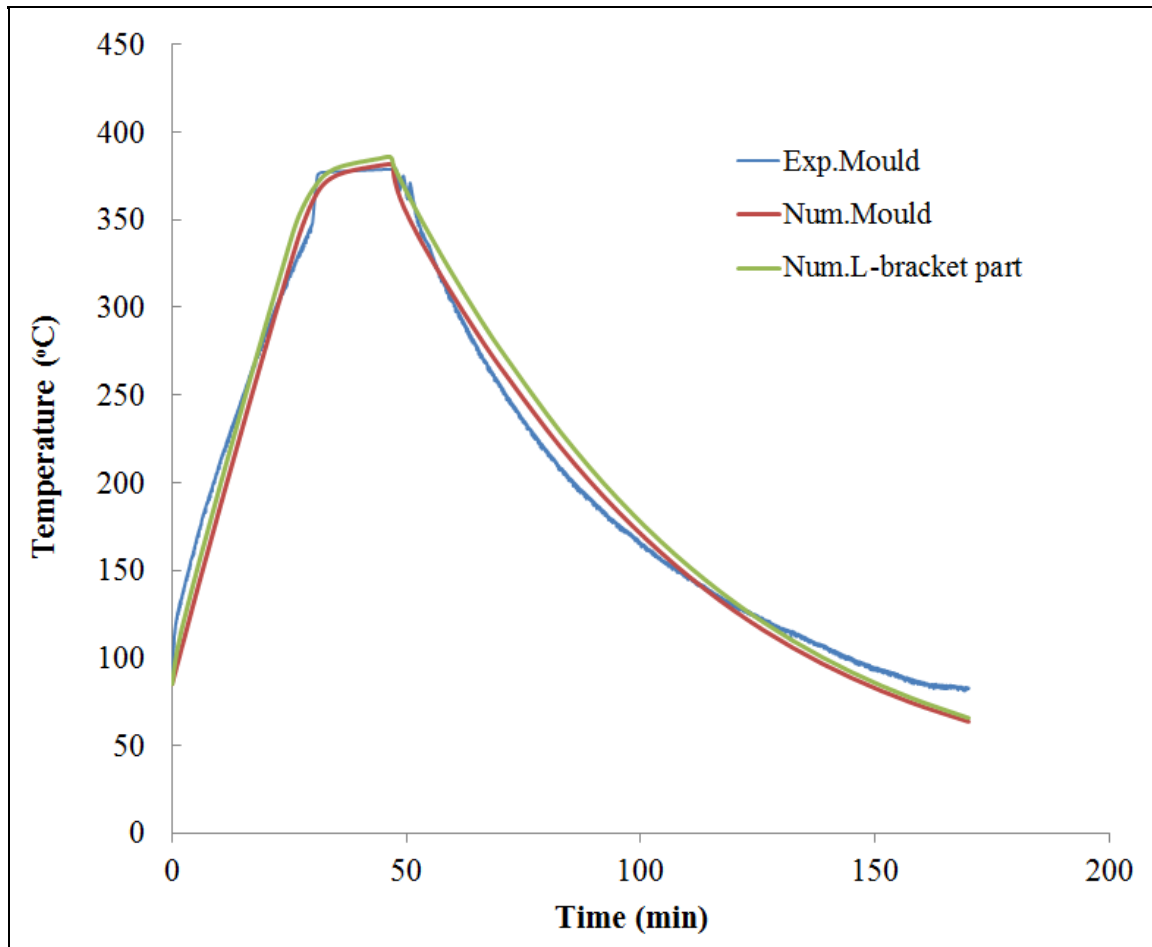


Figure 2.27 Temperature variation versus time inside the mould and L-bracket part

2.6.5 Heating power simulation results

As mentioned in the previous section, the heating time was simulated using the transient thermal analysis module of the commercial COMSOL Multiphysics software. In order to reach the processing temperature and to obtain temperature uniformity throughout the part, the required heating power needing to be applied at the surfaces of the heating cartridges was adjusted using formula (2.7). From Figure 2.27, using formula (2.7) and applying equation (2.4), the heating curve can be divided into three approximated straight lines such that the heating power can be deduced for each heating time step and temperature scale corresponding to different heating rates. Table 2.12 presents the heating step simulation results for L-bracket part.

Table 2.12 Heating step simulation results for L-bracket part

V_p (10^4 mm^3)	H.P ₁ (w)	H.P ₂ (w)	H.P ₃ (w)	H.T ₁ (min)	H.T ₂ (min)	H.T ₃ (min)
11.7589	2710	1200	595	1812	258	724
-	-	N.H.C	C.A (m^2)	H.P.D (w/m^2)	-	-
-	-	2	0.001847	103885	-	-
-	-	4	0.003898	125103	-	-
-	-	2	0.002512	76386	-	-

2.6.6 Heating energy costs calculations

From Table 2.12 and applying equations (2.5) and (2.6), the heating energy and the heating energy costs were calculated. Table 2.13 presents the heating energy and the heating energy costs results for L-bracket part.

Table 2.13 Heating energy and heating energy costs results for L-bracket part

Part volume (10^4 mm^3)	Total heating energy (kwh)	Energy rate (\$/kwh)	Energy costs(\$)
11.758	1.5696	0.0457	0.0717

2.7 Tooling costs estimation for manufacturing ROS parts

2.7.1 Methodology

To perform a cost analysis of the moulds, it is important to consider separately the manufacturing costs of the components and the overheads costs such as design and engineering costs, boxing and shipping costs, capital costs, taxes; and the commercial profits which correspond to the return on investment. The machining costs were calculated using

DFM module of DFMA software while the assembly costs were estimated using DFA one. The machining operations consists of selecting the material, cut from stock and machining, followed by surface polishing and final inspection operations. For cut from stock, the abrasive cut off was used. For machining, the CNC milling machine was used with a parallel vise setup. The machining costs depend on various optional machining parameters and on the labour rate. Polishing and inspection costs were calculated by adjusting the data and the time of operations. The DFA module calculates the costs of the mould assembly according to criteria such as the securing method, symmetry, handling difficulty and insertion difficulty, all depending on operation times and on the labour rate. The material selected for the moulds was high carbon steel. The material data are integrated in the database of the DFM module.

The mould costs estimation results obtained by DFM module for each mould component and for a specified production volume include different costs per part such as material costs, set up costs, process costs, and reject costs, tooling investment costs and manufacturing total cost. The material cost per part is the cost of all material used including the material of the part. The set up cost is the sum of the setup costs for each operation and is equal to the set up time multiplied by set up rate divided by batch size. The process cost is the sum of the processing costs for each operation adjusted for plant efficiency. The reject cost is the sum of costs of the rejected parts following by the highlighted operation. The tooling investment cost per part is the cost of the initial purchase of dies, moulds or it is the sum of all the initial tooling investment costs for each operation. The mould manufacturing cost data were imported into DFA module which calculates the mould assembly cost and the total mould cost. The calculated mould costs results for the all mould components includes assembly labor cost, other operation cost, tool/assembly fixture investment costs, total manufacturing cost, and total mould cost.

2.7.2 Flat mould cost estimation

2.7.2.1 Flat mould manufacture process

The flat mould was composed of the frame and two identical flat plates. The frame consisted of four straight bars. The mould manufacturing process was divided into two steps: the first step was to cut parts from a rectangular bar stock, and the second consisted in cutting and removing materials from the parts. Milling and drilling operations were required to produce all the mould components. The milling operation involved two types of machines, the rough and finish face milling machine, which was used to produce features such as faces, and the rough and finish side and slot milling machine, which was used to produce features such as slots for installing the thermocouples through the mould. The drilling operation consisted in drilling holes in the components of the frame, followed by reaming, tapping or counter drilling operations to attach and secure these components. After the machining, all the surfaces of the mould were polished and inspected. The features manufacturing data for flat mould are presented in ANNEX I.

2.7.2.2 Flat mould assembly process

After the flat mould was machined and polished, it was assembled using socket head cap screws and dowel pins, and then checked to ensure that the mould components fit together properly. Figure 2.28 shows the CAD of the flat mould. The features assembly data for flat mould are presented in Table 2.14.

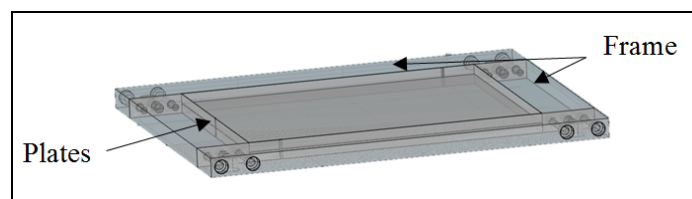


Figure 2.28 CAD of flat mould
Taken from Roy (2014)

Table 2.14 Features assembly data for flat mould

Mould component	Securing method	Symmetry	Handling difficulty	Insertion difficulty	Operation time (s)	RC
Frame A	Secured later	One way	No	Align	1007.6	2
Frame B	Secured later	One way	No	Align	607.6	2
Plates	Secured later	One way	No	Align	507.6	2
Dowel pins	Threads	One way	No	Align	268.8	4
S.H.C.S	Threads with manual fed	One way	No	Align	657.6	8
Flat mould	-				9087.7	1

2.7.2.3 Flat mould cost estimation results

Each mould component contributes to the total mould cost. The mould costs estimation was based on the manufacture and assembly, as well as on the number of components. The flat mould manufacturing cost results obtained by DFM software are presented in Table 2.15.

The cost results obtained by the DFMA program for the flat mould are presented in detail in Table 2.16. The labor rates used in the DFM and DFA softwares are respectively 85\$/hour and 30\$/hour.

Table 2.15 Flat mould manufacturing cost

Mould component	Material cost (\$)	Set up cost(\$)	Process cost(\$)	Rejects costs(\$)	Repeat count	Total costs(\$)
Frame A	11.34	20	59.23	0.99	2	183.12
Frame B	6.5	19.38	39.92	0.64	2	132.88
Top plate	23.48	10.88	35.8	0.8	1	70.96
Bottom plate	23.48	10.88	35.8	0.8	1	70.96
Dowel pins	-	-	-	-	-	1.58
S.H.C.S	-	-	-	-	-	3.36
Flat mould	41.32	50.26	134.95	2.43	1	462.86

Table 2.16 DFMA Flat mould estimated cost

Mould component	Manufacturing cost/part(\$)	Assembly cost/part(\$)	Repeat count	Total costs(\$)
Frame A	91.56	4.94	2	193
Frame B	66.45	2.98	2	138.84
Top plate	70.97	2.49	1	73.45
Bottom plate	70.97	2.49	1	73.45
Dowel pins	1.58	2.64	-	4.22
S.H.C.S	3.36	6.45	-	9.81
Flat mould	462.86	29.91	1	492.77

2.7.2.4 Flat mould costs breakdown

The mould costs are distributed according to the mould components. Figure 2.29 presents the cost breakdown of flat mould.

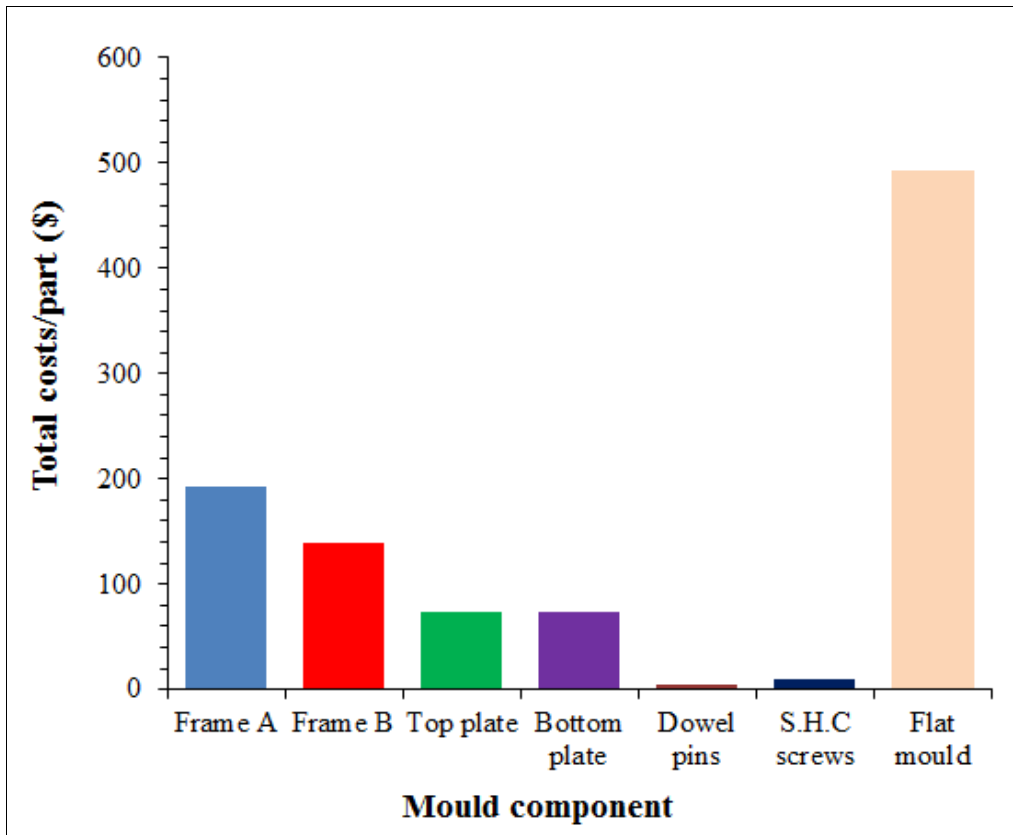


Figure 2.29 Cost breakdown of flat mould

2.7.2.5 Estimated and commercial cost comparison for the flat mould

Table 2.17 presents comparison results between estimated and commercial costs for the flat mould (Roy, 2014).

Table 2.17 Commercial and estimated costs comparison for the flat mould

Cost category	DFMA	Comments	Commercial price
Manufacturing costs (\$)	462.86		-
Assembly costs(\$)	29.91		-
Estimated costs(\$)	492.77	51% of total estimated costs	
Overhead + profit			
Design an Engineering costs(\$)	160	16% of total estimated costs	-
Boxing and shipping costs (\$)	45	5% of total estimated costs	-
Profit(\$)	150	15% of total estimated costs	-
Taxes(\$)	126.95	14.975% of total costs before taxes	-
Total costs(\$)	974.72		1000

2.8 T-shape mould cost estimation

2.8.1 T-shape mould manufacture process

The T-shape mould was manufactured at two locations: the platens and two plates were machined in AMTC, whereas the inserts and the frame were made at McGill University. The T-shape mould was composed of two main parts: the punch and the cavity, with the punch attached to the upper platen and upper plate. The cavity, including two inserts and the frame, were affixed to the bottom platen and bottom plate. The mould manufacturing process is divided into two steps. The first is to cut out parts from a rectangular bar stock, and the second consists in cutting and removing materials from the parts. Milling and drilling operations were required to produce all the mould components. The rough and finish face milling machine was used to produce features such as faces and the rib insert, and the drilling

operation consisted in drilling holes in all the components, followed by reaming, tapping or counter drilling operations to secure and install the heating cartridges, the thermocouples, and the cooling channels in the platens. After the machining operations, all the surfaces of the mould were polished and inspected. Features manufacturing data for T-shape mould are presented in ANNEX II.

2.8.2 T-shape mould assembly process

After the T-shape mould was machined and polished, it was assembled using socket head cap screws and dowel pins, and then checked to ensure that the mould components fit together properly. The mould and the insulators were then affixed to the die sets, thereby assuring alignment during processing. Figure 2.30 show the CADs of the mould cavity and punch assemblies respectively. Table 2.18 presents the features assembly data for T-shape mould.

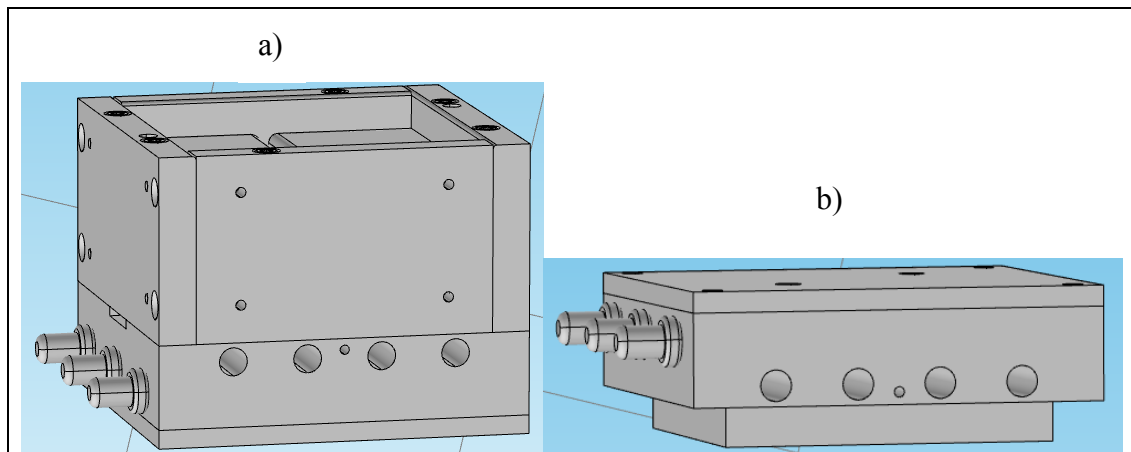


Figure 2.30 CADs of T-shape mould assembly:
a) cavity assembly, b) punch assembly
Reproduced and adapted with the permission of (Landry, 2014)

Table 2.18 Features assembly data for T-shape mould

Mould component	Securing method	Symmetry	Handling difficulty	Insertion difficulty	Operation time (s)	RC
Mould frame A	Secured later	One way	No	Align	2007.6	2
Mould frame B	Secured later	One way	No	Align	2007.6	2
Mould insert with rib	Secured later	One way	No	Align	403.8	1
Mould insert without rib	Secured later	One way	No	Align	403.8	1
Bottom platen	Secured later	One way	No	Align	1103.8	1
Top platen	Secured later	One way	No	Align	1103.8	1
Bottom plate	Secured later	One way	No	Align	1507.6	2
Dowel pins	Threads	One way	No	Align	837.1	16
S.H.C.S	Threads with	One way	No	Align	1210.7	22
T-shape mould	-				10585.8	1

2.8.3 T-shape mould cost estimation results

Each mould component contributes to the total mould cost. The mould cost estimation was based on the manufacture and assembly, as well as on the number of components. The T-shape mould manufacturing cost results obtained by DFM software are presented in Table 2.19. The mould cost results obtained by the DFMA program for the T-shape mould are presented in detail in Table 2.20. The labor rates used in the DFM and DFA modules were respectively Cad \$85/hour and Cad \$30/hour.

Table 2.19 T-shape mould manufacturing cost

Mould component	Material cost(\$)	Set up cost(\$)	Process cost(\$)	Rejects costs(\$)	Repeat count	Total costs(\$)
Frame A	0.93	75.85	159.19	2.22	2	476.36
Frame B	0.7	73.85	136.3	1.88	2	425.46
Insert with rib	1.46	76.65	96.88	1.7	1	176.69
Insert without rib	1.46	74.65	64,39	1.06	1	141.57
Top platen	4.07	91.3	316.21	4.6	1	416.18
Bottom platen	4.07	84.55	258.69	3.73	1	351.04
Top plate	0.81	75.55	111.72	1.57	1	189.65
Bottom plate	0.81	75.55	111.72	1.57	1	189.65
Dowel pins for cavity	-	-	-	-	-	9.32
Dowel pins for punch	-	-	-	-	-	3.72
S.H.C.S for cavity	-	-	-	-	-	6.36
S.H.C.S for punch	-	-	-	-	-	1.88
T-shape mould	15.94	777.65	1550.59	22.43	1	2387.88

Table 2.20 DFMA T-shape mould estimated cost

Mould component	Manufacturing cost/part(\$)	Assembly cost/part(\$)	Repeat count	Total costs(\$)
Frame A	238.18	9.84	2	496.04
Frame B	212.73	9.83	2	445.12
Insert with rib	176.69	3.95	1	180.64
Insert without rib	141.57	4.04	1	145.61
Top platen	416.18	10.82	1	427
Bottom platen	351.04	10.82	1	361.86
Top plate	189.65	7.375	1	197.025
Bottom plate	189.65	7.375	1	197.025
Dowel pins for cavity	9.32	5.675	-	14.995

Table 2.20 (Continued)

Mould component	Manufacturing cost/part(\$)	Assembly cost/part(\$)	Repeat count	Total costs(\$)
Dowel pins for punch	3.72	2.655	-	6.375
S.H.C.S for cavity	6.36	9.605	-	15.965
S.H.C.S for punch	1.88	2.265	-	4.145
Cavity	1776.45	80.805	1	1857.255
Punch	611.43	23.115	1	634.545
T-shape mould	2387.88	103.92	1	2491.8

2.8.4 T-shape mould cost breakdown

The mould costs are distributed according to the mould components. Figure 2.31 presents the cost breakdown of T-shape mould.

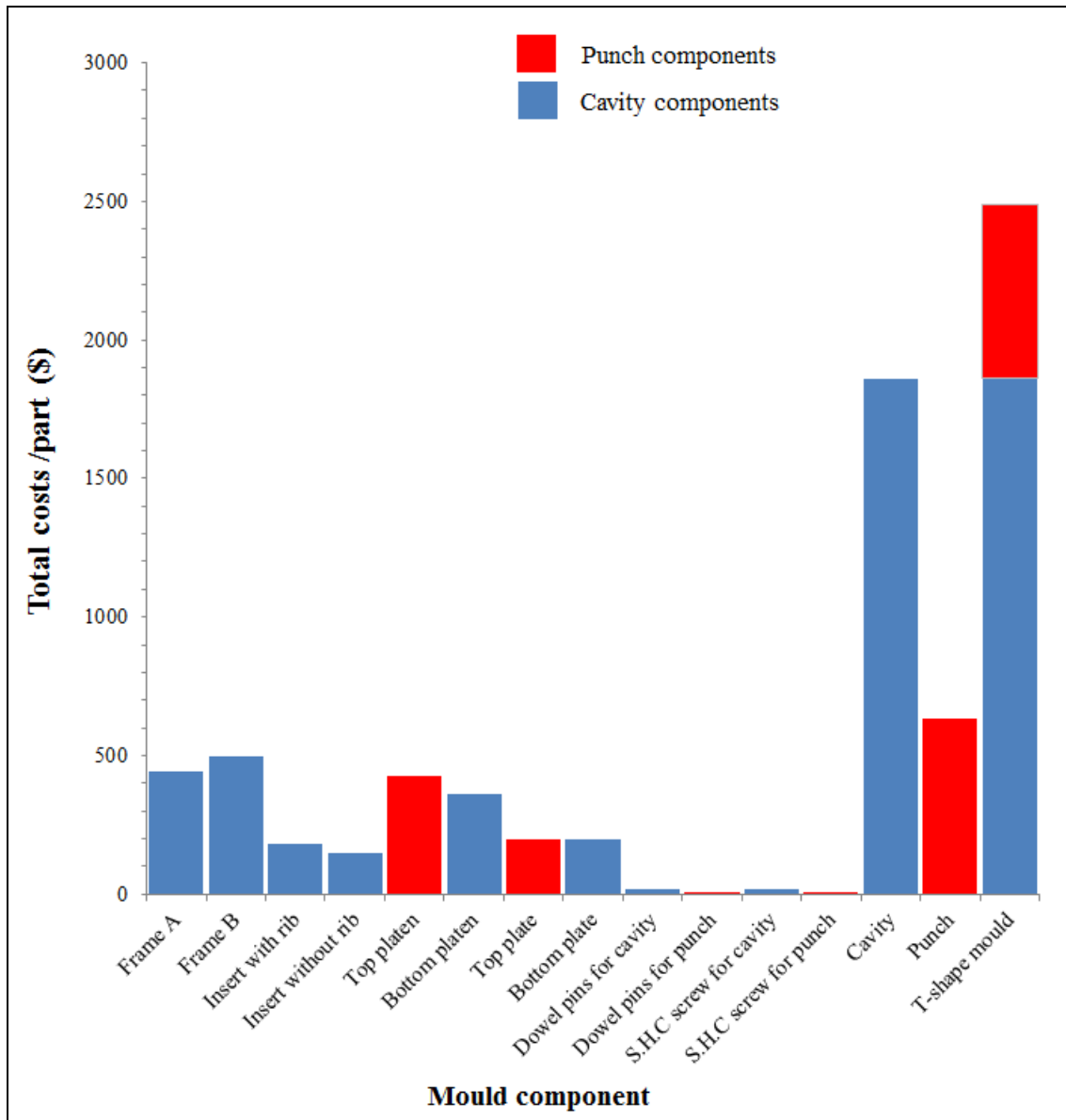


Figure 2.31 Cost breakdown of T-shape mould

2.8.5 Estimated and workshop costs comparison for the T-shape mould

Table 2.21 shows the comparison between the estimated and workshop costs for T-shape mould (LeBlanc, 2015).

Table 2.21 Workshop and estimated costs comparison for T-shape mould

Cost category	DFMA	Workshop
Manufacturing costs (\$)	2387.87	-
Assembly costs (\$)	103.93	-
Design costs (\$)	450	-
Total costs (\$)	2941.8	3000

2.9 L-bracket mould cost estimation

2.9.1 L-bracket mould manufacture process

The L- shape mould was composed primarily of the cavity and the punch. Two cavity closers were produced for use in closing the mould, and a rib insert was integrated in the punch in order to create a rib feature. The upper platen was produced to be used to heat and cool the punch. The mould manufacturing process was divided into two steps: the first was to cut parts from a rectangular bar stock, while the second consisted in cutting and removing materials from the parts. Milling and drilling operations were required to produce all the mould components. For the cavity block, the part was submitted to milling operations to produce features such as faces, slots, and pocket. For the punch block, the part was submitted to milling operations to create features such as faces, slots and the rib; the mould blocks were then submitted to drilling operations in order to produce different holes in all the components, followed by reaming, tapping or counter drilling operations to secure and install the heating cartridges, the thermocouples, and the cooling channels in the platens. After the machining operations, all the surfaces of the mould were polished and inspected. The features manufacturing data for L-bracket mould are presented in ANNEX III.

2.9.2 L-bracket mould assembly process

After the L-shape mould was machined and polished, it was assembled using socket head cap screws and dowel pins, and then checked to ensure that the mould components fit together properly. The moulds and the insulators were then affixed to the die sets, thereby assuring alignment during processing. Figure 2.32 shows the CAD of the L-shape mould fixture.

Table 2.22 presents the features assembly data for L-bracket mould.

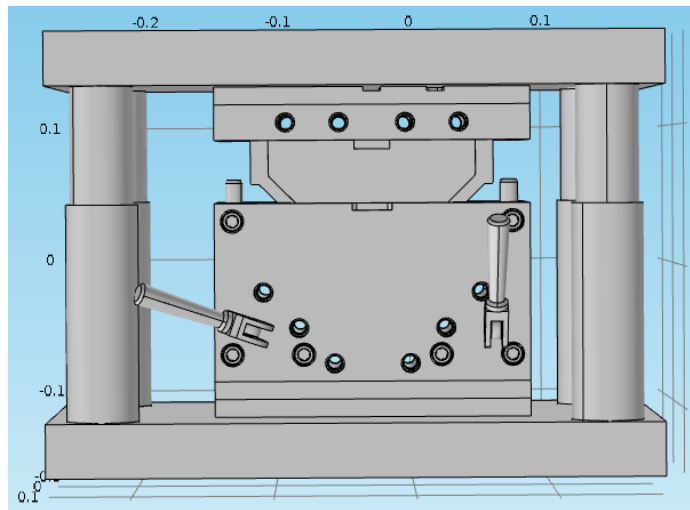


Figure 2.32 CAD of L-bracket mould fixture
Taken from (LeBlanc, 2014b)

Table 2.22 Features assembly data for L-bracket mould

Mould component	Securing method	Symmetry	Handling difficulty	Insertion difficulty	Operation time (s)	RC
Cavity	Secured later	One way	Two hands	Align	1203.8	1
Mould frame	Secured later	One way	Two hands	Align	2607.6	2
Bottom platen	Secured later	One way	No	Align	653.8	1
Punch	Secured later	One way	Two hands	Align	1003.8	1

Table 2.22 (Continued)

Mould component	Securing method	Symmetry	Handling difficulty	Insertion difficulty	Operation time (s)	RC
Punch mould rib	Secured later	One way	No	Align	503.8	1
Mould locker	Secured later	One way	No	Align	707.6	2
Punch cooling	Secured later	One way	Two hands	Align	753.8	1
Dowel pins	threads	One way	No	Align	1197	18
Socket head cap screws	Threads with manual fed	One way	No	Align	8110.4	31
L-bracket mould	-				16741.6	1

2.9.3 L-shape mould cost estimation results

Each mould component contributes to the total mould cost. The mould cost estimation was based on the manufacture and assembly, as well as on the number of components. The L-shape mould manufacturing cost results obtained by DFM software are presented in Table 2.23. The mould cost results obtained by the DFMA program for the L-shape mould are presented in detail in Table 2.24. The labor rates used in the DFM and DFA softwares are respectively 100\$/hour and 30\$/hour.

Table 2.23 L-shape mould manufacturing cost

Mould component	Material cost(\$)	Set up cost(\$)	Process cost(\$)	Rejects costs(\$)	Repeat count	Total costs(\$)
Female cavity	24.47	201.8	3034.51	57.97	1	3318.76
Frame	7.71	161.05	466.34	6.64	2	1283.47
Bottom plate	4.57	120.85	262.16	3.78	1	391.36
Punch	16.92	179.8	1963.48	36.24	1	2196.44
Punch rib	1.16	100.05	236.42	3.19	1	340.82

Table 2.23 (Continued)

Mould component	Material cost(\$)	Set up cost(\$)	Process cost(\$)	Rejects costs(\$)	Repeat count	Total costs(\$)
Locker	0.07	30.25	50.76	0.47	2	163.09
Punch cooling	7.25	141.6	547.33	7.98	1	704.16
Dowel pins for cavity	-	-	-	-	10	60
Dowel pins for punch	-	-	-	-	8	48
S.H.C.S for cavity	-	-	-	-	22	21.12
S.H.C.S for punch	-	-	-	-	9	2.35
L-shape mould	69.93	1126.7	7078.1	123.38	1	8529.5

Table 2.24 DFMA L-shape mould estimated cost

Mould component	Manufacturing cost/part(\$)	Assembly cost/part(\$)	Repeat count	Total costs(\$)
Female cavity	3318.76	11.8	1	3330.56
Frame	641.735	12.785	2	1309.04
Bottom plate	391.36	6.41	1	397.77
Punch	2196.44	9.84	1	2206.28
Punch rib	340.82	4.94	1	345.76
Locker	81.545	3.47	2	170.03
Punch cooling	704.16	7.39	1	711.55
Dowel pins for cavity	60	6.52	10	66.52
Dowel pins for punch	48	5.22	8	53.22
S.H.C screw for cavity	21.12	55.81	22	76.93
S.H.C screw for punch	2.35	25.92	9	28.27
Cavity	5074.71	106.11	1	5180.82
Punch	3454.86	60.25	1	3515.11
L-bracket mould	8529.57	166.36	1	8695.93

2.9.4 L-bracket mould cost breakdown

The mould costs are distributed according to the mould components. Figure 2.33 presents the cost breakdown of L-bracket mould.

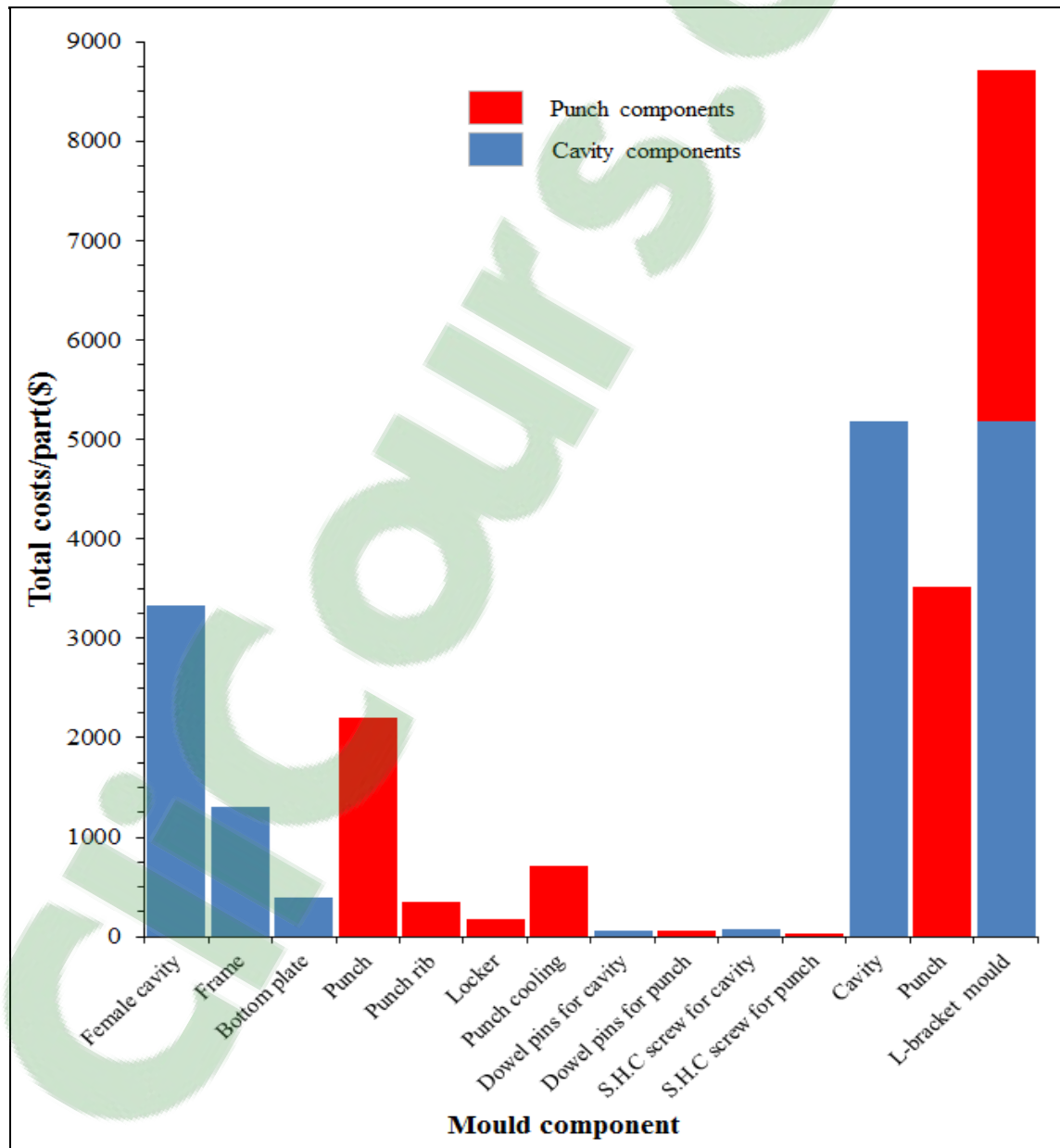


Figure 2.33 Cost breakdown of L-bracket mould

2.9.5 Estimated cost and commercial price comparison for L-shape mould

Table 2.25 presents a comparison between estimated and commercial costs for the L-shape mould (LeBlanc, 2015).

Table 2.25 Estimated cost and commercial price comparison for L-shape mould

Cost category	DFMA	Comments	Commercial
Manufacturing costs (\$)	8529.57	-	-
Assembly costs (\$)	166.36	-	-
Total costs (\$)	8695.93	46% of total estimated costs	-
Overhead + profit			
Design an Engineering costs (\$)	3700	20% of total estimated costs	-
Boxing and shipping costs (\$)	930	5% of total estimated costs	-
Optional FEM Analysis	-	-	-
Profit (\$)	3100	16% of total estimated costs	-
Taxes (\$)	2459.78	14.975% of total costs before taxes	-
Total estimated costs	18885.71		20000

2.10 Discussion of results and conclusion

For the flat plate, during the heating step, the model predicted almost the same temperature throughout the flat plate. However, there was an average difference of around 10% between the simulated and experimental temperatures for three specific locations on the middle surface of the ROS flat plate.

There was no significant difference in the heating time to reach the consolidated temperature of 380 °C from the ambient temperature of 22 °C, between the numerical and experimental results. The experimental heating time was approximately 147 minutes, whereas the simulated heating time was about 157 minutes. For the dwelling period, the average error between the simulated and experimental temperatures was around 2%.

For the cooling step, the average error between the numerical and experimental temperatures was approximately 15%. Conversely, the experimental cooling time (64 minutes) was approximately the same as that obtained by the numerical simulation (63 minutes).

Overall, the process cycle time, including the heating and cooling times estimated by the numerical modelling for a ROS flat plate, was validated thanks to an acceptable error of around 4% between the simulated and experimental times.

For the ROS T-shape part, during the heating step, the model predicted almost the same temperature throughout the part. However, there was an average difference of around 15% between the simulated and experimental temperatures through the thickness of the ROS T-shape part. There was no significant difference in the heating time to reach the consolidated temperature of 380°C from the ambient temperature of 25°C, between the numerical and experimental results. The experimental heating time was approximately 43 minutes, whereas the simulated heating time was about 46 minutes. For the dwelling period, the average error between the simulated and experimental temperatures was around 2%. For the cooling step, the average error between the numerical and experimental temperatures was approximately 1.5%. The experimental cooling time (77 minutes) was approximately the same as that obtained by the numerical simulation (80 minutes). Overall, the process cycle time, including the heating and cooling times estimated by the numerical modelling for a compression moulded thermoplastic composite ROS T-shape part, was validated thanks to an acceptable error of around 4% between the simulated and experimental times.

For the ROS L-bracket part, during the heating step, there was an average difference of around 5% between the simulated and experimental temperatures inside the part. There was no significant difference in the heating time to reach the consolidated temperature of 380 °C from a temperature of 85°C, between the numerical and experimental results. The experimental heating time was approximately 47 minutes, whereas the simulated heating time was about 46 minutes. For the dwelling period, the average error between the simulated and experimental temperatures was around 2%. As a result, the cycle time, including the heating and cooling steps estimated by the numerical modelling for a compression moulded thermoplastic composite ROS L-bracket part, was validated thanks to an acceptable error of around 10% between the simulated and experimental times.

The ROS parts heating energy costs comparison showed that the calculated heating energy costs of the three experimental part forms are different due to different geometries of the heating platens and the moulds used.

For the T and L-shape moulds, the estimated tooling costs results showed that the cavity costs are higher than the punch costs because cavity requires more components to make than for punch. The estimated T-shape mould costs are close to those of workshop. The errors between them are about 2% (only the design and engineering costs were estimated).

The estimated L-shape mould and flat mould costs were close to that of a commercial contractor with the error between them coming in at approximately 6% and 3%, respectively.

For all the ROS parts, by keeping the same cycle time the parts heating energy could be predicted for other similar geometries in function of the volumes of the parts with the condition to be limited to the size of platens and based on the cost results obtained for the three mould forms by the DFMA cost estimation software packages, the mould costs could be extrapolated and applied to other similar mould geometries by changing the projected mould area. Consequently, the tooling and energy costs complexity sizing and complexity scaling

laws for compression process moulded randomly oriented strands prepreg thermoplastics parts will be established in chapter 3.

CHAPTER 3

TOOLING AND ENERGY COSTS SIZING AND COMPLEXITY SCALING LAWS OF COMPRESSION PROCESS MOULDED RANDOMLY ORIENTED STRANDS THERMOPLASTIC EXPERIMENTAL PARTS

3.1 Introduction

The chapter 3 aims on one hand, at establishing the energy costs sizing and complexity scaling laws of compression moulded randomly oriented strands prepreg thermoplastic virtual parts, on the other hand, at generating the tooling costs sizing and complexity laws for virtual moulds.

3.2 Energy costs sizing scaling laws for ROS parts

In order to generate the heating energy costs sizing scaling laws for the ROS parts, the heating power was estimated for other similar geometries scaling with the part volume by keeping the same process cycle time. It is called virtual heating power. The heating power was calculated by multiplying the heating power density to the heating cartridge area and to the number of heating cartridges. The virtual heating powers were determined by changing the volume of the mould, the platens and the composite parts, in other words, by changing the area and the thickness of these components. The compression moulding process cycle time was simulated by the same methodology used in chapter 2 for experimental ROS parts. The thermal energy was calculated by using the necessary power for heating the compression moulding system at the desired temperatures. The heating energy and the energy costs were calculated using the equations (2.5) and (2.6) respectively.

3.2.1 Flat plate

From Tables 2.5, 2.9 and 2.13 it was found that the heating energy consumption of the experimental flat plate was higher than that of other part forms due to high size of heating

platens. Consequently the heating energy scale is not the same order of magnitude as that of other part forms. In order to be able to compare the energy costs of three types of parts virtual flat plates of comparable dimension of T-shape parts were simulated numerically using the same experimental protocol as the T- shape moulding process. The design of the virtual ROS flat plate in 3D is shown in Figure 3.1.

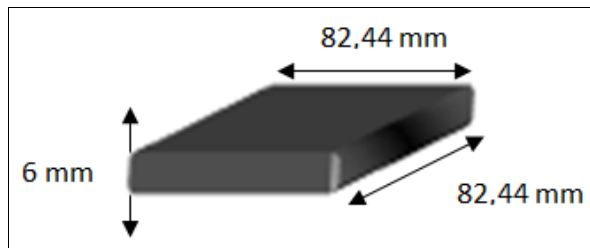


Figure 3.1 Design of ROS flat plate in 3D

3.2.1.1 Heating power simulation results scaling with volume of ROS flat plate

Table 3.1 presents the heating data and the heating power density simulation results scaling with volume of ROS flat plate.

Table 3.1 Heating data and heating power density simulation results scaling with volume of ROS flat plate

V_p (10^4 mm^3)	N.H.C	C.A (m^2)	H.P.D (w/m^2)	H.T (min)	H.P'.D (w/m^2)	H.T' (min)
4.077	8	0.0024	35200	30	10000	15.5
5.698	8	0.003	39200	30	10000	15.5
7491	8	0.0036	43200	30	10000	15.5
9.440	8	0.0042	47500	30	10000	15.5
11.533	8	0.0048	51700	30	10000	15.5

3.2.1.2 Heating energy cost calculation results scaling with volume of ROS flat plate

Table 3.2 presents the calculated heating energy and heating energy costs scaling with volume of ROS flat plate.

Table 3.2 Calculated heating energy and heating energy costs scaling with volume of ROS flat plate

Part volume (10^4 mm^3)	Total heating energy (kwh)	Energy rate (\$/kwh)	Heating energy costs (\$)
4.077	0.3961	0.0457	0.0181
5.698	0.5427	0.0457	0.0248
7.491	0.7114	0.0457	0.0325
9.440	0.9008	0.0457	0.0411
11.533	1.1106	0.0457	0.0507

3.2.2 T-shape part

The design of the ROS T-shape part in 3D is shown in Figure 3.2

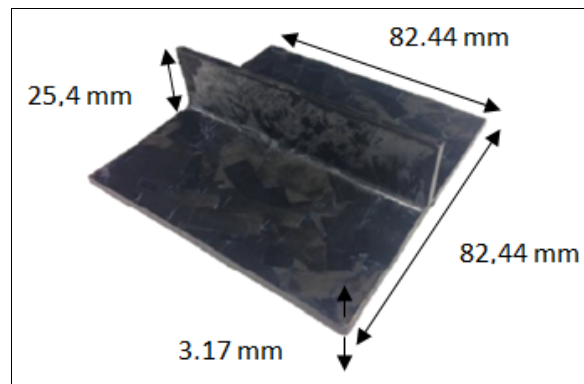


Figure 3.2 Design of the ROS T-shape
Reproduced and adapted with permission
of Leblanc et al. (2014a, p.4)

3.2.2.1 Heating power simulation results scaling with volume of ROS T-shape part

Table 3.3 presents the heating data and the heating power density simulations results scaling with volume of ROS T-shape part.

Table 3.3 Heating data and heating power density simulation results scaling with volume of ROS T-shape part

V_p (10^4 mm^3)	N.H.C	C.A (m^2)	H.P.D (w/m^2)	H.T (min)	H.P'.D (w/m^2)	H.T' (min)
2.817	8	0.0024	54000	30	16000	15.5
4.195	8	0.003	65000	30	16500	15.5
5.842	8	0.0036	76000	30	16500	15.5
7.758	8	0.0042	87500	30	16500	15.5
9.944	8	0.0048	99700	30	16500	15.5

3.2.2.2 Heating energy cost calculation results scaling with volume of ROS T-shape part

Table 3.4 presents the calculated heating energy and heating energy costs scaling with volume of ROS T-shape part.

Table 3.4 Calculated heating energy and heating energy costs scaling with volume of ROS T-shape part

Part volume (10^4 mm^3)	Total heating energy (kwh)	Energy rate (\$/kwh)	Heating energy costs (\$)
2.817	0.6098	0.0457	0.0278
4.195	0.8942	0.0457	0.0408
5.842	1.2411	0.0457	0.0567
7.758	1.6610	0.0457	0.0759
9.944	21459	0.0457	0.0980

3.2.3 L-bracket part

The design of the ROS L-bracket in 3D is shown in Figure 3.3.

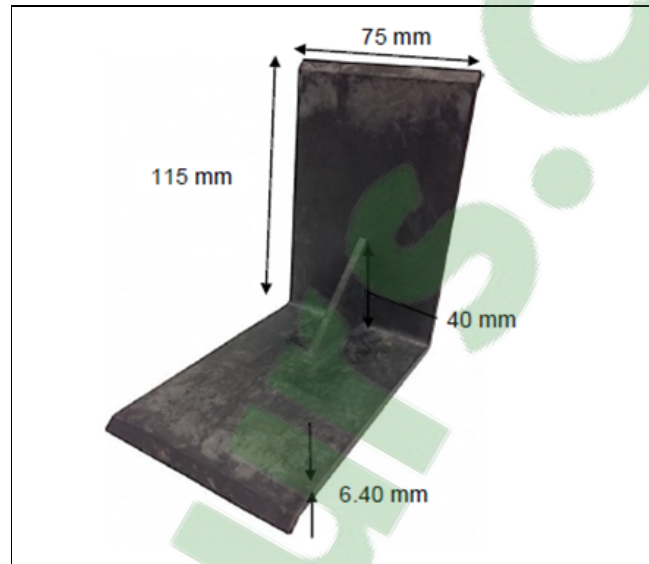


Figure 3.3 Design of the ROS L-bracket
Taken from Leblanc et al. (2014b, p.9)

3.2.3.1 Heating power simulation results scaling with volume of ROS L-bracket part

Tables 3.5 and 3.6 present respectively the heating data, the heating power density simulation results and the heating power calculation results scaling with volume of ROS L-bracket.

Table 3.5 Heating data and heating power density simulation results scaling with volume of ROS L-bracket

V_p (10^4 mm^3)	N.H.C	C.A (m^2)	H.P.D (w/m^2)
11.552	2	0.0018	103885
11.552	4	0.0038	125103
11.552	2	0.0025	76386

Table 3.5 (Continued)

V_p (10^4 mm^3)	N.H.C	C.A (m^2)	H.P.D (w/m^2)
16.143	2	0.0023	122923
16.143	4	0.0048	155880
16.143	2	0.0031	90384
21.222	2	0.0027	133682
21.222	4	0.0058	169203
21.222	2	0.0037	98295
26.743	2	0.0032	140815
26.743	4	0.0068	182717
26.743	2	0.0043	103539
32.674	2	0.0037	146164
32.674	4	0.0078	190354
32.674	2	0.0050	107473

Table 3.6 Heating power calculations results scaling with volume of ROS L-bracket

V_p (10^4 mm^3)	H.P ₁ (w)	H.P ₂ (w)	H.P ₃ (w)	H.T ₁ (min)	H.T ₂ (min)	H.T ₃ (min)
11.552	2710	1200	595	1812	258	724
16.143	3750	1620	775	1812	258	724
21.222	4880	2085	955	1812	258	724
26.743	6010	2595	1125	1812	258	724
32.674	7220	3120	1310	1812	258	724

3.2.3.2 Heating energy cost calculation results scaling with volume of ROS L-bracket

Table 3.7 presents the calculated heating energy and the heating energy costs for the ROS L-bracket scaling with part volume.

Table 3.7 Calculated heating energy and heating energy costs scaling with the volume of ROS L-bracket

Part volume (10⁴ mm³)	Total heating energy (kwh)	Energy rate (\$/kwh)	Energy costs (\$)
11.552	1.5696	0.0457	0.0717
16.143	2.1594	0.0457	0.0986
21.222	2.7977	0.0457	0.1278
26.743	3.4372	0.0457	0.1570
32.674	4.1211	0.0457	0.1883

3.2.3.3 ROS part heating energy sizing scaling laws

Figure 3.4 shows the heating energy of three ROS parts in function of the part volume. Table 3.8 presents the heating energy sizing scaling laws for three ROS part forms.

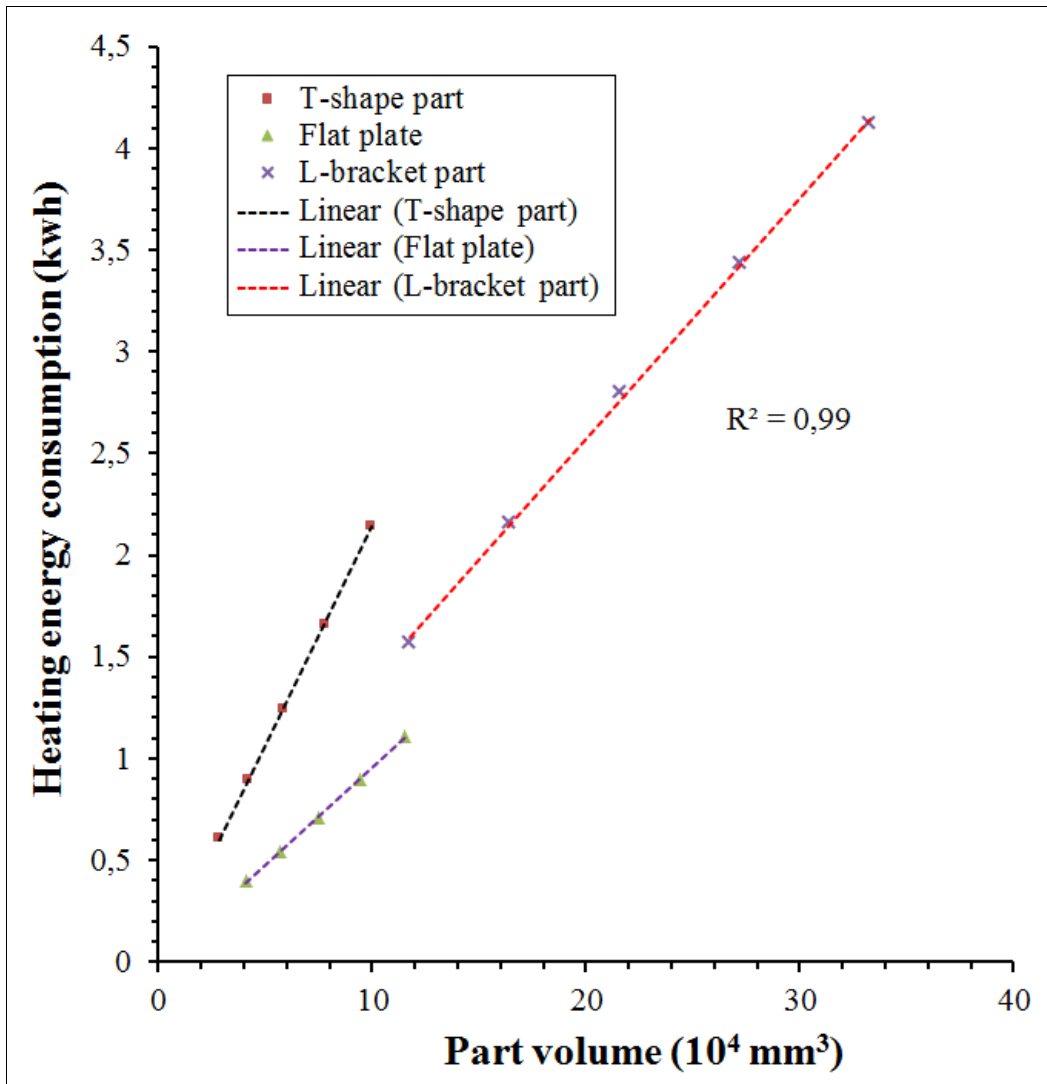


Figure 3.4 Heating energy of three ROS parts in function of the part volume: Flat plate, T-shape and L-bracket

Table 3.8 Heating energy sizing scaling laws for three ROS part forms: Flat plate, T-shape and L-bracket

Part form	Sizing scaling laws	Remarks
L-bracket part	$y = 0.1206 x + 0.2041$	y: Heating energy (kwh) x: Part volume (10 ⁴ mm ³) Heating energy sizing scaling laws are in linear form (trend curve)
T-shape mould	$y = 0.2158 x - 0.0081$	
Flat mould	$y = 0.0959 x - 0.0011$	

3.2.3.4 ROS part heating energy costs sizing scaling laws

Figure 3.5 shows the heating energy costs of three ROS parts in function of the part volume.

Table 3.9 presents the heating energy costs sizing scaling laws for three ROS part forms.

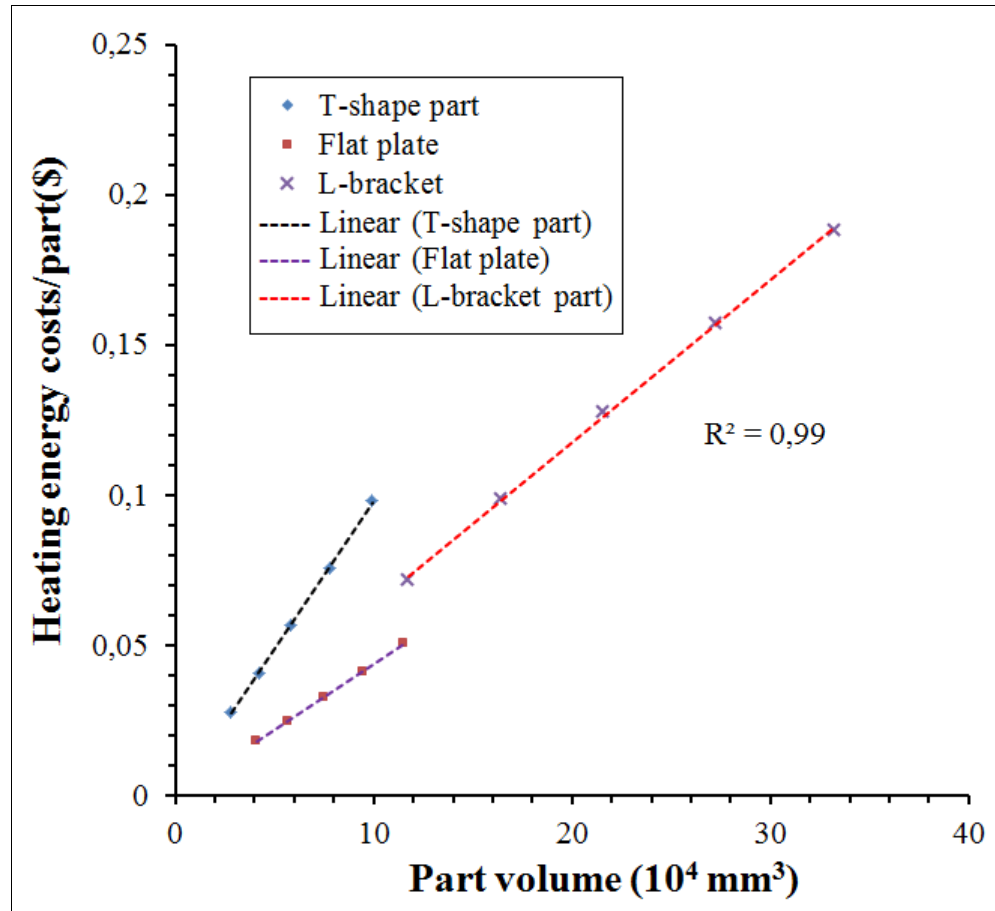


Figure 3.5 Heating energy costs of three ROS parts in function of the part volume: Flat plate, T-shape and L-bracket

Table 3.9 Heating energy costs sizing scaling laws for three ROS part forms

Part form	Sizing scaling laws	Remarks
L-bracket part	$y = 0.0055 x + 0.0093$	y: Heating energy cost (\$) x: Part volume (10^4 mm^3) Heating energy costs scaling law are in linear form (trendline)
T-shape mould	$y = 0.0099 x - 0.0004$	
Flat mould	$y = 0.0044 x - 0.00005$	

3.2.3.5 ROS parts heating energy complexity scaling laws

In order to consider the complexity level of part geometry, the heating energy consumption and the heating energy costs of three part forms were calculated for the same volume of the parts. Figure 3.6 shows the heating energy consumption scaling with complexity of the part.

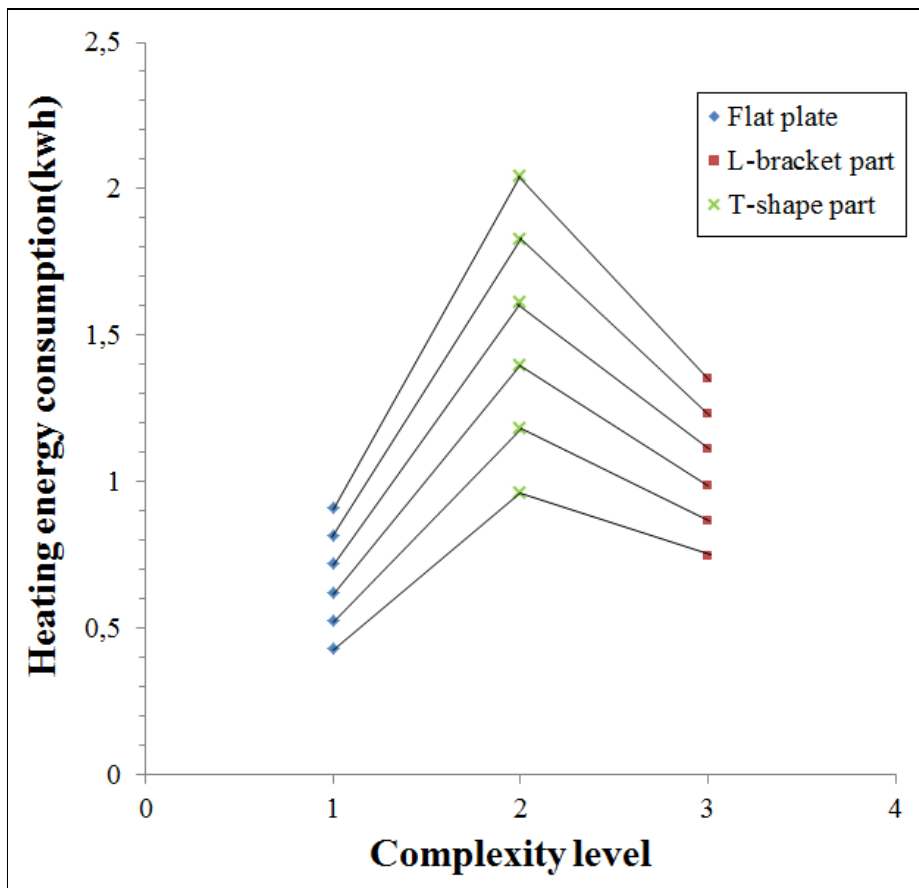


Figure 3.6 Heating energy consumption scaling with complexity of the part

Based on the same volume of the parts, the calculated heating energy for T-shape part is higher than that for L-bracket even if L-bracket is more complex than T-shape part.

3.3 Tooling costs sizing scaling laws for ROS parts

The methodology for estimating the tooling cost of three mould forms using DFMA software of Boothroyd and Dewhurst Inc. was already described in the chapter 2. The mould costs

sizing scaling laws were established by making extrapolation for other mould similar geometry, scaling with projected area of the mould, which is more important variable comparing to the thickness due to low pressure applied to the part. It is about virtual mould. In reality the virtual mould costs were estimated by changing the volume of the mould which means the area and the thickness of the mould. In order to make the cost analysis of the moulds, it important to consider the costs components during the manufacturing process such as the manufacturing and assembly costs calculated by DFMA and overheads such design and engineering costs, boxing and shipping costs, taxes and the commercial profits which correspond to the return on investment. Table 3.10 presents the estimated tooling costs for L-bracket mould, T-shape mould and flat mould scaling with the mould projected area.

Table 3.10 Estimated tooling costs for L-bracket mould, T-shape mould and flat mould scaling with mould projected area

Mould form	Mould projected area (10 ⁴ mm ²)	Mould costs (\$)	
		Manufacturing and assembly costs (DFMA)	Estimated prices
L-bracket mould	2.756	8695.93	18885.71
	3.445	9457.06	20508.16
	4.134	10447.11	22669.75
	4.823	11510.61	24984.77
T-shape mould	1.032	2491.8	5630.10
	1.613	2897.78	6591.26
	2.323	3188.05	7218.19
	3.161	3701.33	8365.96
	4.129	4088.28	9236.26
Flat mould	1.032	2088.01	5108.35
	1.613	2379.87	5817.59
	2.323	2806.21	6848.15
	3.161	3155.59	7709.75
	4.129	3516.64	8602.02

Figure 3.7 shows the tooling costs vs. the projected area for L-bracket mould, T-shape mould and flat mould. Table 3.11 presents the tooling costs sizing scaling laws for L-bracket mould, T-shape mould and flat mould.

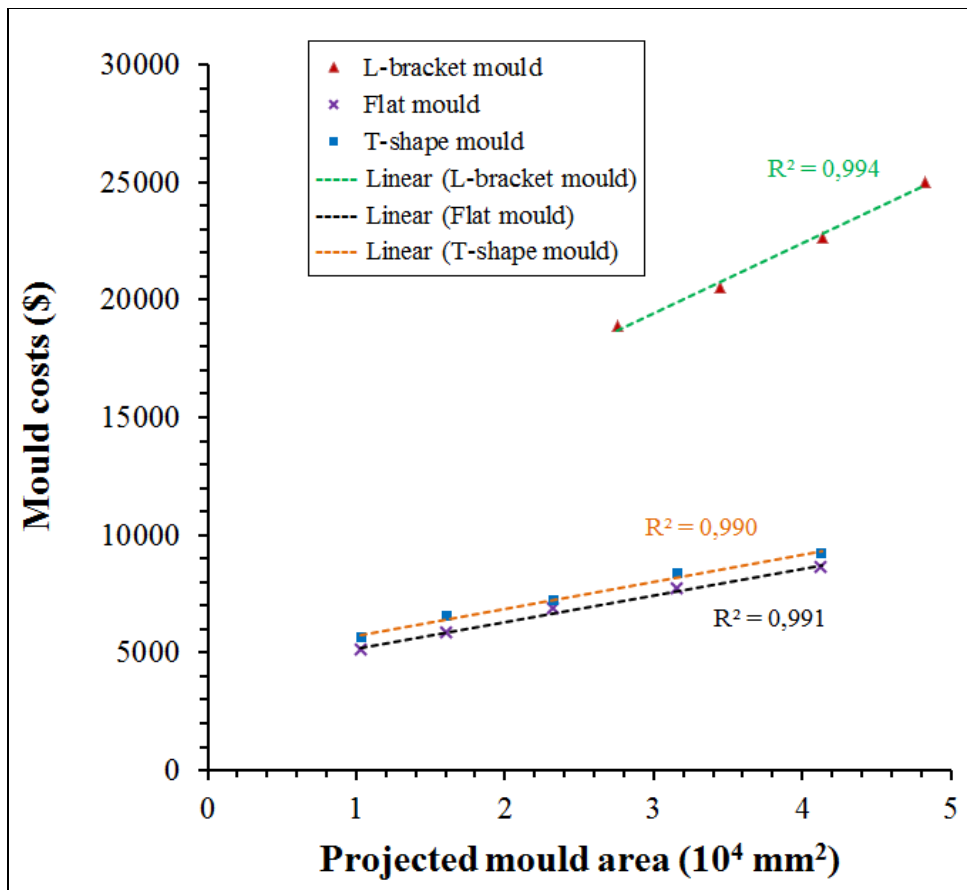


Figure 3.7 Tooling costs vs. projected area for L-bracket mould, T-shape mould and flat mould

Table 3.12 Tooling costs sizing scaling laws for L-bracket mould, T-shape mould and flat mould

Mould form	Sizing scaling laws	Remarks
L-bracket mould	$y = 2969.5 x + 10510$	y : Mould cost (\$) x : Projected mould area (10 ⁴ mm ²) Mould costs sizing scaling laws are in linear form
T-shape mould	$y = 1153.3 x + 4581$	
Flat mould	$y = 1138 x + 4027.3$	

3.4 Tooling costs complexity scaling laws

In order to consider the complexity level, the mould costs were calculated for the same projected area of the mould. Figure 3.8 shows the moulds costs for L-bracket mould, T-shape mould and flat mould scaling with complexity level of the mould.

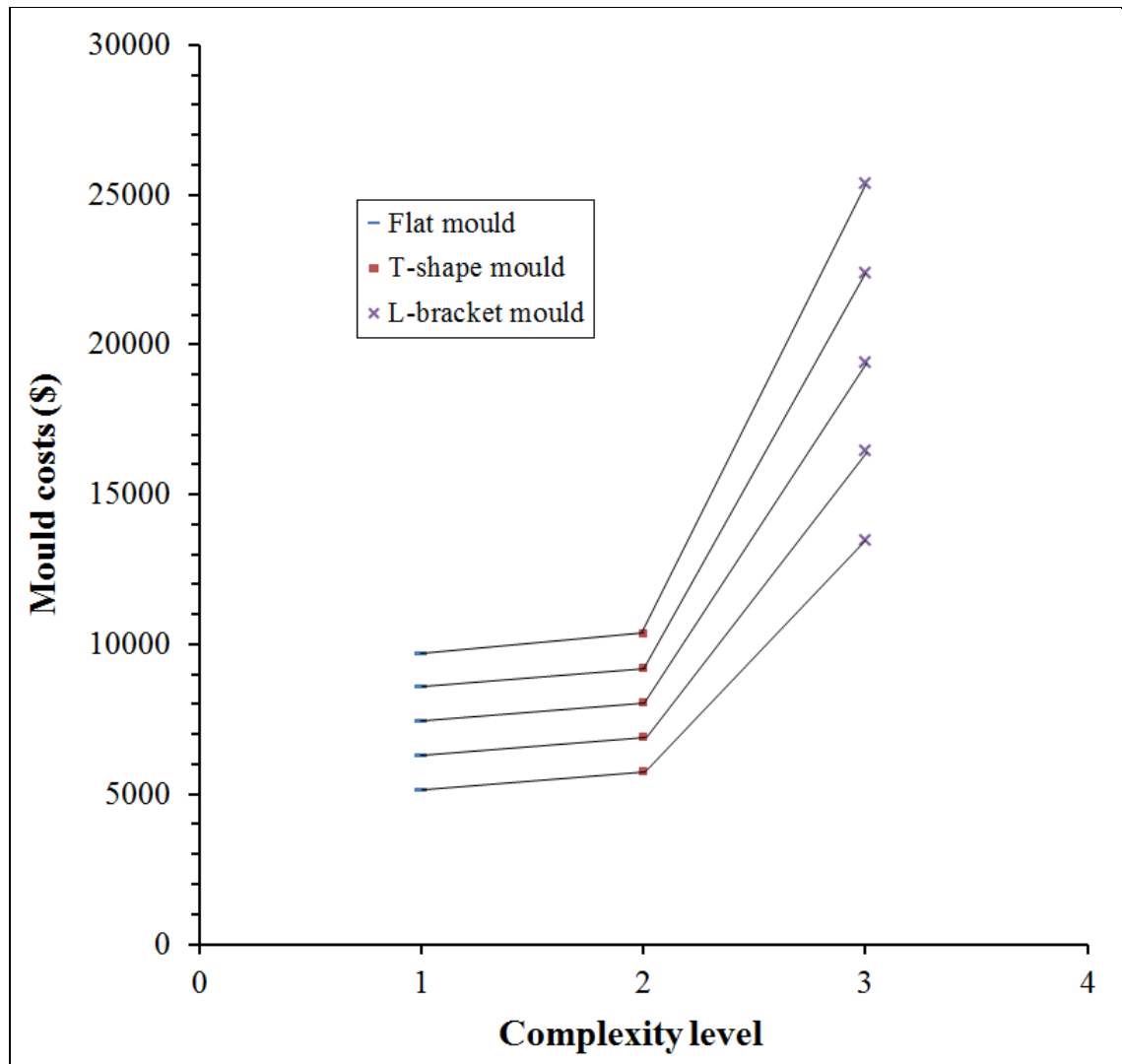


Figure 3.8 Moulds costs for L-bracket mould, T-shape mould and flat mould scaling with complexity level of the mould

3.5 Discussion of results and conclusion

From the heating energy costs calculations for the three ROS part forms scaling with part volume, the heating energy costs sizing scaling laws were established in linear forms for different respective determination coefficients and limited to the size of platens areas.

The heating energy costs comparisons showed that there is a significant difference in terms of heating energy cost between different part forms. The heating energy of T-shape part is higher than those of flat plate and L-bracket. It was concluded that the heating energy does not depend on the complexity of part but it was influenced by the weight of the heated components, on another words, by the volume and the material properties of these components.

From the costs estimations for three moulds forms scaling with the projected area of the mould, the tooling costs sizing scaling laws were established in linear forms for different respective determination coefficients and limited to the size of platens areas.

In order to make tooling costs comparisons, the tooling costs scaling with their projected mould area were normalized in term of the overheads and the profits. In term of complexity, the tooling costs were normalized to the same projected area in order to show the tooling costs complexity laws.

The tooling costs comparisons showed that the L- shape mould costs are higher than T-shape mould costs which are higher that flat mould costs. Therefore, it was concluded that the more complex the mould is the higher the cost.

CHAPTER 4

TOOLING AND ENERGY COSTS ESTIMATION FOR COMPRESSION PROCESS MOULDED UNIDIRECTIONAL FIBRE CARBON PREPREG THERMOPLASTIC EXPERIMENTAL PARTS

4.1 Introduction

The conducted study in this chapter is divided into two sections. The first section presents the techniques and the results of estimation of energy costs for unidirectional carbon fibre prepreg thermoplastic parts manufactured by compression moulding process. As stated in the previous chapter, the process energy includes heating energy and mechanical energy. The mechanical energy is the mechanical power multiplied by the cycle time of the press. The mechanical power is the force applied in compression moulding system by the pressing speed. It was demonstrated that the mechanical energy cost per part is very low and can be neglected (Cardonne, 2015). Thus, they are integrated in investment costs calculation of the press. The second section presents the methodology and the results of estimating the tooling costs used for manufacturing these categories of parts.

4.2 Cycle time simulations and energy costs estimation for UD parts

This section consists to simulate the process cycle time and calculate the heating energy costs for UD concave part. The process cycle time includes the heating time and the cooling time. The heating step was divided in two periods: the first one is preheating of the laminate and the second one is heating of the concave mould. These two periods were simulated by the transient thermal analysis module of the commercial COMSOL Multiphysics® software in order to determine the transient temperature distribution versus the heating time through the laminate and inside the concave mould. The heating power was simulated by adjusting the necessary heat source rate applied respectively at the surfaces of infrared radiators panels and at the surfaces of the heating cartridges in order to get the processing temperature for a

specific heating time. The heating energy and the heating energy costs of the laminate and the concave mould were calculated by applying equations (2.5) and (2.6).

4.2.1 Material

The material used in this study is a prepreg from Royal Tencate Corp, composed of PEEK reinforced by continuous unidirectional carbon fibres. The fibre contains a volume fraction of 59% and has a layer of about 0.14 mm. Different flat plates were moulded using flat mould which was heated by the press platens. The flat plates were laminates made out of 24 plies with a [0/90]₁₂ stacking and they were cut into test blanks of 241.4 mm x 152.4 mm x 3.35 mm. The laminate was preheated in an infrared oven. The infrared oven used to heat the laminate consists of 18 ceramic infrared radiators panels of 1000 w each made by ZrO₂ from (Elstein-Werk). Table 4.1 presents the thermal and physical proprieties of materials (Acuratus, 2013; AZoM, 2001; Callister, 2005; NIST). The thermal and physical proprieties of CF/PEEK were mentioned in chapter 2. Only the proprieties of the steel and the air can be taken from the database of the COMSOL software.

Table 4.1 Physical and thermal properties of ZrO₂

Proprieties	Unit	ZrO ₂	Glass ceramic
Density	(kg/m ³)	6000	3200
Specific heat	J.kg ⁻¹ .K ⁻¹	550	790
Thermal conductivity	W.m ⁻¹ .K ⁻¹	2.5	1.46

4.2.2 Compression moulding process of concave part

The studied part was a concave part moulded using a concave mould which has been designed at the University du Québec à Trois-Rivières (UQTR) and manufactured by a

contractor. The laminate already specified was preheated in an infrared oven and transferred to the concave mould by a support frame in ten seconds then compressed by 50 tons hydraulic press. The concave mould was already preheated by a control system to the desire temperature. A data acquisition system (computer with LABVIEW program) was connected to the infrared sensor of oven, to the thermocouples embedded in the laminate and in the concave mould (punch and cavity) (Lessard, Lebrun et Pham, 2013). The manufacturing cell of the concave part is divided into six activities as shown in Figure 4.1. The experimental set up of manufacturing of concave part is shown in Figure 4.2.

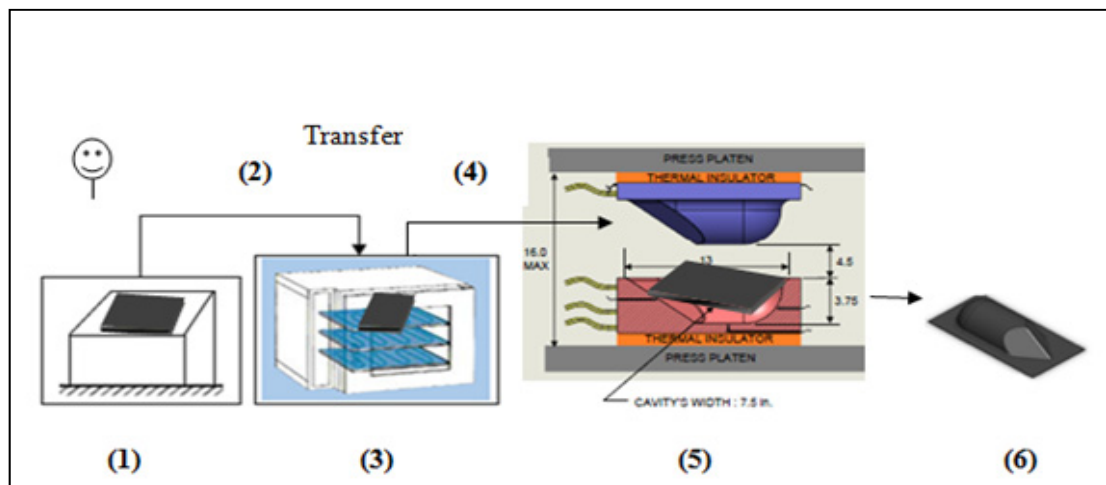


Figure 4.1 Manufacturing cell of concave part. (1) preparation of the laminate, (2) placing the laminate in the IR oven, (3) heating the laminate in the IR oven, (4) transfer of heated laminate to press, (5) compression moulding of part, (6) demoulding of the cooled concave part

Reproduced and adapted with the permission of Lessard et Lebrun (2011)

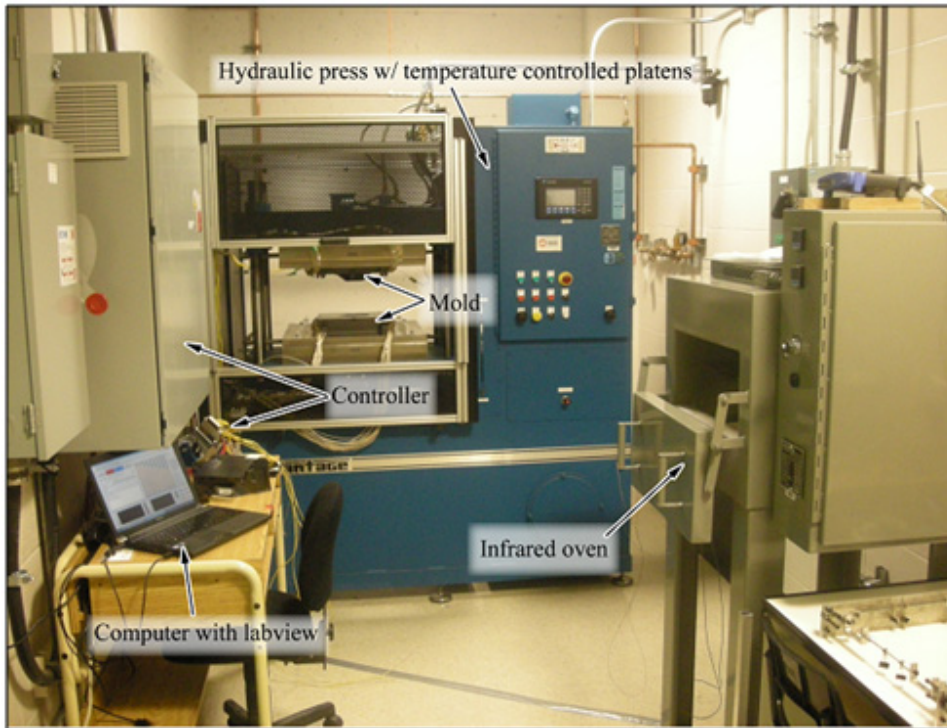


Figure 4.2 Experimental setup
 Taken from Lessard, Lebrun, Pham (2013, p.4)

4.2.2.1 Heating step

- **Preheating of the laminate**

An Infrared oven used to heat the laminate consists of 18 ceramic infrared radiator panels of 1000 w each made of ZiO_2 , which were distributed evenly on the top and the bottom of the oven with regard to the laminate to get a uniform temperature. Each infrared ceramic radiator panel is a square with a side of 125 mm and 21.5 mm high and was embedded in a resistance wire. The distance between the laminate and infrared radiators is 254 mm. These radiators can be used for operating temperatures up to 860 °C and give the radiative intensity up to 64 kw/m² for one heating side with spectral wavelength range of 2 to 10 μ m (Elstein-Werk). Figure 4.3 shows the design of the Elstein ceramic infrared radiators panels. In order to measure and control the temperature inside the laminate, three thermocouples were placed in three different positions through the thickness of the laminate. An infrared temperature

sensor, located in the bottom of the oven and pointing to the lower surface of the laminate, was used to measure and control its temperature with a PID controller(Lessard, Lebrun et Pham, 2013).The position of the thermocouples through the laminate is shown in Figure 4.4.

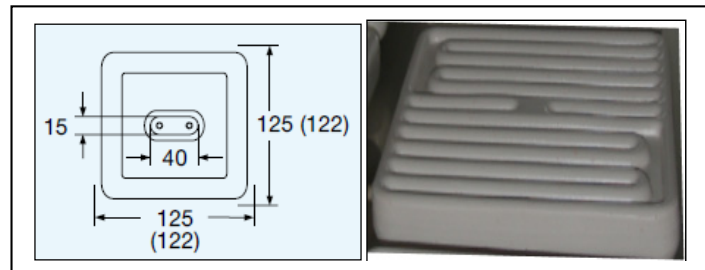


Figure 4.3 Design of Elstein ceramic infrared radiator (HTS series)
Taken from (Elstein-Werk)

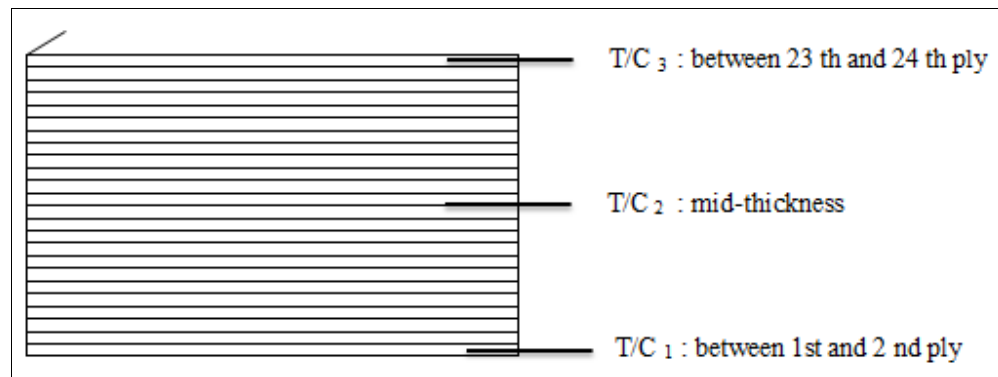


Figure 4.4 Position of thermocouples through the thickness of the laminate

- **Heating of the mould**

Before moulding, the concave mould was heated by cylindrical heating cartridges. The surface of the mould was maintained to the temperature of 360 °C by a temperature control unit using embedded thermocouples. The mould having the geometry of a quarter sphere at one extremity, a half cylinder in the middle and two slanted surfaces at the other extremity(Lessard, Lebrun et Pham, 2013) was manufactured using machining process by a

contractor of the University du Québec à Trois-Rivières (UQTR). The geometry of two halves of the mould and the top and bottom views of the concave part are shown in Figure 4.5.

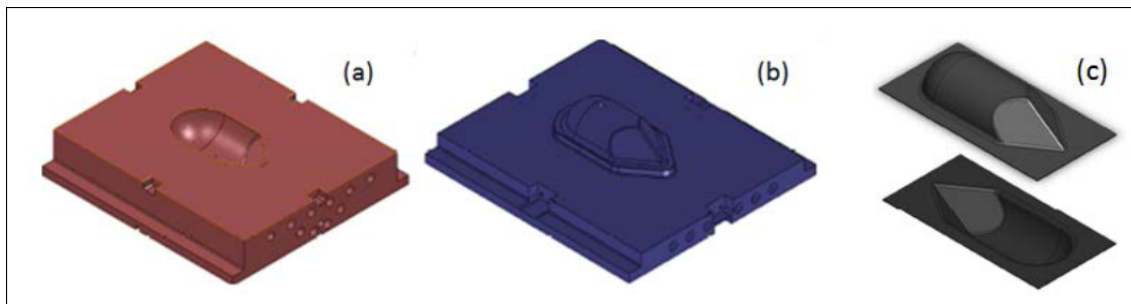


Figure 4.5 a) Cavity block, (b) Punch block,
 (c) Top and bottom views of concave part
 Reproduced and adapted with permission of Lessard (2012a)
 and Lessard et Lebrun (2011)

4.2.2.2 Cooling step

When the laminate was heated up to 420 °C, it was transferred by a support frame from the infrared oven to a P20 tempered steel mould and was put between the punch and the cavity already heated. Afterwards, the mould was closed and the laminate was compressed by a 50 tons press, submitted to a pressure measured and controlled by a pressure transducer integrated in the punch. When the laminate reached the temperature of the mould, it started to cool down by a cooling channel integrated inside the platens to the demoulding temperature. The mould was opened and the part was removed afterwards (Lessard, Lebrun et Pham, 2013).

4.2.3 Mathematical model and heat transfer processes

The heat transfer mechanisms occurring in infrared oven between the IR ceramic radiators, the composite laminate and the IR oven walls during the preheating stage are shown in Figure 4.6. It was assumed that there were no temperature gradients through the thickness of

each ply. Only the natural convection between the composite laminate and the surrounding air was considered in this study. The developed model consists to consider the laminate as a semi-infinite solid submitted to a uniform incident heat flux emitted by the IR ceramic radiators. Admitting that convection heating is under boundary conditions form, the transient temperature through the laminate is given by solving the 3D heat transfer equation (4.1).

$$\rho C_p \frac{\partial T}{\partial t} = \nabla \cdot (k \nabla T) - \nabla \cdot q_r \quad (4.1)$$

Where ρ , C_p , k and q_r are respectively the specific mass, the specific heat capacity, the thermal conductivity of CF/PEEK and the radiative heat flux absorbed by the laminate. The heat capacity C_p is considered to be temperature-dependent. For the other domains, the heat transfer is described by equation (4.2).

$$\rho C_p \frac{\partial T}{\partial t} = \nabla \cdot (k \nabla T) \quad (4.2)$$

The thermo-physical proprieties of the other materials are given as average values in the range of temperature 20 to 450 °C .These properties are presented in Table 4.1. In order to simplify the problem, the radiative flux emitted by the IR ceramic radiators is assumed to be one dimensional across the thickness of laminate in z-direction and to behave like isothermal, grey, diffuse and opaque surfaces with emissivity ϵ supposed to be constant. The solution of heat transfer equation (4.1) can be obtained on two steps: The first step consists to resolve the radiative heat transfer equation in order to obtain the radiative intensity absorbed by the laminate using the radiosity method by taking into account the view factors. However, in the case of the opacity of CF/PEEK composite material, resolving the radiative heat transfer equation is so complicated. In the second step, the absorbed radiative intensity is then implemented into equation (4.1) in order to calculate the transient temperature in the laminate by considering the convective boundary conditions. As the surface of the laminate is opaque, the transmittivity is always set to zero, therefore, two modes of propagations of the radiation

are considered: reflection and absorption. Considering the isotropic propriety of the surface of the laminate, the emissivity and absorptivity are equal according to equation (4.3).

$$\varepsilon = \alpha = 1 - \rho \quad (4.3)$$

The surface emissivities of different materials were taken from the literature. They are presented in Table 4.2.

Table 4.2 Surface emissivities
Taken from Grouve (2012) ;
(Protherm) and Tanaka et al. (2001)

Material	Emissivity
ZiO ₂ (Infrared radiators)	0.65
CF/PEEK (laminate)	0.9
Steel (oven walls)	0.75

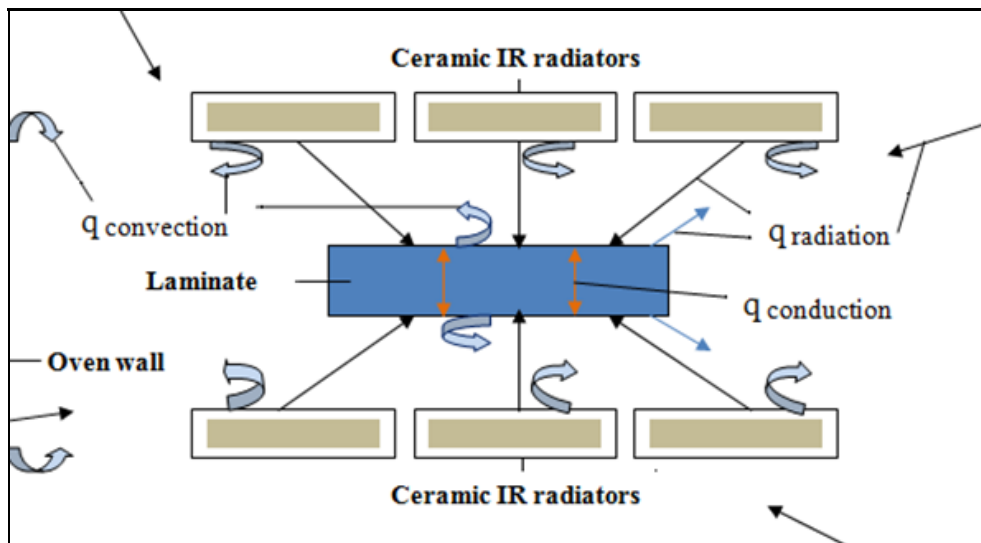


Figure 4.6 Heat transfer mechanisms in the IR oven

4.2.4 Numerical simulations

4.2.4.1 Heating step simulation

The geometry model is composed of the oven walls, ceramic infrared radiators, the air volume inside the oven and the laminate. The model simulates these elements as blocks located at different positions in the space 3D (x,y,z). The oven walls were modeled by surface blocks whereas the other objects were modeled by solid blocks. The infrared radiators blocks were distributed on top and the bottom inside the oven for a superficial heat source rate of 52.3 kw/m², which corresponds to about 80% of the power efficiency. The laminate block was placed in the middle position at the same distance between the top and the bottom infrared radiators. Figure 4.7 shows the geometry of the model for simulation of infrared preheating step. The infrared radiators present symmetrical positions with the respect to the laminate. The time-dependent study is selected in order to know the evolution of temperature in the laminate by steps of time. The heating time was defined in the range from 0 to 260 s with a step of 5 s. It is the necessary time to reach the temperature of 420 °C. The boundary thermal conditions during the pre-heating stage are described as follows: The initial value of temperature in the whole model was fixed to 60°C. The boundary conditions at the surface of the laminate are radiative and convective .They are given by equations (4.4) and (4.5).

$$n.(k\nabla T) = h(T_{air} - T) + \varepsilon(G - \sigma T^4) \quad (4.4)$$

$$(1 - \varepsilon)G = J_0 - \varepsilon\sigma T^4 \quad (4.5)$$

Where G , σ , ε et J_0 are respectively Irradiation, Boltzmann constant, emissivity and radiosity intensity.

In order to get the uniformity of 420°C through the laminate, the heat source rate was reduced to 5000 kw/m². Formula (4.6) was set in the COMSOL program at the surfaces of the laminate such as:

$$(T - 420[\text{degC}]) * (T < 420[\text{degC}]) + 420[\text{degC}] \quad (4.6)$$

Where h is a heat transfer coefficient ($10 \text{ W/m}^2\cdot\text{K}$) (Raj et al., 2011) and T_{air} is the temperature of the air inside the oven. The convective heat transfer mode occurred at all the surfaces of the laminate, whereas the radiative heat transfer was the surface to surface radiation mode. As the laminate was heated in the infrared oven which is a closed domain, the natural convective cannot be applied at the surface the laminate in COMSOL program,. However, an approximation can be made between at the surfaces of the laminate and the nearest surfaces of the air block inside the oven using formula (4.7).

$$h * (bnd_{air} - bnd_{laminate}) \quad (4.7)$$

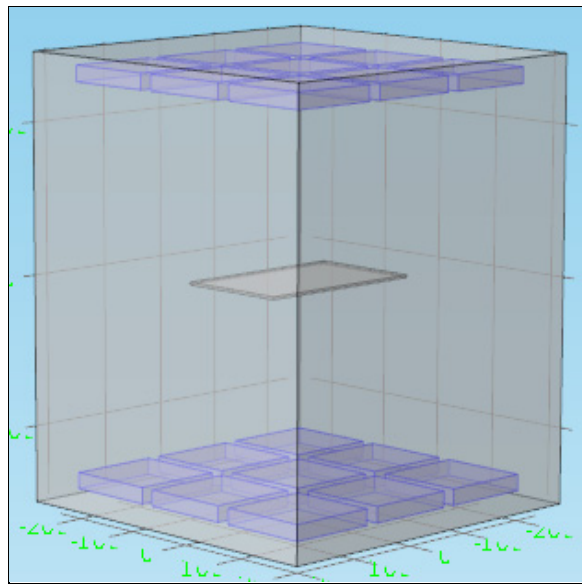


Figure 4.7 Geometry of the model for simulation of infrared pre-heating step

The mould heating time and the distribution of temperature through the mould were simulated using the transient thermal analysis module of the commercial COMSOL software by solving numerically the heat transfer equation (2.1) based on the 3D finite elements method. The time-dependent study was selected in order to assess the evolution of temperature in the concave mould by steps of time. The boundary thermal conditions during

the heating of the concave mould were as follows: for the convective heat transfer, the initial value of air temperature was fixed to 22°C; the initial value of temperature in the whole model was fixed at 25°C . However, for energy calculation, the temperature of 170°C was considered because the concave part was removed at this temperature after cooling stage for a certain production volume. The necessary power density applied at the heating cartridges areas was adjusted in order to reach the temperature 360 °C .The time of maintaining this temperature was also simulated. The upper of the punch block and the bottom of the cavity block were isolated.

The laminate transfer time from the IR oven to the mould was the time corresponding to the decrease of the laminate temperature until 380°C , this time was simulated and defined in the range from 0 to 20 s with a step of 5 s. The time for reaching of the mould temperature was simulated and defined in the range from 0 to 50 s with the step of 5 s.The infrared radiators present symmetrical positions with the respect to the laminate. The geometry characteristics of the pre-heating model are presented in Table 4.3.

Table 4.3 Geometry characteristics of the pre-heating model

Domains		Nature	Dimensions (x, y, z) (mm)	Position (x, y, z) (mm)	
Infrared radiators	Top	Solid blocks	125 x 125 x 21.5	1	(0,0,266.42)
				2	(140.5,0,266.42)
				3	(-140.5,0,266.42)
				4	(0,140.5,266.42)
				5	(0,-140.5,266.42)
				6	(140.5,-140.5,266.42)
				7	(-140.5,-140.5,266.42)
				8	(140.5,140.5,266.42)
				9	(-140.5,140.5,266.42)
	Bottom				Symmetrical positions
Composite plate (CF/PEEK)		Solid block	241.4 x 152.4 x 3.352	(0,0,0)	
Oven walls(steel)		Surface block	481 x 481 x 590	(0,0,0)	
Air volume		Block	481 x 481 x 590	(0,0,0)	

The pre-heating geometry model was meshed with free tetrahedral elements. Figure 4.8 shows the mesh of the model geometry for preheating step simulation.

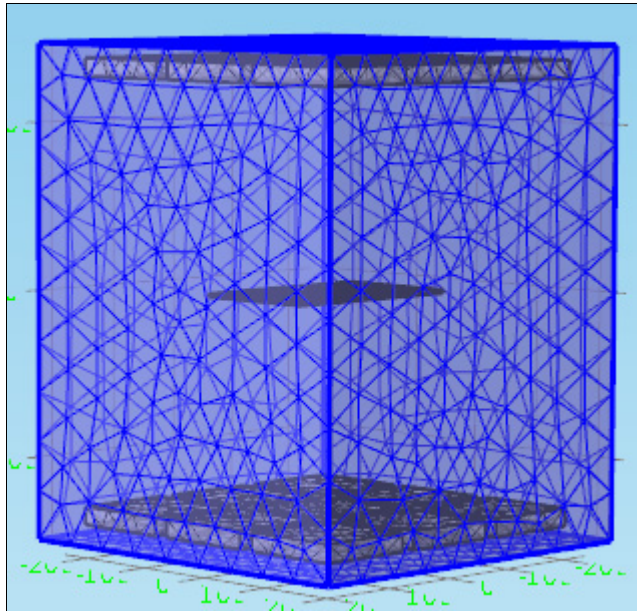


Figure 4.8 Mesh of the model geometry for pre-heating step simulation

4.2.4.2 Cooling step simulation

In order to save the computational time and avoid the meshing problems due to the complexity of the geometry, the compression moulding model was simplified. The mould, the platens, the insulators and the laminate were simulated as the solid blocks in contact each other by considering the same volume of the real geometry.

For cooling stage, cooling channels were added to the geometry of the model. The cooling channel was made of pipes connections. The pipes have the radius of 7.62 mm and 12.7 mm. The model geometry for cooling step simulation is shown in Figure 4.9. The cooling time was defined in the range from 0 to 800 s with a step of 3 s. It is the necessary time to cool down to around 170°C. The boundary thermal conditions during the cooling stage are described as

follows: For the convective heat transfer, the air temperature was fixed to 22°C. The initial value of temperature in the whole model was fixed to 360°C. The velocity of the water through cooling channel was 20 m/s. The finite element mesh of the model for cooling stage comprises free tetrahedral elements with finer size. The geometry characteristics of the cooling model are presented in Table 4.4.

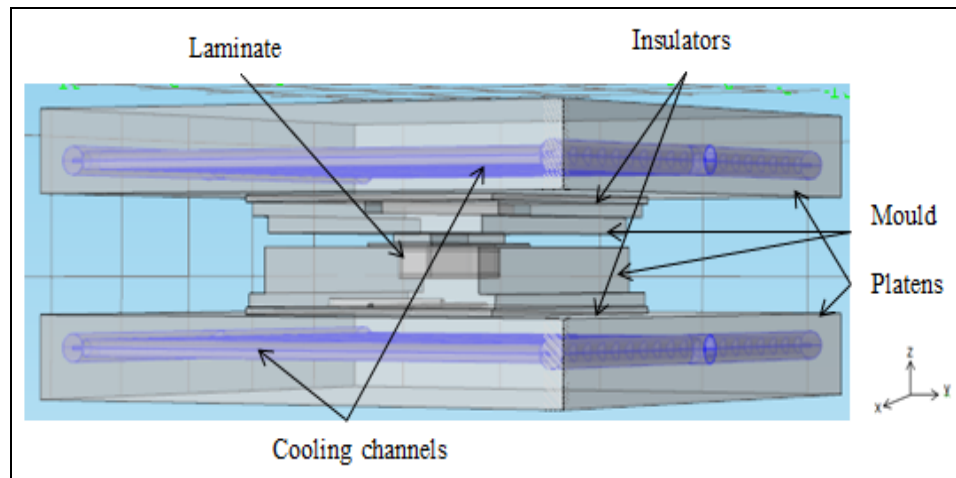


Figure 4.9 Geometry of the model for cooling step simulation

Table 4.4 Geometry characteristics of the cooling model

Domains		Nature	Dimensions (x,y,z) (mm)	Position (mm)
Platens	Top	Block -steel	610 x 610 x 35.56	(0,0,0)
	Bottom			(0,0,124.26)
Thermal insulators	Top	Block-glass-ceramic	330 x 292 x 6.35	(0,0,103.3)
	Bottom			(0,0,20.96)
Cavity mould block		Block-steel	317.5 x 292 x 48.26	(0,0,48.26)
Punch mould block		Block-steel	317.5 x 292 x 65	(0,0,67.62)
Laminate		Solid block (CF/PEEK) Layer : 3.35	168.18 x 84.33 x 44	(0,0,53.75)
Cooling channel		Solid cylinder-steel	R = 7.62; L = 558.8 R = 12.7 ; L = 25.4 R = 12.7 ; L = 566.42	(x,y,z axis)

4.2.5 Experimental and numerical results

The COMSOL heat transfer program was used to simulate the temperature variation in function of the time through a compression moulded carbon/PEEK composite concave part. The obtained numerical results of transient temperature for the present model were compared to experimental data (Lessard, 2014). Figure 4.10 shows the comparison between numerical and experimental temperatures over time at three different locations inside the laminate. For concave mould, the numerical simulation results of heating step were also obtained and were compared to experimental values (Lessard, 2012a). Figure 4.11 shows numerical temperature over time inside the concave mould.

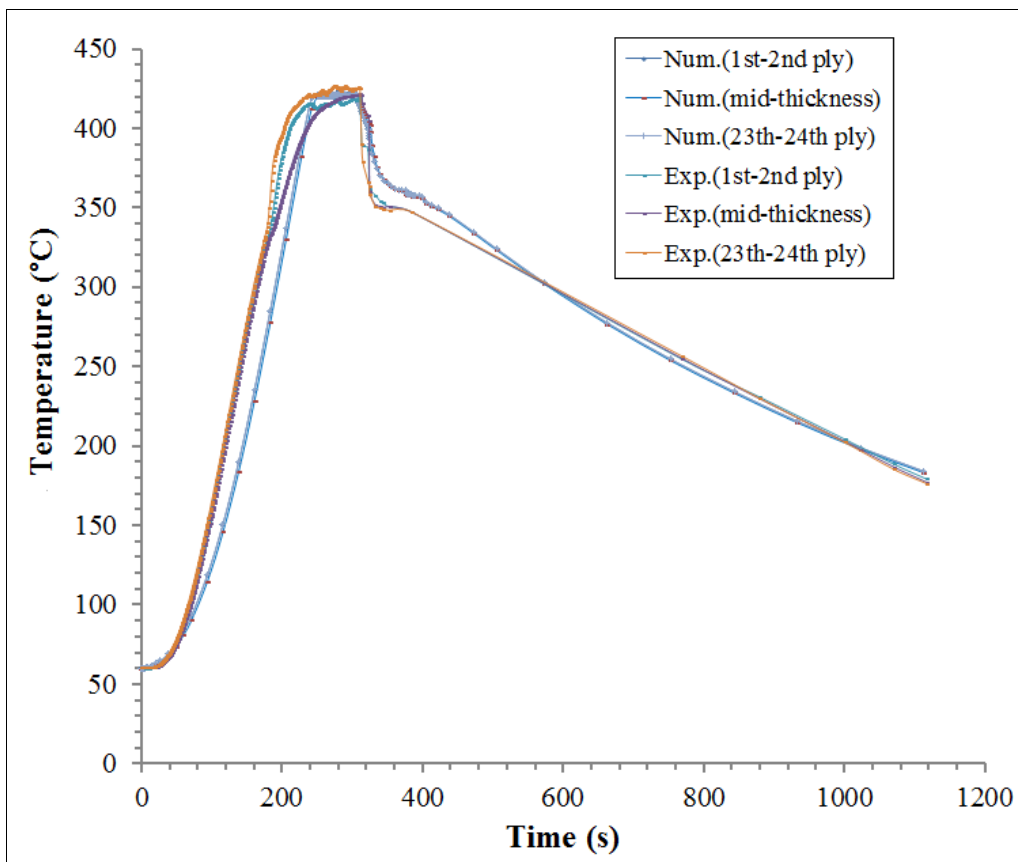


Figure 4.10 Comparison between numerical and experimental temperatures over time for three different locations inside the laminate in z- direction

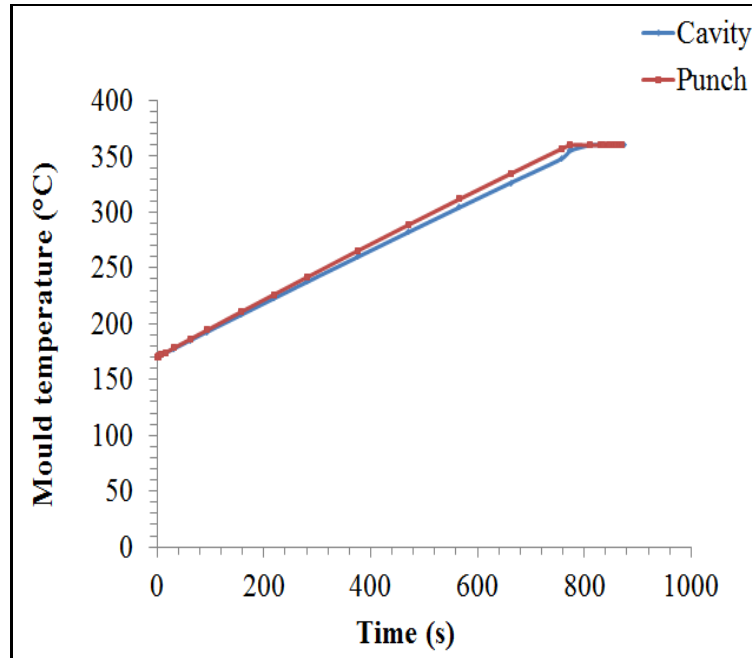


Figure 4.11 Numerical temperature vs. time inside the concave mould

4.2.6 Heating power simulations

As mentioned in the previous section, the heating power was simulated using the transient thermal analysis module of the commercial COMSOL Multiphysics software (based on 3D FEM). For preheating the laminate the same thermal boundary conditions as above were considered: The necessary heat source rate at the surfaces of infrared radiators panels was adjusted in order to get the processing temperature for a specific heating time. In order to maintain the processing temperature, the heat source rate was reduced for a simulated dwelling time.

From Figure 4.10 and using the range of applied heating source rate, the heating power was deducted for each step of heating time and the temperature scale corresponding to different heating rates. Table 4.5 presents the heating power simulation results for the laminate.

Table 4.5 Heating power simulation results for laminate

N.R.P	18		H.P' ₁	H.T' ₁	H.P' ₂	H.T' ₂
V _L (10 ⁴ mm ³)	12.334		(w)	(s)	(w)	(s)
R.P.A	(m ²)	0.015625	14709	259	1406	47
H.P' ₁ .D	(w/m ²)	52300				
H.P' ₂ .D	(w/m ²)	5000				

From Figure 4.11 and using formula (4.8), the mould heating power was deducted for each step of heating time and temperature scale corresponding to different heating rates. Table 4.6 presents the heating power simulation results for the concave mould.

Table 4.6 Heating power simulation results for concave mould

P'₁(w)	t'₁(s)	P'₂(w)	t'₂(s)	P'₃(w)	t'₃(s)	P'₄(w)	t'₄(s)
2640	771	667.14	25	4000	810	862.85	25

4.2.7 Heating energy costs estimation

The total heating energy consumption of concave part includes heating energy consumption of the laminate and that of the concave mould. The heating power of the concave mould comprises the heating power of the cavity and that of the punch. From Table 4.6 and applying equations (2.5) and (2.6), the heating energy and the heating energy costs were calculated. Table 4.7 presents the heating energy and the heating energy cost results for concave part.

Table 4.7 Heating energy and heating energy cost results for concave part

Laminate heating energy (kwh)	Mould heating energy (kwh)	Total heating energy consumption (kwh)	Energy rate (\$/kwh)	Heating energy costs (\$)
1.08	1.476	2.556	0.0457	0.117

4.3 Tooling costs estimations for manufacturing UD parts

This section consists to estimate the tooling costs for manufacturing concave parts. The tooling costs were estimated with the same methodology used in chapter 2.

4.3.1 Concave mould manufacture process

The concave mould is composed of two parts: the cavity and the punch. Each part is 317.5 mm long, 292 mm wide and 55.58 mm high for the cavity, 70.31mm high for the punch. The concave mould manufacturing process is divided in two steps: The first step is to cut two parts from rectangular bar stock. The cavity is made with quarter sphere, half cylinder and two slanted surfaces. The second step is to cut and remove material from the parts. For making the punch and the cavity, it is needed to use milling and drilling operations. For the cavity, the part is submitted to milling operations to make features such as faces, slots, and pocket, and then to drilling operation to make different holes. For the punch block, the part is submitted to milling operations to make features such as faces, slots, and punch and then submitted to drilling operation to make different holes. After the machining operations, all the surfaces of the mould were polished and inspected afterward. The features manufacturing data of concave mould are presented in ANNEX IV. Figure 4.12 shows the CAD of two halves of the concave mould, cavity and punch, which were machined into final shapes.

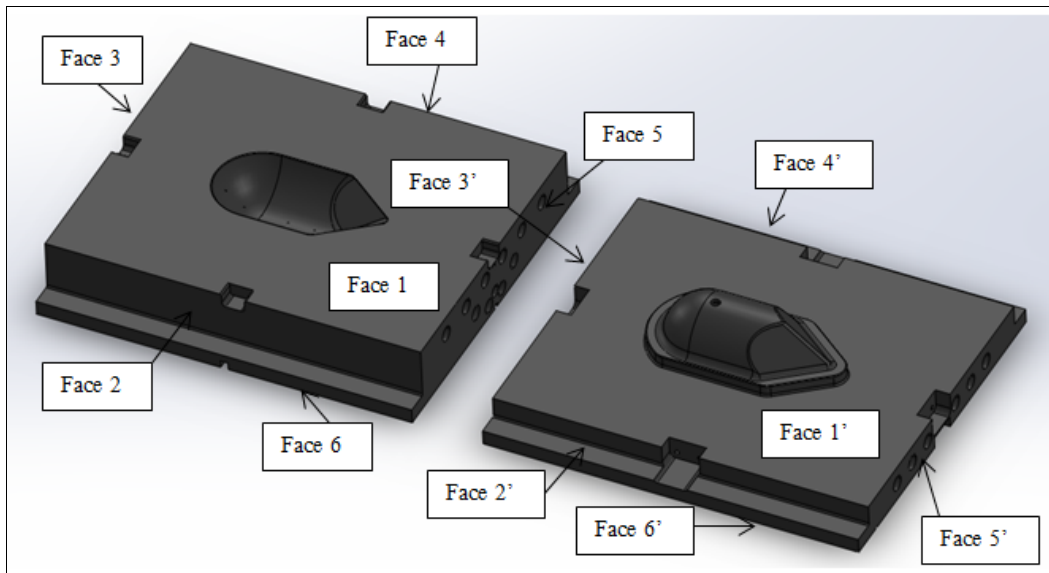


Figure 4.12 CAD of two halves of concave mould: cavity and punch
Reproduced and adapted with permission of Lessard (2013a)

4.3.2 Side lock manufacturing process

The side lock manufacturing process is also divided into two steps. The first step is to cut four parts from rectangular bar form stock. Each part is 41.28 mm long, 31.75 mm wide and 12.7 mm high. The second step is to cut and remove material from the parts. For making one side lock, it is needed to use face milling and two holes drilling operations. Figure 4.13 illustrates the CAD of side lock.

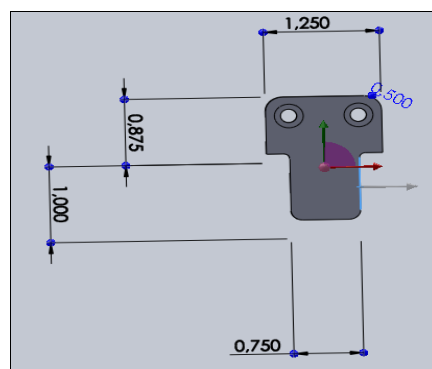


Figure 4.13 CAD of side lock
Taken from Lessard (2013a)

4.3.3 Concave mould assembly process

After machining and polishing, each mould form was assembled and checked to make sure that the two halves mould fit together properly. The alignment is assured by four guide pins which are side lock devices located on mould sides then the mould cavity and the thermal insulator were fixed to the platen by four clamping devices. Figure 4.14 shows the concave mould assembly. Table 4.8 presents the concave mould components assembly data.

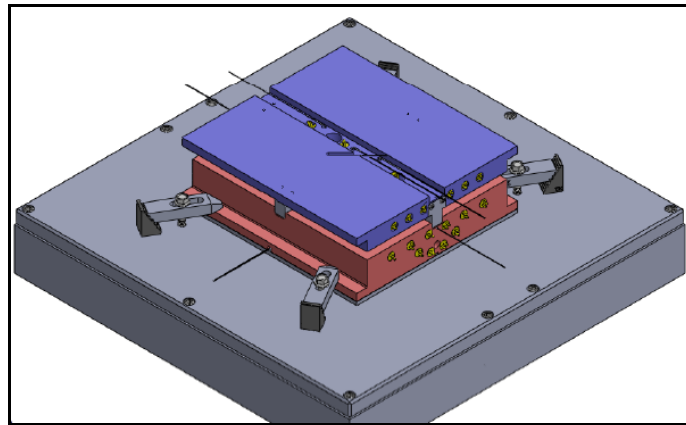


Figure 4.14 Concave mould assembly
Reproduced and adapted with the permission of
Lessard et Lebrun (2011)

Table 4.8 Concave mould components assembly data

Mould component	Securing method	Symmetry	Handling difficulty	Insertion difficulty	RC	Operation time (s)
Punch	Secured later	One way	Two hands	Align	1	1250
Cavity	Secured later	One way	Two hands	Align	1	1250
Side locks	Secured later	One way	-	Align	4	300
Screws and clamping devices	Threads for screws	One way – other way	Two hands	Align	8	3300
Concave mould					1	6100

The manufacturing costs of the concave mould components estimated by DFM software are imported to DFA software for calculating the concave mould assembly costs according to different criteria such as securing method, symmetry, handling difficulty and insertion difficulty.

4.3.4 Concave mould cost estimation results

The concave mould manufacturing cost estimation results obtained by DFM program are presented in Table 4.9. The concave mould total cost estimation results obtained by DFMA are presented in Table 4.10. The labour rates used in the DFM and DFA softwares are respectively Cad \$80/hour and Cad \$30/hour.

Table 4.9 Concave mould manufacturing cost estimation results

Mould component		Cut from stock	Machining	Polishing	Inspection
Cavity	Material	109.55	0	113.5	0
	Set up	3.75	117	0	0
	Processing	0.13	1630.19	39.85	23.53
	Rejects	0	8.69	9.51	9.67
	Total	113.43	1755.88	162.86	33.2
Punch	Material	109.55	0	98.5	0
	Set up	3.75	139.5	0	0
	Processing	0.13	2578.38	61.88	39.71
	Rejects	0	13.46	14.33	14.6
	Total	113.43	2731.34	174.71	54.31
Side locks		154.06			
Screws and clamping devices		19.5			
Cavity		2143.37			
Punch		3768.03			
Concave mould		5911.4			

Table 4.10 DFMA concave mould cost estimation results

Mould component	Manufacturing costs (\$)	Assembly costs(\$)	Repeat count	Total costs (\$)
Cavity	2065.37	12.29	1	2077.66
Punch	3073.79	12.29	1	3086.08
Side locks	154.06	2.98	4	628.16
Screws and clamping devices	19.5	4.13	8	189.04
Cavity	2143.37	28.81	1	2172.18
Punch	3768.03	40.73	1	3808.76
Concave mould	5911.4	69.54	1	5980.94

4.3.5 Concave mould cost breakdown

The concave mould costs are distributed according to the manufacturing and assembly operations of mould components. Figure 4.15 presents the cost breakdown of concave mould.

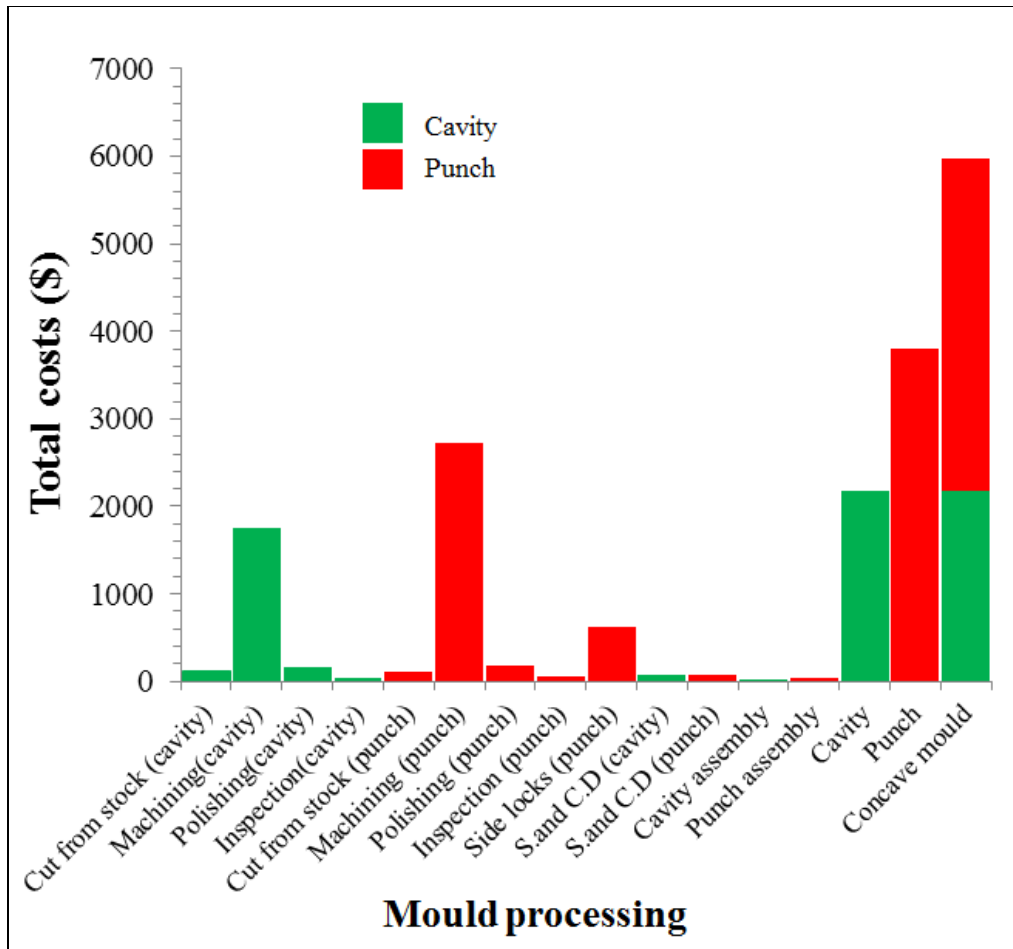


Figure 4.15 Cost breakdown of concave mould

For making comparison between the estimated costs and the actual prices of the mould, the total estimated costs includes the estimated costs by DFMA and other estimated costs such as design and engineering costs, boxing and shipping costs, taxes and profits. Table 4.11 presents DFMA estimated costs and commercial price comparison for the concave mould (Lebrun, 2012).

Table 4.11 DFMA estimated costs and commercial price comparison for the concave mould

Cost category	DFMA	Commercial
Manufacturing costs	5911.4	-
Assembly costs	69.54	-
Overhead + profit		
Design an Engineering costs	2900	-
Boxing and shipping	710	-
Optional FEM Analysis		-
Taxes	1840.57	14.975% of total costs before taxes
Profit	2700	-
Total costs	14131.51	15145

4.4 Discussion of results and conclusion

For the heating step, the model predicted almost the same temperature throughout the laminate. However, there was an average difference of around 10% between the simulated and experimental temperatures for three specific locations on the middle plan of the laminate.

There was no significant difference in the heating time to reach the consolidated temperature of 420°C from the temperature of 60°C, between the numerical and experimental results. The heating time for the experimental plots was 311 s whereas for the numerical simulations was about 306 s. For the transfer of the laminate to the press, reaching the temperature of the mould and beginning of cooling down, the experimental and numerical temperatures variations presented approximately the same trend. For the cooling step, the average error between the numerical and experimental temperatures was approximately 20%. The cycle time including the heating and cooling steps estimated by the numerical modelling for a compression moulded carbon/PEEK composite concave parts was validated.

For the heating the concave mould, there was also no significant difference in heating time to attain 360 °C between the numerical and experimental results. The experimental heating time was 900 s and the numerical one was about 835 s.

The total heating energy consumptions are the sum of the heating energy consumption of the laminate in the oven and that of the concave mould. The concave mould cost results showed that the cost of the punch are higher than that of the cavity due to the higher machining time of the punch and the mould manufacturing costs are higher than assembly costs.

The concave mould costs comparison showed that there is no significant difference between the total estimated costs and the commercial costs. The error between them is about 6%.

By keeping the same cycle time, the concave parts heating energy could be predicted for other similar geometries in function of the volumes of the mould and the concave parts and based on the cost results obtained for the concave mould by the DFMA cost estimation software, the mould costs were extrapolated and applied to other similar mould geometries by changing the projected mould area. Consequently, the tooling and energy costs sizing and complexity scaling laws for compression process moulded unidirectional continuous fibre prepreg sheet thermoplastics parts will be established in chapter 5.

CHAPTER 5

TOOLING AND ENERGY COSTS SIZING AND COMPLEXITY SCALING LAWS FOR COMPRESSION PROCESS MOULDED UNIDIRECTIONAL CONTINUOUS FIBRE REINFORCED THERMOPLASTIC PARTS

5.1 Introduction

Chapter 5 aims on one hand, at establishing the energy costs sizing and complexity scaling laws of compression moulded unidirectional (UD) virtual parts. On the other hand, at generating the tooling costs sizing and complexity laws for virtual moulds, in order to manufacture the (UD) virtual parts.

There were different UD part forms which were designed in order to calculate the costs, to make comparisons between these parts and study the influence of part forms on the final cost.

5.2 Energy costs sizing scaling laws for UD parts

Similarly, this section consists to generate the heating energy costs sizing scaling laws for UD concave part and others UD part forms such as U-shape part, hollow square part, Z-shape part and flat plate. For doing that, the heating energy was estimated for other similar geometries in function of the part volume by keeping the same process cycle time. The compression moulding process cycle time was simulated by the same methodology used in chapter 4 for experimental UD parts. The heating energy and the energy costs were calculated using equations (2.5) and (2.6) respectively.

The heating energy costs scale with part volume which means the area and the thickness of the part. The total heating energy consumption of UD parts includes heating energy consumption of the laminates and that of the moulds. The heating power of the moulds comprises the heating power of the cavity and that of the punch. The heating power was simulated for each step of heating time and the temperature scale.

5.2.1 Concave part

The concave part was composed of a quarter of sphere at one extremity, cylindrical portion in the middle and two inclined flat faces at the other extremity. The thickness is 3.35 mm. Figure 5.1 shows the design of concave part.

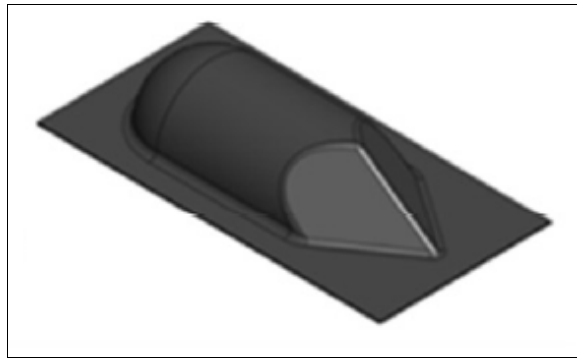


Figure 5.1 Design of concave part
Reproduced and adapted with permission
of Lessard et Lebrun (2011)

5.2.1.1 Heating power simulations results for the laminate

Table 5.1 presents the heating data and heating power simulation results for the laminate scaling with the part volume.

Table 5.1 Heating data and heating power simulation results
for the laminate scaling with the part volume

V_L (10^4 mm^3)	R.P.A (m^2)	R.P.N	H.P' ₁ (w/m^2)	H.T' ₁ (min)	H.P' ₂ (w/m^2)	H.T' ₂ (min)
12.334	0.015625	18	14709.37	259	1406.25	47
15.418	0.015625	18	14807.81	259	1448.44	47
18.502	0.015625	18	14934.37	259	1518.75	47
21.585	0.015625	18	15075	259	1575	47
24.669	0.015625	18	15257.81	259	1653.75	47

The heating energy sizing scaling law was obtained by scaling the heating energy of the laminate with the volume. It was approximated by the linear equation (5.1) (trend line).

$$y = 0.0034 x + 1.0356 \quad (5.1)$$

Where x is part volume (10^4 mm^3); y is heating energy (kwh)

5.2.1.2 Heating power simulation results for the concave mould

Table 5.2 presents the heating power simulation results for the concave mould scaling with the volume of the mould.

Table 5.2 Heating power simulation results for the concave mould scaling with the volume of the mould

Mould Size	P'₁ (w)	t'₁ (s)	P'₂ (w)	t'₂ (s)	P'₃ (w)	t'₃ (s)	P'₄ (w)	t'₄ (s)
V_m	2640	771	667.14	25	4000.04	810	862.85	25
$1.397 \times V_m$	3587.61	771	752.85	25	5575.14	810	1057.14	25
$1.837 \times V_m$	4752.1	771	896.42	25	6996.1	810	1248.57	25
$2.315 \times V_m$	5901.12	771	1045	25	9037.15	810	1440	25
$2.828 \times V_m$	7146.49	771	1144.57	25	10972.72	810	1636.43	25

5.2.1.3 Heating energy cost calculation results for concave part

Table 5.3 presents the calculated heating energy and heating energy costs for the concave part scaling with the part volume.

Table 5.3 Calculated heating energy and heating energy costs for the concave part scaling with the part volume

V_p (10^4 mm^3)	Total heating energy (kwh)	Energy rate (\$/kwh)	Heating energy costs (\$)
12.334	2.556	0.0457	0.117
15.418	3.122	0.0457	0.142
18.502	3.704	0.0457	0.169
21.585	4.423	0.0457	0.202
24.669	5.14	0.0457	0.235

5.2.2 U-shape part

The U-shape part has sides of 45.72 mm and thickness of 3.35 mm. Figure 5.2 shows the CAD of the U-shape part.

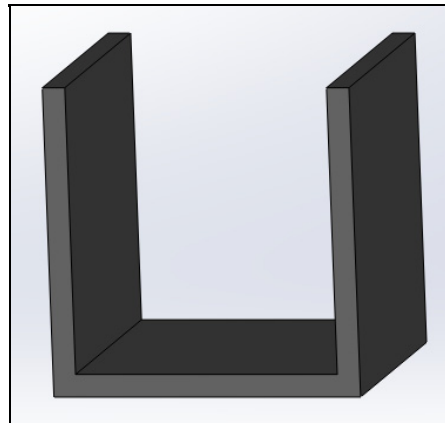


Figure 5.2 CAD of U-shape part

5.2.2.1 Heating energy calculation results for the laminate

From heating energy size scaling law of the laminate, the heating energy of U-shape part can be deducted. Table 5.4 presents the heating energy scaling with volume of the U-shape part.

Table 5.4 Heating energy scaling with the part volume

Part volume (10^4 mm^3)	Laminate heating energy (kwh)
2.102	1.042
2.628	1.044
3.153	1.046
3.679	1.048
4.205	1.049

5.2.2.2 Heating power simulation results for hollow square mould

In order to make a U-shape part, the hollow square mould was used. Table 5.5 presents the heating power simulation results for the hollow square mould scaling with the volume of the mould.

Table 5.5 Heating power simulation results for the hollow square mould scaling with the volume of the mould

Mould Size	P'_1 (w)	t'_1 (s)	P'_2 (w)	t'_2 (s)	P'_3 (w)	t'_3 (s)	P'_4 (w)	t'_4 (s)
V_m	2552	771	545.71	25	4116	810	784.28	25
$1.3975 \times V_m$	3524	771	694.28	25	5672	810	995.71	25
$1.8371 \times V_m$	4612	771	822.85	25	7440	810	1197.14	25
$2.315 \times V_m$	5750	771	951.42	25	9320	810	1418.57	25
$2.828 \times V_m$	7016	771	1108.57	25	11288	810	1641.43	25

5.2.2.3 Heating energy cost calculation results for U-shape part

Table 5.6 presents the calculated heating energy and heating energy costs for U-shape part scaling with part volume.

Table 5.6 Calculated heating energy and heating energy costs for U-shape part scaling with the part volume

Part volume (10^4 mm^3)	Total heating energy (kwh)	Energy rate (\$/kwh)	Heating energy costs (\$)
2.102	2.524	0.0457	0.115
2.628	3.087	0.0457	0.141
3.153	3.722	0.0457	0.170
3.679	4.393	0.0457	0.200
4.205	5.111	0.0457	0.233

5.2.3 Hollow square part

The hollow square part has sides of 45.72 mm and thickness of 3.35 mm. Figure 5.3 shows the CAD of the hollow square part.

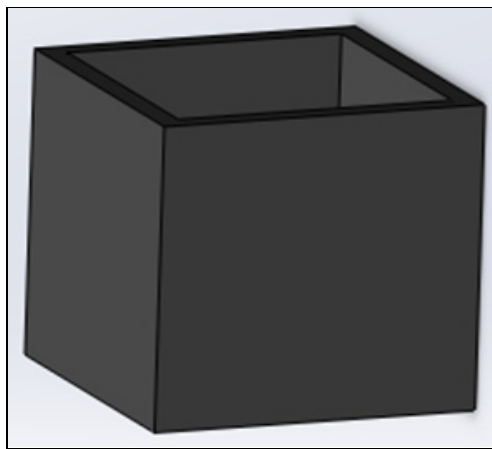


Figure 5.3 CAD of hollow square part

5.2.3.1 Heating energy cost calculation results for the laminate

From heating energy size scaling laws of the laminate, the heating energy of hollow square part can be deducted. Table 5.7 presents the heating energy scaling with the part volume.

Table 5.7 Heating energy scaling with part volume

Part volume (10^4 mm^3)	Laminate heating energy (kwh)
6.307	1.057
8.814	1.065
11.587	1.075
14.602	1.085
17.837	1.096

5.2.3.2 Heating power simulation results for hollow square mould

In order to make a hollow square part, the hollow square mould was used. Table 5.8 presents the heating power simulation results for the hollow square mould scaling with the volume of the mould.

Table 5.8 Heating power simulation results for the hollow square mould scaling with the volume of the mould

Mould Size	P'_1 (w)	t'_1 (s)	P'_2 (w)	t'_2 (s)	P'_3 (w)	t'_3 (s)	P'_4 (w)	t'_4 (s)
V_m	2552	771	545.71	25	4116	810	784.28	25
$1.3975 \times V_m$	3524	771	694.28	25	5672	810	995.71	25
$1.8371 \times V_m$	4612	771	822.85	25	7440	810	1197.14	25
$2.315 \times V_m$	5750	771	951.42	25	9320	810	1418.57	25
$2.828 \times V_m$	7016	771	1108.57	25	11288	810	1641.43	25

5.2.3.3 Heating energy cost calculation results for hollow square part

Table 5.9 presents the calculated heating energy and heating energy costs for hollow square parts scaling with part volume.

Table 5.9 Calculated heating energy and heating energy costs for hollow square parts scaling with part volume

Part volume (10^4 mm^3)	Total heating energy (kwh)	Energy rate (\$/kwh)	Heating energy costs (\$)
6.307	2.539	0.0457	0.116
8.814	3.108	0.0457	0.142
11.587	3.750	0.0457	0.171
14.602	4.430	0.0457	0.202
17.837	5.157	0.0457	0.235

5.2.4 Z-shape part

The Z-shape part has sides of 45.72 mm and thickness of 3.35 mm. Figure 5.4 shows the CAD of the Z-shape part.

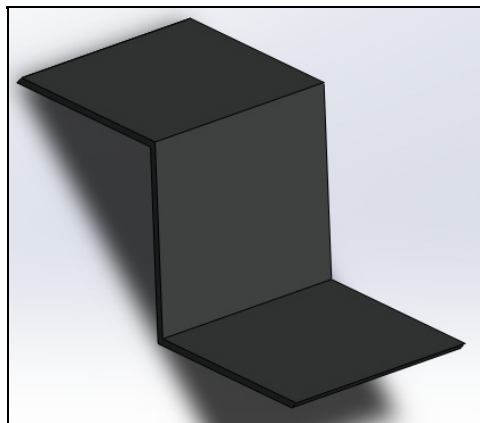


Figure 5.4 CAD of Z-shape part

5.2.4.1 Heating power calculations results for the laminate

From heating energy size scaling laws of the laminate, the heating energy of Z-shape part can be deducted. Table 5.10 presents the heating energy scaling with the part volume.

Table 5.10 Heating energy scaling with part volume

Part volume (10^4 mm^3)	Laminate heating energy (kwh)
1.888	1.042
2.638	1.044
3.469	1.047
4.371	1.050
5.340	1.053

5.2.4.2 Heating power simulation results for Z-shape mould

In order to make a Z-shape part, the Z-shape mould was used. Table 5.11 presents the heating power simulation results for the Z-shape mould scaling with the volume of the mould.

Table 5.11 Heating power simulation results for the Z-shape mould scaling with the volume of the mould

Mould Size	P'_1 (w)	t'_1 (s)	P'_2 (w)	t'_2 (s)	P'_3 (w)	t'_3 (s)	P'_4 (w)	t'_4 (s)
V_m	2735	771	726	810	4099	25	1000	25
$1.3975 \times V_m$	3733	771	817	810	5651	25	1223	25
$1.8371 \times V_m$	4831	771	927	810	7393	25	1313	25
$2.315 \times V_m$	6008	771	1045	810	9221	25	1412	25
$2.828 \times V_m$	7247	771	1161	810	11263	25	1522	25

5.2.4.3 Heating energy cost calculation results for Z-shape part

Table 5.12 presents the calculated heating energy and heating energy costs for Z-shape part scaling with the part volume.

Table 5.12 Calculated heating energy and heating energy costs for Z-shape part scaling with part volume

Part volume (10⁴ mm³)	Total heating energy (kwh)	Energy rate (\$/kwh)	Heating energy costs (\$)
1.888	2.562	0.0457	0.117
2.638	3.129	0.0457	0.143
3.469	3.761	0.0457	0.172
4.371	4.428	0.0457	0.202
5.340	5.158	0.0457	0.235

5.2.5 Flat plate

The flat plate has sides of 45.72 mm and thickness of 3.35 mm. Figure 5.5 shows the CAD of the flat plate.

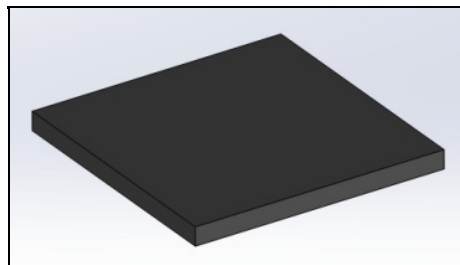


Figure 5.5 CAD of flat plate

5.2.5.1 Heating power calculation results for the laminate

From heating energy size scaling laws of the laminate, the heating energy of flat plate can be deducted. Table 5.13 presents the heating energy scaling with the volume of the flat plate.

Table 5.13 Heating energy scaling with the volume of flat plate

Part volume (10^4 mm^3)	Laminate heating energy (kwh)
0.700	1.038
0.876	1.038
1.051	1.039
1.226	1.039
1.401	1.040

5.2.5.2 Heating power simulation results for flat mould

In order to make a flat plate, the flat mould was used. Table 5.14 presents the heating power simulation results for the flat mould scaling with the volume of the mould.

Table 5.14 Heating power simulation results for the flat mould scaling with volume of the mould

Mould Size	P'_1 (w)	t'_1 (s)	P'_2 (w)	t'_2 (s)	P'_3 (w)	t'_3 (s)	P'_4 (w)	t'_4 (s)
V_m	2450	770	505	25	2380	810	490	25
$1.3975 \times V_m$	3350	770	659	25	3260	810	626	25
$1.8371 \times V_m$	4392	770	788	25	4228	810	762	25
$2.315 \times V_m$	5450	770	932	25	5300	810	898	25
$2.828 \times V_m$	6640	770	1074	25	6410	810	1036	25

5.2.5.3 Heating energy cost calculation results for flat plate

Table 5.15 presents the heating energy and heating energy costs calculations for flat plate scaling with the part volume.

Table 5.15 Calculated heating energy and heating energy costs for flat plate scaling with part volume

Part volume (10⁴ mm³)	Total heating energy (kwh)	Energy rate (\$/kwh)	Heating energy costs (\$)
0.700	2.104	0.0457	0.096
0.876	2.497	0.0457	0.114
1.051	2.940	0.0457	0.134
1.226	3.410	0.0457	0.155
1.401	2.745	0.0457	0.125

5.2.6 UD part heating energy sizing scaling laws

Figure 5.6 shows the heating energy of five UD parts in function of the part volume. Table 5.16 presents the heating energy sizing scaling laws for five UD part forms.

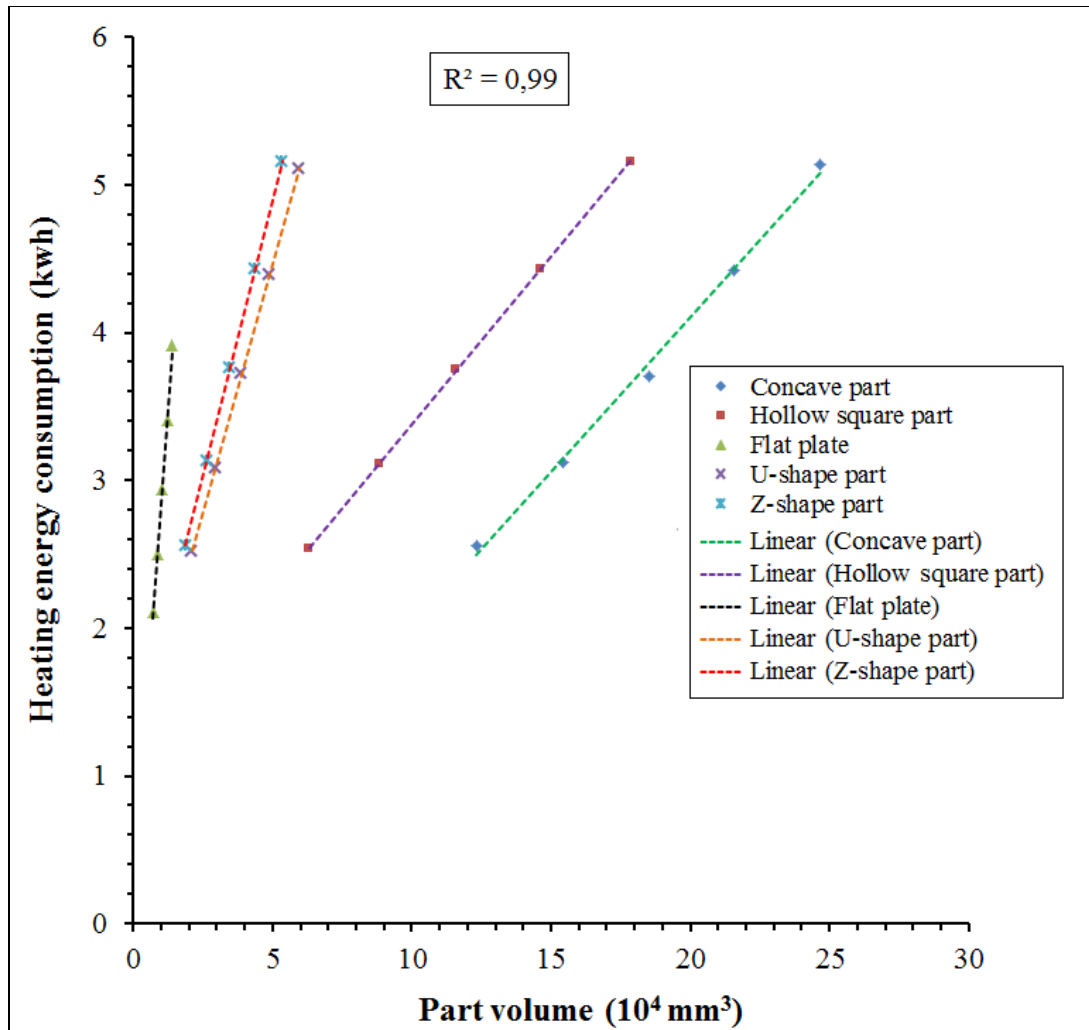


Figure 5.6 Heating energy of five UD parts in function of part volume: concave part, hollow square part, U-shape part, Z-shape part, Flat plate

Table 5.16 Heating energy sizing scaling laws for five UD part forms: concave part, hollow square part, U-shape part, Z-shape part, Flat plate

Part form	Sizing scaling laws	Remarks
Concave part	$y = 0.2098 x - 0.0924$	y: Heating energy (kwh) x: Part volume (10 ⁴ mm ³) Heating energy sizing scaling laws are in linear form (trendlines)
Hollow square part	$y = 0.2272 x + 1.1084$	
U-shape part	$y = 1.2328 x - 0.1206$	
Z-shape part	$y = 0.7515 x + 1.1463$	
Flat plate	$y = 2.5908 x + 0.2506$	

5.2.7 UD part heating energy costs sizing scaling laws

Figure 5.7 shows the heating energy costs of five UD parts in function of the part volume. Table 5.17 presents the heating energy costs sizing scaling laws for five UD part forms.

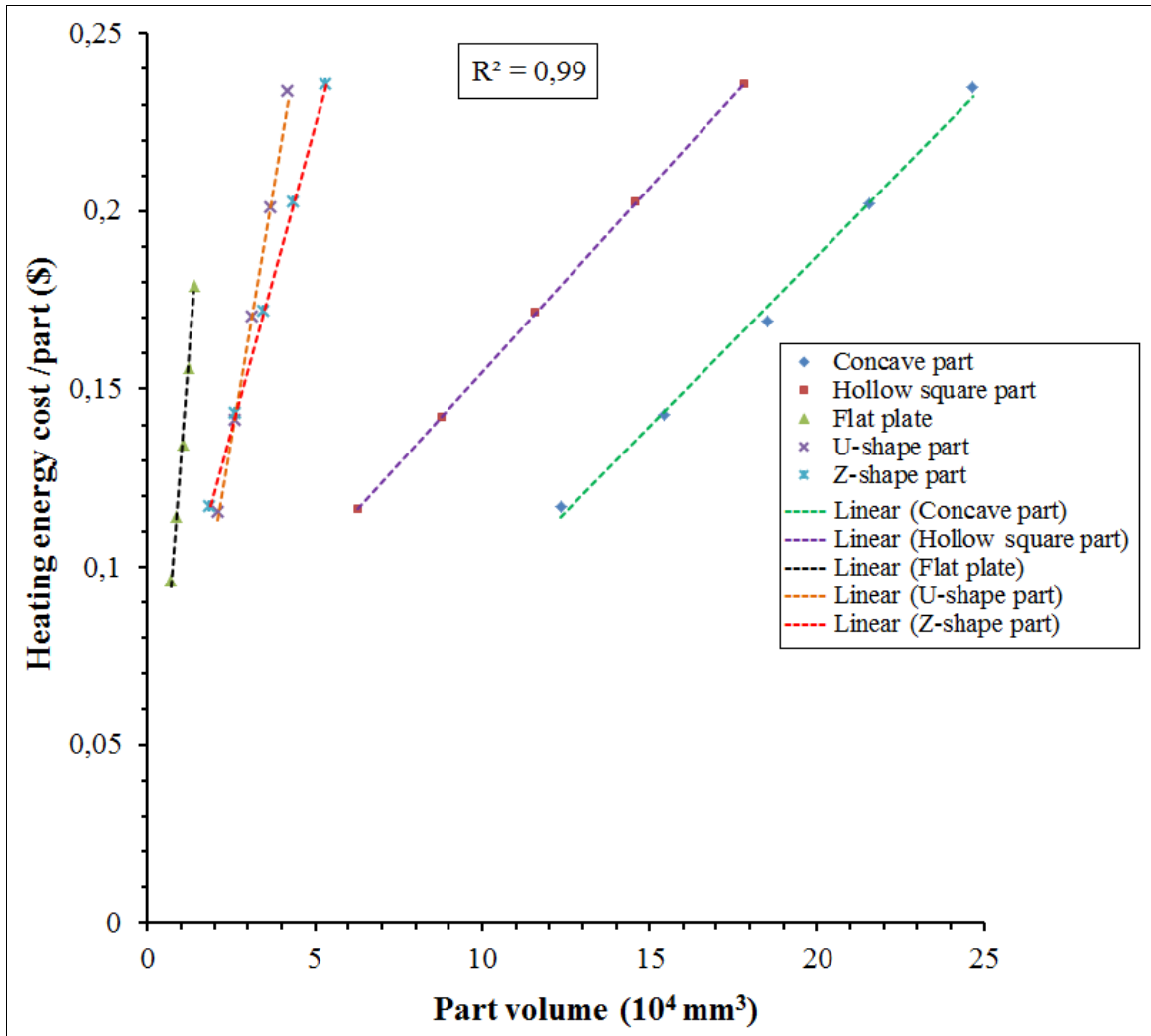


Figure 5.7 Heating energy costs of five UD parts in function of part volume: concave part, hollow square part, U-shape part, Z-shape part, Flat plate

Table 5.17 Heating energy costs sizing scaling laws for five UD part forms: concave part, hollow square part, U-shape part, Z-shape part, Flat plate

Part form	Sizing scaling laws	Remarks
Concave part	$y = 0.0096 x - 0.0042$	y: Energy cost (\$) x : Part volume (10^4 mm^3) Energy costs sizing scaling laws are in linear form (trend curve)
Hollow square part	$y = 0.0104 x + 0.0507$	
U-shape part	$y = 0.0563 x - 0.0055$	
Z-shape part	$y = 0.0343 x + 0.0524$	
Flat plate	$y = 0.1184 x + 0.0115$	

5.3 Mould costs sizing scaling laws for UD parts

The methodology for estimating the tooling costs of four mould forms using DFMA softwares was already described in chapter 4. The mould costs sizing scaling laws were established by making extrapolation for other mould similar geometry scaled with projected area of the mould.

In order to make the cost analysis of the moulds, it important to consider the costs components during the manufacturing process such as the manufacturing and assembly costs calculated by DFMA and overheads such design and engineering costs, boxing and shipping costs, capital costs and taxes and the commercial profits which correspond to the return on investment. Table 5.18 presents the estimated tooling costs for concave mould, hollow square mould, flat mould and Z-shape mould scaling with the mould projected area.

Table 5.18 Estimated tooling costs for concave mould, hollow square mould, flat mould and Z-shape scaling with mould projected area

Mould form	Mould projected area (10 ⁴ mm ²)	Mould costs (\$)	
		Manufacturing and assembly costs	Estimated prices
Concave mould	9.274	5980.94	14131.51
	11.593	7150.79	16856.24
	13.911	8788	20796.68
	16.23	10450	24639.14
	18.548	12440	29272.64
Hollow square mould	9.274	4818.25	11483.99
	11.593	5703.23	13593.76
	13.911	6929.44	16651.58
	16.23	8077.52	19598.13
	18.548	9309.9	22035.02
Flat mould	9.274	3956.62	9837.974
	11.593	4266.42	10579.333
	13.911	4812.52	11960.297
	16.23	5438.14	13490.178
	18.548	6139.66	15245.294
Z-shape mould	9.274	5071.89	12591.94
	11.593	6026.97	14926.02
	13.911	7389.07	18337.44
	16.23	8811	21892.91
	18.548	10009	24822.33

Figure 5.8 shows the estimated moulds costs vs. the projected area of concave mould, hollow square mould, flat mould and Z-shape mould.

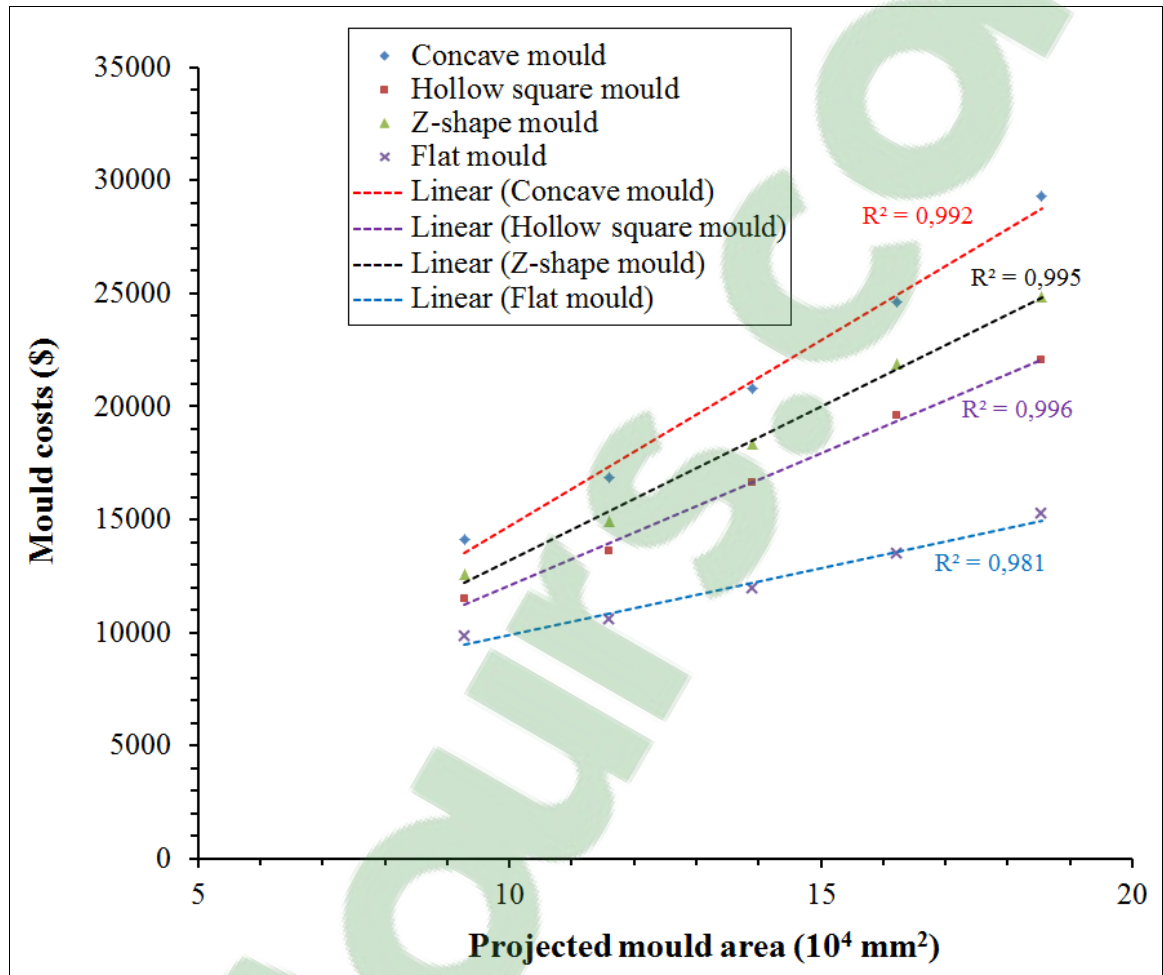


Figure 5.8 Estimated moulds costs vs. projected area of concave mould, hollow square mould, flat mould and Z-shape mould

Table 5.19 presents the mould costs sizing scaling laws for concave mould, hollow square mould, flat mould and Z-shape mould.

Table 5.19 Mould costs sizing scaling laws for concave mould, hollow square mould, flat mould and Z-shape mould

Mould form	Sizing scaling laws	Remarks
Concave mould	$y = 1641.8 x - 1699.9$	y: Mould cost (\$) x: Mould projected area (10 ⁴ mm ²) Mould costs sizing scaling laws are in linear form
Hollow square mould	$y = 1169.1x + 408.64$	
Flat mould	$y = 591.99 x + 3987.3$	
Z-shape mould	$y = 1355.5x - 342.47$	

5.4 Mould costs complexity scaling laws for UD parts

In order to consider the complexity level, the mould costs of different part forms were calculated for the same projected area of the mould. Figure 5.9 shows the moulds costs for concave mould, hollow square mould, flat mould and Z-shape mould scaling with complexity level of the mould.

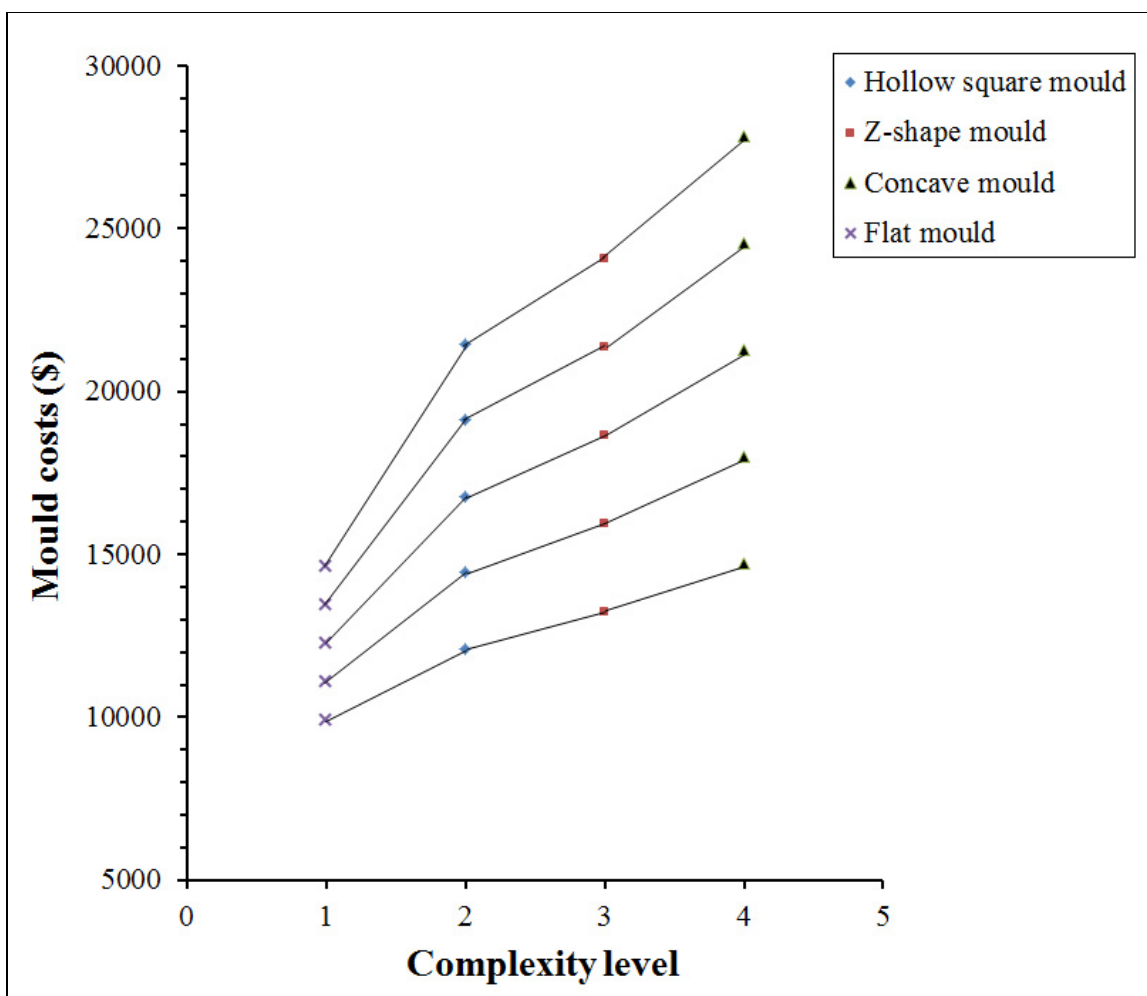


Figure 5.9 Moulds costs for concave mould, hollow square mould, flat mould and Z-shape mould scaling with complexity level of the mould

5.5 Discussion of results and conclusion

The total heating energy consumptions which are the sum of the heating energy consumption of the laminate in the oven and that of the concave mould scale with the volumes of the laminate. From the heating energy costs results for different UD part forms scaling with part volume, the heating energy costs sizing scaling laws were established which are in linear forms and are limited to the size of platens areas.

For the concave part, U-shape part, hollow square part and Z-shape part, there is no significant difference in term of heating energy costs between them. The heating energy costs do not depend on the volume of the part. For the flat plate the heating energy costs are lower than those of the other UD parts due to lower volume of the flat mould.

From the estimated costs for four moulds forms scaling with their projected area, the tooling costs sizing scaling laws were established which are in linear forms and are limited to the size of platens areas.

The costs comparison between different mould forms showed that the concave mould costs are very higher than those of the other mould forms due to a high complexity level of the concave mould. Therefore, based on the estimated tooling costs scaling with complexity level, it was concluded that the more complex the mould is the higher the cost.

In order to make the right decision about the manufacturing process selection for an economical production, it is important to study other processes and to make comparisons between them. In the present case study, the compression moulding process which was involved in the previous chapters and the autoclave process for making thermosets parts for which the costs estimation will be presented in chapter 6.

CHAPTER 6

COSTS ESTIMATION FOR THERMOSET COMPOSITE PARTS MANUFACTURED BY AUTOCLAVE PROCESS

6.1 Introduction

Chapter 6 is devoted to estimating the costs of thermoset composite parts made by an autoclave process in order to make a cost comparison with those manufactured by a compression moulding process and to determine the cost effective technique of manufacturing the composite materials. This chapter focuses especially, on one hand, on the estimation of manufacturing process cycle time for the same part forms which were already designed in chapter 2 and chapter 4, and on the other hand, on the estimation of tooling costs for manufacturing these categories of parts.

In the case of no available data for calculating the lay-up time using the 1st order model, the lay-up time was calculated by applying the power law ACCEM model. The rate categories presented in Table 6.1 are similar for all the studied mould forms and for all the studied part geometries(Haffner, 2002; Hexcel, 2013).

Table 6.1 The rate categories for the cost calculation

Rate category	Unit	Value
Invar	\$/kg	22.04
Density of invar	kg/m ³	8055
Density of AS4/8552	kg/m ³	1578
Labour	\$/hr	100
Autoclave operating	\$/hr	20
Machining operating	\$/hr	250
Plasma cutting operating	\$/hr	150
Welding + press operating	\$/hr	50
Heat treatment	\$/kg	3.31
Inspection	\$/hr	200

The autoclave equipment was estimated using a regression method of approximately 350 k\$ for an internal volume of 39.64 m³ (Haffner, 2002). Figure 6.1 shows autoclave equipment (Hoa, 2009).

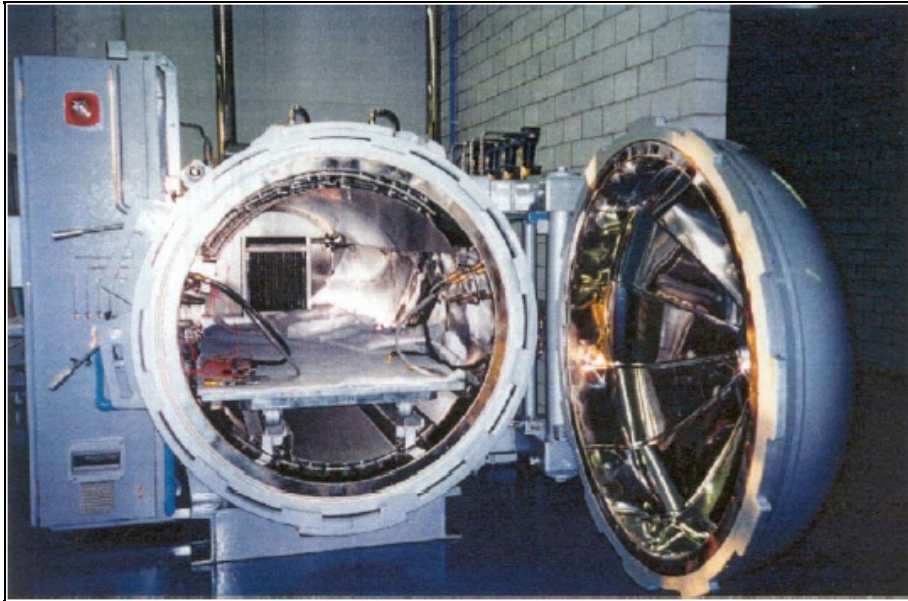


Figure 6.1 Autoclave equipment
Taken from Hoa (2009)

For tooling costs, according to (Haffner, 2002) the mould costs estimation was based on selecting the material and different manufacturing steps such as plasma cutting of support structure, welding of support structure, machining of support structure, forming and fitting face sheet, welding and deburring of mould face, heat treatment, rough and finish machining of mould face, polishing, inspection, details installation and in-house transportation. It was considered that the total estimated mould costs include the manufacturing costs of the components and the overhead costs such as design and engineering costs, boxing and shipping costs, capital costs, taxes; and the commercial profits which correspond to the return on investment.

6.2 Flat plate

The flat plate has a dimension of 355.6 mm x 304.8 mm with 6 mm of thickness (El wazziki et Ngo, 2014). Table 6.2 presents the other material costs for making flat plate by lay-up and autoclave cure (Fuchs, 2003; Ruoshi, 2012).

Table 6.2 Other material costs for making flat plate
by lay-up and autoclave cure
Adapted from Fuchs (2003, p.82) and Ruoshi (2012, p.29)

Material category	Supplier	Cost rate	Quantity	Cost
Release agent	Airtech	0.148\$/ml	30 ml	4.44 \$
Breather	Airtech	5.032\$/m ²	0.108 m ²	0.543 \$
Release film	Airtech	4.021\$/m ²	0.108 m ²	0.434 \$
Sealant tape	Airtech	4.78\$/unit	0.75	3.585 \$
Vacuum bag	Airtech	1.957\$/m ²	0.144 m ²	0.282 \$
Adhesive	-	17.5 \$/kg	0.1 kg	1.75 \$
Bleeder	Airtech	1.075\$/m ²	0.108 m ²	0.116 \$
Total cost	-	-	-	11.15 \$

6.2.1 Process manufacturing time estimation

The process manufacturing time includes all the steps necessary to produce a part such as cleaning of the mould, applying the release agent, transferring the mould to the autoclave, etc. The formulas for calculating the process times in ACCEM model are presented in Figure 6.1 (Neoh, 1995). The steps 4 to 6 and from 13 to 18 were not used as long as they were already estimated by the methodology of lay-up time estimation. For step 45, the Autoclave cure cycle time that was recommended by the manufacturer of composite Hexcel for their prepreg fibres AS4/8552 is 262.67 min.

6.2.1.1 Layup time estimation

The lay-up time of each ply of the UD material was estimated by equation (6.1) (Haffner, 2002).

$$t_{Ply} = \tau_0 \cdot \left(\sqrt{\left(\frac{L}{\nu_0 \cdot \tau_0} + 1 \right)^2} - 1 \right) \quad (6.1)$$

Where ν_0 is the steady state velocity of the process; τ_0 is the time constant which represents the time to attain the steady state of the process and L is the length of the flat plate. For 304,8 mm width UD tape prepreg, the two process parameters ν_0 and τ_0 can be obtained by curve fitting the hyperbolic model with the power law ACCEM model. The lay-up time was determined by multiplying the layup time for each ply by the number of plies for the flat plate. The total lay-up time is the sum of all the calculated lay-up times. The data and the results for estimating the manufacturing time of flat plate are presented in Table 6.3.

Table 6.3 Flat plate manufacturing time estimation results

1st order model			
Component	Item	Value	Comments
Flat plate	ν_0 (ft/min)	2.63	For 304.8 mm width UD tape
	τ_0 (min)	0.666	
	L (ft)	1.166	
	t_{Ply} (min)	0.886	Equation (6.1)
	Number of plies	36	Flat plate thickness/ ply thickness. Ply thickness specified by Hexcel corp.

Table 6.3 (Continued)

Lay- up ACCEM model			
Process step plan	Step description	Time (min)	
1	clean lay-up tool surface	0.06	
2	apply release agent to surface	0.09	
3	position template and tape down	0.33	
4	304.8 mm manual ply deposition		For calculating total lay-up time
5	304.8 mm hand assist deposition		For calculating total lay-up time
6	tape layer (720 ipm)		For calculating total lay-up time
7	transfer from plate to stack	9.75	
8	transfer from stack to tool	0.27	
9	clean curing tool	0.06	
10	apply release agent to curing tool	0.12	
11	transfer lay-up to curing tool	0.27	
12	debulking (disposable bag)	4.82	
13	sharp male bend		For calculating total lay-up time
14	sharp female bend		For calculating total lay-up time
15	male radial		For calculating total lay-up time
16	female radial		For calculating total lay-up time
17	stretch flange		For calculating total lay-up time
18	shrink flange		For calculating total lay-up time
19	setup	4.20	
20	gather details, prefit, disassemble, clean	1.17	
21	apply adhesive	0.55	Applied for the highest length
22	assemble detail parts	0.27	
23	trim part	0.34	
24	apply porous separator	0.12	

Table 6.3 (Continued)

Lay- up ACCEM model			
Process step plan	Step description	Time (min)	
25	apply bleeder plies	9.68	
26	apply non-porous sep. film	0.12	
27	apply vent colth	0.27	
28	install vacuum fittings	0.37	
29	install thermocouples	0.97	
30	apply seal strips	0.58	
31	apply disposable bag	0.08	
32	seal edges	1.94	
33	connect vacuum Lines, apply vacuum	0.37	
34	smooth down	0.08	
35	check seals	0.06	
36	disconnect vacuum Lines	0.19	
37	check autoclave interior	1.80	
38	load lay-up in tray	0.27	
39	roll tray installation	1.50	
40	connect thermocouples	0.55	
41	connect vacuum Lines, apply vacuum	0.37	
42	check bag, seal and fittings	1.58	
43	close autoclave	1.15	
44	set recorders	3.36	
45	cure cycle		
46	cycle check	4.80	
47	shut down	0.20	

Table 6.3 (Continued)

Lay- up ACCEM model			
Process step plan	Step description	Time (min)	
48	remove charts	0.19	
49	open autoclave door	1.15	
50	disconnect thermocouples leads	0.21	
51	disconnect vacuum Lines	0.19	
52	roll tray out of autoclave	0.72	
53	remove lay-up from tray	0.27	
54	remove disposable bag	0.11	
55	remove thermocouples	0.57	
56	remove vacuum fittings	0.17	
57	remove vent cloth	0.09	
58	remove non-porous separator film	0.09	
59	remove bleeder plies	0.09	
60	remove porous separator film	0.09	
61	put used material aside	0.07	
62	remove lay-up	0.08	
63	clean tool	0.08	
Total process time		56.92	
Total lay-up time		31.93	
Cure cycle		262.67	Specified and recommended by Hexcel manufacturer
Total manufacturing process cycle		351.52	

6.2.2 Flat mould cost estimation

The flat mould is composed of two main components to be welded: The support structure and the mould plate. The support structure was made of several plates welded each other for good resistance to pressure during polymerization. Each one is about 12.7 mm thick and 152.4 mm high. The mould plate which was made of 19 mm thick flat plate has a dimension of 25.4 mm greater on each side than that of the mould face for setting up and sealing of plastic wrap to create the void. The mould plate and the support structure plates were submitted to machining operations respectively, for forming 6 mm thick plate mould cavity and the hollow rectangular cavities permitting the circulation of air through them during the autoclave cure cycle. The design of the flat mould is shown in Figure 6.2. Table 6.4 presents the flat mould manufacture process data. Table 6.5 presents the cost details for flat mould.

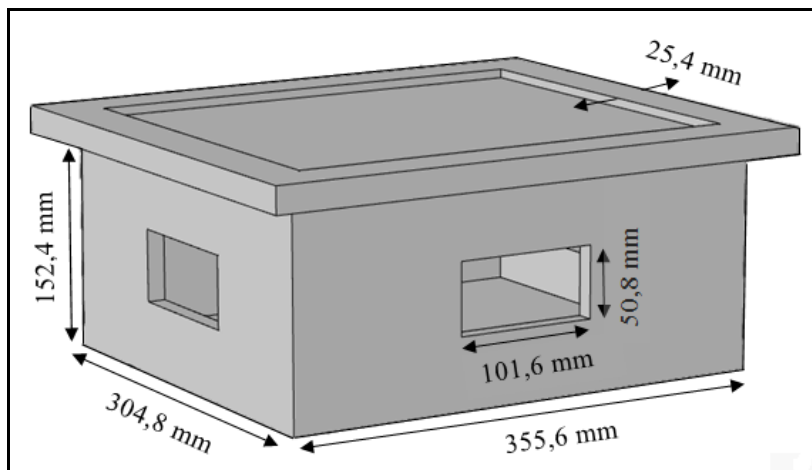


Figure 6.2 Design of flat mould for autoclave process with support structure

Table 6.4 Flat mould manufacture process data

Items	Value	Unit	Comments
Support structures			
Number of parallel plates	2		
Number of transversal plates	2		
Thickness	12.7	mm	
Area of parallel plates	$46.4 \cdot 10^3$	mm ²	152.4 mm height at plate extremities
Area of transversal plates	$54.2 \cdot 10^3$	mm ²	152.4 mm height at plate extremities
Material weight	20.59	kg	
Plasma cutting			
Hole cutouts in parallel plates	304.8	mm	Simple hole of 50.8 mm per 101.6 mm
Hole cutouts in transversal plates	304.8	mm	Same as parallel plate
Number of holes in parallel plates	1		
Number of holes in transversal plates	1		
Total cutting length	$1.22 \cdot 10^3$	mm	Average
Average cutting speed	$1.52 \cdot 10^3$	mm/min	
Plasma cutting time	0.013	hr	
Welding			
Number of welding seams	4		
Length of each seam	$1.52 \cdot 10^2$	mm	
Total seam length	$6.1 \cdot 10^2$	mm	Average
Welding speed	$1.4 \cdot 10^2$	mm/min	
Welding time	0.073	hr	
Machining			
Total machining length	$26.41 \cdot 10^2$	mm	Average
Cutting speed	$1.65 \cdot 10^2$	mm/min	
Machining time	0.267	hr	
plasma cutting face sheet elements			
Number of face elements	1		No plasma cutting
Perimeter of faces	$13.21 \cdot 10^2$	mm	

Table 6.4 (Continued)

Items	Value	Unit	Comments
Welding face			
Welding face length	13.21 10 ²	mm	
Welding face time	0.157	hr	
Deburring			
Deburring speed	101.6	mm/min	
Deburring time	0.216	hr	
Machining face			
Surface area	10.83 10 ⁴	mm ²	
Cutting depth (Roughing)	6.35	mm	
Material volume	660.73 10 ³	mm ³	
Roughing speed	65.55 10 ³	mm ³	
Finishing speed	6.4 10 ³	mm ²	
Rough machining time	0.168	hr	
Finish machining time	0.28	hr	
Polishing			
Polishing speed	3.2 10 ³	mm ²	
polishing time	0.56	hr	

Table 6.5 Cost details for flat mould

Processing plan for flat mould	Time (hr)	Costs (\$)	Comments
Support structure			
Support structure material		453.96	
Plasma cutting	1.01	253.33	15 min per plate for installation
Welding	1.47	220.91	1hr of setup + 10 min at each welding change for inspection
Machining	1.81	632.69	1hr de setup + 30 min to replace the part
Total support structure		1560.89	
Face sheet			
Face sheet material		2.55	Thickness of 19 mm
Fitting sheet to structure	0.25	25	15 min per plate for fitting

Table 6.5 (Continued)

Processing plan for flat mould	Time (hr)	Costs (\$)	Comments
Welding	2.16	323.64	1hr of setup + 15 min at each welding change for inspection
Deburring	0.47	46.67	No cost for rotary tool for grinding
Heat treatment		141.43	Thermal treatment with transportation included
Rough machining	1.17	408.8	1hr of setup
Finish machining	0.28	98	no setup
Polishing	0.81	81	15 min of setup, no cost for polishing tool
Inspection / leak check	0.58	115.84	40% of machining time (rough + finish)
Mount details		117.37	5% of manufacturing cost
In-house transportation	1	100.10	10% of manufacturing time
Manufacturing costs	11.01	2564.77	
Material costs		456.51	
Total costs		3021.28	
Overhead + profit			
Design and engineering		2800	30% of total cost
Boxing and shipping		470	5% of total cost
Optional FEM analysis		-	No complexity
Profit		1875	20% of total cost
Taxes		1222.9	14.975% of cost before taxes
Estimated total price		9389.18	

6.3 T-shape part

The T-shape part dimension of 76.2 mm x 76.2 mm x 3.17 mm was chosen according to the same width UD tape specified in ACCEM model (76.2 mm width tape). This part can be manufactured by assembly of three components, two L-shape parts and one flat plate. The lay-up can be done for these three components separately with a thickness of 1.585 mm each. Table 6.6 presents the other material costs for making a T-shape part by lay-up and autoclave cure (Fuchs, 2003; Ruoshi, 2012).

Table 6.6 Other material costs for making a T-shape part
by lay-up and autoclave cure
Adapted from Ruoshi (2012, p.29) and Fuchs (2003, p.82)

Material category	Supplier	Cost rate	Quantity	Cost
Release agent	Airtech	0.148\$/ml	25 ml	3.7 \$
Breather	Airtech	5.032\$/m ²	0.015 m ²	0.075 \$
Release film	Airtech	4.021\$/m ²	0.015 m ²	0.06 \$
Sealant tape	Airtech	4.78\$/unit	0.65	3.107 \$
Vacuum bag	Airtech	1.957\$/m ²	0.045 m ²	0.088 \$
Adhesive	-	17.5 \$/kg	0.15 kg	2.625 \$
Bleeder	Airtech	1.075\$/m ²	0.015 m ²	0.016 \$
Total cost				9.671 \$

6.3.1 Process manufacturing time estimation

The formulas for calculating the process times in ACCEM model for a T-shape part are the same as for a flat plate and the autoclave cure cycle time was also the same. However, a time for filling up the void gap between the components was considered. This step was designated by the AA and located between the steps 22 and 23 in Figure 6.1 (Neoh, 1995).

6.3.1.1 Lay-up time estimation

For flat plate component, the lay-up time of each ply of the UD material was estimated using equation (6.2) (LeBlanc et al., 1976). For the two L-shape components, equations (6.2), (6.3) and (6.4) were applied respectively for flat shape (no bend), male shape and female shape bends. The total lay-up time was obtained by summing the flat plate lay-up time and two L-shape lay-up times.

$$t_{ply} = 0.0014 L^{0.6018} \quad (6.2)$$

$$\text{For male shape } t_{ply} = 0.00007 L_b \quad (6.3)$$

$$\text{For female shape } t_{ply} = 0.00016 L_b \quad (6.4)$$

Where L is the length of the flat plate component; L_b is the length of the bend. The lay-up time was determined by multiplying the lay-up time for each ply by the number of plies for each component of the T-shape part. The total lay-up time is the sum of all the calculated layup times. The data and the results for estimating the manufacturing time of the T-shape part are presented in Table 6.7.

Table 6.7 T-shape part manufacturing time estimation results

Lay-up ACCEM model			
Component	Item	Value	Comments
Flat plate	L (mm)	76.2	
	t_{ply} (min)	0.163	Equation (6.2)
	Number of plies	8	T-shape thickness / ply thickness Ply thickness specified by Hexcel corp.

Table 6.7 (Continued)

Lay-up ACCEM model				
Component	Item		Value	Comments
Flat plate	Total lay-up time (min)		1.304	(t_1)
L-shape	L_b (mm)		76.2	
	t'_1 (min)	Male shape	0.012	Equation (6.3)
	t'_2 (min)	Female shape	0.029	Equation (6.4)
	Total lay-up time (min)		1.632	$t_2 = t_1 + 8(t'_1 + t'_2)$
Process step plan	Step description		Time (min)	Comments
1	clean lay-up tool surface		0.01	
2	apply release agent to surface		0.01	
3	position template and tape down		0.07	
4	76.2 mm manual ply deposition			For calculating total lay-up time
5	76.2 mm hand assist deposition			For calculating total lay-up time
6	tape layer (720ipm)			For calculating total lay-up time
7	transfer from plate to stack		0.59	
8	transfer from stack to tool		0.07	
9	clean curing tool		0.01	
10	apply release agent to curing tool		0.04	
11	transfer layup to curing tool		0.07	

Table 6.7 (Continued)

Process step plan	Step description	Time (min)	Comments
12	Debulking (disposable bag)	2.14	
13	sharp male bend		For calculating total lay-up time
14	sharp female bend		For calculating total lay-up time
15	male radial		For calculating total lay-up time
16	female radial		For calculating total lay-up time
17	stretch flange		For calculating total lay-up time
18	shrink flange		For calculating total lay-up time
19	setup	4.20	
20	Gather, details, prefit, disassemble, clean	0.42	
21	apply adhesive	0.08	Joining bend and flat plate components
22	assemble detail parts	0.07	
AA	Filling the gap between components	9.07	Based on step #6 formula
23	trim part	0.22	
24	apply porous separator film	0.04	
25	apply bleeder plies	0.67	
26	apply non-porous separator film	0.04	
27	apply vent colth	0.08	
28	install vacuum fittings	0.37	
29	install thermocouples	0.37	
30	apply seal strips	0.33	
31	apply disposable bag	0.03	
32	seal edges	1,12	
33	connect vacuum Lines, apply vacuum	0.37	
34	smooth down	0.03	
35	check seals	0.04	
36	disconnect vacuum Lines	0.19	

Table 6.7 (Continued)

Process step plan	Step description	Time (min)	Comments
37	check autoclave interior	1.80	
38	load lay-up in tray	0.07	
39	roll tray installation	1,50	
40	connect thermocouples	0.55	
41	connect vacuum Lines, apply vacuum	0.37	
42	check bag, seal and fittings	1.11	
43	close autoclave	1.15	
44	set recorders	3.36	
45	cure cycle		
46	cycle check	4.80	
47	shut down	0.20	
48	remove charts	0.19	
49	open autoclave door	1.15	
50	disconnect thermocouples leads	0.21	
51	disconnect vacuum Lines	0.19	
52	roll tray out of autoclave	0.72	
53	remove lay-up from tray	0.07	
54	remove disposable bag	0.03	
55	remove thermocouples	0.57	
56	remove vacuum fittings	0.17	
57	remove vent cloth	0.03	
58	remove non-porous separator film	0.03	
59	remove bleeder plies	0.03	
60	remove porous separator film	0.03	
61	put used material aside	0.02	
62	remove lay-up	0.01	
63	clean tool	0.03	
Total		39.15	
T-shape lay-up		4.57	
Cure cycle		262.67	Specified and recommended by Hexcel manufacturer
Total manufacturing process cycle		306.39	

6.3.2 Tooling costs estimation

The T-shape mould is composed of four main parts: The flat mould, two L-shape moulds and a support structure. The flat mould was made of 19 mm thick flat plate which was submitted to the machining operation in order to obtain 1.587 mm depth machined cavity and four drilled holes on the extremities of the flat plate. Moreover, the flat mould has a dimension of 25.4 mm greater on each side for setting up and sealing of plastic wrap to create the void. The vacuum pump was set up in the gap between the three components. The support structure consists of different plates of 101.6 mm high each which were welded and fixed to the flat mould. The support plates were machined in order to obtain the hollow square cavities permitting the circulation of air through them during the autoclave cure cycle. The two L-shape mould parts were made of 19 mm thick plates. Each bend L was shaped by a hydraulic press and was machined in order to obtain a 1.587 mm thick cavity and four drilled holes for assembly of the two L-shape mould parts together and the flat mould. A drilled hole was machined in one L-shape component in order to set up the vacuum pump. The designs of flat mould and L-shape mould components are shown in Figure 6.3 and Figure 6.4 respectively. The design of T-shape mould assembly with support structure is shown in Figure 6.5. Table 6.8 presents the T-shape mould manufacture process data. Table 6.9 presents the cost details for T-shape mould.

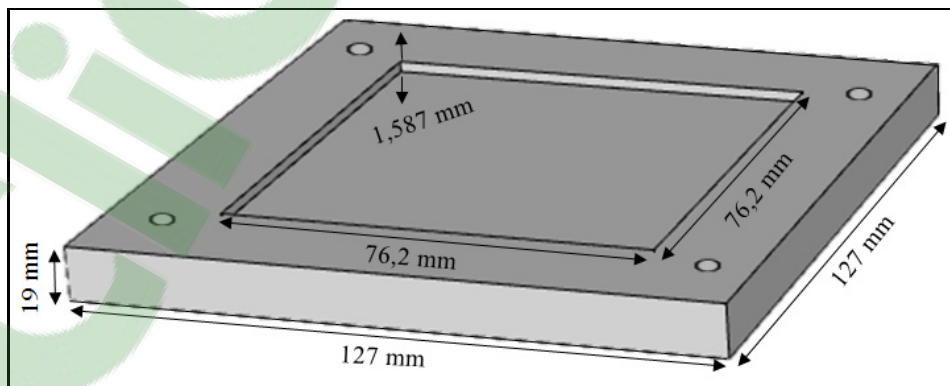


Figure 6.3 Flat mould component

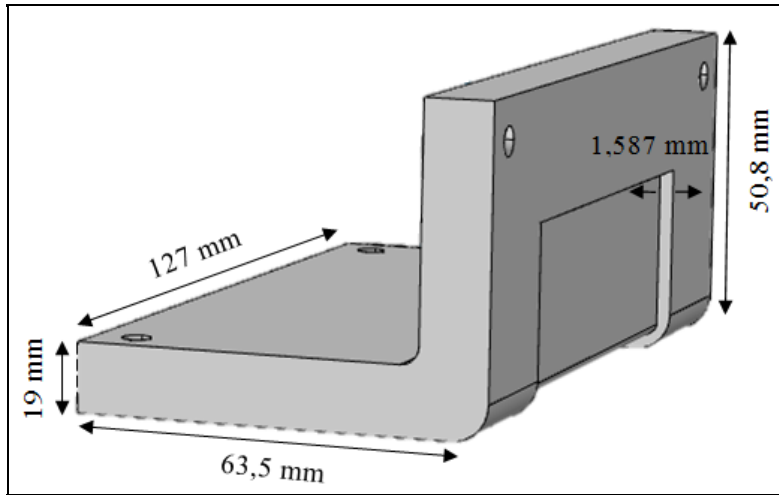


Figure 6.4 L-shape mould component

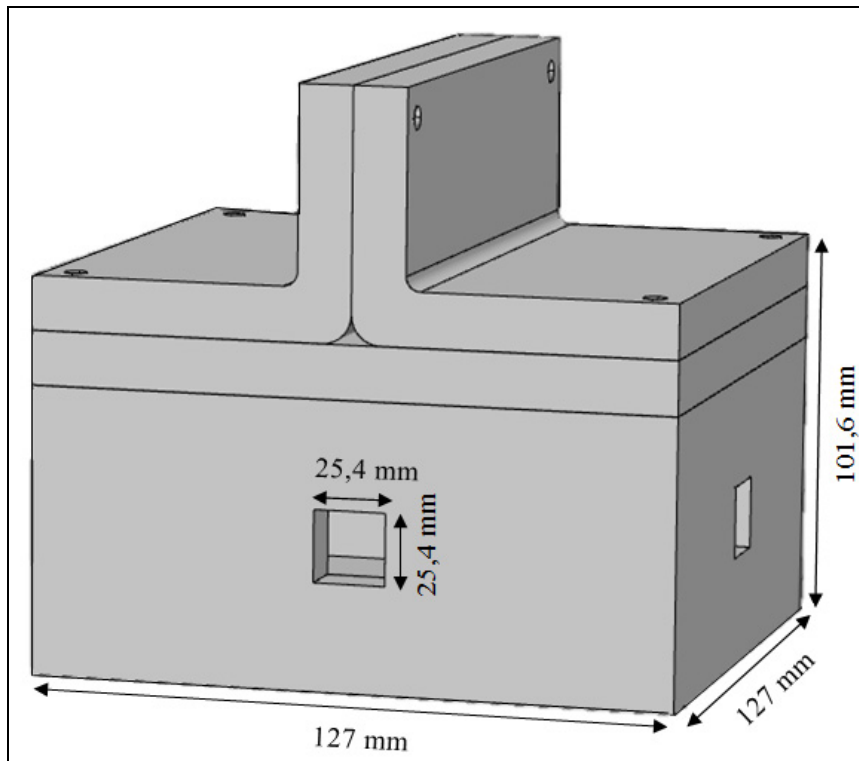


Figure 6.5 T-shape mould assembly with support structure

Table 6.8 T-shape mould manufacture process data

Items		Value	Unit	
Support structures				
Number of parallel plates		2		
Number of transversal plates		2		
Thickness		12.7	mm	
Area of parallel plates		$12.9 \cdot 10^3$	mm ²	101.6 mm height at plate extremities
Area of transversal plates		$12.9 \cdot 10^3$	mm ²	101.6 mm height at plate extremities
Material weight		5.28	kg	
Plasma cutting				
Hole cutouts in parallel plates		101.6	mm	Simple hole of 25.4 mm per 25.4 mm
Hole cutouts in transversal plates		101.6	mm	Same as parallel plate
Number of holes in parallel plates		1		
Number of holes in transversal plates		1		
Total cutting length		406.4	mm	Average
Average cutting speed		$1.524 \cdot 10^3$	mm/min	
Total cutting time		0.27	min	
Welding				
Number of welding seams		4		
Length of each seam		101.6	mm	
Total seam length		406.4	mm	Average
Welding speed		$0.14 \cdot 10^3$	mm/min	
Welding time		2.91	min	
Machining				
Total machining length		$1.016 \cdot 10^3$	mm	Average
Cutting speed		$0.165 \cdot 10^3$	mm/min	
Machining time		6.15	min	
plasma cutting face sheet elements				No plasma cutting
Number of face elements		3		
Perimeter of faces	Base	$0.508 \cdot 10^3$	mm	1 face
	L-shape	$0.482 \cdot 10^3$		2 faces

Table 6.8 (Continued)

Welding face			
Welding face length	$0.305 \cdot 10^3$	mm	
Welding face time	2.18	min	
Deburring			
Deburring speed	$0.101 \cdot 10^3$	mm/min	
Deburring time	3	min	
Machining face		L-part	Base
Surface area	$4.839 \cdot 10^3$	mm ²	$5.806 \cdot 10^3$
Cutting depth (Roughing)	1.59	mm	1.59
Material volume	$7.681 \cdot 10^3$	mm ³	$9.218 \cdot 10^3$
Roughing speed	$65.548 \cdot 10^3$	mm ³ /min	$65.548 \cdot 10^3$
Finishing speed	$6.451 \cdot 10^3$	mm ² /min	$6.451 \cdot 10^3$
Rough machining time	0.12	min	0.14
Finish machining time	0.75	min	0.05
Polishing			
Polishing speed	$3.226 \cdot 10^3$	mm ²	$3.226 \cdot 10^3$
Polishing time	1.5	min	1.8

Table 6.9 Cost details for T-shape mould

Processing plan for flat mould	Time (hr)	Costs	Comments
Support structure			
Support structure material		116.40	
Plasma cutting	1	251.11	15 min per plate for installation
Welding	1.45	217.27	1hr of setup + 10 min at each welding change for inspection
Machining	1.60	480.77	1hr de setup + 30 min to replace the part
Total support structure		1065.55	
L-shape (2 parts)			
L-shape material		98.21	19 mm thick sheet
forming	0.50	75.00	15 min per plate for forming + press rate at 50\$/hr

Table 6.9 (Continued)

Rough machining	2.00	601.17	1 hr of setup + 30 min to replace the part (replace one time), 2 parts
Finish machining	1.03	307.50	no setup + 30 min to replace the part (replace one time), 2 parts
Drilling hole	0.37	110.00	0.3 hr setup of machine , 0.3 min/hole , 8 holes per part , 5 min setup per hole , operation rate is the same as press rate
Threaded hole	0.28	84.00	2.1min/hole , 8 holes
Heat treatment	-	28.00	heat treatment including transport
Polishing	0.30	30	15 min of setup, no cost for polishing tool
Inspection / leak check	1.21	121.16	40% of machining time (rough + finish)
Base			
Base material costs		54.56	19 mm thick sheet
Fitting base to structure	0.25	25	15 min per plate for fitting
Welding	2.04	305.45	1hr of setup + 15 min at each welding change for inspection
Drilling hole	0.333	67.15	0.3 hr setup of machine , 0.4 min/hole , 4 holes per part , 0.1 min setup per hole , operation rate is the same as press rate
Threading hole	0.14	42	2.1min/hole, 4 holes
Heat treatment		28.37	Thermal treatment with transportation included
Rough machining	1	300.70	1hr of setup
Finish machining	0.001	0.28	No setup
Polishing	0.28	28	15 min of setup, no cost for polishing tool
Inspection / leak check	0.4	80.26	40% of machining time (rough + finish)
Fasteners		1.7	4 units (0.25\$/ screw) + 2 units (0.35\$/screw)
Assembly	0.08	8	0.8 min/screw
Mount details		176.88	5% of manufacturing cost
In-house transportation	1.586	158.6	10% of manufacturing time

Table 6.9 (Continued)

Manufacturing costs	15.86	3528.37	
Material costs		217.16	
Total		3745.53	
Overhead + profit			
Design and engineering cost		4000	30% of manufacturing cost
Boxing and shipping cost		670	5% of total cost
Optional FEM analysis		134	level of complexity : medium
Profit		2700	20% of total
Taxes		1684.62	14.975% of cost before taxes
Estimated total price		12934.15	

6.4 L-bracket

The L-shape part dimension of 230 mm x 76.2 mm x 6.4 mm with 115 mm leg length and 40 mm rib high was chosen according to the same width UD tape specified in ACCEM model (76.2 mm width tape). This part can be manufactured by assembly of two components, an L-profile and a triangular plate as a rib. Table 6.10 presents the other material costs for making an L-bracket part by lay-up and autoclave cure (Fuchs, 2003; Ruoshi, 2012).

Table 6.10 Other material costs for making an L-bracket part by lay-up and autoclave cure
Adapted from Ruoshi (2012, p.29) and Fuchs (2003, p.82)

Material category	Supplier	Cost rate	Quantity	Cost
Release agent	Airtech	0.148\$/ml	25 ml	3.7 \$
Breather	Airtech	5.032\$/m ²	0.019 m ²	0.095 \$
Release film	Airtech	4.021\$/m ²	0.019 m ²	0.076 \$
Sealant tape	Airtech	4.78\$/unit	0.7	3.346 \$
Vacuum bag	Airtech	1.957\$/m ²	0.039 m ²	0.076 \$
Adhesive	-	17.5 \$/kg	0.15 kg	2.625 \$
Bleeder	Airtech	1.075\$/m ²	0.019 m ²	0.02 \$
Total cost				9.938 \$

6.4.1 Process manufacturing time estimation

Similarly, the formulas for calculating the process times in ACCEM model are the same as flat plate and T-shape part. The autoclave cure cycle time was also the same.

6.4.1.1 Layup time estimation

For the L-shape component, the lay-up time of each ply of the UD material was estimated using equations (6.2), (6.3) and (6.4) (LeBlanc et al., 1976) which were applied respectively for flat shape (no bend), male shape and female shape bends. For the triangular plate, equation (6.2) was applied by making the assumption that the lay-up time corresponds approximately to half of the width UD tape specified in ACCEM model (76.2 mm width tape) for a flat plate having a 80 mm side (see Figure (6.6)). The lay-up time for each component was determined by multiplying the lay-up time of each ply by the number of plies. The total lay-up time was obtained by summing the triangular plate lay-up time and the L-shape lay-up time.

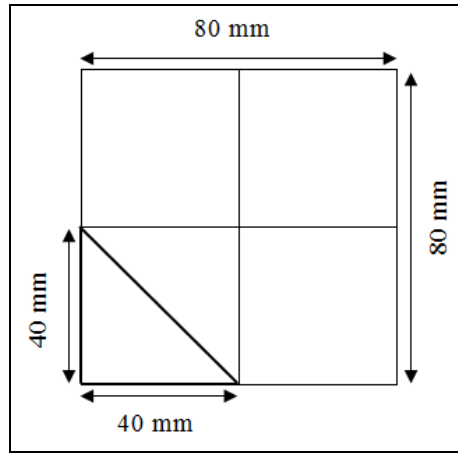


Figure 6.6 Design of the triangular flat plate

Where L is the length of the component; L_b is the length of the bend. The data and the results for estimating the manufacturing time of the L-shape part are presented in Table 6.11.

Table 6.11 L-bracket manufacturing time estimation results

Lay-up ACCEM model				
component				Comments
L-shape	Flat-shape (without bend)	L (mm)		76.2
		t_{ply} (min)		0.163
		Number of plies		8
		layup time (min)		1.304
			$t_1 = 8 \times 0.163$	
	L-bend	L_b (mm)		76.2
		t'_1 (min)	Male shape	0.012
t'_2 (min)		Female shape	0.029	
		Equation (6.3)		
		Equation (6.4)		

Table 6.11 (Continued)

Lay-up ACCEM model				
		Number of plies	8	Flat plate thickness / ply thickness Ply thickness specified by Hexcel corp.
		Lay-up time (min)	1.632	$t_2 = t_1 + 8(t'_1 + t'_2)$
Rib		L (mm)	76.2	
		t'_{Ply} (min)	0.081	$= 0.5 \times t_{Ply}$
		Number of plies	8	Flat plate thickness / ply thickness Ply thickness specified by Hexcel corp.
		Lay-up time (min)	0.648	$t_3 = 8 \times 0.081$
Power law ACCEM model				
Process step plan	Step description	Time (min)		
1	clean lay-up tool surface	0.011		
2	apply release agent to surface	0.017		
3	position template and tape down	0.090		
4	76.2 mm manual ply deposition			For calculating total lay-up time
5	76.2 mm hand assist deposition			For calculating total lay-up time
6	tape layer (720 ipm)			For calculating total lay-up time
7	transfer from plate to stack	0.693		
8	transfer from stack to tool	0.087		
9	clean curing tool	0.011		
10	apply release agent to curing tool	0.017		

Table 6.11 (Continued)

Power law ACCEM model			
Process step plan	Step description	Time (min)	
11	transfer lay-up to curing tool	0.087	
12	debulking (disposable bag)	2.320	
13	sharp male bend		For calculating total lay-up time
14	sharp female bend		For calculating total lay-up time
15	male radial		For calculating total lay-up time
16	female radial		For calculating total lay-up time
17	stretch flange		For calculating total lay-up time
18	shrink flange		For calculating total lay-up time
19	setup	4.200	
20	gather details, prefit, disassemble, clean	0.481	
21	apply adhesive	0.101	Joining bend and rib components
22	assemble detail parts	0.087	
23	trim part	0.222	
24	apply porous separator film	0.034	
25	apply bleeder plies	0.597	
26	apply non-porous separator film	0.034	
27	apply vent colth	0.112	
28	install vacuum fittings	0.372	

Table 6.11 (Continued)

Power law ACCEM model			
Process step plan	Step description	Time (min)	
29	install thermocouples	0.972	
30	apply seal strips	0.407	
31	apply disposable bag	0.022	
32	seal edges	1.374	
33	connect vacuum Lines, apply vacuum	0.366	
34	smooth down	0.011	
35	check seals	0.043	
36	disconnect vacuum Lines	0.186	
37	check autoclave interior	1.800	
38	load lay-up in tray	0.087	
39	roll tray installation	1.500	
40	connect thermocouples	0.552	
41	connect vacuum Lines, apply vacuum	0.366	
42	check bag, seal and fittings	1.237	
43	close autoclave	1.152	
44	set recorders	3.360	
45	cure cycle		
46	cycle check	4.800	
47	shut down	0.199	
48	remove charts	0.192	

Table 6.11 (Continued)

Power law ACCEM model			
Process step plan	Step description	Time (min)	
49	open autoclave door	1.152	
50	disconnect thermocouples leads	0.210	
51	disconnect vacuum Lines	0.186	
52	roll tray out of autoclave	0.720	
53	remove lay-up from tray	0.087	
54	remove disposable bag	0.030	
55	remove thermocouples	0.570	
56	remove vacuum fittings	0.174	
57	remove vent cloth	0.026	
58	remove non-porous separator film	0.026	
59	remove bleeder plies	0.026	
60	remove porous separator film	0.026	
61	put used material aside	0.019	
62	remove lay-up	0.022	
63	clean tool	0.022	
Total		31.49	
Lay-up		2.28	
Cure cycle		262.67	Specified and recommended by Hexcel manufacturer
Total manufacturing process cycle		296.44	

6.4.2 Tooling costs estimation

The L-shape mould is composed of three main components to be assembled: The L-shape part, the support structure and the rib. The L-shape part was made of 25.4 mm thick plate having 6.4 mm depth machined cavity, the bend L was shaped by a hydraulic press. The support structure was made of several plates welded together and with the L-shape part of good resistance to pressure during polymerization. Each one is about 12.7 mm thick and 152.4 mm high. The support plates were machined in order to obtain the hollow cavities permitting the circulation of air through them during the autoclave cure cycle. The rib of the mould was made in two steps. The first step consists to assemble 25.4 mm thick plates which were cut in triangular form by plasma cutting and a flat plate having the same thickness as the first part and was bent by hydraulic press. The second step consists of machining these two parts in order to make the half rib cavity and drilled holes for assembly. A drilled hole was machined in L-shape component in order to set up the vacuum pump. The mould rib manufacturing was completed by repeating the first step and assembling the two machined components. The L-shape plates has a dimension of 25.4 mm greater on each side for setting up and sealing of plastic wrap to create the void. Finally, the all mould components were assembled. The designs of L-shape mould components are shown in Figure 6.7. The design of L-shape mould assembly with support structure is shown in Figure 6.8. The L-shape mould manufacture process data are presented in Table 6.12. Table 6.13 presents the cost details for L-shape mould.

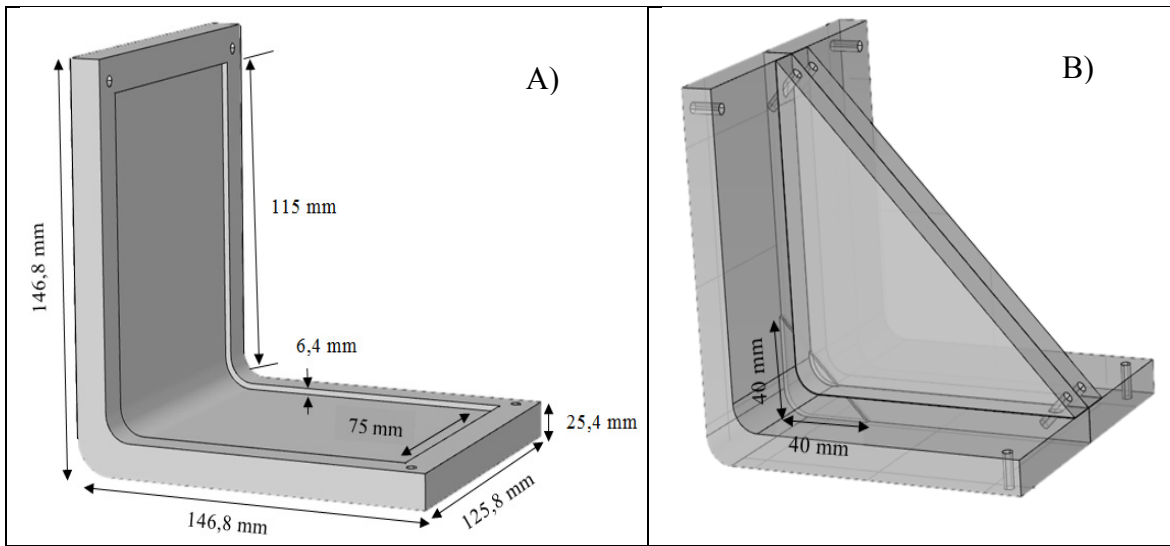


Figure 6.7 Design of L-shape mould components:
 A) L-shape cavity B) L-shape rib cavity

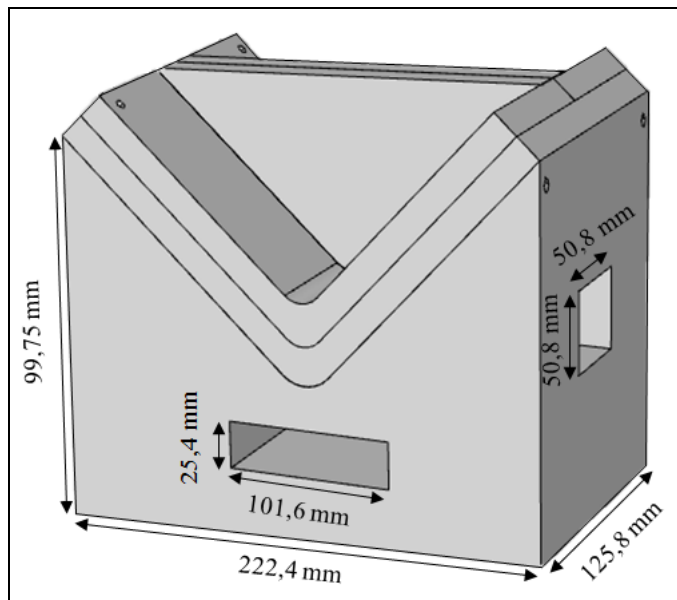


Figure 6.8 Design of L-shape mould assembly
 with support structure

Table 6.12 L-shape mould manufacture process data

Items	Value	Unit	
Support structures			
Number of parallel plates	2		
Number of transversal plates	2		
Thickness	12.7	mm	
Area of parallel plates	22 10 ³	mm ²	152.4 mm height at plate extremities
Area of transversal plates	19.35 10 ³	mm ²	152.4 mm height at plate extremities
Material weight	8.46	kg	
Plasma cutting			
Contour of mould form	585.72	mm	
Contour of hole in parallel plates	254	mm	Simple hole: 25.4 mm x 101.6 mm
Contour of hole in transversal plates	203.2	mm	Simple hole: 50,8 mm x 50,8 mm
Number of holes in parallel plates	1		
Number of holes in transversal plates	1		
Total cutting length	1.5 10 ³	mm	
Cutting speed	1.52	mm/min	Average
Cutting time	0.016	hr	
L-part			
Welding			
Number of welding seams	4		
Length of each seam	152.4	mm	
Total seam length	609.6	mm	
Welding speed	0.14	mm/min	Average
Welding time	0,072	hr	
Machining			
Total machining length	1.17	mm	
Cutting speed	165.1	mm/min	Average
Machining time	0.118	hr	
plasma cutting face sheet elements			
Number of face elements	1		No plasma cutting
Perimeter of faces	612.65	mm	

Table 6.12 (Continued)

Items	Value	Unit	
Welding face			
Welding face length	917.45	mm	
Welding face time	0.11	hr	
Deburring			
Deburring speed	101.6	mm/min	
Deburring time	0.15	hr	
Brace (rib)			
L-part			
Machining face			
Surface area	$17.53 \cdot 10^3$	mm^2	
Cutting depth (Roughing)	6.4	mm	
Material volume	$112.24 \cdot 10^3$	mm^3	
Roughing speed	$65.55 \cdot 10^3$	mm^3/min	
Finishing speed	$6.45 \cdot 10^3$	mm^2/min	
Rough machining time	0.028	hr	
Finish machining time	0.045	hr	
Brace (rib)			
Machining face			
Surface area	800	mm^2	
Cutting depth (Roughing)	6.4	mm	
Material volume	$5.12 \cdot 10^3$	mm^3	
Roughing speed	$65.55 \cdot 10^3$	mm^3/min	
Finishing speed	$6.45 \cdot 10^3$	mm^2/min	
Rough machining time	0.024	hr	Including machining of vacuum pump
Finish machining time	0.009	hr	
Polishing			
Polishing speed	$3.23 \cdot 10^3$	mm^2	For both L-part and rib
polishing time	0.016	hr	Including machining of vacuum pump
Welding face brace			
Total seam length	663.45	mm	
Welding speed	140	mm/min	Average
Welding time	0.08	hr	

Table 6.12 (Continued)

Items	Value	Unit	
Plasma cutting brace			
Number of face elements	1		
Perimeter of each face element	92.81	mm	
Cutting speed	$1.52 \cdot 10^3$	mm/min	Average
Cutting time	0.001	hr	
Deburring brace			
Deburring speed	101.6	mm/min	
Deburring time	0.109	hr	

Table 6.13 Cost details for L-shape mould

Support structure material cost		186.50	
Plasma cutting	1.02	254.10	15 min per plate for installation
Welding	1.47	220.91	1 hr of setup + 10 min at each welding change for inspection
Machining	1.62	566.39	1 hr de setup + 30 min to replace the part
Heat treatment		27.98	heat treatment including transport
Total support structure costs		1223.51	
L-part			
L-part material costs		95.01	25.4 mm thick sheet
Forming	0.25	37.50	15 min par plaque pour le formage + coût presse à 50\$/h
Fitting base to structure	0.25	25.00	15 min per plate for fitting
Welding	2.61	391.42	1 hr of setup + 15 min at each welding change for inspection
Deburring	0.40	40.05	No cost for rotary tool for grinding
Rough machining	1.53	534.99	1 hr of setup + 30 min to replace the part (replace one time)
Finish machining	0.55	190.86	no setup + 30 min to replace the part (replace one time)

Table 6.13 (Continued)

L-part			
Drilling hole	0.33	114.33	0.3 hr setup machine , 0.3 min/hole , 4 holes per part , 0.1 min setup per hole , operation cost with same press
Threading hole	0.14	14.00	2.1min/hole , 4 holes
Heat treatment		28.50	heat treatment including transport
Polishing	0.02	2.27	15 min of setup, no cost for polishing tool
Inspection / leak check	0.83	82.95	40% of machining time (rough + finish)
Brace - part			
Brace part material cost		197.24	25.4 mm thick sheet
Forming	0.25	37.50	15 min par plaque pour le formage + coût presse à 50\$/h
Plasma cutting	0.25	37.65	15 min per plate for installation
Welding	1.75	261.87	1 hr of setup + 10 min at each welding change for inspection
Deburring	0.11	10.88	No cost for rotary tool for grinding
Rough machining	1.02	358.42	1 hr of setup
Finish machining	1.01	353.37	No setup
Drilling hole	0.33	114.33	0.3 hr setup machine , 0.3 min/hole , 8 holes per part , 5 min setup per hole, operation cost with same press
Threading hole	0.28	28.00	2,1min/hole ; 2 holes tapping
Heat treatment		55.20	heat treatment including transport
Polishing	0.01	1.09	15 min of setup, no cost for polishing tool
Inspection / leak check	0.81	81.35	40% of machining time (rough + finish)

Table 6.13 (Continued)

Brace - part			
Fasteners		2	4 units (0.35\$/ screw) + 4 units(0.15\$/screw)
Assembly	0.35	35	Handling + alignment
Mount details		193.55	5% of manufacturing cost
in-house transportation	1.68	168.30	10% of manufacturing time
Manufacturing costs	16.83	4269.76	
Material costs		478.75	
Total costs		4748.51	
Overhead + profit			
Design and engineering		4700	30% of manufacturing cost
Boxing and shipping		790	5% of total cost
Optional FEM analysis		250	level of complexity : medium
Profit		3150	20% of total
Taxes		2042.37	14.975% of cost before taxes
Estimated total price		15680.88	

6.5 Cost analysis

The costs of the composite thermoset parts manufactured by an autoclave process, including different cost elements can be calculated using the same technique as the compression moulded composite thermoplastic parts costs which were calculated in an Excel spreadsheet (For more details, see costs calculation Excel spreadsheet for flat plate, T-shape and L-bracket part in ANNEX V, ANNEX VI and ANNEX VII respectively).

The energy costs were estimated according to Song, Youn et Gutowski (2009) who estimated the heating energy consumption during the autoclave cure of 21.9 MJ/kg (6.083 kWh/kg). The energy costs were obtained by multiplying the total weight of the manufactured parts by the energy consumption per part. In the present case study, one part was used. The other cost calculations were based on the industrial and academic data assumptions such as:

- Material costs for lay-up and autoclave cure include costs of the prepreg, release agent, breather, release film, sealant tape, vacuum bag, adhesive, and bleeder. The prepreg material price is 152\$/kg (Haffner, 2002) and the material burden rate is 15%. The material cost was calculated by applying equation (7.10);
- One parallel stream and one of machine/stream are chosen for equipment and tooling;
- The installations and training costs of autoclave equipment are assumed to be 35k\$;
- The installations and training costs for tooling are assumed to be 200 \$;
- For building costs, the footprint/stream is assumed to be 18.58 m² for autoclave equipment, 2.23 m² of lay-up surface, 74.322 m² for material and finished part storage;
- For working capital cost estimation, the capital recovery period and the cost of capital r are assumed to be 13 months and 30% respectively;
- The useful life t of the autoclave equipment and the cost of capital r are being assumed to be 10 years and 30% respectively.

For the three studied parts, the costs calculations were based on 2% of rejects and 80% of the productivity, which corresponds to production volumes of 257 flat plates, 295 T-shape parts and 305 L-bracket parts.

For all thermoset studied parts, the total cost per part is the sum of material cost, labour cost, energy cost, equipment cost, tooling cost, building cost, cost of working capital and overhead cost. The obtained cost breakdowns show how each category of cost contribute to the total cost.

6.5.1 Flat mould

Table 6.14 presents the estimated costs for the thermoset flat plate. Figure 6.9 shows the cost breakdown of the thermoset flat plate.

Table 6.14 Estimated cost for the thermoset flat plate

Cost category	Cost per part (\$)
Material cost	162.54
Labour cost	747.08
Energy cost	0.29
Equipment cost	552.7
Tooling cost	22.37
Building cost	23.91
Cost of working capital	320.36
Overhead cost	1494.16
Total cost	3323.42

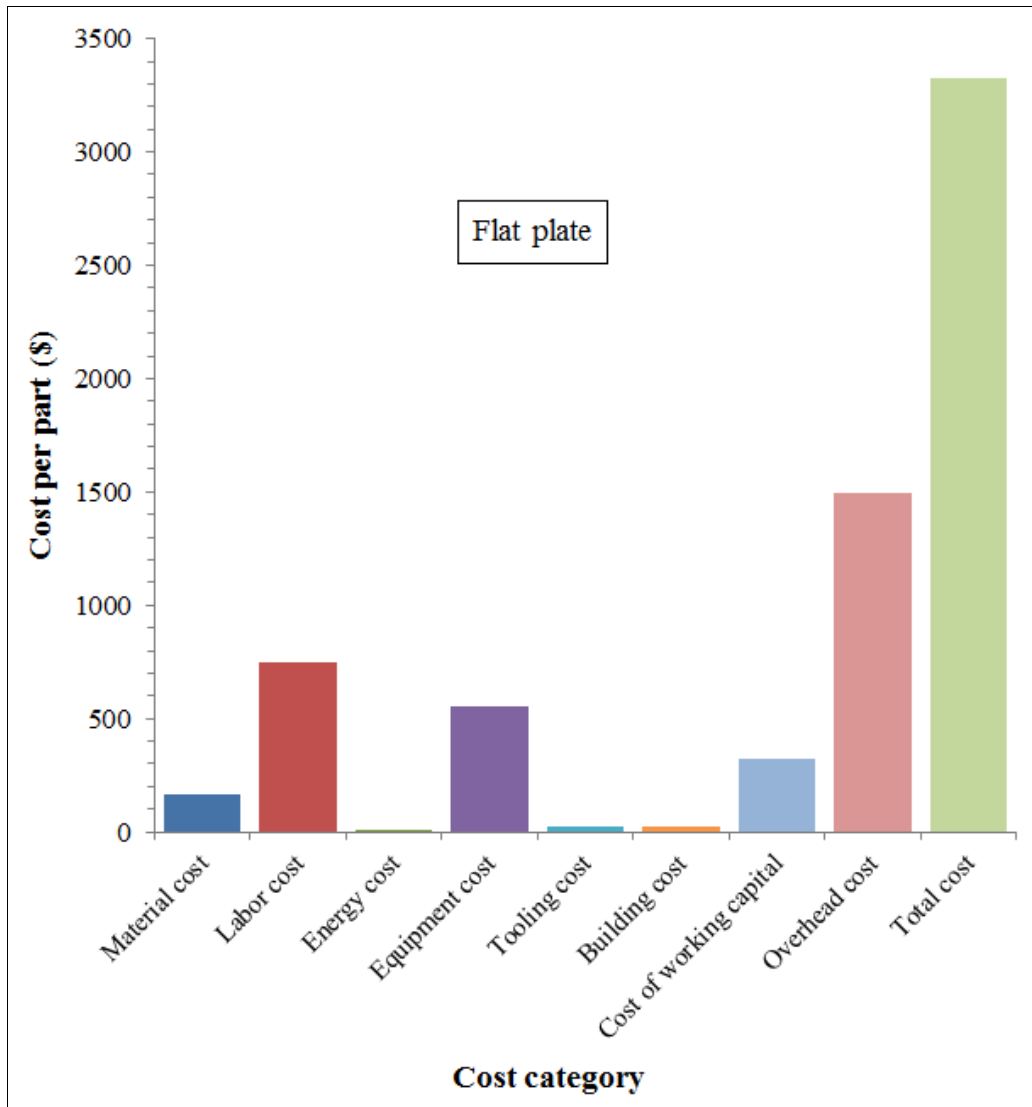


Figure 6.9 Cost breakdown of the thermoset flat plate

6.5.2 T-shape part

Table 6.15 presents the estimated costs for the thermoset T-shape part. Figure 6.10 shows the cost breakdown of the thermoset T-shape part.

Table 6.15 Estimated costs for the thermoset T-shape part

Cost category	Cost/part(\$)
Material cost	10.73
Labor cost	572.74
Energy cost	0.019
Equipment cost	481.5
Tooling cost	24.95
Building cost	20.82
Cost of working capital	205.44
Overhead cost	1145.49
Total cost	2461.71

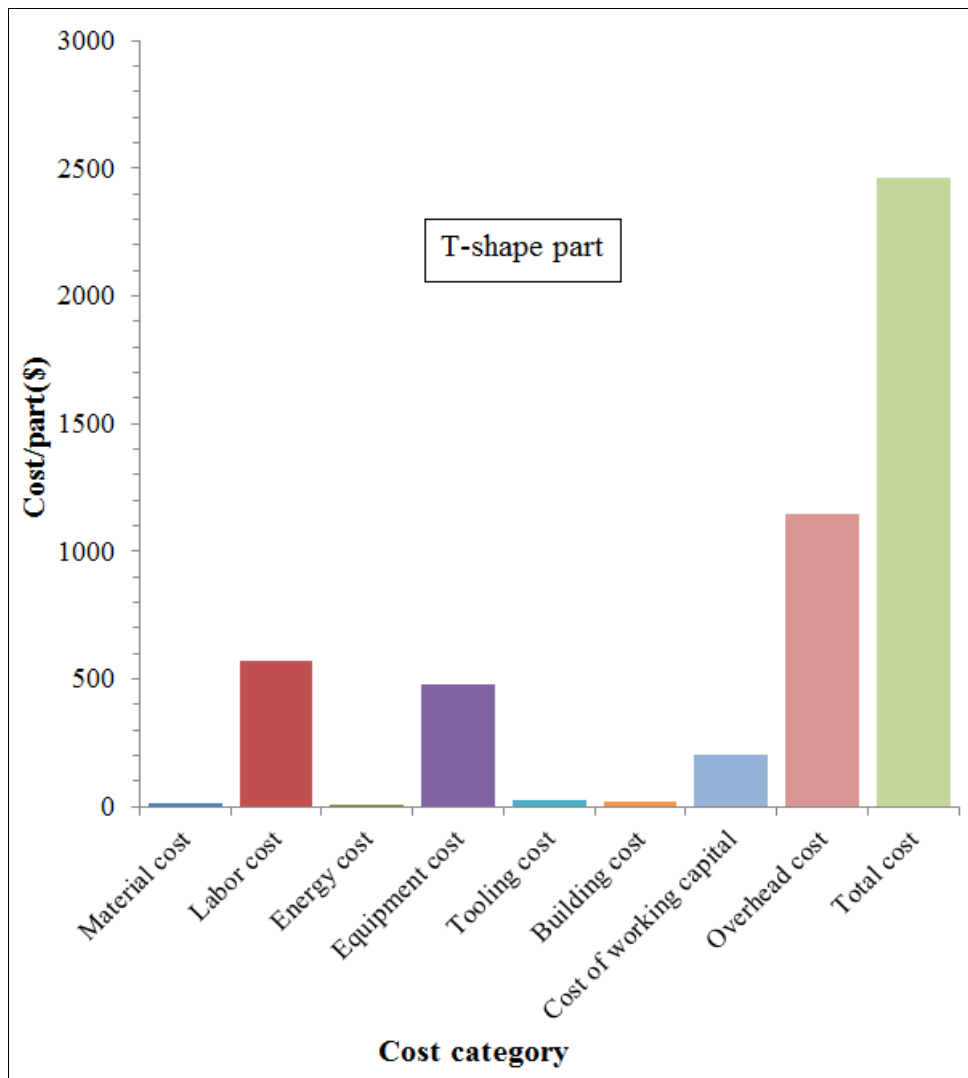


Figure 6.10 Cost breakdown of the thermoset T-shape part

6.5.3 L-bracket part

Table 6.16 presents the estimated costs for the thermoset L-bracket part. Figure 6.11 shows the cost breakdown of the thermoset L-bracket part.

Table 6.16 Estimated costs for the thermoset L-bracket part

Costs category	Cost per part (\$)
Material cost	28.87
Labor cost	553.97
Energy cost	0.05
Equipment cost	465.72
Tooling cost	29.18
Building cost	20.14
Cost of working capital	205.23
Overhead cost	1107.94
Total cost	2411.10

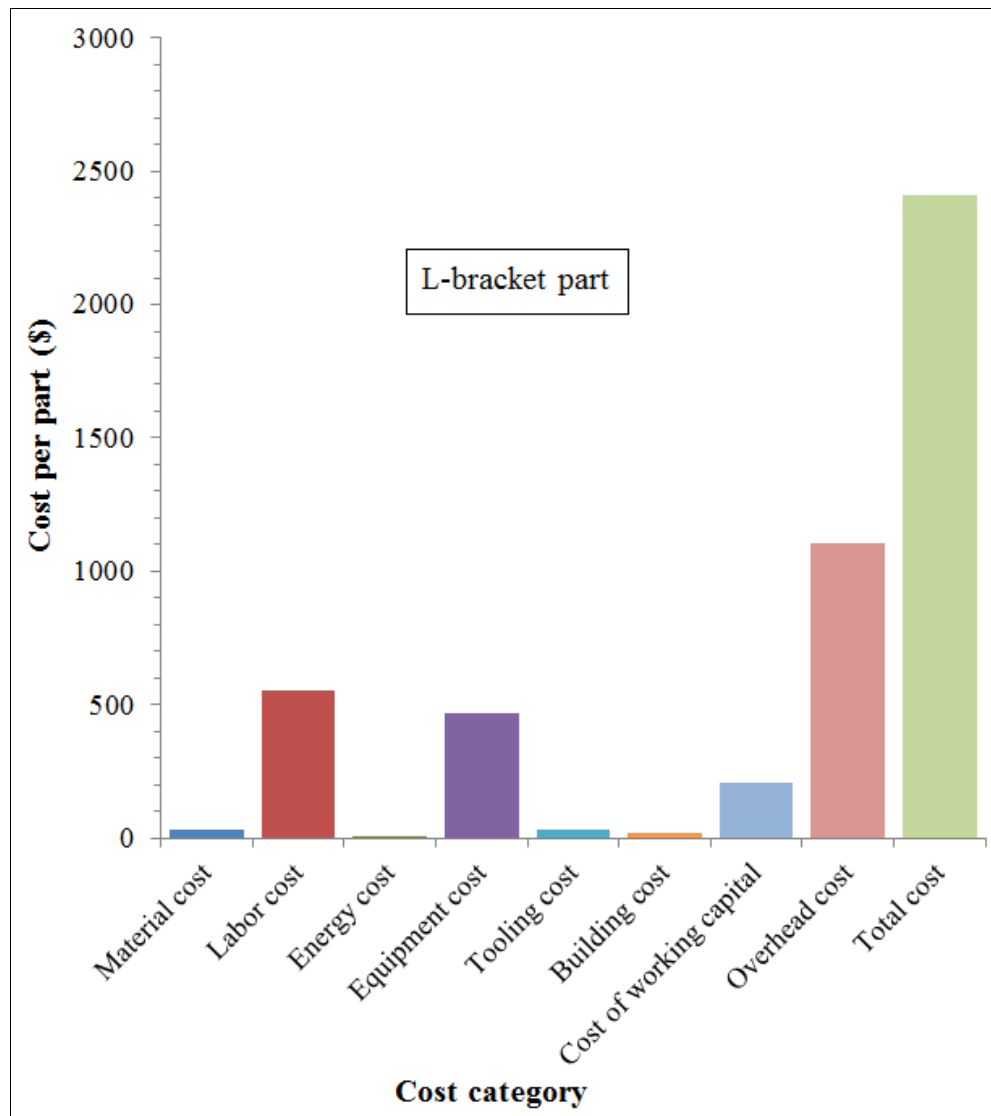


Figure 6.11 Cost breakdown of the thermoset L-bracket part

6.6 Discussion of results and conclusion

The manufacturing cost analysis for thermoset composites parts made by an autoclave process using the same approach than those for thermoplastic composites parts made by a compression moulding process were performed in an Excel spreadsheet. The manufacturing process cycle times for the studied parts and the tooling costs were estimated using the theories of Haffner (2002) and Neoh (1995). The estimation of other costs was based on

assumptions. The cycle times estimation results showed that there was no significant difference between cycle times for manufacturing three part forms such as flat plate, T-shape part and L-shape part due to the same cure cycle which was specified and recommended by Hexcel manufacturer. The estimated tooling cost comparison showed that the L-shape mould cost was higher than that of the T-shape mould which was higher than that of flat mould, due to different manufacturing times of the moulds. The manufacturing times difference was due to the number and the dimension of mould components to make.

From the obtained cost results, for all the thermoset studied parts, it was found that overhead cost dominates the total cost per part due to high labour cost as the overhead cost was assumed to be two times of labour cost. The labour and equipment cost are the important cost elements in the cost analysis of thermoset parts manufactured by autoclave process. The high equipment price and high labour rate lead respectively to high equipment cost and high labour cost. The energy costs are the lowest cost element due to lower energy consumption.

The total cost results showed that there was significant cost difference between flat plate and T-shape, L-bracket parts manufactured by autoclave process due to different geometries of these parts. The cost of flat plate is higher than that of T-shape and L-bracket parts due to higher manufacturing process cycle time and higher material cost, which all are due a great geometry of the flat plate. So it is important to decrease two cost drivers: equipment price and labor rate for reducing the manufacturing cost.

In order to make comparison between the costs of thermoset parts manufactured by autoclave process and thermoplastic parts manufactured by a compression moulding process, it is necessary to calculate the total cost of the parts. The manufacturing cost analysis for thermoplastic composite parts made by compression moulding processes studied in the previous chapters will be presented in chapter 7.

CHAPTER 7

MANUFACTURING COST ANALYSIS FOR THERMOPLASTIC COMPOSITE COMPRESSION MOULDED AEROSPACE COMPONENTS

7.1 Introduction

The manufacturing costs calculations were performed in Excel spreadsheet by applying different costs equations and imputing different industrial and academic data. The industrial data were obtained from a meeting of researchers of ETS and industrial partners on cost modeling by considering assumptions (see Table 7.2). The energy consumptions scaling laws and the tooling costs scaling laws already established under equation linear form in chapters 3 and 5 were integrated in the Excel program.

7.2 Manufacturing costs

According to (Haffner, 2002), the manufacturing costs include different costs elements. Commonly, the manufacturing costs can be divided into two categories of costs: variables costs and fixed costs. The total manufacturing costs are defined as the sum of fixed costs and variables costs. These manufacturing costs are presented in Table 7.1.

Table 7.1 Typical manufacturing costs

Variable costs	Fixed cost
Material	Equipment and tooling
Direct labor	Setup and maintenance
Energy	Capital cost
Operation	Management
....	Floorspace
....	Overheads, etc.

7.2.1 Manufacturing cost elements

The variables costs and fixed costs include the individual cost elements such as material costs labor, tooling costs, etc...The costs elements can be estimated on different ways. According to Gutowski and his disciples: (Haffner, 2002; Neoh, 1995), they were estimated on an annual base.

- **Operation conditions**

The manufacturing costs of the part depend on the operation conditions such as the production volume, the labor productivity and the capacity utilization of the production.

The production volume can be divided into two categories: the actual production volume and the effective production volume. The actual production volume corresponds to amount of products specified by the customer. The effective production volume is the actual production volume by considering the proportion of produced parts to be rejected. The company should produce more than the annual actual production volume. The effective production volume (Haffner, 2002, p. 121) is expressed by equation (7.1).

$$Eff. Prod. Vol = \frac{Annual Prod. Vol}{(1 - Reject Rate)} = Eff. Number of Run \times \frac{Parts}{Run} \quad (7.1)$$

In order to produce the effective production volume, it is needed to make an effective number of runs. The run means a certain quantity of produced parts between setups.

- **Labor productivity**

The labor productivity is the relationship between the annual production time and the annual available time. The annual production time is the time spent annually on actual production (breaks, downtime, etc. are considered). The annual production time (Haffner, 2002, p. 121) is expressed by equation (7.2).

$$\text{Ann. Prod. Time} = \frac{\text{Cycle time}}{\text{Run}} \times \text{Eff. Number of Runs} \quad (7.2)$$

The cycle time per run is defined as the summation of all the processing times and set up times for each processing step symbolized by letter i . The cycle time per run (Haffner, 2002, p. 133) was given by equation (7.3).

$$\frac{\text{Cycle Time}}{\text{Run}}_i = \frac{\text{Setup}}{\text{Run}} + \left(\frac{\text{Delay}}{\text{Operation}} + \frac{\text{Proc.time}}{\text{Operation}} \right) \times \left(\frac{\text{Operations}}{\text{Part}} \right) \times \left(\frac{\text{Parts}}{\text{Run}} \right) \quad (7.3)$$

The annual available time per run (Haffner, 2002, p. 121) was defined as the number of working days per year and the number of hours per shift and the number of shifts per day. It is expressed by equation (7.4).

$$\text{Ann. Avail. Time} = \frac{\text{Working Days}}{\text{Year}} \times \frac{\text{Shifts}}{\text{Day}} \times \frac{\text{Hours}}{\text{Shift}} \quad (7.4)$$

Therefore, the labor productivity run (Haffner, 2002, p. 121) is expressed by equation (7.5).

$$\text{Labor Productivity} = \frac{\text{Ann. Prod. Time}}{\text{Ann. Avail. Time}} \quad (7.5)$$

- **Capacity**

The production capacity (Haffner, 2002, p. 122) was defined as the number of parallel production stream to be installed for completing the customer demand using the available resources. The capacity is affected by the annual available time, the cycle time, and labor productivity. The number of parallel stream was formulated by equation (7.6) (Haffner, 2002, p. 122). The capacity utilization was given by equation (7.7).

$$\text{Number of Parallel Stream} = \frac{\text{Eff. Number of Runs} \times \text{Cycle Time/Run}}{\text{Ann. Avail. Time} \times \text{Labor Productivity}} \quad (7.6)$$

$$\text{Capacity Utilization} = \frac{\text{Eff. Number of Runs} \times \frac{\text{Cycle Time}}{\text{Run}}}{\text{Number of Parallel Stream} \times \text{Ann. Avail. Time}} \quad (7.7)$$

7.2.1.1 Variable costs

- **Material costs**

The annual material cost depends firstly, on the annual amount of material used in a process in term of weight with the consideration of the material scrap rate, secondly, on the material rate. The material rate is a material cost percentage, which takes account for the material price and overhead related to the material consumption such as material handling, material transportation, material storing, etc. These material overheads are expressed annually as material burden rate in equation (7.8) (Haffner, 2002, p. 123).

$$\text{Matl. Burden Rate} = \frac{\text{Ann. Matl. Overhead}}{\text{Ann. Matl. Req.} \times \text{Matl. Price}} \quad (7.8)$$

The material rate is then given by equation (7.9) (Haffner, 2002, p. 123).

$$\text{Matl. Rate} = \text{Matl. Price} \times (1 + \text{Matl. Burden Rate}) \quad (7.9)$$

Therefore, the annual material cost is given by equation (7.10) (Haffner, 2002, p. 123) :

$$\text{Ann. Matl. Cost} = \frac{\text{Part Weight} \times \text{Eff. Prod. Vol.}}{(1 - \text{Matl. Scrap Rate})} \times \text{Matl. Rate} \quad (7.10)$$

- **Labor costs**

The annual labor costs take account for different parameters such as labor rate, labor time per run, labor productivity. The labor time per run depends on the number of workers. It is expressed by equation (7.11) (Haffner, 2002, p. 124).

$$\frac{\text{Labor Time}}{\text{Run}} = \frac{\text{Cycle Time}}{\text{Run}} \times \text{Number of Workers} \quad (7.11)$$

The labor rate takes account the hourly wages (depending on the industry), and the overheads costs, which includes the administrative costs, supervising costs and others costs related to the amount of work realized. The annual labor overhead is given as a labor burden rate in equation (7.12) (Haffner, 2002, p. 124).

$$\text{Labor Burden Rate} = \frac{\text{Ann. Labor Overhead}}{\text{Hourly Wages} \times \text{Ann. Paid time}} \quad (7.12)$$

The labor rate is expressed in equation (7.13) (Haffner, 2002, p. 124).

$$\text{Labor Rate} = \text{Hourly Wages} \times (1 + \text{Labor Burden Rate}) \quad (7.13)$$

Therefore, the annual labor costs are expressed by equation (7.14) (Haffner, 2002, p. 124).

$$\text{Ann. Labor Costs} = \frac{\text{Eff. Number of Runs} \times \frac{\text{Labor Time}}{\text{Run}} \times \text{Labor Rate}}{\text{Labor Productivity}} \quad (7.14)$$

- **Energy costs**

The annual energy costs are expressed in function of annual energy consumption and energy price. The energy consumption depends on the machinery used and operation time. The annual energy consumption is given by equation (7.15).

$$\text{Ann. Energy Consumption} = \left(\frac{\text{Power consumption}}{\text{Cycle time}} \right) \times \frac{\text{Labor time}}{\text{Run}} \quad (7.15)$$

The annual energy costs are given in equation (7.16) (Haffner, 2002, p. 125).

$$\text{Ann. Energy Costs} = \text{Ann. Energy Consumption} \times \text{Energy Price} \quad (7.16)$$

7.2.1.2 Fixed costs

- **Equipment costs**

The investment costs are associated to equipment which consists of the price of equipment and its total installation and training costs. They are expressed in equation (7.17) (Haffner, 2002, p. 125).

$$\text{Investment Costs} = \text{Number of Parallel Streams} \times \text{Machines/Stream} \times (\text{Machine Price} + \text{Installation Costs} + \text{Training Costs}) \quad (7.17)$$

As these investments costs have to be annualized as loan and have to be paid during the useful life t of the equipment, the costs of capital r (generally scales between 10% and 50%) are considered for the payment of interests. The annual maintenance costs are also included. Therefore the annual investment costs are expressed by equation (7.18)(Haffner, 2002,p.126).

$$Ann. Invest. Costs = Invest. Costs \times \left(\frac{1}{r} - \frac{1}{r \cdot (1+r)^t} \right)^{-1} + Ann. Maint. Costs \quad (7.18)$$

- **Tooling costs**

The same way is used to calculate tooling costs as equipment costs, but the useful life of tooling t and their annual maintenance costs can be different (Haffner, 2002, p. 127).

- **Building costs**

Building costs are defined as the floor space price multiplied by the area specified for all the equipment, offices, stores etc. The investment costs for buildings are expressed by equation (7.19) (Haffner, 2002, p. 127).

$$Invest. Costs = Floorspace Price \times number\ of\ Parallel\ Streams \times \frac{Footprint}{Stream} \quad (7.19)$$

- **Costs of working capital**

Working capital is the total investment needed to produce a part before the sale. It depends on the total variable costs and the capital recovery period (the time from the first investment until the payment of the sold product). Working capital is given by equation (7.20) (Haffner, 2002, p. 128).

$$Working\ Capital = \frac{Ann. Variables\ Costs}{12} \times Capital\ Recovery\ Period \quad (7.20)$$

The costs of working capital take account for the discount rate r , because the working capital is very high for long-term projects. So the costs of working capital are estimated by the equation (7.21) (Haffner, 2002, p. 128).

$$\text{Costs of Working Capital} = \text{Working Capital} \times \frac{r}{12} \times \text{Cap. Recov. Period} \quad (7.21)$$

7.2.1.3 Overheads costs

These costs depend on the historic cost data and structure of business of each company. They can include administrations costs, sales, accounting, research and development, etc. The overheads costs are considered proportional to the total number of labor time or to the quantity of processed material (Haffner, 2002, p. 128).

7.2.1.4 Unit costs

The unit costs are calculated by the summation of the total variables costs and fixed costs, divided by the annual production volume such as expressed in equation (7.22) (Haffner, 2002, p. 129).

$$\text{Unit costs} = \frac{\text{Ann. Variable Costs}}{\text{Ann. Prod. Vol.}} + \frac{\text{Ann. Fixed Costs}}{\text{Ann. Prod. Vol.}} \quad (7.22)$$

7.3 Costs analysis

The cost analysis of thermoplastic parts manufactured by compression moulding process includes costs analysis of ROS parts and that of UD parts.

- **Assumptions**

According to a meeting of researchers of ETS and industrial partners on cost modeling, the obtained industrial data were based on assumptions. Table 7.2 presents the industrial data on cost modeling.

Table 7.2 Industrial data on cost modeling

Item	Bombardier	BHTC	Marquez
Dimension of the component (mm)	127 x 76 x 76	457 x 457 x 76	457 x 457 x 25.4
Production volume	400/year	-	50/year
Cost of one press (x tons, table 914 mm x 914mm) including installation cost	-	-	400k\$ for 400 tons
Utilization time of the press	-	-	2000hr/year
Cost of one heating oven (914 mm x 914 mm x 914 mm)	-	-	25k\$
Maintenance of machinery	5% of the buying cost	-	-
Machinery depreciation	10 years	-	10 years
Energy cost	-	-	-
Building cost	-	-	53.82 \$/m ²
Taxes	-	-	10.7\$/ m ²
Tooling cost	-	-	-
Tooling depreciation	-	-	3 years
Labor cost	80\$/hr	100\$/hr	60\$/hr
Raw material cost (CETEX TC1200 PEEK/AS4; 134g; 34%RC)	-	217.04\$/kg For 6.35 mm: 48.33\$/m ² For 12.7 mm : 50.05\$/m ² For 25.4 mm: 53.7\$/m ² For 158.75 mm strip: 39.72\$/m ² Set up charge for slitting: 2k\$/batch	-

For parts manufacturing cost calculation, it was considered the following detailed assumptions:

- The calculation of annual available time per run was based on 240 days per year, 1 shift per day and 8 hours per day (see equation 7.4);
- The number effective per run was one;
- The material and labor burden rates were assumed to be 10%;
- The hourly wages was 80\$/hour (average rate);
- The prices of MTS machine and die set were assumed to be 9.8 k\$ for manufacturing ROS flat plates and T-shape parts and 11.28 k\$ for manufacturing ROS L-shape parts;
- One parallel stream and one of machine/stream were chosen for equipment and tooling;
- The installations and training costs of MTS machine press were assumed to be 700 \$ for manufacturing ROS parts;
- The useful life t of the press and the cost of capital r were assumed to be 10 years and 30% respectively;
- The prices of electrical, control system and labview software were assumed to be 6 k\$;
- For ROS parts, the installations and training costs of electrical, control system and labview software were assumed to be 12 k\$ with 400 \$ for annual maintenance costs. For UD parts, they were assumed to be 6 k\$ with 12 k\$ for annual maintenance costs;
- The price of automatic cutter was assumed to be 1.4 k\$ with 500 \$ for installations costs and training costs, 400 \$ for annual maintenance costs;
- For ROS parts, the tooling installations and training costs were assumed to be 600 \$. For UD parts, they were assumed to be 1k\$, with the useful life t and the cost of capital r were assumed to be 3 years and 30% respectively;
- For estimation of costs of working capital, the capital recovery period and the cost of capital r were assumed to be 13 months and 30% respectively;
- The annual overheads were assumed to be two times of the annual labor costs;
- The price of press was assumed to be 125k\$ for manufacturing UD parts;
- The installation and training costs of press for manufacturing UD parts were assumed to be 400 \$;

- The price of one infrared oven for heating UD parts with dimension of 481 mm x 481 mm x 590 mm was assumed to be 10.42 k\$;
- The installation and training costs of infrared oven were assumed to be 200 \$;
- For building costs, the footprint/stream was assumed to be 1.022 m² for press, 0.464 m² for automatic cutter, 74.322 m² for material and finished part storage and 0.929 m² for infrared oven.

7.3.1 ROS parts

In order to run the costs model for calculating the manufacturing costs of ROS parts, the tooling costs have to be adjusted by adding other costs associated to accessories of the mould such as heating cartridges, cooling system, insulators and thermocouples. The tooling costs sizing scaling laws already established were adjusted by the accessories costs scaling, with projected area of the mould using the same costs coefficients, whereas the costs of the electrical, control system, labview and die set costs were included in equipment costs calculations.

For flat plates and T-shape parts, the costs calculations were based on a production volume of 1000 parts, 2% of rejects and 79.7% of the productivity. For L-bracket parts, the costs calculations were based on a production volume of 500 parts, 2% of rejects and 83.7% of the productivity.

7.3.1.1 Flat plate

For estimating flat mould and accessories costs, the coefficients were 74% for the tooling costs and 26% for mould accessories. Table 7.3 presents the estimated costs for ROS flat plate. Figure 7.1 shows the cost breakdown of ROS flat plate. For more details see costs calculation Excel spreadsheet for ROS flat plate in ANNEX VIII.

Table 7.3 Estimated costs for ROS flat plate

Cost category	Cost per part (\$)
Material cost	14.19
Labor cost	168.96
Energy cost	0.02
Equipment cost	11.12
Tooling cost	3.69
Building cost	4.90
Cost of working capital	64.49
Overhead cost	337.92
Total cost	605.28

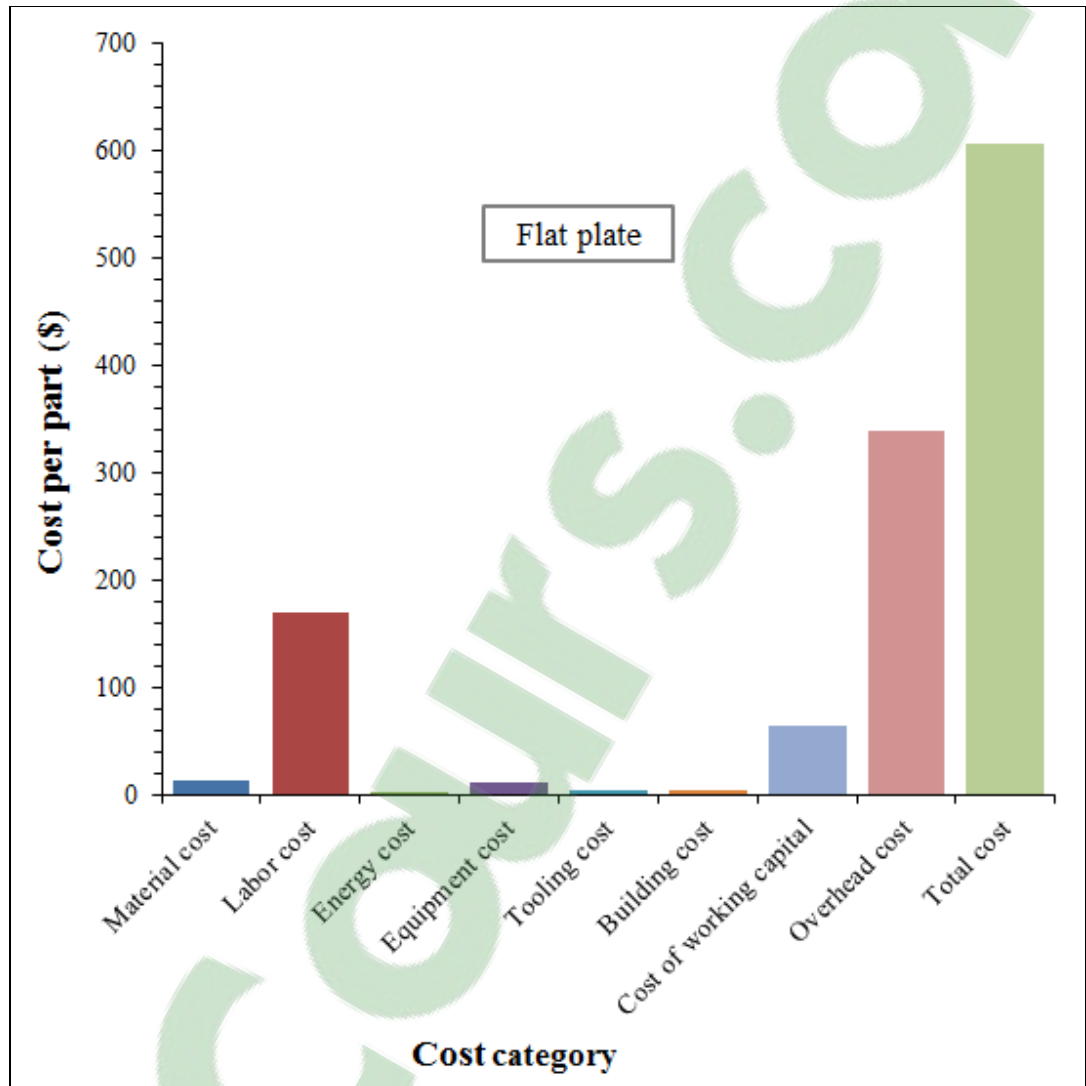


Figure 7.1 Cost breakdown of ROS flat plate

7.3.1.2 T-shape part

For estimating T-shape mould and accessories costs, the coefficients were 75.8% for the tooling costs and 24% for mould accessories costs. Table 7.4 presents the estimated costs for (ROS) T-shape part. Figure 7.2 shows the cost breakdown of T-shape part. For more details see costs calculation Excel spreadsheet for ROS T-shape part in ANNEX IX.

Table 7.4 Estimated costs for (ROS) T-shape part

Cost category	Cost per part (\$)
Material cost	9.81
Labor cost	168.96
Energy cost	0.03
Equipment cost	11.12
Tooling cost	4.16
Building cost	4.90
Cost of working capital	62.95
Overhead cost	337.92
Total cost	599.85

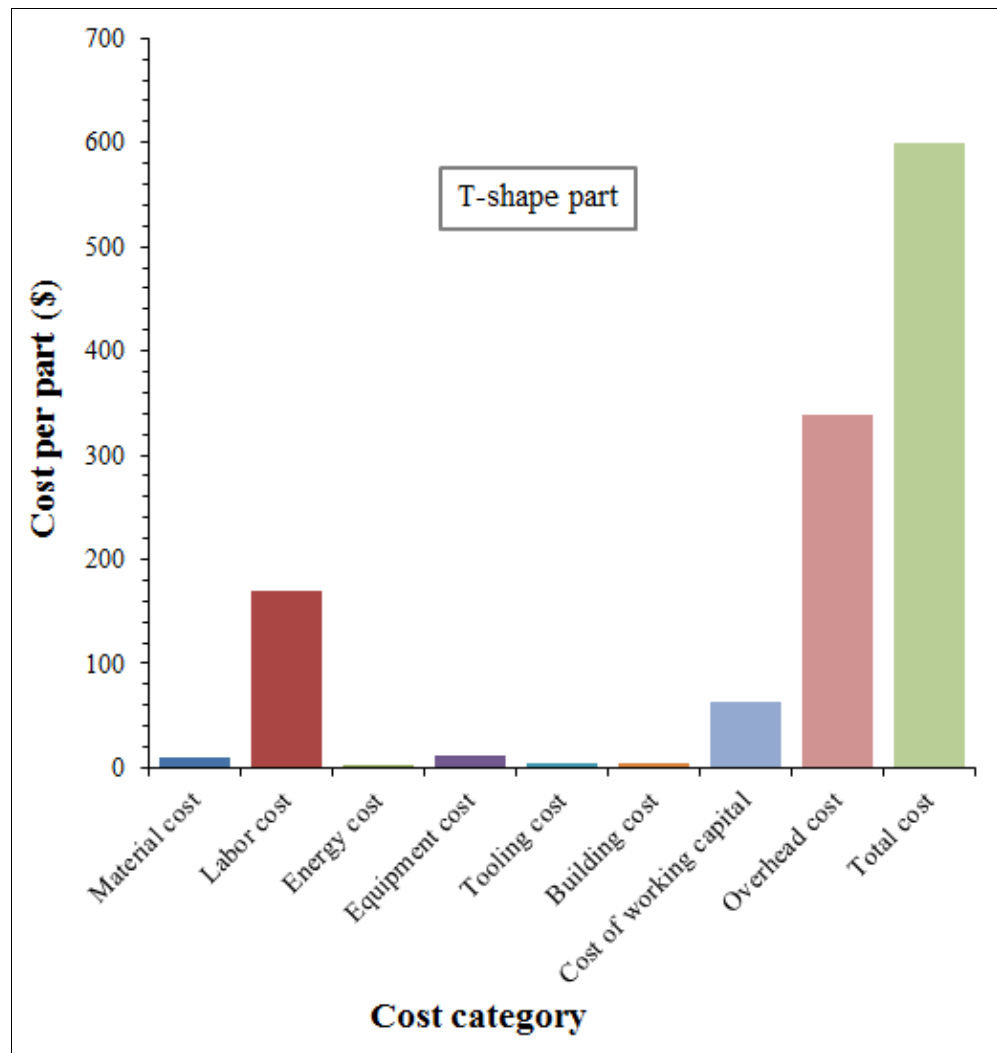


Figure 7.2 Cost breakdown of (ROS) T-shape part

7.3.1.3 L-bracket part

For estimating L-bracket mould and accessories costs, the coefficients were 88.8% for the tooling costs and 11.2% for mould accessories costs. Table 7.5 presents the estimated costs for (ROS) L-bracket part. The cost breakdown of L-bracket part is shown Figure 7.3. For more details see costs calculation Excel spreadsheet for ROS L-bracket part in ANNEX X.

Table 7.5 Estimated costs for (ROS) L-bracket part

Cost category	Cost per part (\$)
Material cost	40.20
Labor cost	337.92
Energy cost	0.07
Equipment cost	23.35
Tooling cost	24.25
Building cost	9.79
Cost of working capital	133.16
Overhead cost	675.84
Total cost	1244.59

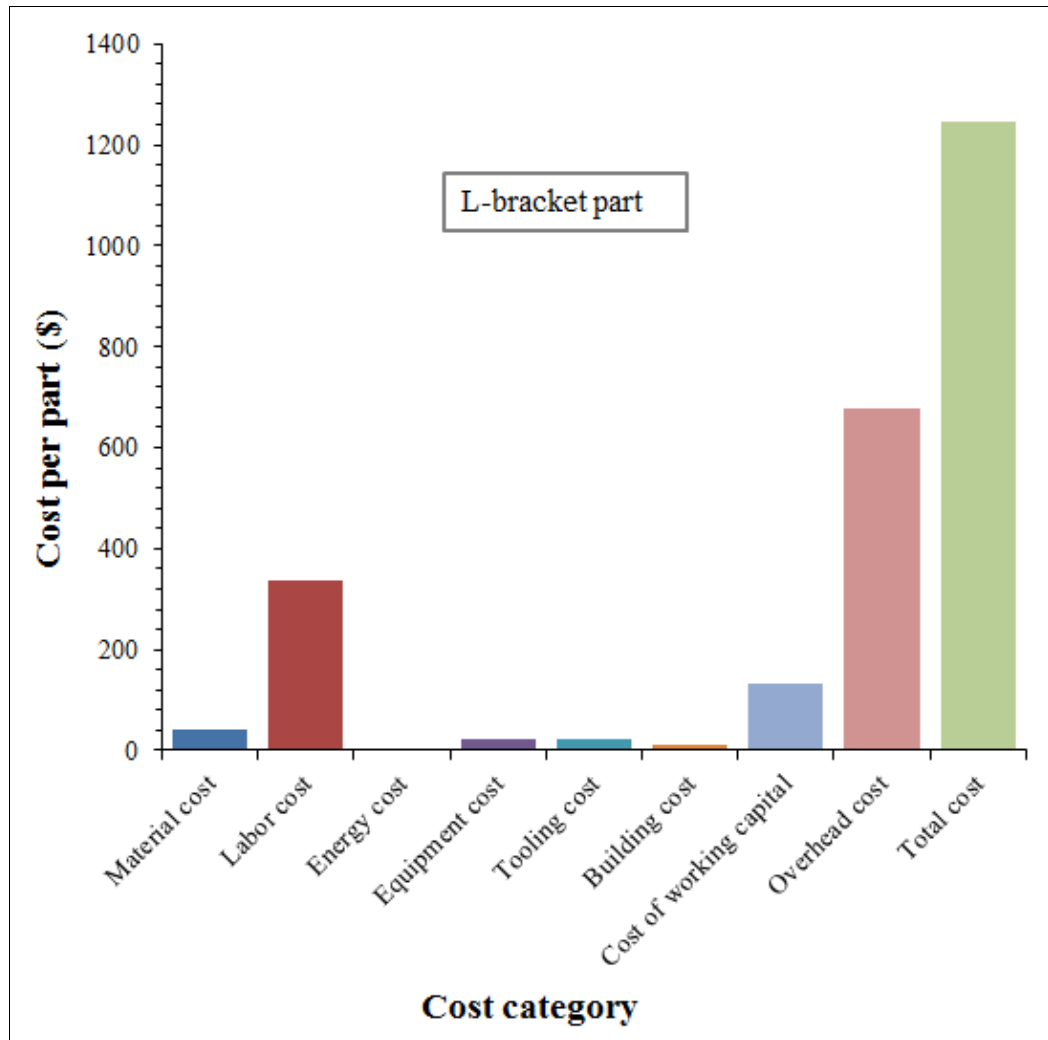


Figure 7.3 Cost breakdown of (ROS) L-bracket part

7.3.2 UD parts

In order to run the costs model for calculating the manufacturing costs of UD parts, the tooling costs have to be adjusted by adding other costs associated to accessories of the mould such as heating cartridges, clamps, screws, thermocouples, pressure transducer, mould plate support and sheet support system. The tooling costs sizing scaling laws already established were adjusted by the accessories costs, scaling with projected area of the mould using the same costs coefficients such as 66.3% for the tooling costs and 33.7% for mould accessories

costs, whereas the costs of the electrical, control system and labview costs were included in equipment costs calculations. The costs calculations were based on a production volume of 4500 parts, 3% of rejects and 73.8% of the productivity.

7.3.2.1 Concave part

Table 7.6 presents the estimated costs for (UD) concave part. Figure 7.4 shows the cost breakdown of (UD) concave part. For more details see costs calculation Excel spreadsheet for (UD) concave part in ANNEX XI.

Table 7.6 Estimated costs for (UD) concave part

Cost category	Cost per part (\$)
Material cost	19.87
Labor cost	37.55
Energy cost	0.12
Equipment cost	12.64
Tooling cost	2.67
Building cost	1.09
Cost of working capital	20.26
Overhead cost	75.09
Total cost	169.30

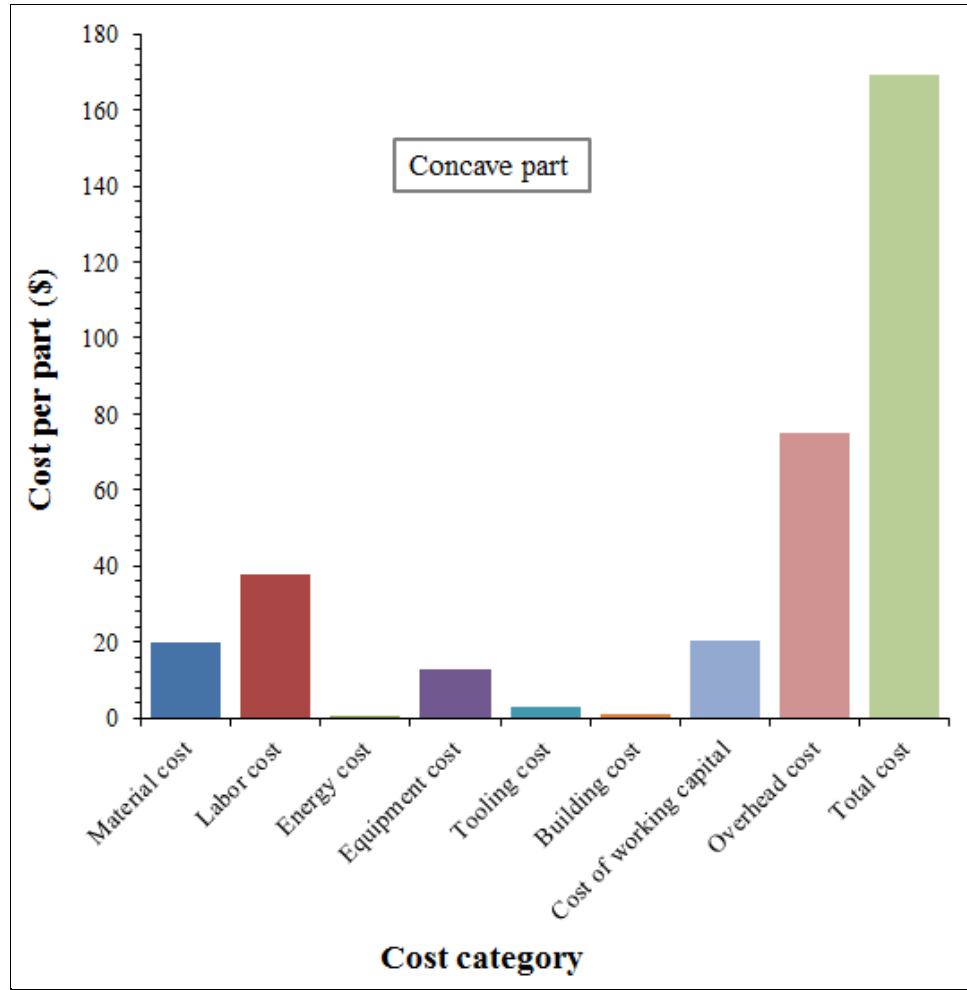


Figure 7.4 Cost breakdown of (UD) concave part

7.3.2.2 Hollow square part

Table 7.7 presents the estimated costs for (UD) hollow square part. Figure 7.5 shows the cost breakdown of (UD) hollow square part. For more details see costs calculation Excel spreadsheet for (UD) hollow square part in ANNEX XII.

Table 7.7 Estimated costs for (UD) hollow square part

Cost category	Cost per part (\$)
Material cost	22.41
Labor cost	37.55
Energy cost	0.07
Equipment cost	12.64
Tooling cost	2.23
Building cost	1.09
Cost of working capital	21.13
Overhead cost	75.09
Total cost	172.22

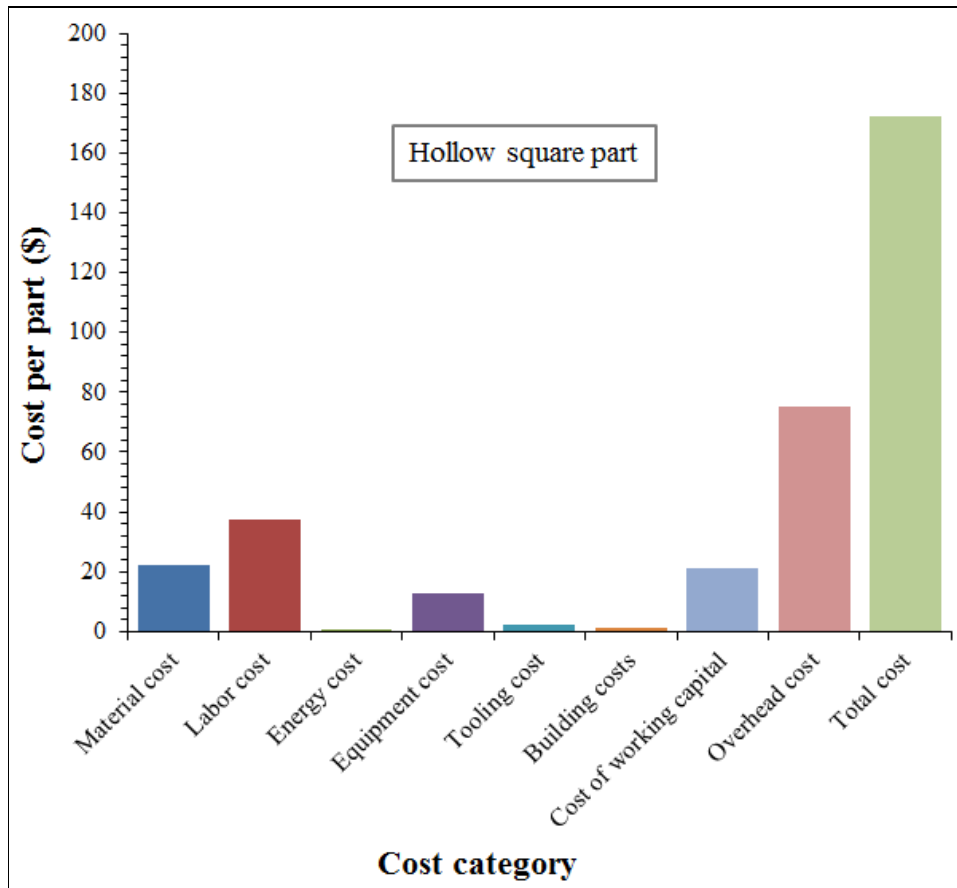


Figure 7.5 Cost breakdown of (UD) hollow square part

7.3.2.3 U-shape part

Table 7.8 presents the estimated costs for (UD) U-shape part. Figure 7.6 shows cost breakdown of (UD) U-shape part. For more details see costs calculation Excel spreadsheet for (UD) U-shape part in ANNEX XIII.

Table 7.8 Estimated costs for (UD) U-shape part

Cost category	Cost per part (\$)
Material cost	7.47
Labor cost	37.55
Energy cost	0.12
Equipment cost	12.64
Tooling cost	2.23
Building cost	1.09
Cost of working capital	15.89
Overhead cost	75.09
Total cost	152.08

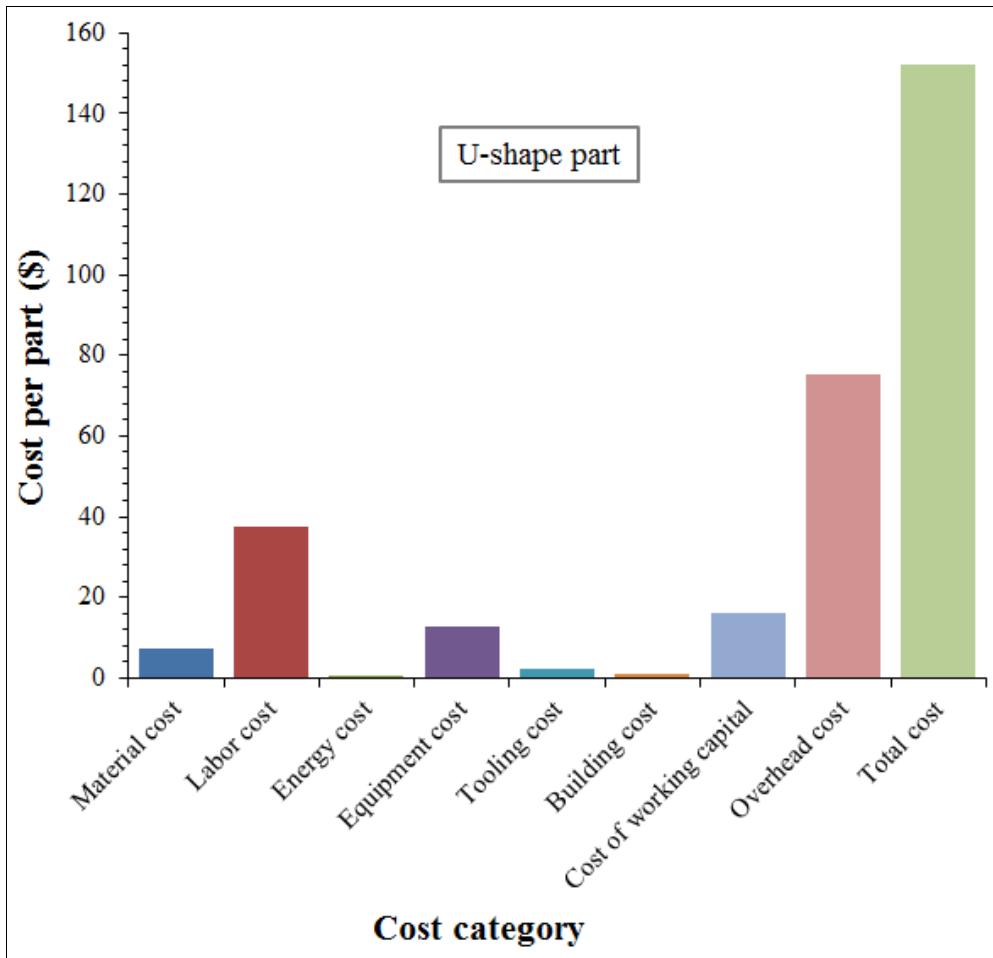


Figure 7.6 Cost breakdown of (UD) U-shape part

7.3.2.4 Z-shape part

Table 7.9 presents the estimated costs for (UD) Z-shape part. Figure 7.7 shows cost breakdown of (UD) Z-shape part. For more details see costs calculation Excel spreadsheet for (UD) Z-shape part in ANNEX XIV.

Table 7.9 Estimated costs for (UD) Z-shape part

Cost category	Cost per part (\$)
Material cost	6.71
Labor cost	37.55
Energy cost	0.12
Equipment cost	12.64
Tooling cost	2.29
Building cost	1.09
Cost of working capital	15.62
Overhead cost	75.09
Total cost	151.12

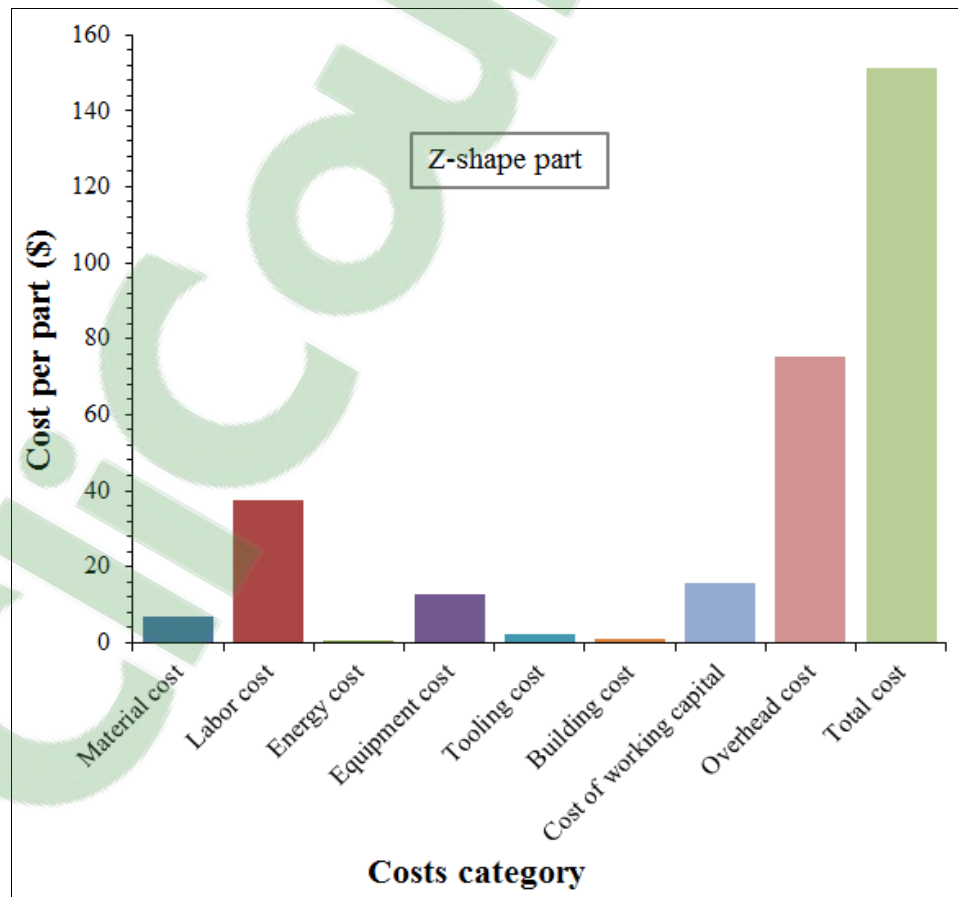


Figure 7.7 Cost breakdown of (UD) Z-shape part

7.3.2.5 Flat plate

Table 7.10 presents the estimated costs for (UD) flat plate. Figure 7.8 shows cost breakdown of (UD) flat plate. For more details see costs calculation Excel spreadsheet for (UD) flat plate in ANNEX XV.

Table 7.10 Estimated costs for (UD) flat plate

Cost category	Cost per part (\$)
Material cost	2.49
Labor cost	37.55
Energy cost	0.10
Equipment cost	12.64
Tooling cost	1.83
Building cost	1.09
Cost of working capital	14.13
Overhead cost	75.09
Total cost	144.92

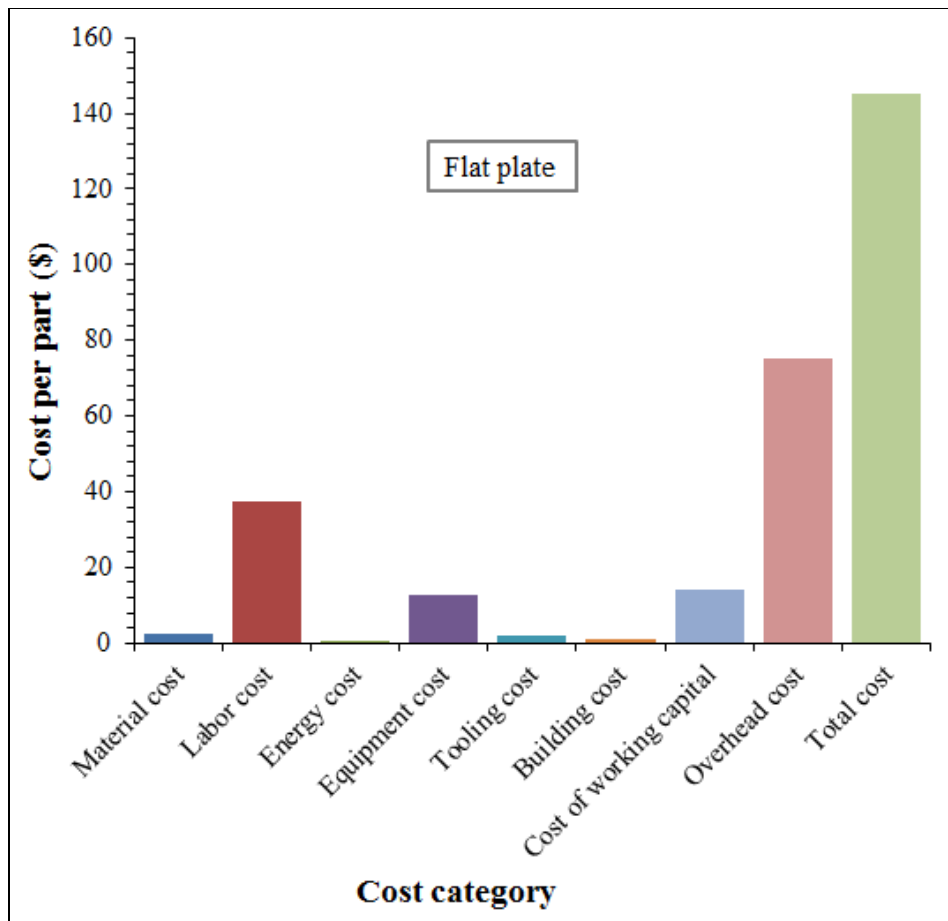


Figure 7.8 Cost breakdown of (UD) flat plate

7.4 Autoclave process and compression moulding parts manufacturing costs comparisons

This section consists to make comparisons between the manufacturing costs of thermoplastic parts made by compression moulding process and those of thermoset parts made by autoclave process in order to determine the cost effective technique of manufacturing the composite materials. The costs calculations of thermoset parts made by autoclave process were performed in Excel spreadsheet by applying cost data and the cost equations already mentioned.

There are three categories of parts made by hand lay-up from UD continuous fibers prepreg AS4/8552 and processed by autoclave cure. The studied parts are: flat plate, T-shape part and L-bracket part. The tooling costs estimation and manufacturing time estimation methodology were based on the works of Haffner (2002) and Neoh (1995) and they were adapted to the studied parts. In order to make costs comparisons, the same dimension of the parts and the same productivity were selected. Table 7.11 presents the cost comparisons between the manufacturing costs of thermoplastic parts made by compression moulding process and those of thermoset parts made by autoclave process.

Table 7.11 Comparisons between compression moulding process and autoclave process parts manufacturing costs

Part form	Part dimension (mm)	Productivity	Cost/part (Compression moulding process) (\$)	Cost/part (Autoclave process) (\$)
Flat plate	355.6 x 304.8 x 6	80%	1843.2	3323.42
T-shape part	Flange: 76.2 x 76.2 x 3.17 Rib: 76.2 x 25.4 x 3.17	80%	595.79	2461.71
L-bracket part	Flange: 115 x 75 x 6.4 Rib: 40 x 40 x 6.4	80%	1299.36	2411.10

7.5 Discussion of results and conclusion

The cost breakdowns showed how each cost category contributes to the total cost per part. For all ROS and UD parts, the costs analysis of parts manufactured by compression moulding process showed that the overhead cost is the highest cost element due to high labor cost. The labour costs are higher due to high labour rate. The manufacturing costs for ROS parts are higher than those of UD parts due to long cycle time for making ROS parts.

The energy cost is the lowest cost element due to low heating energy consumption. The manufacturing cost of L-bracket part is higher than that of flat plate and T-shape part due to high process cycle time, an important geometry of the part and high size of the mould and equipment used.

The cost comparison between ROS and UD parts showed that the manufacturing costs of ROS parts are higher than those of UD parts due high process cycle time.

The comparisons between compression moulding process and autoclave process parts manufacturing costs showed that the manufacturing costs of one part manufactured by autoclave process is higher than those of a part manufactured by compression moulding process due to long cure cycle and higher investment equipment costs. It was concluded that the compression moulding process is more economic with respect to autoclave process.

GENERAL CONCLUSION

The main objective of this research study was to develop a cost estimation model in order to evaluate manufacturing costs of experimental and new carbon fiber thermoplastic composite parts made by two different compression moulding processes based on process physical laws. The first one aimed at making ROS parts, whereas the second one aimed at making UD parts. This cost analysis model was based on different costs equations, different assumed academic and industrial data which were integrated in Microsoft Excel spread sheet for calculating costs elements such as material, labour, energy, tooling, machinery, building costs, etc...and then calculating the total cost per part. The physical laws are the heat transfer equations applied during the process cycle time. The sensitivity cost analysis permit to identify the cost drivers which are effects on production costs and then help engineers and designers to make good decision about cost effectiveness of the manufacturing processes. A new cost estimating tool for thermoplastic composites aerospace parts manufactured by compression moulding process was developed and used to predict the costs.

Two cost modules were involved in this study: The energy costs and tooling costs for making ROS and UD parts. Firstly, the energy costs were calculated for experimental parts and tooling costs were estimated for experimental moulds. Secondly, the energy costs were calculated for virtual parts and tooling costs were estimated for virtual moulds using extrapolation technique. Consequently, the energy and tooling costs sizing scaling laws were established under linear equations forms (trend curves) with their respective determination coefficients and with the condition to be limited to the size of platens areas. The heating energy extrapolations scaling with the volumes of the parts were based on the same process cycle times which were simulated and validated experimentally. These energy and tooling costs linear equations were imputed in Excel program in order to calculate the cost for new parts which have not been made.

The process cycle time, including the heating and cooling times estimated by the numerical modelling for was validated thanks to an acceptable error of around 4% for a ROS flat plate

and T-shape part, around 10% for L-Bracket part between the simulated and experimental times.

The ROS parts heating energy costs comparison showed that the calculated heating energy costs of the three experimental part forms are different due to different geometries of the heating platens and the moulds used. For all the categories of parts by keeping the same cycle time, the parts heating energies were predicted for other similar geometries in function of the volumes of the parts with the condition to be limited to the size of platens.

For the T-shape and L-shape mould, the estimated tooling costs results showed that the cavity costs are higher than the punch costs because making the cavity requires more components than those of the punch and the mould manufacturing costs were higher than mould assembly costs. The estimated mould cost for T-shape mould is close to that of workshop. The errors between them are about 2% (only the design and engineering costs were estimated).

For L-shape and flat mould, it was found that the L-shape mould and flat mould costs were close to that of a commercial contractor with the error between them coming in at approximately 6% and 3%, respectively.

The machining process is the most important cost driver in the mould cost analysis of two studied cases. The milling operations costs represent the highest cost rate because they depend on numbers and dimension of milled featured by considering that recommended milling parameters do not change.

Based on the cost results obtained for the different mould forms by the DFMA cost estimation software packages, the mould costs were extrapolated and applied to other similar mould geometries by changing the projected mould area. The tooling costs sizing scaling laws were established in linear forms (trend curves) with their respective determination coefficients and with the condition to be limited to the size of platens areas.

In order to make tooling costs comparisons, the tooling costs scaling with their projected mould area were normalized in term of the overheads and the profits.

The tooling costs comparisons showed that the L- shape mould costs were higher than T- shape mould costs which are higher than the flat mould costs. Therefore, it was concluded that the more complex the mould is the higher the cost.

The cycle time including the heating and cooling times estimated by the numerical modelling for a compression moulded carbon/PEEK composite concave part was validated thanks to an acceptable error of around 5% between the simulated and experimental times.

The total heating energy consumptions are the sum of the heating energy consumption of the laminate in the oven and that of the concave mould. Consequently keeping the same cycle time, the concave parts heating energy was predicted for other similar geometries in function of the volumes of the mould and of the concave parts.

The concave mould results showed that the cost of the punch are higher than that of the cavity due to the higher machining time of the punch, and the mould manufacturing costs are higher than assembly costs.

The concave mould costs analysis showed that there was no significant difference between the total estimated costs and the commercial costs. The error between them is about 6%.

From the heating energy costs results for different UD part forms scaling with part volume, the heating energy costs sizing scaling laws were established which are in linear forms (trend curves) with the condition to be limited to the size of platens areas.

For the concave part, U-shape part, hollow square part and Z-shape part, there is no significant difference in term of heating energy costs between them. Overall, the heating energy costs do not depend on the volume of the part.

For the flat plate the heating energy costs are lower than those of the other UD parts due to lower volume of the flat mould.

For UD parts, from the estimated costs for four moulds forms scaling with their projected area, the tooling costs sizing scaling laws were established which are in linear forms (trend curves) with their respective determination coefficients and with the condition to be limited to the size of platens areas.

The costs comparisons between different mould forms for making UD parts showed that the concave mould costs are very higher than those of the other mould forms due to a high complexity level of the concave mould.

For ROS parts, the cost analysis showed that manufacturing cost per one L-bracket part is higher than that of one flat plate and one T-shape part. That was due to higher process cycle time which is a cost driver yielding higher labour cost and higher overheads as well.

For UD parts, the cost analysis showed that there is no significant difference between the parts manufacturing costs and that the higher cost driver is the process cycle time. Overall, In order to optimize the manufacturing costs it is necessary to reduce the process cycle time.

The comparisons results between compression moulding process and autoclave process manufacturing costs showed that for a similar part, the autoclave process was the most costly process due to long cure cycle and equipment investment.

RECOMENDATIONS

The cost estimation model developed in this study for calculating parts costs manufactured by compression moulding process was based on small production volume. In this case, it is not worthy to optimize. In the case of important production volume, cost optimization could be possible by making combinations of different production parameters such as number of mould used, number of equipment, etc...

From cost analysis results that the cycle time is the main cost driver which has effects on total manufacturing cost of the part, it will be important to develop optimization methods such as mould design for manufacturing the composite parts made of a given material in such way to minimize the temperature variation through the mould in order to reduce the process cycle time. However, the influence of reducing cycle time on the quality of the part is ignored. For that reason, another research study is recommended to be realised for this issue.

APPENDIX I

LIST PUBLICATION LIST

CONFERENCE PUBLICATIONS

- **M. El Wazziki**, A. D. Ngo, G. Lebrun, H. Lessard. *Application of DFMA concept to evaluate the tooling cost for carbon fibre reinforced thermoplastic composites compression moulding processes*. Proceeding of the 28th annual International Forum On Design for Manufacturing and Assembly, Rhode Island, USA, June 12-14, 2013;
- **M. El Wazziki**, A. D. Ngo. *Modelling of compression moulding process cycle time for carbon fibre reinforced thermoplastic flat panels*. The 10th Canada-Japan Workshop on Composites. Vancouver, Canada, August 19-21, 2014;
- **M. El Wazziki**, A. D. Ngo. *Modelling of compression moulding process cycle time and application of DFMA concept to evaluate the tooling costs for carbon fibre reinforced thermoplastic composites T-shape parts*. The 20th International Conference on Composites Materials. Copenhagen, Denmark, July 19-24, 2015;
- **M. El Wazziki**, A. D. Ngo. *Modeling of compression moulding process cycle time for carbon fibre reinforced thermoplastic concave parts*. The Canadian International Conference on Composites, Edmonton, Alberta, August 18-20, 2015;

JOURNAL SUBMISSION

- **M. El Wazziki**, A. D. Ngo. *Tooling and energy costs estimation of compression process moulding randomly oriented strands thermoplastic experimental parts*. Journal of Cost Analysis and Parametrics, January 24, 2016, ID: UCAP-2016-0005.

ANNEX I

FEATURES MANUFACTURING DATA FOR FLAT MOULD

Table A-I-1

Mould component	Features	Machining operations	Dimension					Repeat count	Operation time	Comments
			W	L ₁	D ₁	d	L ₂			
			mm	mm	mm	mm	mm		s	
Frame A (2)	Faces	Rough and finish face milling	57.15	89.1	1.56			2	141	
			12.7	57.15	3.33			2	94	
			12.7	89.1	3.175			2	123	
	Holes	Drilling				2.5	2.5	12	214	(pointing)
						2.5	8.5	4	488	(thermocouples)
						3.5	8.5	4	291	For horizontal securing
						2.5	8.5	4	118	For dowel pins
		Reaming				2.5	8.5	4	93	For dowel pins
		Tapping				3.5	8.5	4	202	
		Drilling				3.5	50.8	1	314	For vertical securing
		Counterdrilling				7.4	3.5	1	-	For head screw
		Polishing							1506	
Inspection								1220		
Frame B (2)	Faces	Rough and finish face milling	57.15	107.95	1.95			2	350	
			12.7	57.15	3.968			2	188	

		Holes		12.7	107.95	3.175			2	306	
			Drilling				2.5	2.5	16	419	(pointing)
							3.5	9.58	4	283	For horizontal securing
			Counterdrilling				5	3.5	4	-	For head screw
			Tapping				3.5	6.1	4	126	
			Drilling				2.5	8.5	4	183	(thermocouples)
			Drilling				3.5	50.8	2	323	For vertical securing
			Counterdrilling				7.4	3.5	2	-	For head screw
			Reaming				2.5	8.5	1	44	For dowel pins
			Drilling				2.5	4.5	5	229	For dowel pins
			Reaming				2.5	4.5	5	247	For dowel pins
			Drilling				4.5	4.5	1	48	For dowel pins
			Reaming				4.5	4.5	1	26	For dowel pins
			Polishing							1596	
			Inspection								1260
Platens	Up	Faces	Rough and finish face milling	107.95	107.95	1.4			2	502	
				35	107.95	3.175			4	648	
				9.58	101.6	9.58			2	650	
				9.58	82.44	9.58			2	547	
		Holes	Drilling				2.5	2.5	19	720	(pointing)
							5.5	22.62	4	308	For vertical securing
			Tapping				5.5	22.62	4	279	For vertical securing
			Drilling				5.5	6.1	2	153	For dowel pins
			Reaming				5.5	6.1	2	219	For dowel pins
			Drilling				5.5	30.284	2	277	For vertical securing

			Tapping				6.875	40.25	2	184	For vertical securing
			Counterdrilling				8.52	4.086	2	-	For head screw
			Drilling				3.834	101.6	4	903	Heating cartridges
			Counterdrilling				8.52	4.086	4	-	For head screw
			Drilling				3.834	101.6	3	683	Cooling channels
			Tapping				3.834	8	3	57	Cooling channels
			Drilling				2.43	49	1	162	thermocouple
			Polishing							1281	
			Inspection							1880	
		Bottom	Faces	Rough and finish face milling	107.95	107.95	1.4			2	494
				35	107.95	3.175			4	648	
				9.58	101.6	9.58			2	556	
				9.58	82.44	9.58			2	469	
	Holes		Drilling				2.5	2.5	15	415	(pointing)
							3.834	101.6	3	683	Cooling channels
			Tapping				3.834	8	3	103	Cooling channels
			Drilling				3.834	101.6	4	953	Heating cartridges
							5.5	22.62	4	296	For vertical securing
			Counterdrilling				8.52	4.86	4	-	For head screw
		Drilling				4.86	6.1	2	87	For dowel pins	
	Reaming				4.86	6.1	2	69	For dowel pins		
	Drilling				6.1	6.1	2	131	For dowel pins		
	Reaming				6.1	6.1	2	65	For dowel pins		

			Polishing							1256	
			Inspection							1850	
Plate (2)	Up and bottom	Faces	Rough and finish face milling	107.95	107.95	0.495			2	664	
				6.35	107.95	3.175			4	740	
		Holes	Drilling				2.5	2.5	6	57	(pointing)
							5.5	5.36	4	212	For vertical securing
			Tapping				5.5	5.36	4	126	For vertical securing
			Drilling				6.1	5.36	2	116	
			Polishing							1106	
			Inspection							800	
Flat mould			Total manufacturing time						31781		

ANNEX II

FEATURES MANUFACTURING DATA FOR T-SHAPE MOULD

Table A-II-1

Mould component	Features	Machining operations	Dimension					Repeat count	Operation time	Comments
			W	L ₁	D ₁	d	L ₂			
			mm	mm	mm	mm	mm		s	
Frame A (2)	Faces	Rough and finish face milling	57.15	89.1	1.56			2	141	
			12.7	57.15	3.33			2	94	
			12.7	89.1	3.175			2	123	
	Holes	Drilling				2.5	2.5	12	214	(pointing)
						2.5	8.5	4	488	(thermocouples)
						3.5	8.5	4	291	For horizontal securing
						2.5	8.5	4	118	For dowel pins
		Reaming			2.5	8.5	4	93	For dowel pins	
		Tapping			3.5	8.5	4	202		
		Drilling			3.5	50.8	1	314	For vertical securing	
		Counterdrilling			7.4	3.5	1	-	For head screw	
		Polishing						1506		
	Inspection						1220			
Frame B (2)	Faces	Rough and finish face milling	57.15	107.95	1.95			2	350	
			12.7	57.15	3.968			2	188	
			12.7	107.95	3.175			2	306	
	Holes	Drilling				2.5	2.5	16	419	(pointing)

			grinding	41.22	82.44	0.089			2	72			
				31.64	41.22	0.089			2	62			
			Polishing							1362			
			Inspection							1800			
Platens	Up	Faces	Rough and finish face milling	107.95	107.95	1.4			2	502			
				35	107.95	3.175			4	648			
				9.58	101.6	9.58			2	650			
				9.58	82.44	9.58			2	547			
				Holes	Drilling				2.5	2.5	19	720	(pointing)
									5.5	22.62	4	308	For vertical securing
					Tapping				5.5	22.62	4	279	For vertical securing
					Drilling				5.5	6.1	2	153	For dowel pins
					Reaming				5.5	6.1	2	219	For dowel pins
					Drilling				5.5	30.284	2	277	For vertical securing
					Tapping				6.875	40.25	2	184	For vertical securing
					Counterdrilling				8.52	4.086	2	-	For head screw
					Drilling				3.834	101.6	4	903	Heating cartridges
					Counterdrilling				8.52	4.086	4	-	For head screw
					Drilling				3.834	101.6	3	683	Cooling channels
					Tapping				3.834	8	3	57	Cooling channels
					Drilling				2.43	49	1	162	thermocouple
					Polishing								1281
				Inspection								1880	
		Bottom	Faces	Rough and finish face milling	107.95	107.95	1.4			2	494		
35	107.95				3.175			4	648				
9.58	101.6				9.58			2	556				

				9.58	82.44	9.58			2	469		
		Holes	Drilling				2.5	2.5	15	415	(pointing)	
								3.834	101.6	3	683	Cooling channels
			Tapping				3.834	8	3	103	Cooling channels	
			Drilling				3.834	101.6	4	953	Heating cartridges	
								5.5	22.62	4	296	For vertical securing
			Counterdrilling				8.52	4.86	4	-	For head screw	
			Drilling				4.86	6.1	2	87	For dowel pins	
			Reaming				4.86	6.1	2	69	For dowel pins	
			Drilling				6.1	6.1	2	131	For dowel pins	
			Reaming				6.1	6.1	2	65	For dowel pins	
			Polishing							1256		
			Inspection							1850		
Plate (2)	Up and bottom	Faces	Rough and finish face milling	107.95	107.95	0.495			2	664		
				6.35	107.95	3.175			4	740		
		Holes	Drilling				2.5	2.5	6	57	(pointing)	
							5.5	5.36	4	212	For vertical securing	
			Tapping				5.5	5.36	4	126	For vertical securing	
			Drilling				6.1	5.36	2	116		
			Polishing								1106	
			Inspection								800	
T-shape mould			Total manufacturing time						37639			

ANNEX III

FEATURES MANUFACTURING DATA FOR L-SHAPE MOULD

Table A-III-1

Mould component	Features	Machining operations	Dimension						Repeat count	Operation time	Comments	
			W	L ₁	D ₁	d	L ₂	A				D ₂
			mm	mm	mm	mm	mm					s
Cavity	Faces	Rough and finish face milling	133.35	228.6	3.775					2	1538	
			82.55	133.35	4.612					2	822	
			133.35	228.6	3.862					2	1344	
	Pocket	Rough and finish pocket end mill						50.625	75	1	18187	
								62	75	1	27858	
	Holes	Drilling (face 1)				6.35	6.35			18	419	(pointing)
						12.187	14.062			4	178	For dowel pins
		Reaming				12.187	14.062			4	317	For dowel pins
		Drilling (face 1)				9.375	75			6	992	For cooling channels
						7.493	16.866			6	260	Frame-cavity horizontal fixation
		Tapping				7.493	16.866			6	218	Frame-cavity horizontal fixation

					7.5	75			2	685	Frame-cavity horizontal fixation
					6.35	6.35			18	495	(pointing)
					12.187	14.062			4	533	For dowel pins
					12.187	14.062			4	353	For dowel pins
					7.493	16.866			6	479	Frame-cavity horizontal fixation
					7.493	16.866			6	296	Frame-cavity horizontal fixation
					1	6.35			4	46	(pointing)
					2.812	62.6			1	225	(thermocouples)
					9.375	138.657			2	1070	Heating cartridges
					2.812	91			1	643	(thermocouple)
					6.35	6.35			4	199	(pointing)
					9.375	138.657			2	1070	Heating cartridges
					6.35	6.35			6	168	(pointing)
					7.5	12.187			2	116	For dowel pins
					7.5	12.187			2	155	For dowel pins
					7.5	12.187			4	152	Bottom vertical fixation
					6.35	6.35			2	151	(pointing)

						11.25	18.75			2	282	For dowel pins
		Reaming				11.25	18.75			2	180	For dowel pins
	Faces	Surface traverse grinding	125.625	219.375	0.089					2	1584	Surface finish
			75	125.625	0.089					2	880	Surface finish
		Polishing									26533	
		Inspection									6900	
Frame (2)	Faces	Rough and finish face milling	27	228.6	3.862					2	850	
			27	133.35	4.612					2	548	
			133.35	228.6	0.844					2	3354	
	Slots	Rough and finish side and slot milling	15	28.125	4.687					1	244	For alignment
			3.426	89.08	1.7					2	195	Slots
			3.426	73.09	1.7					2	166	Slots
			3.426	57.1	1.7					2	138	Slots
			3.426	41.11	1.7					2	110	Slots
			3.426	106.21	1.7					1	115	Slot
	Holes	Drilling				6.35	6.35			4	97	(pointing)
						7.5	21.562			4	236	For dowel pins
		Reaming				7.5	21.562			4	264	For dowel pins
		Surface traverse grinding	--			25.312	219.375	0.089		2	276	Surface finish
		Drilling				6.35	6.35			14	327	(pointing)
					7.5	25.312			2	112	Frame-cavity horizontal fixation	

						9.375	25.312			12	874	
		Tapping				9.375	25.312			6	341	For cooling channels
		Counterdrilling				16	9.375			6	-	For head screw
		Drilling				6.35	6.35			2	59	(pointing)
						9.375	125.625			2	819	Frame-bottom plate fixation
		Counterdrilling				17.2	10.214			2	-	For head screw
		Inspection									4900	
Punch	Faces	Rough and finish face milling	82.55	177.8	2.775					2	1128	
			82.55	114.3	4.55					2	774	
			114.3	177.8	3.775					2	1048	
	Holes	Drilling				6.35	6.35			12	281	(pointing)
						7.5	14.062			2	73	For dowel pins
		Reaming				7.5	14.062			2	86	For dowel pins
		Drilling				9.375	50.625			2	214	Heating cartridges
						9.375	75			2	323	Heating cartridges
						2.812	90			1	1268	Thermocouples
						2.812	75.86			1	792	Thermocouples
	Tapping				7.5	14.062			4	66		
	L-faces	Rough and finish peripheral end milling	75	77	5.625					2	2845	
			75	77	38.5					2	4245	
	Slot	Rough and finish side and slot milling	36.562	73.125	18.281					1	2139	For rib fixation
Holes	Drilling				6.35	6.35			2	51	(pointing)	

						12.187	12.187			2	95	For dowel pins
		Reaming				12.187	12.187			2	121	For dowel pins
		Drilling				6.35	6.35			1	28	(pointing)
						7.5	10			1	34	For dowel pin
		Counterdrilling				11.25	4			1	-	For head screw
	Slots	Rough and finish face milling	41.62	144.375	3.281					2	5400	Slots
			24.375	144.375	3.281					2	3368	Slots
	Faces	Surface traverse grinding	75	108.75	0.089					2	716	Surface finish
			5.625	75	0.089					2	350	Surface finish
			35.35	82.5	0.089					1	241	Surface finish
			17.675	36.43	0.089					2	328	Surface finish
		Polishing									30038	
		Inspection									4500	
	Punch rib	Faces	Rough and finish face milling	38.1	76	0.769					4	1612
38.1				38.1	1.437					2	438	
Holes		Drilling				6.35	6.35			2	59	(pointing)
						7.687	13.125			2	97	For dowel pins
		Reaming				7.687	13.125			2	138	For dowel pins
		Drilling				6.35	6.35			1	32	(pointing)
						4.687	11.25			1	37	Rib fixation
Tapping					4.687	11.25			1	22	Rib fixation	
Slots	Rough and finis side and slot milling	5.625	23.437	23.437					1	1031	For rib insertion	

		Polishing									5506		
		Inspection									1300		
Cooling punch	Faces	Rough and finish face milling	25.4	228.6	3.862					2	1412		
			25.4	133.35	4.612					2	880		
			133.35	228.6	1.39							4490	
	Holes	Drilling				6.35	6.35				4	97	(pointing)
						10.4	125.625				4	1064	Cooling channels
		Tapping				14	11.347				4	415	Cooling channels
		Drilling				6.35	6.35				12	281	(pointing)
						9.375	24.375				8	593	
		Tapping				9.375	24.375				4	529	Punch and cooling punch fixation
		Drilling				7.5	24.375				2	132	For dowel pins
		Reaming				7.5	24.375				2	237	For dowel pins
		Drilling				18.75	24.375				2	249	Lockers fixation
		Reaming				18.75	24.375				2	189	For dowel pins
		Drilling				18.75	24.375				2	249	Lockers fixation
						1.875	24.375				2	97	Thermocouples
Faces	Surface traverse grinding	125.625	219.375	0.089						2	1414	Surface finish	
	Inspection										2700		
Lockers	Faces	Rough and finish face milling	19.05	31.75	3.175						2	200	
			6.35	19.05	1.812						2	160	
			6.35	31.75	2.02						2	150	
	Holes	Drilling				1	1				2	20	(pointing)

						2.34	4.687			2	153	Liners fixation
		Tapping				2.34	4.687			2	134	Liners fixation
		Counterdrilling				4.47	2.55			2	-	For head screw
		Inspection									900	
Bottom plate	Faces	Rough and finish face milling	16	228.6	3.862					2	700	
			16	133.35	4.612					2	448	
			133.35	228.6	1.437					2	2158	
	Holes	Drilling				6.35	6.35			10	235	(pointing)
						9.375	13.125			4	367	For vertical securing
		Tapping				9.375	13.125			4	87	For vertical securing
		Drilling				7.5	13.125			6	416	
		Tapping				7.5	13.125			4	95	For vertical securing
		Reaming				7.5	13.125			2	165	For dowel pins
	Faces	Surface traverse grinding	125.625	219.375	0.089					2	484	Surface finish
	Inspection									1800		
L-shape mould		Total manufacturing time									203877	

ANNEX IV

FEATURES MANUFACTURING DATA FOR CONCAVE MOULD

Table A-IV-1

Mould component	Features	Machining operations	Dimension						Repeat count	Operation time	Comments	
			W	L ₁	D ₁	d	L ₂	A				D ₂
			mm	mm	mm	mm	mm	mm ²		mm		s
Cavity	Faces	Rough and finish face milling	355.6	355.6	16.662					2	1264	Adjust the selected dimension All the faces
			88.9	355.6	19.05					2	638	
			88.9	355.6	31.75					2	994	
			19.05	317.5	42.875					2	3208	Face 2 and face 4
	Slots	Rough and finish side and slot milling	14.3	18.898	10.973					4	1262	Face 1
			4.775	200.101	3.175					1	459	Face 6
			6.35	135.839	6.35					1	726	
	Holes	Drilling (face 3)				2.54	2.54			11	203	Pointing
						12.7	98.552			2	804	Heating cartridges
						12.7	155.702			8	3306	
						1.6	87.63			1	190	thermocouple

					2.54	2.54			12	215	Pointing	
		Drilling (face 5)			12.7	98.552			2	804	Heating cartridges	
					12.7	155.702			8	3306		
					1.6	104.394			1	228	thermocouple	
		Tapping (face 5)			0.188	5.588			1	69	Vacuum channel	
		Drilling (face 6)			2.54	2.54			11	203	Pointing	
						12.7	98.552			2	804	Heating cartridges
						12.7	155.702			8	3306	
						1.905	25.4			4	481	Vacuum channels
						1.905	28.575			1	111	
						1.905	33.02			1	119	
						1.905	39.878			1	138	
						1.905	44.45			1	169	
		Counterdrilling (face 6)			3.81	9.525			8	290	Vacuum channels	
		Drilling (face 6)			3.175	53.34			1	168	thermocouples	
						3.175	28.702			1		158
						3.175	44.45			1		180
Pocket		Rough and finish pocket end mill					53.742	30.48	1	4374		

		(face 1)												
		Polishing									2710			
		Inspection									3600			
Punch	Faces	Rough and finish face milling	355.6	355.6	19.05					2	805	Adjust the selected dimension All the faces		
			88.9	355.6	19.05					2	308			
			88.9	355.6	31.75					2	319			
														Punch faces (Face 1')
			104.14	635	39.83					2	3925			
			78.74	83.82	39.83					1	1036			
			73.66	83.82	39.83					1	1055			
			18.34	27.69	39.83					1	413			
	19.41	97.54	39.83					1	680					
	83.82	165.1	11.05					1	723					
	Holes	Drilling (face 2',3',4',5')				2.54	2.54			8	344	Pointing		
						4.45	33.02			8	911	Side locks screws fixation		
		Tapping (face 2',3',4',5')				4.45	33.02			8	978			
	Faces Slots	Rough and finish face milling (face 2',4')	19.05	317.5	19.05					2	1690			
			82.55	114.3	4.55					2	774			
			114.3	177.8	3.775					2	1048			
		Rough and finish side and slot milling (face 2',3',4',5')	12.7	31.75	19.05					4	2024			
			6.35	35.03	6.35					1	273			
			27	317.5	9.525					1	2735			
	Holes	Drilling (face 3')				12.7	155.702			6	3725	Heating cartridges		
Drilling (face 5')					12.7	155.702			6	3725				
Drilling (face 6')					2.54	2.54			7	152	Pointing			

						10.16	69.85			1	301	Heating cartridges		
						10.16	50.8			1	216			
						10.16	44.45			1	192			
		Counterdrilling (face 6')						1.905	34.29			1	210	
								1.905	27.94			1	165	
								1.905	21.59			1	131	
								1.905	16.51			1	110	
		Drilling (face 6')						2.54	31.75			1	102	Thermocouples
								2.54	44.45			1	137	
								2.54	38.1			1	115	
								2.54	25.4			1	92	
		Counterdrilling (face 6')						19.05	25.4			1	152	Pressure transducer
								6.35	50.8			1	185	
								10.16	12.7			1	111	
								8.89	3.175			1	96	
				Polishing									5410	
Inspection											2700			
Side locks	Faces	Rough and finish face milling	19.05	76.2	9.525					2	244	Adjust the selected dimension All the faces		
			19.05	50.8	17.46					2	354			
			50.8	76.2	3.175					2	236			
			6.48	22.23	12.7					2	196			
			2.54	3.81	12.7					1	62			
	Holes	Drilling				4.45	12.7			2	141			

		Tapping				4.45	8.26			2	55	
		Counterdrilling				8.25	4.45			2	77	
		Polishing									576	
		Inspection									365	
Concave mould	Total manufacturing time										69953	

ANNEX V

COST CALCULATION EXCEL SPREADSHEET FOR THERMOSET FLAT PLATE MANUFACTURED BY AUTOCLAVE PROCESS

Table A-V-1

Cost elements		Items	Input	Equations	Output	Descriptions
Material costs	Production volume	Ann. Prod. Vol.	257	(7.1)		Hypothesis
		Reject Rate (%)	2%			Hypothesis
		(1 - Reject Rate)			0.98	
		Eff. Prod. Vol.		(7.1)	262.24	
	Productivity	Working days	240	(7.4)		
		shifts	1	(7.4)		
		Hours	8	(7.4)		
		Ann. Avail. Time (h)		(7.4)	1920	
		Cycle Time (min)/part	351.52			layup(31.92 min) + process(56.92 min)+ cure cycle(262.67min)
		Cycle Time (h)/part	5.85	(7.2)		
		Cycle Time (h)/Run	1536.40	(7.2)		[Cycle Time/60] (h)/part x Eff. Prod. Vol.
		Eff. Numbers of Runs	1	(7.2)		
		Ann. Prod. Time(h)		(7.2)	1536.40	
		Labor productivity		(7.5)	0.80	
	Part parameters	Length(mm)	355.6			
Width(mm)		304.8				

		Thickness(mm)	6			
		part volume(mm ³)			650321.28	
		part volume(m ³)			65.032E-05	Length x Width x Thickness
		Density(kg/m ³)	1578			
		Part weight (kg)			1.026	Density x plate volume
		Matl .Burden. Rate (%)	15%	(7.8)		Hypothesis
		(1 + Mat .Burden Rate)		(7.9)	1.15	
		Material price(\$/lbs)	60	(7.9)		
		Material rate(\$/lbs)		(7.9)	69	
		Material rate(\$/kg)		(7.9)	152.12	This intermediate to be inputted in (7.10)
		Ann. Matl. Costs (\$)		(7.10)	41773.34	
Labour costs		Labor Burden Rate (%)		(7.12)		
		(1 + Labor Burden Rate)		(7.13)		
		Hourly wages(\$/h)		(7.13)		
		Labor rate (\$/h)		(7.13)	100	This intermediate to be inputted in (7.14)
		Number of workers	1			Hypothesis
		Labor time/Run(h)	1536.40	(7.11)		Already calculated (cycle time/ Run)
		Annual labor costs (\$)		(7.14)	192000	
Energy costs		Energy consumption (kwh)/kg	6.083			Energy is 21.9 MJ/ kg
		energy consumption(kwh)/part		(7.15)	6.24	This intermediate to be inputted in (7.16)
		Annual energy consumption(kwh)			1637.12	

		Energy price (\$/kwh)	0.0457			Industrial rate
		Annual energy costs (\$)		(7.16)	74.82	
		Total annual variable costs (\$)			233848.16	
Equipment costs		Autoclave price (\$)	350000			
		Number of parallel streams	1			Hypothesis
		Number of machines/stream	1			Hypothesis
		Installations costs and training costs (\$)	35000			
		Investment costs (\$)		(7.17)	385000	This intermediate to be inputted in (7.18)
		Annual maintenance costs (\$)	17500			5% cost of Autoclave
		r (%)	30%			Hypothesis
		t (years)	10			Useful life of the autoclave
		$A = (1+r)^t$			13.78	
		$1/A$			0.072	
		$(r \cdot A)^{-1}$			0.24	
		$B = r^{-1}$			3.33	
		$[B(1-A^{-1})]^{-1}$			0.32	
		Annual investment costs (\$)		(7.18)	142033.42	
		Layup Material accessories (\$)	11.15			
		Total. Ann. Invest. Costs (\$)			142044.57	
Tooling costs		Mould price (\$)	9389.18			
		Number of parallel streams	1			Hypothesis

		Number of machines/stream	1			Hypothesis	
		Installations costs and training costs (\$)	200				
		Investment costs (\$)		(7.17)	9589.18	This intermediate to be inputted in (7.18)	
		Annual maintenance costs (\$)	469.46			5% cost of mould	
		r (%)	30%			Hypothesis	
		t(years)	3			Useful life of the mould	
		$A = (1+r)^t$			2.197		
		1/A			0.45		
		$(r \cdot A)^{-1}$			1.52		
		$B = r^{-1}$			3.33		
		$[B(1-A^{-1})]^{-1}$			0.55		
		Ann. Invest. Costs (\$)		(7.18)	5749.52		
Building costs	Autoclave	Floor space price(\$/ft ²)	6				
		Footprint/stream(ft ²)	200				
		Invest. Costs (\$)		(7.19)	1200		
	Layup surface	Floor space price (\$/ft ²)	6				
		Footprint/stream (ft ²)	24				
		Invest. Costs (\$)		(7.19)	144		
	Material and finished part storage	Floor space price (ft ²)	6				
		Area (ft ²)	800				
		Invest. Costs (\$)		(7.19)	4800		
		Total building costs (\$)				6144	

Costs of working capital	Capital recovery period (months)	13			Hypothesis
	Working Capital		(7.20)	253335.51	This intermediate to be inputted in (7.21)
	r (%)	30 %			Hypothesis
	Costs of working capital (\$)		(7.21)	82334.04	
Ann. Overhead costs	2 x Annual labor costs (\$)			384000	
	Total annual fixed costs (\$)			620272.13	
Unit cost/part (\$)			(7.22)	3323.43	

ANNEX VI

COST CALCULATION EXCEL SPREADSHEET FOR THERMOSET T-SHAPE PART MANUFACTURED BY AUTOCLAVE PROCESS

Table A-VI-1

Cost elements		Items	Input	Equations	Output	Descriptions	
Material costs	Production volume	Ann. Prod. Vol.	257	(7.1)		Hypothesis	
		Reject Rate (%)	2%			Hypothesis	
		(1 - Reject Rate)				0.98	
		Eff. Prod. Vol.			(7.1)	262.24	
	Productivity	Working days	240		(7.4)		
		shifts	1		(7.4)		
		Hours	8		(7.4)		
		Ann. Avail. Time (h)			(7.4)	1920	
		Cycle Time (min)/part	306.39				layup(4.56 min) + process(39.15 min)+ cure cycle(262.67min)
		Cycle Time (h)/part	5.106		(7.2)		
		Cycle Time (h)/Run	1537.16		(7.2)		[Cycle Time/60] (h)/part x Eff. Prod. Vol.
		Eff. Numbers of Runs	1		(7.2)		
		Ann. Prod. Time(h)			(7.2)	1536.40	
		Labor productivity			(7.5)	0.80	
	Part parameters	Flange length(mm)	76.2				
Flange width(mm)		76.2					

		Flange thickness(mm)	3.17			
		Rib length(mm)	76.2			
		Rib width(mm)	25.4			
		Rib thickness(mm)	3.17			
		part volume(m ³)			2.454E-05	\sum Length x Width x Thickness
		Density(kg/m ³)	1578			
		Part weight (kg)			0.067	Density x plate x volume
		Matl .Burden. Rate (%)	15%	(7.8)		Hypothesis
		(1 + Mat .Burden Rate)		(7.9)	1.15	
		Material price(\$/lbs)	60	(7.9)		
		Material rate(\$/lbs)		(7.9)	69	
		Material rate(\$/kg)		(7.9)	152.12	This intermediate to be inputted in (7.10)
	Ann. Matl. Costs (\$)		(7.10)	3166.29		
Labour costs		Labor Burden Rate (%)	10	(7.12)		
		(1 + Labor Burden Rate)		(7.13)	1.1	
		Hourly wages(\$/h)	80	(7.13)		
		Labor rate (\$/h)		(7.13)	88	This intermediate to be inputted in (7.14)
		Number of workers	1			Hypothesis
		Labor time/Run(h)	1537.16	(7.11)		Already calculated (cycle time/ Run)
		Annual labor costs (\$)		(7.14)	168960	
Energy costs		Energy consumption (kwh)/kg	6.083			Energy is 21.9 MJ/ kg
		energy consumption(kwh)/part		(7.15)	0.412	This intermediate to be inputted in (7.16)

		Annual energy consumption(kwh)			124.089	
		Energy price (\$/kwh)	0.0457			Industrial rate
		Annual energy costs (\$)		(7.16)	5.67	
		Total annual variable costs (\$)			172131.96	
Equipment costs		Autoclave price (\$)	350000			
		Number of parallel streams	1			Hypothesis
		Number of machines/stream	1			Hypothesis
		Installations costs and training costs (\$)	35000			
		Investment costs (\$)		(7.17)	385000	This intermediate to be inputted in (7.18)
		Annual maintenance costs (\$)	17500			5% cost of Autoclave
		r (%)	30%			Hypothesis
		t (years)	10			Useful life of the autoclave
		$A = (1+r)^t$				13.78
		1/A				0.072
		$(r \cdot A)^{-1}$				0.24
		$B = r^{-1}$				3.33
		$[B(1-A^{-1})]^{-1}$				0.32
		Annual investment costs (\$)		(7.18)	142033.42	
		Layup Material accessories (\$)	9.671			
	Total. Ann. Invest. Costs (\$)				142043.1	
Tooling		Mould price (\$)	12934.15	(7.18)		

costs		Number of parallel streams	1	(7.18)		Hypothesis
		Number of machines/stream	1	(7.18)		Hypothesis
		Installations costs and training costs (\$)	200	(7.18)		
		Investment costs (\$)		(7.18)	13134.15	This intermediate to be inputted in (7.18)
		Annual maintenance costs (\$)	129.34	(7.19)		5% cost of mould
		r (%)	30%	(7.19)		Hypothesis
		t(years)	3	(7.19)		Useful life of the mould
		$A = (1+r)^t$			2.197	
		1/A			0.45	
		$(r \cdot A)^{-1}$			1.52	
		$B = r^{-1}$			3.33	
		$[B(1-A^{-1})]^{-1}$		(7.19)	0.55	
		Ann. Invest. Costs \$		(7.19)	7361.35	
Building costs	Autoclave	Floor space price(\$/ft ²)	6			
		Footprint/stream(ft ²)	200			
		Invest. Costs \$)		(7.19)	1200	
	Layup surface	Floor space price (\$/ft ²)	6			
		Footprint/stream (ft ²)	24			
		Invest. Costs (\$)		(7.19)	144	
	Material and finished part storage	Floor space price (ft ²)	6			
		Area (ft ²)	800			
		Invest. Costs (\$)		(7.19)	4800	
	Total building costs			6144		

		(\\$)				
Costs of working capital		Capital recovery period (months)	13			Hypothesis
		Working Capital		(7.20)	186476.29	This intermediate to be inputted in (7.21)
		r (%)	30%			Hypothesis
		Costs of working capital (\$)		(7.21)	60604.8	
Ann. Overhead costs		2 x Annual labor costs (\$)			337920	
		Total annual fixed costs (\$)			554073.24	
Unit cost/part (\$)				(7.22)	2461.71	

ANNEX VII

COST CALCULATION EXCEL SPREADSHEET FOR THERMOSET L-SHAPE PART MANUFACTURED BY AUTOCLAVE PROCESS

Table A-VII-1

Cost elements		Items	Input	Equations	Output	Descriptions	
Material costs	Production volume	Ann. Prod. Vol.	305	(7.1)		Hypothesis	
		Reject Rate (%)	2%			Hypothesis	
		(1 - Reject Rate)				0.98	
		Eff. Prod. Vol.		(7.1)		311.22	
	Productivity	Working days	240	(7.4)			
		shifts	1	(7.4)			
		Hours	8	(7.4)			
		Ann. Avail. Time (h)		(7.4)		1920	
		Cycle Time (min)/part	296.44				layup(1,79 min) + process(31,42 min)+ cure cycle(262.67min)
		Cycle Time (h)/part	4.94	(7.2)			
		Cycle Time (h)/Run	1537.65	(7.2)			[Cycle Time/60] (h)/part x Eff. Prod. Vol.
		Eff. Numbers of Runs	1	(7.2)			
		Ann. Prod. Time(h)		(7.2)		1537.65	
		Labor productivity		(7.5)		0.80	
	Part parameters	length(mm)	230				
		width(mm)	75				

		thickness(mm)	6.4			
		Rib side(mm)	40			
		Rib thickness(mm)	6.4			
		part volume(m ³)			5.12E-06	Σ Length x Width x Thickness
		Density(kg/m ³)	1578			
		Part weight (kg)			0.182	Density x plate x volume
		Matl .Burden. Rate (%)	15%	(7.8)		Hypothesis
		(1 + Mat .Burden Rate)		(7.9)	1.15	
		Material price(\$/lbs)	60	(7.9)		
		Material rate(\$/lbs)		(7.9)	69	
		Material rate(\$/kg)		(7.9)	152.12	This intermediate to be inputted in (7.10)
		Ann. Matl. Costs (\$)		(7.10)	8806.34	
Labour costs		Labor Burden Rate (%)	10%	(7.12)		
		(1 + Labor Burden Rate)		(7.13)	1.1	
		Hourly wages(\$/h)	80	(7.13)		
		Labor rate (\$/h)		(7.13)	88	This intermediate to be inputted in (7.14)
		Number of workers	1			Hypothesis
		Labor time/Run(h)	1273.13	(7.11)		Already calculated (cycle time/ Run)
		Annual labor costs (\$)		(7.14)	168960	
Energy costs		Energy consumption (kwh)/kg	6.083			Energy is 21.9 MJ/ kg
		energy consumption(kwh)/part		(7.15)	1.108	This intermediate to be inputted in (7.16)
		Annual energy consumption(kwh)			345.12	
		Energy price (\$/kwh)	0.0457			Industrial rate

		Annual energy costs (\$)		(7.16)	15.77	
		Total annual variable costs (\$)			177782.11	
Equipment costs		Autoclave price (\$)	350000			
		Number of parallel streams	1			Hypothesis
		Number of machines/stream	1			Hypothesis
		Installations costs and training costs (\$)	35000			
		Investment costs (\$)		(7.17)	385000	This intermediate to be inputted in (7.18)
		Annual maintenance costs (\$)	17500			5% cost of Autoclave
		r (%)	30%			Hypothesis
		t (years)	10			Useful life of the autoclave
		$A = (1+r)^t$			13.78	
		1/A			0.072	
		$(r \cdot A)^{-1}$			0.24	
		$B = r^{-1}$			3.33	
		$[B(1-A^{-1})]^{-1}$			0.32	
		Annual investment costs (\$)		(7.18)	142033.42	
		Layup Material accessories (\$)	9.94			
		Total. Ann. Invest. Costs (\$)			142043.37	
Tooling costs		Mould price (\$)	15680.88	(7.18)		
		Number of parallel streams	1	(7.18)		Hypothesis
		Number of machines/stream	1	(7.18)		Hypothesis

		Installations costs and training costs (\$)	200	(7.18)			
		Investment costs (\$)		(7.18)	15880,88	This intermediate to be inputted in (7.18)	
		Annual maintenance costs (\$)	156.81	(7.19)		5% cost of mould	
		r (%)	30%	(7.19)		Hypothesis	
		t(years)	3	(7.19)		Useful life of the mould	
		$A = (1+r)^t$			2.197		
		1/A			0.45		
		$(r \cdot A)^{-1}$			1.52		
		$B = r^{-1}$			3.33		
		$[B(1-A^{-1})]^{-1}$		(7.19)	0.55		
		Ann. Invest. Costs \$		(7.19)	8901.24		
Building costs	Autoclave	Floor space price(\$/ft ²)	6				
		Footprint/stream(ft ²)	200				
		Invest. Costs \$)		(7.19)	1200		
	Layup surface	Floor space price (\$/ft ²)	6				
		Footprint/stream (ft ²)	24				
		Invest. Costs (\$)		(7.19)	144		
	Material and finished part storage	Floor space price (ft ²)	6				
		Area (ft ²)	800				
		Invest. Costs (\$)		(7.19)	4800		
		Total building costs (\$)			6144		
Costs of working capital		Capital recovery period (months)	13			Hypothesis	
		Working Capital		(7.20)	190966.84	This intermediate to be inputted in (7.21)	

		r (%)	30%			Hypothesis
		Costs of working capital (\$)		(7.21)	62064.22	
Ann. Overhead costs		2 x Annual labor costs (\$)			337920	
		Total annual fixed costs (\$)			557602.73	
Unit cost/part (\$)				(7.22)	2411.10	

ANNEX VIII

COST CALCULATION EXCEL SPREADSHEET FOR ROS FLAT PLATE MANUFACTURED BY COMPRESSION MOULDING PROCESS

Table A-VIII-1

Cost elements		Items	Input	Equations	Output	Descriptions	
Material costs	Production volume	Ann. Prod. Vol.	1000	(7.1)		Hypothesis	
		Reject Rate (%)	2%			Hypothesis	
		(1 - Reject Rate)				0.98	
		Eff. Prod. Vol.		(7.1)		1020.41	
	Productivity	Working days	240	(7.4)			
		Shifts	1	(7.4)			
		Hours	8	(7.4)			
		Ann. Avail. Time (h)		(7.4)		1920	
		Cycle Time (min)/part	90				
		Cycle Time (h)/part	1.5	(7.2)			
		Cycle Time (h)/Run	1530.61	(7.2)			[Cycle Time/60] (h)/part x Eff. Prod. Vol.
		Eff. Numbers of Runs	1	(7.2)			
		Ann. Prod. Time(h)		(7.2)		1530.61	
		Labor productivity		(7.5)		0.8	
	Part parameters	Length(mm)	82.44				
Width(mm)		82.44					

		Thickness(mm)	6			
		Part volume(mm ³)			40758.336	
		Part volume(m ³)			4.075E-05	Length x Width x Thickness
		Density(kg/m ³)	1540			
		Part weight (kg)			0.063	Density x plate volume
		Matl .Burden. Rate (%)	10%	(7.8)		Hypothesis
		(1 + Mat .Burden Rate)		(7.9)	1.1	
		Material price(\$/lbs)	89.5	(7.9)		
		Material rate(\$/lbs)		(7.9)	98.45	
		Material rate(\$/kg)		(7.9)	217.05	This intermediate to be inputted in (7.10)
		Ann. Matl. Costs (\$)		(7.10)	14185.18	
Labour costs		Labor Burden Rate (%)	10%	(7.12)		Hypothesis
		(1 + Labor Burden Rate)		(7.13)	1.1	
		Hourly wages(\$/h)	80	(7.13)		
		Labor rate (\$/h)		(7.13)	88	This intermediate to be inputted in (7.14)
		Number of workers	1			Hypothesis
		Labor time/Run(h)	1530.61	(7.11)		Already calculated (cycle time/ Run)
		Annual labor costs (\$)		(7.14)	168960	
Energy costs		Energy consumption (kwh)/part			0.39	y = 0.0959 x – 0.0011
		Annual energy consumption(kwh)		(7.15)	397.73	This intermediate to be inputted in (7.16)
		Energy price (\$/kwh)	0.0457			Industrial rate
		Annual energy costs (\$)		(7.16)	18.18	
		Total annual variable costs			183163.36	

		(\$)				
Equipment costs		MTS machine price and die set (\$)	9800			
		Number of parallel streams	1		Hypothesis	
		Number of machines/stream	1		Hypothesis	
		Installations costs and training costs (\$)	700			
		Investment costs (\$)		(7.17)	10500	This intermediate to be inputted in (7.18)
		Annual maintenance costs (\$)	490			5% cost of press
		r (%)	30%			Hypothesis
		t (years)	10			Useful life of the press
		$A = (1+r)^t$			13.79	
		1/A			0.07	
		$(r \cdot A)^{-1}$			0.24	
		$B = r^{-1}$			3.33	
		$[B(1-A^{-1})]^{-1}$			0.32	
		Annual investment costs (\$)		(7.18)	3886.37	
			Electrical and Control system and labview software	6000		
		Number of parallel streams	1			Hypothesis
		Number of machines/stream	1			Hypothesis
		Installations costs and training costs (\$)	12000			
		Investment costs (\$)		(7.17)	18000	This intermediate to be inputted in (7.18)
		Annual maintenance costs (\$)	400			5% cost of Ele.Con.Sys.Labv

	r (%)	30%			Hypothesis
	t(years)	10			Hypothesis
	$A = (1+r)^t$			13.79	
	$1/A$			0.07	
	$(r \cdot A)^{-1}$			0.24	
	$B = r^{-1}$			3.33	
	$[B(1-A^{-1})]^{-1}$			0.32	
	Annual investment costs (\$)		(7.18)	6222.34	
	Automatic cutter(\$)	1400			
	Number of parallel streams	1			Hypothesis
	Number of machines/stream	1			Hypothesis
	Installations costs and training costs (\$)	500			
	Investment costs (\$)		(7.17)	1900	This intermediate to be inputted in (7.18)
	Annual maintenance costs (\$)	400			5% cost of cutter
	r(%)	30%			Hypothesis
	t(years)	10			Hypothesis
	$A = (1+r)^t$			13.79	
	$1/A$			0.07	
	$(r \cdot A)^{-1}$			0.24	
	$B = r^{-1}$			3.33	
	$[B(1-A^{-1})]^{-1}$			0.32	
	Annual investment costs (\$)		(7.18)	1014.58	
	Total. Ann. Invest. Costs (\$)			11123.29	

Tooling costs		Projected mould area (mm²)	8819			
		Accessories and mould costs (\$)	5993.06			$y = 1357.7x + 4795.7$
		Number of parallel streams	1			
		Number of machines/stream	1			
		Installations costs and training costs (\$)	600			
		Investment costs (\$)		(7.17)	6593.06	This intermediate to be inputted in (7.18)
		Annual maintenance costs (\$)	59.93			5% cost of mould and accessories
		r (%)	30%			Hypothesis
		t(years)	3			Useful life of the mould and accessories
		$A = (1+r)^t$			2.2	
		1/A			0.46	
		$(r \cdot A)^{-1}$			1.52	
		$B = r^{-1}$			3.33	
		$[B(1-A^{-1})]^{-1}$			0.55	
			Ann. Invest. Costs \$		(7.18)	3690.24
Building costs	Press	Floor space price(\$/ft ²)	6			
		Footprint/stream(ft ²)	11			
		Invest. Costs \$)		(7.19)	66	
	Automatic cutter	Floor space price (\$/ft ²)	6			
		Footprint/stream (ft ²)	5			
		Invest. Costs (\$)		(7.19)	30	
	Material and finished part storage	Floor space price (ft ²)	6			
Area (ft ²)		800				

		Invest. Costs (\$)		(7.19)	4800	
		Total building costs (\$)			4896	
Costs of working capital		Capital recovery period (months)	13			Hypothesis
		Working Capital		(7.20)	198426.97	This intermediate to be inputted in (7.21)
		r (%)	30%			Hypothesis
		Costs of working capital (\$)		(7.21)	64488.77	
Ann. Overhead costs		2 x Annual labor costs (\$)			337920	
		Total annual fixed costs (\$)			422118.30	
Unit cost/part (\$)				(7.22)	605.28	

ANNEX IX

COST CALCULATION EXCEL SPREADSHEET FOR ROS THERMOPLASTIC T-SHAPE PART MANUFACTURED BY COMPRESSION MOULDING PROCESS

Table A-IX-1

Cost elements		Items	Input	Equations	Output	Descriptions	
Material costs	Production volume	Ann. Prod. Vol.	1000	(7.1)		Hypothesis	
		Reject Rate (%)	2%			Hypothesis	
		(1 - Reject Rate)				0.98	
		Eff. Prod. Vol.		(7.1)		1020.41	
	Productivity	Working days	240	(7.4)			
		shifts	1	(7.4)			
		Hours	8	(7.4)			
		Ann. Avail. Time (h)		(7.4)		1920	
		Cycle Time (min)/part	90				
		Cycle Time (h)/part	1.5	(7.2)			
		Cycle Time (h)/Run	1530.61	(7.2)			[Cycle Time/60] (h)/part x Eff. Prod. Vol.
		Eff. Numbers of Runs	1	(7.2)			
		Ann. Prod. Time(h)		(7.2)		1530.61	
		Labor productivity		(7.5)		0.8	
	Part parameters	Flange length(mm)	82.44				
Flange width(mm)		82.44					

		Flange thickness(mm)	3.17				
		Rib length(mm)	82.44				
		Rib width(mm)	25.4				
		Rib thickness(mm)	3.17				
		part volume(m ³)				2.82E-05	\sum Length x Width x Thickness
		Density(kg/m ³)	1540				
	Part weight (kg)				0.043	Density x plate volume	
		Matl .Burden Rate (%)	10%	(7.8)			Hypothesis
		(1 + Mat .Burden Rate)		(7.9)		1.1	
		Material price(\$/lbs)	89.5	(7.9)			
		Material rate(\$/lbs)		(7.9)		98.45	
		Material rate(\$/kg)		(7.9)		217.045	This intermediate to be inputted in (7.10)
Ann. Matl. Costs (\$)			(7.10)		9808.34		
Labour costs	Labor Burden Rate (%)	10%	(7.12)			Hypothesis	
	(1 + Labor Burden Rate)		(7.13)		1.1		
	Hourly wages(\$/h)	80	(7.13)				
	Labor rate (\$/h)		(7.13)		88	This intermediate to be inputted in (7.14)	
	Number of workers	1				Hypothesis	
	Labor time/Run(h)	1530.61	(7.11)			Already calculated (cycle time/ Run)	
	Annual labor costs(\$)		(7.14)		168960		
Energy costs	Energy consumption (kwh)/part				0.6	$y = 0.0959x - 0.0011$	
	Annual energy consumption(kwh)		(7.15)		612.32	This intermediate to be inputted in (7.16)	

		Energy price(\$/kwh)	0.0457			Industrial rate
		Annual energy costs (\$)		(7.16)	27.983	
		Total annual variable costs (\$)			178796.32	
Equipment costs		MTS machine price and die set (\$)	9800			
		Number of parallel streams	1			Hypothesis
		Number of machines/stream	1			Hypothesis
		Installations costs and training costs (\$)	700			
		Investment costs (\$)		(7.17)	10500	This intermediate to be inputted in (7.18)
		Annual maintenance costs (\$)	490			5% cost of press
		r (%)	30%			Hypothesis
		t (years)	10			Useful life of the press
		$A = (1+r)^t$				13.78
		$1/A$				0.072
		$(r \cdot A)^{-1}$				0.241
		$B = r^{-1}$				3.33
		$[B(1-A^{-1})]^{-1}$				0.32
		Annual investment costs (\$)		(7.18)	3886.36	
		Electrical and Control system and labview software (\$)	6000			
		Number of parallel streams	1			Hypothesis
		Number of machines/stream	1			Hypothesis
	Installations costs and training costs (\$)	12000				
	Investment costs (\$)		(7.17)	18000	This intermediate to be inputted in (7.18)	

	Annual maintenance costs (\$)	400			5% cost of Ele.Con.Sys.Labv
	r (%)	30%			Hypothesis
	t(years)	10			Hypothesis
	$A = (1+r)^t$			13.78	
	1/A			0.072	
	$(r \cdot A)^{-1}$			0.24	
	$B = r^{-1}$			3.33	
	$[B(1-A^{-1})]^{-1}$			0.32	
	Annual investment costs (\$)		(7.18)	6222.34	
	Automatic cutter (\$)	1400			
	Number of parallel streams	1			Hypothesis
	Number of machines/stream	1			Hypothesis
	Installations costs and training costs (\$)	500			
	Investment costs (\$)		(7.17)	1900	This intermediate to be inputted in (7.18)
	Annual maintenance costs (\$)	400			5% cost of Cutter
	r (%)	30%			Hypothesis
	t(years)	10			Hypothesis
	$A = (1+r)^t$			13.78	
	1/A			0.072	
	$(r \cdot A)^{-1}$			0.241	
	$B = r^{-1}$			3.33	
	$[B(1-A^{-1})]^{-1}$			0.32	
	Annual investment costs (\$)		(7.18)	1014.58	
	Total. Ann. Invest. Costs (\$)			11123.28	

Tooling costs		Projected mould area (mm²)	8819			
		Accessories and mould costs (\$)	6831.21			$y = 1357.7x + 4795.7$
		Number of parallel streams	1			
		Number of machines/stream	1			
		Installations costs and training costs (\$)	600			
		Investment costs (\$)		(7.17)	7431.21	This intermediate to be inputted in (7.18)
		Annual maintenance costs (\$)	68.31			5% cost of mould and accessories
		r (%)	30%			Hypothesis
		t(years)	3			Useful life of the mould and accessories
		$A = (1+r)^t$			2.197	
		1/A			0.455	
		$(r \cdot A)^{-1}$			1.517	
		$B = r^{-1}$			3.33	
		$[B(1-A^{-1})]^{-1}$			0.55	
		Ann. Invest. costs(\$)		(7.18)	4160.13	
Building costs	Press	Floor space price(\$/ft ²)	6			
		Footprint/stream(ft ²)	11			
		Invest. Costs (\$)		(7.19)	66	
	Automatic cutter	Floor space price (\$/ft ²)	6			
		Footprint/stream(ft ²)	5			
		Invest. Costs(\$)		(7.19)	30	
	Material and finished part storage	Floor space price(ft ²)	6			
		Area (ft ²)	800			

		Invest. Costs(\$)		(7.19)	4800	
		Total building costs (\$)			4896	
Costs of working capital		Capital recovery period (months)	13			Hypothesis
		Working Capital		(7.20)	193696.02	This intermediate to be inputted in (7.21)
		r (%)	30%			Hypothesis
		Costs of working capital (\$)		(7.21)	62951.2	
Ann. Overhead costs		2 x Annual labor costs (\$)			337920	
		Total annual fixed costs (\$)			421050.63	
Unit cost/part(\$)				(7.22)	599.84	

ANNEX X

COST CALCULATION EXCEL SPREADSHEET FOR ROS THERMOPLASTIC L-SHAPE PART MANUFACTURED BY COMPRESSION MOULDING PROCESS

Table A-X-1

Cost elements		Items	Input	Equations	Output	Descriptions	
Material costs	Production volume	Ann. Prod. Vol.	500	(7.1)		Hypothesis	
		Reject Rate (%)	2%			Hypothesis	
		(1 - Reject Rate)				0.98	
		Eff. Prod. Vol.		(7.1)	510.2		
	Productivity	Working days	240	(7.4)			
		shifts	1	(7.4)			
		Hours	8	(7.4)			
		Ann. Avail. Time (h)		(7.4)	1920		
		Cycle Time (min)/part	189				
		Cycle Time (h)/part	3.15	(7.2)			
		Cycle Time (h)/Run	1607.14	(7.2)			[Cycle Time/60] (h)/part x Eff. Prod. Vol.
		Eff. Numbers of Runs	1	(7.2)			
		Ann. Prod. Time(h)		(7.2)	1607.14		
		Labor productivity		(7.5)	0.84		
	Part parameters	Length(mm)	115				
Width(mm)		75					

		Thickness(mm)	6.4			
		Rib side(mm)	40			
		Rib thickness(mm)	6.4			
		part volume(mm ³)			115520	$\sum \text{Length} \times \text{Width} \times \text{Thickness}$
		part volume(m ³)			11.55E-05	$\sum \text{Length} \times \text{Width} \times \text{Thickness}$
		Density(kg/m ³)	1540			
		Part weight (kg)			0.178	Density x plate volume
		Matl .Burden Rate (%)	10%	(7.8)		Hypothesis
		(1 + Mat .Burden Rate)		(7.9)	1.1	
		Material price(\$/lbs)	89.5	(7.9)		
		Material rate(\$/lbs)		(7.9)	98.45	
Material rate(\$/kg)			(7.9)	217.045	This intermediate to be inputted in (6.10)	
	Ann. Matl. Costs (\$)		(7.10)	20102.3		
Labour costs	Labor Burden Rate (%)	10%	(7.12)		Hypothesis	
	(1 + Labor Burden Rate)		(7.13)	1.1		
	Hourly wages(\$/h)	80	(7.13)			
	Labor rate (\$/h)		(7.13)	88	This intermediate to be inputted in (7.14)	
	Number of workers	1			Hypothesis	
	Labor time/Run(h)	1607.14	(7.11)		Already calculated (cycle time/ Run)	
	Annual labor costs (\$)		(7.14)	168960		
Energy costs	Energy consumption (kwh)/part			1.59	$y = 0.0959x - 0.0011$	
	Annual energy consumption(kwh)		(7.15)	814.93	This intermediate to be inputted in (7.16)	

		Energy price(\$/kwh)	0.0457			Industrial rate
		Annual energy costs(\$)		(7.16)	37.24	
		Total annual variable costs (\$)			189099.54	
Equipment costs		MTS machine price and die set (\$)	11280			
		Number of parallel streams	1			Hypothesis
		Number of machines/stream	1			Hypothesis
		Installations costs and training costs(\$)	700			
		Investment costs (\$)		(7.17)	11980	This intermediate to be inputted in (7.18)
		Annual maintenance costs (\$)	564			5% cost of press
		r (%)	30%			Hypothesis
		t (years)	10			Useful life of the press
		$A = (1+r)^t$				13.78
		$1/A$				0.072
		$(r \cdot A)^{-1}$				0.24
		$B = r^{-1}$				3.33
		$[B(1-A^{-1})]^{-1}$				0.32
		Annual investment costs(\$)		(7.18)	4439.09	
		Electrical and Control system and labview software (\$)	6000			
		Number of parallel streams	1			Hypothesis
		Number of machines/stream	1			Hypothesis

	Installations costs and training costs (\$)	12000			
	Investment costs (\$)		(7.17)	18000	This intermediate to be inputted in (7.18)
	Annual maintenance costs (\$)	400			5% cost of Ele.Con.Sys.Labv
	r (%)	30%			Hypothesis
	t(years)	10			Hypothesis
	$A = (1+r)^t$			13.78	
	1/A			0.072	
	$(r \cdot A)^{-1}$			0.24	
	$B = r^{-1}$			3.33	
	$[B(1-A^{-1})]^{-1}$			0.32	
	Annual investment costs (\$)		(7.18)	6222.34	
	Automatic cutter (\$)	1400			
	Number of parallel streams	1			Hypothesis
	Number of machines/stream	1			Hypothesis
	Installations costs and training costs (\$)	500			
	Investment costs (\$)		(7.17)	1900	This intermediate to be inputted in (7.18)
	Annual maintenance costs (\$)	400			5% cost of cutter
	r(%)	30%			Hypothesis
	t(years)	10			Hypothesis
	$A = (1+r)^t$			13.78	
	1/A			0.072	

		$(r \cdot A)^{-1}$			0.24	
		$B = r^{-1}$			3.33	
		$[B(1-A^{-1})]^{-1}$			0.32	
		Annual investment costs (\$)		(7.18)	1014.58	
		Total. Ann. Invest. Costs (\$)			11676.01	
Tooling costs		Projected mould area (mm²)	27558.9			
		Accessories and mould costs (\$)	21034.57			$y = 1357.7x + 4795.7$
		Number of parallel streams	1			
		Number of machines/stream	1			
		Installations costs and training costs (\$)	600			
		Investment costs (\$)		(7.17)	21634.57	This intermediate to be inputted in (7.18)
		Annual maintenance costs (\$)	210.34			5% cost of mould and accessories
		r (%)	30%			Hypothesis
		t(years)	3			Useful life of the mould and accessories
		$A = (1+r)^t$			2.197	
		1/A			0.45	
		$(r \cdot A)^{-1}$			1.51	
		$B = r^{-1}$			3.33	
		$[B(1-A^{-1})]^{-1}$			0.55	
		Ann. Invest. Costs (\$)		(7.18)	12122.92	
	Press	Floor space price(\$/ft ²)	6			

Building costs		Footprint/stream(ft ²)	11				
		Invest. Costs(\$)		(7.19)	66		
	Automatic cutter		Floor space price (\$/ft ²)	6			
			Footprint/stream(ft ²)	5			
			Invest. Costs (\$)		(7.19)	30	
	Material and finished part storage		Floor space price(ft ²)	6			
			Area (ft ²)	800			
			Invest. Costs (\$)		(7.19)	4800	
			Total building costs (\$)			4896	
	Costs of working capital		Capital recovery period (months)	13			Hypothesis
		Working Capital (\$)		(7.20)	204857.83	This intermediate to be inputted in (7.21)	
		r (%)	30%			Hypothesis	
			Costs of working capital (\$)		(7.21)	66578.8	
Ann. Overhead costs		2 x Annual labor costs (\$)			337920		
		Total annual fixed costs (\$)			433193.73		
Unit cost/part (\$)				(7.22)	1244.58		

ANNEX XI

**COST CALCULATION EXCEL SPREADSHEET FOR UD THERMOPLASTIC
CONCAVE PART MANUFACTURED BY COMPRESSION MOULDING PROCESS**

Table A-XI-1

Cost elements		Items	Input	Equations	Output	Descriptions	
Material costs	Production volume	Ann. Prod. Vol.	4500	(7.1)		Hypothesis	
		Reject Rate (%)	3%			Hypothesis	
		(1 - Reject Rate)				0.97	
		Eff. Prod. Vol.		(7.1)		4639	
	Productivity	Working days	240	(7.4)			
		shifts	1	(7.4)			
		Hours	8	(7.4)			
		Ann. Avail. Time (h)		(7.4)		1920	
		Cycle Time (min)/part	18.33				
		Cycle Time (h)/part	0.305	(7.2)			
		Cycle Time (h)/Run	1417.47	(7.2)			[Cycle Time/60] (h)/part x Eff. Prod. Vol.
		Eff. Numbers of Runs	1	(7.2)			
		Ann. Prod. Time(h)		(7.2)		1417.47	
		Labor productivity		(7.5)		0.74	
	Part parameters	Length(mm)	241.4				
Width(mm)		152.4					

		Thickness(mm)	3.352			
		part volume(mm ³)			123347.36	Length x Width x Thickness
		part volume(m ³)			12.33E-05	Length x Width x Thickness
		Density(kg/m ³)	1540			
		Part weight (kg)			0.189	Density x plate volume
		Matl .Burden. Rate (%)	10%	(7.8)		Hypothesis
		(1 + Mat .Burden Rate)		(7.9)	1.1	
		Material price(\$/lbs)	89.5	(7.9)		
		Material rate(\$/lbs)		(7.9)	98.45	
		Material rate(\$/kg)		(7.9)	217.045	This intermediate to be inputted in (7.10)
		Ann. Matl. Costs (\$)		(7.10)	89437.35	
Labour costs		Labor Burden Rate (%)	10%	(7.12)		Hypothesis
		(1 + Labor Burden Rate)		(7.13)	1.1	
		Hourly wages(\$/h)	80	(7.13)		
		Labor rate (\$/h)		(7.13)	88	This intermediate to be inputted in (7.14)
		Number of workers	1			Hypothesis
		Labor time/Run(h)	1417.47	(7.11)		Already calculated (cycle time/ Run)
		Annual labor costs (\$)		(7.14)	168960	
Energy costs		Energy consumption (kwh)/part			2.495	$y = 0.2098x - 0.0924$
		Annual energy consumption(kwh)		(7.15)	11576.289	This intermediate to be inputted in (7.16)
		Energy price (\$/kwh)	0.0457			Industrial rate
		Annual energy costs (\$)		(7.16)	529.036	

		Total annual variable costs (\$)			258926.39	
Equipment costs		Press (\$)	125000			
		Number of parallel streams	1			Hypothesis
		Number of machines/stream	1			Hypothesis
		Installations costs and training costs (\$)	400			
		Investment costs (\$)		(7.17)	125400	This intermediate to be inputted in (7.18)
		Annual maintenance costs (\$)	6250			5% cost of press
		r (%)	30%			Hypothesis
		t (years)	10			Useful life of the press
		$A = (1+r)^t$			13.78	
		$1/A$			0.072	
		$(r \cdot A)^{-1}$			0.24	
		$B = r^{-1}$			3.33	
		$[B(1-A^{-1})]^{-1}$			0.32	
		Annual investment costs (\$)		(7.18)	46812.31	
		Electrical and Control system and labview software	10420			
		Number of parallel streams	1			Hypothesis
		Number of machines/stream	1			Hypothesis
		Installations costs and training costs (\$)	200			
		Investment costs (\$)		(7.17)	18000	This intermediate to be inputted in (7.18)
		Annual maintenance costs (\$)	521			5% cost of Ele.Con.Sys.Labv

	r (%)	30%			Hypothesis
	t(years)	10			Hypothesis
	$A = (1+r)^t$			13.78	
	1/A			0.072	
	$(r \cdot A)^{-1}$			0.241	
	$B = r^{-1}$			3.33	
	$[B(1-A^{-1})]^{-1}$			0.32	
	Annual investment costs (\$)		(7.18)	6122.34	
	IR Oven (\$)	6000			
	Number of parallel streams	1			Hypothesis
	Number of machines/stream	1			Hypothesis
	Installations costs and training costs (\$)	12000			
	Investment costs (\$)		(7.17)	10620	This intermediate to be inputted in (7.18)
	Annual maintenance costs (\$)	300			5% cost of oven
	r(%)	30%			Hypothesis
	t(years)	10			Useful life of oven
	$A = (1+r)^t$			13.78	
	1/A			0.072	
	$(r \cdot A)^{-1}$			0.24	
	$B = r^{-1}$			3.33	
	$[B(1-A^{-1})]^{-1}$			0.32	
	Annual investment costs (\$)		(7.18)	3956.18	
	Total. Ann. Invest. Costs (\$)			56890.84	

Tooling costs		Projected mould area (mm²)	9.27			
		Accessories and mould costs (\$)	20483.81			$y = 1357.7x + 4795.7$
		Number of parallel streams	1			Hypothesis
		Number of machines/stream	1			Hypothesis
		Installations costs and training costs (\$)	1000			
		Investment costs (\$)		(7.17)	21483.81	This intermediate to be inputted in (7.18)
		Annual maintenance costs (\$)	204.84			5% cost of mould and accessories
		r (%)	30%			Hypothesis
		t(years)	3			Useful life of the mould and accessories
		$A = (1+r)^t$			2.19	
		1/A			0.45	
		$(r \cdot A)^{-1}$			1.51	
		$B = r^{-1}$			3.33	
		$[B(1-A^{-1})]^{-1}$			0.55	
		Ann. Invest. Costs \$)		(7.18)	12034.39	
Building costs	Press	Floor space price(\$/ft ²)	6			
		Footprint/stream(ft ²)	11			
		Invest. Costs \$)		(7.19)	66	
	IR Oven	Floor space price (\$/ft ²)	6			
		Footprint/stream (ft ²)	10			
		Invest. Costs (\$)		(7.19)	60	
Material	Floor space price (ft ²)	6				

	and finished part storage	Area (ft ²)	800			
		Invest. Costs (\$)		(7.19)	4800	
		Total building costs (\$)			4926	
Costs of working capital		Capital recovery period (months)	13			Hypothesis
		Working Capital		(7.20)	280503.59	This intermediate to be inputted in (7.21)
		r (%)	30%			Hypothesis
		Costs of working capital (\$)		(7.21)	91163.66	
Ann. Overhead costs		2 x Annual labor costs (\$)			337920	
		Total annual fixed costs (\$)			502934.9	
Unit cost/part (\$)				(7.22)	169.3	

ANNEX XII

**COST CALCULATION EXCEL SPREADSHEET FOR UD THERMOPLASTIC HOLLOW
SQUARE PART MANUFACTURED BY COMPRESSION MOULDING PROCESS**

Table A-XII-1

Cost elements		Items	Input	Equations	Output	Descriptions	
Material costs	Production volume	Ann. Prod. Vol.	4500	(7.1)		Hypothesis	
		Reject Rate (%)	3%			Hypothesis	
		(1 - Reject Rate)				0.97	
		Eff. Prod. Vol.		(7.1)		4639	
	Productivity	Working days	240	(7.4)			
		shifts	1	(7.4)			
		Hours	8	(7.4)			
		Ann. Avail. Time (h)		(7.4)		1920	
		Cycle Time (min)/part	18.33				
		Cycle Time (h)/part	0.305	(7.2)			
		Cycle Time (h)/Run	1417.47	(7.2)			[Cycle Time/60] (h)/part x Eff. Prod. Vol.
		Eff. Numbers of Runs	1	(7.2)			
		Ann. Prod. Time(h)		(7.2)		1417.47	
		Labor productivity		(7.5)		0.74	
	Part parameters	Length(mm)	137.16				
Width(mm)		137.16					

		Thickness(mm)	3.3528			
		part volume(mm ³)			63075.77	Length x Width x Thickness
		part volume(m ³)			6.30E-05	Length x Width x Thickness
		Density(kg/m ³)	1540			
		Part weight (kg)			0.097136695	Density x plate volume
		Matl .Burden. Rate (%)	10%	(7.8)		Hypothesis
		(1 + Mat .Burden Rate)		(7.9)	1.1	
		Material price(\$/lbs)	89.5	(7.9)		
		Material rate(\$/lbs)		(7.9)	98.45	
		Material rate(\$/kg)		(7.9)	217.045	This intermediate to be inputted in (7.10)
		Ann. Matl. Costs (\$)		(7.10)	100829.1114	
Labour costs		Labor Burden Rate (%)	10%	(7.12)		Hypothesis
		(1 + Labor Burden Rate)		(7.13)	1.1	
		Hourly wages(\$/h)	80	(7.13)		
		Labor rate (\$/h)		(7.13)	88	This intermediate to be inputted in (7.14)
		Number of workers	1			Hypothesis
		Labor time/Run(h)	1417.47	(7.11)		Already calculated (cycle time/ Run)
		Annual labor costs (\$)		(7.14)	168960	
Energy costs		Energy consumption (kwh)/part			1.541481626	y = 0.2272 x + 1.1084
		Annual energy consumption(kwh)		(7.15)	7150.933262	This intermediate to be inputted in (7.16)
		Energy price (\$/kwh)	0.0457			Industrial rate
		Annual energy costs (\$)		(7.16)	326.7976501	
		Total annual variable			270115.909	

		costs (\$)				
Equipment costs		Press (\$)	125000			
		Number of parallel streams	1			Hypothesis
		Number of machines/stream	1			Hypothesis
		Installations costs and training costs (\$)	400			
		Investment costs (\$)		(7.17)	125400	This intermediate to be inputted in (7.18)
		Annual maintenance costs (\$)	6250			5% cost of press
		r (%)	30%			Hypothesis
		t (years)	10			Useful life of the press
		$A = (1+r)^t$			13.78	
		1/A			0.072	
		$(r \cdot A)^{-1}$			0.241	
		$B = r^{-1}$			3.33	
		$[B(1-A^{-1})]^{-1}$			0.32	
		Annual investment costs (\$)		(7.18)	46812.31	
		IR Oven (\$)	10420			
		Number of parallel streams	1			Hypothesis
		Number of machines/stream	1			Hypothesis
		Installations costs and training costs (\$)	200			
		Investment costs (\$)		(7.17)	10620	This intermediate to be inputted in (7.18)
		Annual maintenance costs (\$)	521			5% cost of oven

	r (%)	30%			Hypothesis
	t (years)	10			Useful life of oven
	$A = (1+r)^t$			13.78	
	1/A			0.072	
	$(r \cdot A)^{-1}$			0.24	
	$B = r^{-1}$			3.33	
	$[B(1-A^{-1})]^{-1}$			0.32	
	Annual investment costs (\$)		(7.18)	3956.18	
	Electrical and Control system and labview software	6000			
	Number of parallel streams	1			Hypothesis
	Number of machines/stream	1			Hypothesis
	Installations costs and training costs (\$)	12000			
	Investment costs (\$)		(7.17)	18000	This intermediate to be inputted in (7.18)
	Annual maintenance costs (\$)	300			5% cost of Ele.Con.Sys.Labv
	r (%)	30%			Hypothesis
	t(years)	10			Hypothesis
	$A = (1+r)^t$			13.78	
	1/A			0.072	
	$(r \cdot A)^{-1}$			0.241	
	$B = r^{-1}$			3.33	
	$[B(1-A^{-1})]^{-1}$			0.32	

		Annual investment costs (\$)		(7.18)	6122.34	
		Total. Ann. Invest. Costs (\$)			56890.84	
Tooling costs		Projected mould area (mm²)	92741.75			
		Accessories and mould costs (\$)	16916.83103			$y = 1753.3x + 656.42$
		Number of parallel streams	1			Hypothesis
		Number of machines/stream	1			Hypothesis
		Installations costs and training costs (\$)	1000			
		Investment costs (\$)		(7.17)	17916.83103	This intermediate to be inputted in (7.18)
		Annual maintenance costs (\$)	169.16			5% cost of mould and accessories
		r (%)	30%			Hypothesis
		t(years)	3			Useful life of mould and accessories
		$A = (1+r)^t$				2.197
		1/A				0.455166136
		$(r \cdot A)^{-1}$				1.517220452
		$B = r^{-1}$				3.333333333
		$[B(1-A^{-1})]^{-1}$				0.550626566
		Ann. Invest. Costs (\$)		(7.18)	10034.65146	
Building costs	Press	Floor space price(\$/ft ²)	6			
		Footprint/stream(ft ²)	11			
		Invest. Costs (\$)		(7.19)	66	
	IR Oven	Floor space price (\$/ft ²)	6			

		Footprint/stream (ft ²)	10				
		Invest. Costs (\$)		(7.19)	60		
	Material and finished part storage		Floor space price (ft ²)	6			
			Area (ft ²)	800			
			Invest. Costs (\$)		(7.19)	4800	
		Total building costs (\$)			4926		
Costs of working capital		Capital recovery period (months)	13			Hypothesis	
		Working Capital		(7.20)	292625.5681	This intermediate to be inputted in (7.21)	
		r (%)	30%			Hypothesis	
		Costs of working capital (\$)		(7.21)	95103.30964		
Ann. Overhead costs		2 x Annual labor costs (\$)			337920		
		Total annual fixed costs (\$)			504874.8001		
Unit cost/part (\$)				(7.22)	172.22		

ANNEX XIII

**COST CALCULATION EXCEL SPREADSHEET FOR UD THERMOPLASTIC
U-SHAPE PART MANUFACTURED BY COMPRESSION MOULDING PROCESS**

Table A-XIII-1

Cost elements		Items	Input	Equations	Output	Descriptions	
Material costs	Production volume	Ann. Prod. Vol.	4500	(7.1)		Hypothesis	
		Reject Rate (%)	3%			Hypothesis	
		(1 - Reject Rate)				0.97	
		Eff. Prod. Vol.		(7.1)		4639	
	Productivity	Working days	240	(7.4)			
		shifts	1	(7.4)			
		Hours	8	(7.4)			
		Ann. Avail. Time (h)		(7.4)		1920	
		Cycle Time (min)/part	18.33				
		Cycle Time (h)/part	0.305	(7.2)			
		Cycle Time (h)/Run	1417.47	(7.2)			[Cycle Time/60] (h)/part x Eff. Prod. Vol.
		Eff. Numbers of Runs	1	(7.2)			
		Ann. Prod. Time(h)		(7.2)		1417.47	
		Labor productivity		(7.5)		0.74	
	Part parameters	Length(mm)	137.16				
Width(mm)		45.72					

		Thickness(mm)	3.3528			
		part volume(mm ³)			21025.25	Length x Width x Thickness
		part volume(m ³)			2.102E-05	Length x Width x Thickness
		Density(kg/m ³)	1540			
		Part weight (kg)			0.032	Density x plate volume
		Matl .Burden. Rate (%)	10%	(7.8)		Hypothesis
		(1 + Mat .Burden Rate)		(7.9)	110%	
		Material price(\$/lbs)	89.5	(7.9)		
		Material rate(\$/lbs)		(7.9)	98.45	
		Material rate(\$/kg)		(7.9)	217.045	This intermediate to be inputted in (7.10)
		Ann. Matl. Costs (\$)		(7.10)	33609.7	
		Labor Burden Rate (%)	10%	(7.12)		Hypothesis
		(1 + Labor Burden Rate)		(7.13)	1.1	
		Hourly wages(\$/h)	80	(7.13)		
		Labor rate (\$/h)		(7.13)	88	This intermediate to be inputted in (7.14)
		Number of workers	1			Hypothesis
		Labor time/Run(h)	1417.47	(7.11)		Already calculated (cycle time/ Run)
		Annual labor costs (\$)		(7.14)	168960	
		Energy consumption (kwh)/part			2.47	$y = 1.2328x - 0.1206$
		Annual energy consumption(kwh)		(7.15)	11464.79	This intermediate to be inputted in (7.16)
		Energy price (\$/kwh)	0.0457			Industrial rate
		Annual energy costs (\$)		(7.16)	523.94	
		Total annual variable costs (\$)			203093.64	

Equipment costs		Press (\$)	125000			
		Number of parallel streams	1			Hypothesis
		Number of machines/stream	1			Hypothesis
		Installations costs and training costs (\$)	400			
		Investment costs (\$)		(7.17)	125400	This intermediate to be inputted in (7.18)
		Annual maintenance costs (\$)	6250			5% cost of press
		r (%)	30%			Hypothesis
		t (years)	10			Useful life of the press
		$A = (1+r)^t$			13.78	
		$1/A$			0.072	
		$(r \cdot A)^{-1}$			0.241	
		$B = r^{-1}$			3.33	
		$[B(1-A^{-1})]^{-1}$			0.32	
		Annual investment costs (\$)		(7.18)	46812.31	
		IR Oven (\$)	10420			
		Number of parallel streams	1			Hypothesis
		Number of machines/stream	1			Hypothesis
		Installations costs and training costs (\$)	200			
		Investment costs (\$)		(7.17)	10620	This intermediate to be inputted in (7.18)
		Annual maintenance costs (\$)	521			5% cost of oven
		r (%)	30%			Hypothesis
		t (years)	10			Useful life of oven
		$A = (1+r)^t$			13.78	

		$1/A$			0.072	
		$(r \cdot A)^{-1}$			0.24	
		$B = r^{-1}$			3.33	
		$[B(1-A^{-1})]^{-1}$			0.32	
		Annual investment costs (\$)		(7.18)	3956.18	
		Electrical and Control system and labview software	6000			
		Number of parallel streams	1			Hypothesis
		Number of machines/stream	1			Hypothesis
		Installations costs and training costs (\$)	12000			
		Investment costs (\$)		(7.17)	18000	This intermediate to be inputted in (7.18)
		Annual maintenance costs (\$)	300			5% cost of Ele.Con.Sys.Labv
		r (%)	30%			Hypothesis
		t(years)	10			Hypothesis
		$A = (1+r)^t$			13.78	
		$1/A$			0.072	
		$(r \cdot A)^{-1}$			0.241	
		$B = r^{-1}$			3.33	
		$[B(1-A^{-1})]^{-1}$			0.32	
		Annual investment costs (\$)		(7.18)	6122.34	
		Total. Ann. Invest. Costs (\$)			56890.84	
Tooling costs		Projected mould area (mm²)	92741.75			
		Accessories and mould costs (\$)	16916.83			$y = 1753.3 x + 656.42$

		Number of parallel streams	1			Hypothesis	
		Number of machines/stream	1			Hypothesis	
		Installations costs and training costs (\$)	1000				
		Investment costs (\$)		(7.17)	17916.83	This intermediate to be inputted in (7.18)	
		Annual maintenance costs (\$)	169.16			5% cost of mould and accessories	
		r (%)	30%			Hypothesis	
		t(years)	3			Useful life of mould and accessories	
		$A = (1+r)^t$			2.197		
		$1/A$			0.45		
		$(r \cdot A)^{-1}$			1.51		
		$B = r^{-1}$			3.33		
		$[B(1-A^{-1})]^{-1}$			0.55		
		Ann. Invest. Costs \$		(7.18)	10034.65		
Building costs	Press	Floor space price(\$/ft ²)	6				
		Footprint/stream(ft ²)	11				
		Invest. Costs \$)		(7.19)	66		
	IR Oven	Floor space price (\$/ft ²)	6				
		Footprint/stream (ft ²)	10				
		Invest. Costs (\$)		(7.19)	60		
	Material and finished part storage	Floor space price (ft ²)	6				
		Area (ft ²)	800				
		Invest. Costs (\$)		(7.19)	4800		
		Total building costs (\$)			4926		

Costs of working capital	Capital recovery period (months)	13			Hypothesis
	Working Capital		(7.20)	220018.11	This intermediate to be inputted in (7.21)
	r (%)	30%			Hypothesis
	Costs of working capital (\$)		(7.21)	71505.88	
Ann. Overhead costs	2 x Annual labor costs (\$)			337920	
	Total annual fixed costs (\$)			481277.37	
Unit cost/part (\$)			(7.22)	152.08	

ANNEX XIV

**COST CALCULATION EXCEL SPREADSHEET FOR UD THERMOPLASTIC
Z-SHAPE PART MANUFACTURED BY COMPRESSION MOULDING PROCESS**

Table A-XIV-1

Cost elements		Items	Input	Equations	Output	Descriptions	
Material costs	Production volume	Ann. Prod. Vol.	4500	(7.1)		Hypothesis	
		Reject Rate (%)	3%			Hypothesis	
		(1 - Reject Rate)				0.97	
		Eff. Prod. Vol.		(7.1)		4639	
	Productivity	Working days	240	(7.4)			
		shifts	1	(7.4)			
		Hours	8	(7.4)			
		Ann. Avail. Time (h)		(7.4)		1920	
		Cycle Time (min)/part	18.33				
		Cycle Time (h)/part	0.305	(7.2)			
		Cycle Time (h)/Run	1417.47	(7.2)			[Cycle Time/60] (h)/part x Eff. Prod. Vol.
		Eff. Numbers of Runs	1	(7.2)			
		Ann. Prod. Time(h)		(7.2)		1417.47	
		Labor productivity		(7.5)		0.74	
	Part parameters	Length(mm)	130.048				
		Width(mm)	43.307				

		Thickness(mm)	3.3528			
		part volume(mm ³)			18882.93	Length x Width x Thickness
		part volume(m ³)			0.0000188829	Length x Width x Thickness
		Density(kg/m ³)	1540			
		Part weight (kg)			0.0291	Density x plate volume
		Matl .Burden. Rate (%)	10%	(7.8)		Hypothesis
		(1 + Mat .Burden Rate)		(7.9)	1.1	
		Material price(\$/lbs)	89.5	(7.9)		
		Material rate(\$/lbs)		(7.9)	98.45	
		Material rate(\$/kg)		(7.9)	217.045	This intermediate to be inputted in (7.10)
		Ann. Matl. Costs (\$)		(7.10)	30185.11	
Labour costs		Labor Burden Rate (%)	10%	(7.12)		Hypothesis
		(1 + Labor Burden Rate)		(7.13)	1.1	
		Hourly wages(\$/h)	80	(7.13)		
		Labor rate (\$/h)		(7.13)	88	This intermediate to be inputted in (7.14)
		Number of workers	1			Hypothesis
		Labor time/Run(h)	1417.47	(7.11)		Already calculated (cycle time/ Run)
		Annual labor costs (\$)		(7.14)	168960	
Energy costs		Energy consumption (kwh)/part			2.56	$y = 0,7515 x + 1,1463$
		Annual energy consumption(kwh)		(7.15)	11900.67	This intermediate to be inputted in (7.16)
		Energy price (\$/kwh)	0.0457			Industrial rate
		Annual energy costs (\$)		(7.16)	543.86	
		Total annual variable			199688.97	

		costs (\$)				
Equipment costs		Press (\$)	125000			
		Number of parallel streams	1		Hypothesis	
		Number of machines/stream	1		Hypothesis	
		Installations costs and training costs (\$)	400			
		Investment costs (\$)		(7.17)	125400	This intermediate to be inputted in (7.18)
		Annual maintenance costs (\$)	6250			5% cost of press
		r (%)	30%			Hypothesis
		t (years)	10			Useful life of the press
		$A = (1+r)^t$			13.78	
		$1/A$			0.072	
		$(r \cdot A)^{-1}$			0.241	
		$B = r^{-1}$			3.33	
		$[B(1-A^{-1})]^{-1}$			0.32	
		Annual investment costs (\$)		(7.18)	46812.31	
		IR Oven (\$)	10420			
		Number of parallel streams	1			Hypothesis
		Number of machines/stream	1			Hypothesis
		Installations costs and training costs (\$)	200			
		Investment costs (\$)		(7.17)	10620	This intermediate to be inputted in (7.18)
		Annual maintenance costs (\$)	521			5% cost of oven

	r (%)	30%			Hypothesis
	t (years)	10			Useful life of oven
	$A = (1+r)^t$			13.78	
	$1/A$			0.072	
	$(r \cdot A)^{-1}$			0.24	
	$B = r^{-1}$			3.33	
	$[B(1-A^{-1})]^{-1}$			0.32	
	Annual investment costs (\$)		(7.18)	3956.18	
	Electrical and Control system and labview software	6000			
	Number of parallel streams	1			Hypothesis
	Number of machines/stream	1			Hypothesis
	Installations costs and training costs (\$)	12000			
	Investment costs (\$)		(7.17)	18000	This intermediate to be inputted in (7.18)
	Annual maintenance costs (\$)	300			5% cost of Ele.Con.Sys.Labv
	r (%)	30%			Hypothesis
	t(years)	10			Hypothesis
	$A = (1+r)^t$			13.78	
	$1/A$			0.072	
	$(r \cdot A)^{-1}$			0.241	
	$B = r^{-1}$			3.33	
	$[B(1-A^{-1})]^{-1}$			0.32	

		Annual investment costs (\$)		(7.18)	6122.34	
		Total. Ann. Invest. Costs (\$)			56890.84	
Tooling costs		Projected mould area (mm²)	92741.75			
		Accessories and mould costs (\$)	17425.57			$y = 2001,9 x - 1140,4$
		Number of parallel streams	1			Hypothesis
		Number of machines/stream	1			Hypothesis
		Installations costs and training costs (\$)	1000			
		Investment costs (\$)		(7.17)	18425.57	This intermediate to be inputted in (7.18)
		Annual maintenance costs (\$)	174.25			5% cost of mould and accessories
		r (%)	30%			Hypothesis
		t(years)	3			Useful life of mould and accessories
		$A = (1+r)^t$			2.197	
		1/A			0.45	
		$(r \cdot A)^{-1}$			1.51	
		$B = r^{-1}$			3.33	
		$[B(1-A^{-1})]^{-1}$			0.55	
			Ann. Invest. Costs (\$)		(7.18)	10319.86
Building costs	Press	Floor space price(\$/ft ²)	6			
		Footprint/stream(ft ²)	11			
		Invest. Costs (\$)		(7.19)	66	
	IR Oven	Floor space price (\$/ft ²)	6			

		Footprint/stream (ft ²)	10			
		Invest. Costs (\$)		(7.19)	60	
	Material and finished part storage	Floor space price (ft ²)	6			
		Area (ft ²)	800			
		Invest. Costs (\$)		(7.19)	4800	
		Total building costs (\$)			4926	
Costs of working capital		Capital recovery period (months)	13			Hypothesis
		Working Capital		(7.20)	216329.72	This intermediate to be inputted in (7.21)
		r (%)	30%			Hypothesis
		Costs of working capital (\$)		(7.21)	70307.15	
Ann. Overhead costs		2 x Annual labor costs (\$)			337920	
		Total annual fixed costs (\$)			480363.86	
Unit cost/part (\$)				(7.22)	151.12	

ANNEX XV

**COST CALCULATION EXCEL SPREADSHEET FOR UD THERMOPLASTIC
FLAT PLATE MANUFACTURED BY COMPRESSION MOULDING PROCESS**

Table A-XV-1

Cost elements		Items	Input	Equations	Output	Descriptions	
Material costs	Production volume	Ann. Prod. Vol.	4500	(7.1)		Hypothesis	
		Reject Rate (%)	3%			Hypothesis	
		(1 - Reject Rate)				0.97	
		Eff. Prod. Vol.		(7.1)		4639	
	Productivity	Working days	240	(7.4)			
		shifts	1	(7.4)			
		Hours	8	(7.4)			
		Ann. Avail. Time (h)		(7.4)		1920	
		Cycle Time (min)/part	18.33				
		Cycle Time (h)/part	0.305	(7.2)			
		Cycle Time (h)/Run	1417.47	(7.2)			[Cycle Time/60] (h)/part x Eff. Prod. Vol.
		Eff. Numbers of Runs	1	(7.2)			
		Ann. Prod. Time(h)		(7.2)		1417.47	
		Labor productivity		(7.5)		0.74	
	Part parameters	Length(mm)	45.72				
		Width(mm)	45.72				
		Thickness(mm)	3.352				

		part volume(mm ³)			7008.42	Length x Width x Thickness	
		part volume(m ³)			7.008E-06	Length x Width x Thickness	
		Density(kg/m ³)	1540				
		Part weight (kg)			0.0108	Density x plate volume	
		Matl .Burden. Rate (%)	10%	(7.8)			Hypothesis
		(1 + Mat .Burden Rate)		(7.9)	1.1		
		Material price(\$/lbs)	89.5	(7.9)			
		Material rate(\$/lbs)		(7.9)	98.45		
		Material rate(\$/kg)		(7.9)	217.045		This intermediate to be inputted in (7.10)
		Ann. Matl. Costs (\$)		(7.10)	11203.23		
	Labour costs		Labor Burden Rate (%)	10%	(7.12)		Hypothesis
		(1 + Labor Burden Rate)		(7.13)	1.1		
		Hourly wages(\$/h)	80	(7.13)			
		Labor rate (\$/h)		(7.13)	88	This intermediate to be inputted in (7.14)	
		Number of workers	1			Hypothesis	
		Labor time/Run(h)	1417.47	(7.11)		Already calculated (cycle time/ Run)	
		Annual labor costs (\$)		(7.14)	168960		
Energy costs		Energy consumption (kwh)/part			2.066	$y = 0.2098x - 0.0924$	
		Annual energy consumption(kwh)		(7.15)	9585.75	This intermediate to be inputted in (7.16)	
		Energy price (\$/kwh)	0.0457			Industrial rate	
		Annual energy costs (\$)		(7.16)	438.069		
		Total annual variable costs (\$)			180601.3		

Equipment costs		Press (\$)	125000			
		Number of parallel streams	1			Hypothesis
		Number of machines/stream	1			Hypothesis
		Installations costs and training costs (\$)	400			
		Investment costs (\$)		(7.17)	125400	This intermediate to be inputted in (7.18)
		Annual maintenance costs (\$)	6250			5% cost of press
		r (%)	30%			Hypothesis
		t (years)	10			Useful life of the press
		$A = (1+r)^t$			13.78	
		1/A			0.072	
		$(r \cdot A)^{-1}$			0.241	
		$B = r^{-1}$			3.33	
		$[B(1-A^{-1})]^{-1}$			0.32	
		Annual investment costs (\$)		(7.18)	46812.31	
		IR Oven (\$)	10420			
		Number of parallel streams	1			Hypothesis
		Number of machines/stream	1			Hypothesis
		Installations costs and training costs (\$)	200			
		Investment costs (\$)		(7.17)	10620	This intermediate to be inputted in (7.18)
		Annual maintenance costs (\$)	521			5% cost of oven
		r (%)	30%			Hypothesis
		t (years)	10			Useful life of oven

		$A = (1+r)^t$			13.78	
		$1/A$			0.072	
		$(r \cdot A)^{-1}$			0.24	
		$B = r^{-1}$			3.33	
		$[B(1-A^{-1})]^{-1}$			0.32	
		Annual investment costs (\$)		(7.18)	3956.18	
		Electrical and Control system and labview software	6000			
		Number of parallel streams	1			Hypothesis
		Number of machines/stream	1			Hypothesis
		Installations costs and training costs (\$)	12000			
		Investment costs (\$)		(7.17)	18000	This intermediate to be inputted in (7.18)
		Annual maintenance costs (\$)	300			5% cost of Ele.Con.Sys.Labv
		r (%)	30%			Hypothesis
		t(years)	10			Hypothesis
		$A = (1+r)^t$			13.78	
		$1/A$			0.072	
		$(r \cdot A)^{-1}$			0.241	
		$B = r^{-1}$			3.33	
		$[B(1-A^{-1})]^{-1}$			0.32	
		Annual investment costs (\$)		(7.18)	6122.34	
		Total. Ann. Invest. Costs (\$)			56890.84	
Tooling		Projected mould area (mm²)	92741.75			

costs		Accessories and mould costs (\$)	13700.58			$y = 1357.7x + 4795.7$
		Number of parallel streams	1			Hypothesis
		Number of machines/stream	1			Hypothesis
		Installations costs and training costs (\$)	1000			
		Investment costs (\$)		(7.17)	14700.58535	This intermediate to be inputted in (7.18)
		Annual maintenance costs (\$)	137			5% cost of mould and accessories
		r (%)	30%			Hypothesis
		t(years)	3			Useful life of mould and accessories
		$A = (1+r)^t$			2.197	
		1/A			0.455166136	
		$(r \cdot A)^{-1}$			1.517220452	
		$B = r^{-1}$			3.333333333	
		$[B(1-A^{-1})]^{-1}$			0.550626566	
			Ann. Invest. Costs (\$)		(7.18)	8231.538692
Building costs	Press	Floor space price(\$/ft ²)	6			
		Footprint/stream(ft ²)	11			
		Invest. Costs (\$)		(7.19)	66	
	IR Oven	Floor space price (\$/ft ²)	6			
		Footprint/stream (ft ²)	10			
		Invest. Costs (\$)		(7.19)	60	
	Material and finished part storage	Floor space price (ft ²)	6			
Area (ft ²)		800				

		Invest. Costs (\$)		(7.19)	4800	
		Total building costs (\$)			4926	
Costs of working capital		Capital recovery period (months)	13			Hypothesis
		Working Capital		(7.20)	195651.41	This intermediate to be inputted in (7.21)
		r (%)	30%			Hypothesis
		Costs of working capital (\$)		(7.21)	63586.71	
Ann. Overhead costs		2 x Annual labor costs (\$)			337920	
		Total annual fixed costs (\$)			471555.08	
Unit cost/part (\$)				(7.22)	144.92	

LIST OF BIBLIOGRAPHICAL REFERENCES

- Abrams, Lisa M., et Jose M. Castro. 2003. « Predicting molding forces during sheet molding compound (SMC) compression molding. I: Model development ». *Polymer composites*, vol. 24, n° 3, p. 291-303.
- Acuratus. 2013. « Thermal and mechanical properties ». In *Standard product, MACOR® Machinable Glass Ceramic*. <http://accuratus.com/macorprps1.html>. Accessed February 5, 2016.
- Åkermo, M., et B. Tomas Åström. 2000. « Modelling component cost in compression moulding of thermoplastic composite and sandwich components ». *Composites Part A: Applied Science and Manufacturing*, vol. 31, n° 4, p. 319-333.
- AZoM. 2001. « Zirconia - ZrO₂, Zirconium Dioxide ». In *properties data*. <<http://www.azom.com/properties.aspx?ArticleID=133>>. Accessed February 4, 2016.
- Barlow, Darren, Chris Howe, Graham Clayton et Stephan Brouwer. 2002. « Preliminary study on cost optimisation of aircraft composite structures applicable to liquid moulding technologies ». *Composite structures*, vol. 57, n° 1, p. 53-57.
- Berenberg, Barry. 2003. « Improving autoclave performance ». *High Performance Composites*, vol. 11, n° 2, p. 27-36.
- Boothroyd, G. 1974. « Automatic Handling of Small Parts ». In *Proc. International Production Engineering Conference*. (Tokyo), p. 475.
- Boothroyd, Geoffrey, et al. 1994. « Product design for manufacture and assembly ». *Computer-Aided Design*, vol. 26, n° 7, p. 505-520.
- Callister, W.D. 2005. *Thermal Properties : Chapter 17: Fundamentals of Materials Science and Engineering, 2 nd Ed*. Hoboken NJ : John Wiley & Sons, Inc, 16 p.
- Cardonne, Martin. 2015. *Mechanical energy cost of a hydraulic press during the forming cycle of composite parts*. Coll. « Internal report for COMP412 CRIAQ project ». Montreal: École de technologie supérieure, 181 p.
- Cauberghs, Julien. 2011. « Out-of-Autoclave Manufacturing of Aerospace Representative Parts ». Master Thesis in Engineering. McGill University, 104 p.

- Curran, R., Mark P., Raghunathan S., Benard E., Crosby S., Castagne S. et Mawhinney P. 2005. « Integrating aircraft cost modeling into conceptual design ». *Concurrent Engineering*, vol. 13, n° 4, p. 321-330.
- Dewhurst, P., et G. Boothroyd. 1988. « Early cost estimating in product design ». *Journal of Manufacturing systems*, vol. 7, n° 3, p. 183-191.
- Dysert, L.R. 2008. « An introduction to parametric estimating ». *1984 AACE International Transactions*, vol. 3, p. 1-7.
- Eaglesham, Mark Alan. 1998. « A decision support system for advanced composites manufacturing cost estimation ». Dissertation of Doctor of Philosophy in Industrial and Systems Engineering. Faculty of the Virginia Polytechnic Institute and State University, 246 p.
- El Asli, Neila. 2008. « Approche hybride basée sur les machines à vecteurs de support et les algorithmes génétiques pour l'estimation des coûts de fabrication ». Mémoire de Maîtrise en Génie de production Automatisée. École de technologie supérieure, 119 p.
- El wazziki, M., et A.D. Ngo. 2014. « Modelling of compression moulding process cycle time for carbon fibre reinforced thermoplastic flat panels ». In *10th Canada-Japan Workshop on Composites*. (Vancouver, Canada), p. 9.
- Elstein-Werk. « Ceramic infrared panel radiators ». In *Datasheets heaters-panel heaters, HTS series*. www.elstein.com. Accessed June 20, 2013.
- Fuchs, Erica R.H. 2003. « The significance of production cost inputs in regional technology choice: Composite automotive body-in-whites in the us versus china ». Master Thesis in Sciences, Engineering System Division. Massachusetts Institute of Technology.
- Grouve, Wouter Johannes Bernardus. 2012. « Weld strength of laser-assisted tape-placed thermoplastic composites ». Ph. D Thesis. University of Twente, Enschede, the Netherlands, 169 p.
- Gutowski, Timothy G., et al. 1994. « Development of a theoretical cost model for advanced composite fabrication ». *Composites Manufacturing*, vol. 5, n° 4, p. 231-239.
- Gutowski, Timothy George Peter. 1997. *Advanced composites manufacturing*. New York, N.Y.: J. John Wiley & Sons, 581 p.
- Haffner, S.M., et T.G. Gutowski. 1999. « Manufacturing time estimation laws for composite materials ». In *NSF Conference*. Vancouver, BC:[sn].

- Haffner, Sascha Marcel. 2002. « Cost modeling and design for manufacturing guidelines for advanced composite fabrication ». Ph.D Thesis in Mechanical Engineering. Massachusetts Institute of Technology, 493 p.
- Hexcel, Corp. 2013. « HexPly 8852 ® product data ». In *Le site de Hexcel corp. En ligne* .<http://www.hexcel.com/Resources/DataSheets/Prepreg-Data-Sheets/8552_eu.pdf>. Accessed February 15, 2016.
- Hoa, Suong V. 2009. *Principles of the Manufacturing of Composite Materials*. Destech publications, Inc., 352 p.
- Kaufmann, Markus, Dan Zenkert et Christophe Mattei. 2008. « Cost optimization of composite aircraft structures including variable laminate qualities ». *Composites Science and Technology*, vol. 68, n° 13, p. 2748-2754.
- Kim, Jung-Seok, et al. 2001. « Practical design of tapered composite structures using the manufacturing cost concept ». *Composite structures*, vol. 51, n° 3, p. 285-299.
- Kumar, Jayanthi, et Elizabeth Kendall. 1999. « Complexity based cost estimation model for composite aerospace structures ». *CRC-ACS CP*, vol. 99004.
- Landry, Benoit. 2014. *CAD of T-shape mould*. Department of Mechanical Engineering, McGill University.
- LeBlanc, D. 2014a. *Temperature profile versus time through the thickness of ROS T- shape parts*. Coll. « Excel spreadsheet data ». McGill University, Montreal.
- LeBlanc, D. 2014b. *Temperature profile versus time inside the L-bracket mould and design of L-bracket mould*. Coll. « Excel spreadsheet data and CAD file ». Department of Mechanical Engineering , McGill University.
- LeBlanc, D. 2015. *T-shape mould and L-shape mould prices*. Coll. « Internal data ». McGill University, Montreal.
- LeBlanc, Dominic, Benoit Landry, Arthur Levy, Pascal Hubert, Steven Roy et Ali Yousefpour. 2014a. « Compression moulding of complex parts using randomly-oriented strands thermoplastic composites ». In *Proceeding of the International SAMPE Symposium and Exhibition, Seattle WA, USA*. p. 2-4.
- LeBlanc, Dominic, Arthur Levy, Pascal Hubert, Steven Roy et Ali Yousefpour. 2014b. « Compression moulding of stiffened brackets using randomly oriented strands thermoplastic composites ». In *CAMX 2014.Orlando,FL* p. 2-9.

- LeBlanc, Donald J., A. Kokawa, T. Bettner, F. Timson et J. Lorenzara. 1976. *Advanced Composites Cost Estimating Manual (ACCEM)*. AFFDL-TR-76-87, Northrop Corporation, Hawthorne, California, 54 p.
- Lebrun, G. 2012. *Commercial price of concave mould*. Coll. « CRIAQ project COMP412 ». UQTR.
- Lessard, H. 2012a. *Mould design progression*. Coll. « Presentation for CRIAQ COMP412 research project ». UQTR.
- Lessard, H. 2013a. *CAD of of concave mould and side lock*. Coll. « Internal data ». UQTR.
- Lessard, H. 2014. *Experimental temperatures vs. time for three measurements inside the compression moulded CF/PEEK laminate*. Coll. « Internal data ». UQTR.
- Lessard, H., et G. Lebrun. 2011. « Experimental analysis and modeling of PEEK/carbon parts reinforced with short and continuous carbon fibers ». In *Presentation for CRIAQ project COMP412*. p. 2.
- Lessard, H., G. Lebrun et T. Pham. 2013. *Experimental evaluation of the thermostamping process for a complex 3D composite Part made of unidirectional CF/PEEK prepregs*. Coll. « Internal report, CRIAQ COMP412 project ».
- Levy, Arthur. 2014. *Physical and thermal proprieties of CF/thermoplastic composites materials*. Coll. « Internal data ». Montreal: McGill University.
- Ma, Weitao. 2011. « Cost modelling for manufacturing of aerospace composites ». Master Thesis in Sciences. School of applied sciences, 126 p.
- Mabson, G. E., B. W. Flynn, L. B. Ilcewicz et D. L. Graesser. 1994. « THE USE OF COSTADE IN DEVELOPING COMPOSITE COMMERCIAL AIRCRAFT FUSELAGE STRUCTURES' ». In *35th Structures, Structural Dynamics, and Materials Conference*. (Hilton Head,SC,U.S.A.), p. 1384-1393.
- Marina, Selezneva. 2011. *Compression moulding of thermoplastics composites materials Literature Review Mech-700*. Mc Gill University, 14 p.
- Neoh, Ein-Teck. 1995. « Adaptive framework for estimating fabrication time ». Ph.D Thesis in Mechanical Engineering. Massachusetts Institute of Technology, 453 p.
- Neoh, Ein Teck, Timothy G. Gutowski et Greg Dillon. 1995. « Framework for estimating fabrication time of advanced composites manufacturing processes ». *Materials challenge diversification and the future*, p. 1584-1594.

- NIST, WebBook de Chimie. « zirconium dioxide ». In *Base de données standard de référence NIST*. <http://webbook.nist.gov/chemistry/>. Accessed February 4, 2016.
- Pantelakis, Sp. G., Ch. V. Katsiropoulos, G.N. Labeas et H. Sibois. 2009. « A concept to optimize quality and cost in thermoplastic composite components applied to the production of helicopter canopies ». *Composites Part A: Applied Science and Manufacturing*, vol. 40, n° 5, p. 595-606.
- Picher-Martel, Gilles-Philippe, et Marina Selezneva. 2011. *Moulding of a flat plate : preliminary tests* Presentation for CRIAQ project COMP412. Montreal: Mc Gill University, 9 p.
- Protherm. « Infrared Basics ». In *Electric IR Heating Equipment. En ligne* .<http://www.pro-therm.com/infrared_basics.php>. Accessed June 15, 2013.
- Raj, John Diamond, Sohan Birla, Krishnamoorthy Pitchai, Jeyamkondan Subbiah et David Jones. 2011. « Modeling of Microwave Heating of a Rotating Object in Domestic Oven ». In *Excerpt from the Proceedings of the 2011 Comsol Conference, Boston*.
- Ramkumar, RL, RB Vastava et SK Saha. 1991. « Manufacturing cost model for composites ». In *Proc. 23rd International SAMPE Technical Conf.* p. 982-94.
- Roy, Steven. 2014. *Wabash press specifications, CAD of flat mould and flat mould price*. Coll. « Internal data ». Montreal: Aerospace Manufacturing Technology Centre
- Ruoshi, T. 2012. « Cost analysis on L-shape composite component manufacturing ». Master Thesis in Sciences(Industrial Engineering). Concordia University, 95 p.
- Selezneva, M, G-P Picher-Martel, B Landry, D Trudel-Boucher, S Roy, L Khoun, M Hojjati, L Lessard et P Hubert. 2012. « Compression moulding of discontinuous-fibre carbon/PEEK composites: study of mechanical properties ». In *International SAMPE Technical Conference*.
- Selezneva, Marina. 2013. *Temperature profile versus time at three positions for the same thickness of ROS flat plate*. Coll. « Excel spreadsheet data ». Mc Gill University.
- Shehab, E., et H. Abdalla. 2002. « An intelligent knowledge-based system for product cost modelling ». *The international journal of advanced manufacturing technology*, vol. 19, n° 1, p. 49-65.
- Song, Young S., Jae R. Youn et Timothy G. Gutowski. 2009. « Life cycle energy analysis of fiber-reinforced composites ». *Composites Part A: Applied Science and Manufacturing*, vol. 40, n° 8, p. 1257-1265.

- Tanaka, H, S Sawai, K Morimoto et K Hisano. 2001. « Measurement of spectral emissivity and thermal conductivity of zirconia by thermal radiation calorimetry ». *Journal of thermal analysis and calorimetry*, vol. 64, n° 3, p. 867-872.
- Verrey, J., M.D. Wakeman, V. Michaud et J.-A.E. Manson. 2006. « Manufacturing cost comparison of thermoplastic and thermoset RTM for an automotive floor pan ». *Composites Part A: Applied Science and Manufacturing*, vol. 37, n° 1, p. 9-22.
- Ye, Jinrui, Boming Zhang et Haiming Qi. 2009. « Cost estimates to guide manufacturing of composite waved beam ». *Materials & Design*, vol. 30, n° 3, p. 452-458.